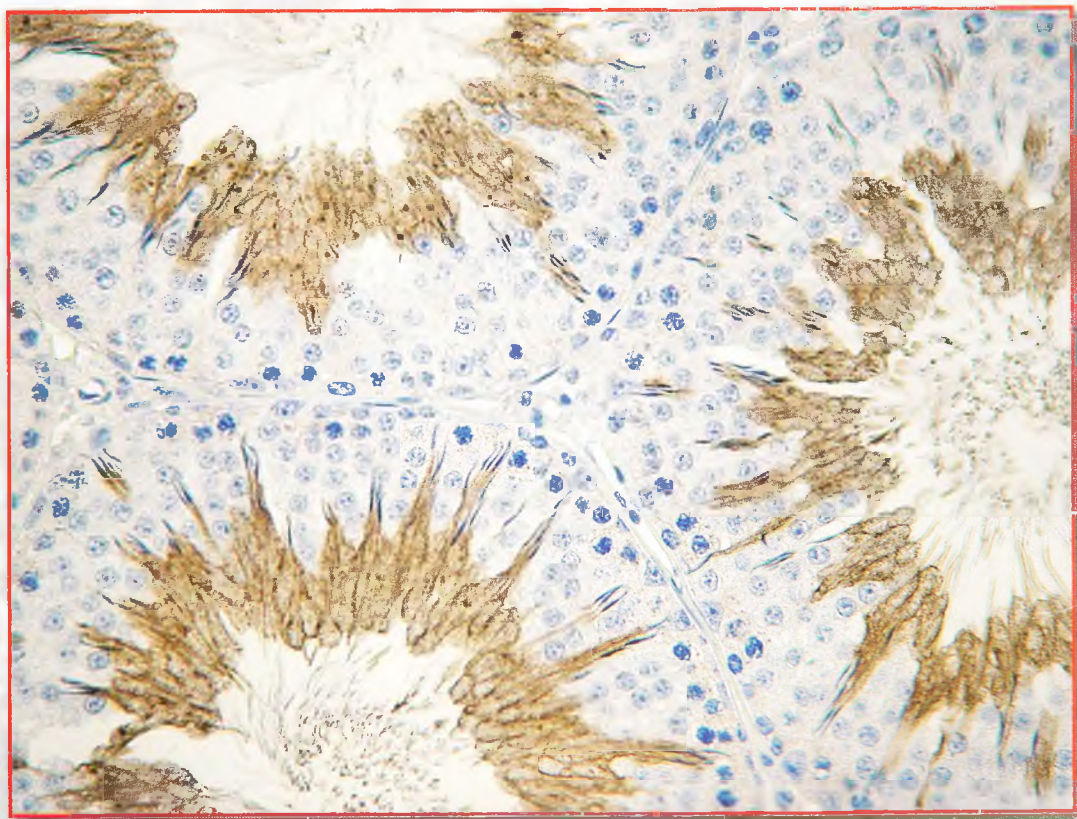


Acta morphologica et anthropologica (17)



Prof. Marin Drinov Academic Publishing House

Acta morphologica et anthropologica

is the continuation of
Acta cytobiologica et morphologica

Editorial Board

Y. Yordanov (Editor-in-Chief), N. Atanassova (Deputy Editor-in-Chief),
M. Gantcheva (Secretary)

Members: D. Angelov (Germany), M. Davidoff (Germany), D. Deleva,
M. Dimitrova, E. Godina (Russia), D. Kadiysky, D. Kordzaya (Geor-
gia), N. Lazarov, Ts. Marinova, A. Nacheva, E. Nikolova, W. Ovtscharoff,
S. Tornjova-Randelova, V. Vassilev, A. Vodenicharov

© БАН, Институт по експериментална морфология, патология и антропология с музей. 2011

Prof. Marin Drinov Academic Publishing House
Bulgaria, 1113 Sofia, Acad. G. Bonchev Str., Bl. 6

Коректор Б. Кременски
Графичен дизайнер Д. Василева
Формат 70×100/16 Печ. коли 13

Печатница на Академично издателство „Проф. Марин Дринов“
София 1113, ул. „Акад. Г. Бончев“, бл. 5

Acta morphologica et anthropologica (17)

17 • Sofia • 2011

Institute of Experimental Morphology, Pathology and Anthropology with Museum
Bulgarian Anatomical Society

Contents

Editorial

- Y. Yordanov – 4th Koprivshitsa Morphological Days, 8th National Conference of Anthropology,
4-6 of June, 2010 3

Morphology

- D. Kadiysky, M. Svetoslavova – Morphological Analysis of Brain Microanatomy via
Lycopersicon Esculentum Histochemistry 5
- N. Lazarov, K. Usunoff, D. Itzev, A. Rolfs, A. Wree, O. Schmitt – Orexinergic
Innervation of the Rat Extended Amygdala 10
- E. Petrova, A. Dishkelov, E. Vasileva – Effect of Hypoxia on Glycolipids in Rat Brain
Myelin 15
- E. Zaprianova, D. Deleva, V. Kolyovska, B. Sultanov – Clinical Significance of
serum anti-ganglioside Antibodies in Multiple Sclerosis 19
- L. Surchev, S. Surcheva – Quantitative Assessment of a Peripheral Nerve in Chronic
Constriction Injury Model of Neuropathic Pain 25
- L. Surchev, S. Surcheva, M. Vlaskovska, L. Kasakov – Effect of Gender and Sex
Hormones on Chronically Injured Nerve as a Model of Neuropathic Pain 31
- M. Gantcheva – Livedo Vasculitis 38
- I. Ilieva, S. Ivanova, P. Tzvetkova, B. Nikolov – Ultrastructure Studies of Abnormal
Sperm in the Pathology of the Male Reproductive System. Deviations in Sperm Head 44
- S. Ivanova, I. Ilieva, P. Tzvetkova – Azoospermia – Clinical and Cytological Manifestations
..... 48
- V. Ormandzhieva – Morphometric Parameters of the Rat Choroid Plexus Blood Vessels ... 56
- I. Stefanov, A. Vodenicharov, N. Tsandev – Blood Supply of Canine Paranasal Sinus
..... 62
- I. Vasilev, V. Vasilev, D. Andreev – Morphogenesis of the Hip Joint. Plastination-
Histological and Electron Microscopic Studies 68
- P. Zaharieva – Ultrastructural Characteristics of the Layer Stratum Compactum in Feline
Stomach Mucosa 75
- N. Atanasova, E. Lakova, S. Popovska, M. Donchev, G. Krasteva, V. Nikolov
– Expression of Testicular Angiotensin I – Converting Enzyme in Ageing Spontaneously
Hypertensive Rats 79

Y. Gluhcheva, M. Madzharova, V. Atanasov, R. Zhorova, J. Ivanova, M. Mitewa – Effects of Cobalt(II) Compounds on Some Hematological Parameters in Developing Mice	84
Y. Gluhcheva, M. Madzharova, V. Atanasov, R. Zhorova, M. Mitewa, E. Pavlova, J. Ivanova – The Affect of Cobalt Salts on Some Weight Indices in Developing Mice	89
M. Madzharova, Y. Gluhcheva, E. Pavlova, N. Atanassova – Impact of Cobalt Chloride on Testis and Male Fertility in Adulthood	95
R. Todorova, M. Dimitrova, I. Ivanov – Novel Fluorescent Histochemical Technique for γ -Glutamyl Transpeptidase Activity Determination	99
V. Pavlova, M. Dimitrova, E. Nikolova – TNF- α Augments Enzyme Expression in the Small Intestine of Developing Mice	104
M. Georgieva, M. Gabrovska – Double Staining Technique for Rat Foetus Skeleton in Teratological Studies	109
D. Arnaudova, A. Arnaudov, E. Sapundzhiev – Metabolic Glycogen Activity in Hepatocytes of Fish from a Water Source Containing Heavy Metals	114
E. Sapundzhiev – Comparative Analysis of Two Embryo Freezing Methods	119
D. Sivrev, Zl. Trifonov – Eyeball Plastination with Polyester Co-Polymers	125
D. Sivrev, Zl. Trifonov, A. Georgieva – Preparing Eye Slices with Biodur P40	129
N. Dimitrov, D. Sivrev, M. Andonova, I. Borisov – Dynamics of Changes in Central and Peripheral Lymphoid Organs in Rats Treated Intraperitoneally with Lipopolysaccharide of E. Coli	133
P. Kancheva – A Modern View of the Bulgarian Anatomical Terminology	138
D. Paskalev, D. Radoinova, B. Galunska – Dr. Zaharina Dimitrova (1873-1940): A Pioneer in Research of the Pineal Gland's (Corpus Pineale) Microstructure	143
D. Radoinova, Y. Kolev – Cases of Bodily Injuries During Arrest and in Custody	148
<i>Anthropology</i>	
E. Andreenko – Psychometric Characteristics of Adolescents from Plovdiv, Aged 19-20	151
M. Nikolova, D. Boyadjiev – Relation Between Body Composition and Some Social Factors and Habits in Children and Adolescents	156
Sl. Tineshev – Morpho-Functional Characteristics of Students from Plovdiv	163
I. Yankova, Y. Zhecheva – Dependence Between Maternal Weight Gain During Pregnancy and Some Newborns Anthropometrical Sizes	168
Y. Zhecheva, I. Yankova – Body Fat Distribution in Bulgarian Children and Adolescents Estimated by the Conicity Index	175
F. Ahmed-Popova, M. Mantarkov, S. Sivkov, V. Akabaliiev – Discrimination Effect of the Biomarkers Minor Physical Anomalies between Schizophrenic Patients and Mentally Healthy Subjects	182
N. Atanassova-Timeva, A. Katsarov – Anthropological Characterization and Correlations of Mandibular Branch	188
A. Baltadjiev, G. Baltadjiev – Bioelectrical Impedance Analysis (BIA) of Body Composition in Children with Diabetes Mellitus Type 1	193
A. Katsarov, N. Atanassova-Timeva, E. Ivanova – Epiphyseal Complex and Growth Arrest	197
S. Todorov – Cephaloscopic Characterization of Acromegalic Patients – Preliminary Announcement	204

Editorial

4th Koprivshitsa Morphological Days 8th National Conference of Anthropology 4-6 of June, 2010

Y. Yordanov

During 4-6 of June, 2010, the already traditional 4th Koprivshitsa Morphological Days and the 8th National Conference of Anthropology were carried out in the Municipality of the Koprivshitsa town. The organizers of this event were the Institute of Experimental Morphology and Anthropology with Museum at Bulgarian Academy of Sciences, the Bulgarian Anatomical Society, the Bulgarian Anthropological Society and the Municipality of the Koprivshitsa town.

108 scientists took part in this scientific forum – anatomists, cytologists, histologists, embryologists and anthropologists from different scientific groups from all over the country – IEMAM – BAS; Medical University – Sofia; Sofia University “St. Kliment Ohridski” – Faculty of Medicine, University of Forestry – Faculty of Veterinary Medicine; Medical University – Plovdiv; Plovdiv University “P. Hilendarski” – Faculty of Biology; Medical University – Varna; Trakia University – St. Zagora (Faculty of Medicine and Faculty of Veterinary Medicine); Pleven Medical University. Scientists from Germany (Stuttgart, Köln), Russia (Moscow), Serbia (Nis, Kragujevac) and Republic Kosovo (Pristina) reported the results of their investigations.

The Conference was inaugurated by the director of IEMAM – BAS Prof. Dr. Yordan Yordanov. After his salutatory to the participants, Dr. Yordanov bestow upon the Koprivshitsa town a sculpture portrait of Hadji Nencho Palaveev a made by him – well-known citizen and benefactor of Koprivshitsa town. The present was cordial welcomed by the mayor of the town Mr. Lubomir Tsekov.

The Mayor of the Koprivshitsa town Mr. Lubomir Tsekov, Prof. Vasil Vasilev – Chairman of honor of the Bulgarian Anatomical Society, Prof. Dr. K.-H. Korfsmeier and Prof. Dr. J. Koebke gave a warm welcome to the participants.

During the six sessions of the conference and three poster sessions, 31 reports and 56 posters were presented. The results of the investigations were animatedly discussed not only during the sessions but also during the informal talks. Members of different scientific groups discussed creation of new general projects.

The organization and the scientific level of the presented works got high assessment from Bulgarian and foreign scientists.

Morphology

Morphological Analysis of Brain Microanatomy via *Lycopersicon* *Esculentum* Histochemistry

D. Kadiysky, M. Svetoslavova

Department of Experimental Morphology, Institute of Experimental Morphology, Pathology and Anthropology with Museum, Bulgarian Academy of Sciences, Sofia

The description of the brain microanatomy always depends on the development of the histological and histochemical methods of coloration. The specificity of each histological or histochemical procedure limits the number of the visualized structures in the tissue. Thus, in the central nervous system (CNS) as results of the performing of *Lycopersicon esculentum* lectin histochemistry on cryostat and paraffin sections could be found marked two different types of object: lectin(+) cells and lectin(+) non-cellular bigger structures.

In the present study we describe local appearance, tissue distribution and visual topography and identity of the *Lycopersicon esculentum*(+) tissue structures in adult hamster brain. Briefly, this investigation is a test for the very contested between the neuromorphologists specificity of the staining histochemical procedure with *Lycopersicon esculentum* lectin.

Key words: TL (tomato lectin) histochemistry, brain microvasculature microglia.

Introduction

Now many assays are available to monitor the morphology of the CNS microanatomy. Some of them are very specific and more or less sensitive in the visualization of different brain structures. In the last two decades in brain marking *Lycopersicon esculentum* is used. In the scientific studies *Lycopersicon esculentum* positive (+) structures are known usually as TL(+) objects (by a terminological abbreviation of *tomato lectin*). Nevertheless, the application of a histochemical procedure with *Lycopersicon esculen-*

tum lectin in golden Syrian hamster's brain we found considerably detailed picture of the cellular and vascular structures. Previously, we have demonstrated that the generality of the positive to TL structures in the hamster brain really represents transversally cut small capillary vessels [6]. But in several CNS zones due to the *Lycopersicon esculentum* affinity for poly-N-acetyl lactosamine sugar residues [11] this lectin binds to microglial population in CNS. During the multidirectional searches for the microglia visualization and imaging in the last decade of the 20th century TL was assumed for long period as more or less specific marker for microglial cells in mammal brain as result of the abundance of the above cited residues [1]. Recently the interest to the microglia histochemical imaging rises because microglial population from the cells in mammal's brain is firmly established as a key cellular element in the CNS. They are recognized to serve as brain and spinal cord's innate immune system [9]. The known markers for microglia are cell-type specific and they do not label other glia or neurons [4]. Today, we have a number of well-established markers for microglial cells in mammal's brain. But from them only single specific molecular markers do not label peripheral macrophages or other micro anatomical components [8]. At the same time this controversy is not real reason for the abandonment of several markers for coloration in contemporary brain histochemistry. Some of them as above-mentioned *Lycopersicon esculentum* lectin continue to be used for microglial identification in CNS [10].

In our study by the use of the dual histochemical specificity of the *Lycopersicon esculentum* lectin we try to evaluate the hamster brain microanatomy.

Material and Methods

Animals: Adult five-week-old female outbred golden Syrian hamsters – *Mesocricetus auratus* (17 animals) were used as a source for obtaining of healthy brain tissue.

Histological procedure: The brains were fixed in Carnoy's solution at room temperature overnight. Serial transversal sections 5-7 μ thick were obtained from selected levels using Leica paraffin microtome after embedding in paraffin.

Lycopersicon esculentum lectin histochemistry: Commercially available biotinylated – *Lycopersicon esculentum* lectin (VECTOR Labs, Cat.No. B-1175) diluted in freshly prepared working solution of 10 μ g/ml PBS buffer (phosphate buffer saline), enriched with CaCl_2 (1mM), MgCl_2 (0.1 mM) and stabilized with Natrium azide (0,08%) was used for histochemical procedure. Recommended working dilution was applied on dewaxed and rehydrated paraffin sections from both healthy hamster brains and after blocking of the endogenous peroxydases on tissue sections with 2,5% H_2O_2 in methanol.

Incubation of the section with *Lycopersicon esculentum* lectin was performed at 20 °C for 2 h followed by application of ABC reagent kit and DAB substrate kit for peroxidase. The rinsing buffer (phosphate buffer saline) during the whole procedure was enriched with CaCl_2 (1mM) and MgCl_2 (0.1 mM).

Controls: Whole staining procedure without lectin.

Studied brain regions: Cortex, thalamus, cerebellum.

Microscopy: Light microscopy and interferential contrast microscopy (Nomarski optics).

Results

Previously in our investigations is demonstrated that in healthy hamster CNS *Lycopersicon esculentum* lectin histochemistry reveals different kinds of positive objects – ones with determined cellular shape bodies, and others – obviously non-cellular elements belonging to the brain microanatomy [1]. The first ones – TL(+) cells possess very irregular shapes with ramified and amoeboid morphologies. Elongated cells with several processes and less or more rounded cells are labelled generally. These cells are structurally absolutely identical to microglia and are seen abundantly in the hamster brains (Fig. 1).

Intriguingly, we observed great variations in the forms of the non-cellular TL(+) objects when samples of the brain tissue were taken from different zones. For example in the study of the hamster cortex microanatomy (using proposed histochemical pro-

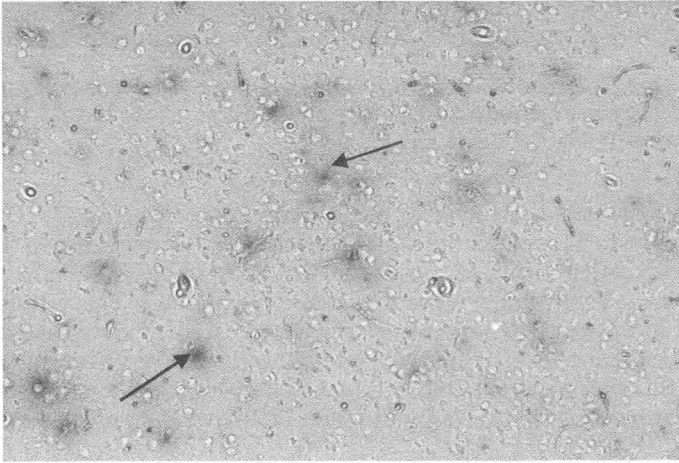


Fig. 1. TL(+) cellular objects with ramified and amoeboid morphologies (arrows) and smaller in size non-cellular objects between them representing a map of the brain microvasculature. Cortex, $\times 160$

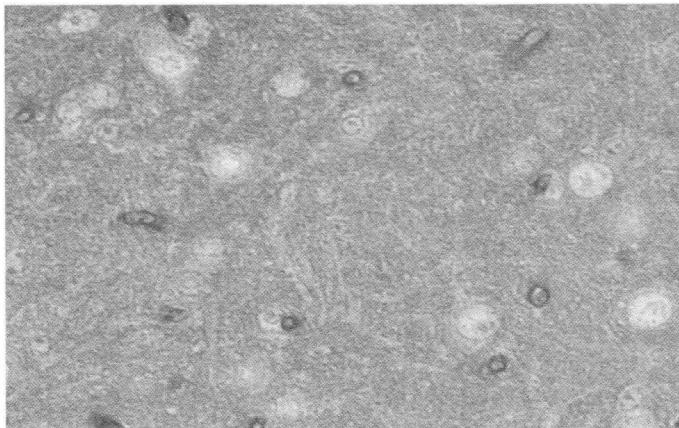


Fig. 2. Different forms of marked by TL histochemistry structures in Thalamus, $\times 400$

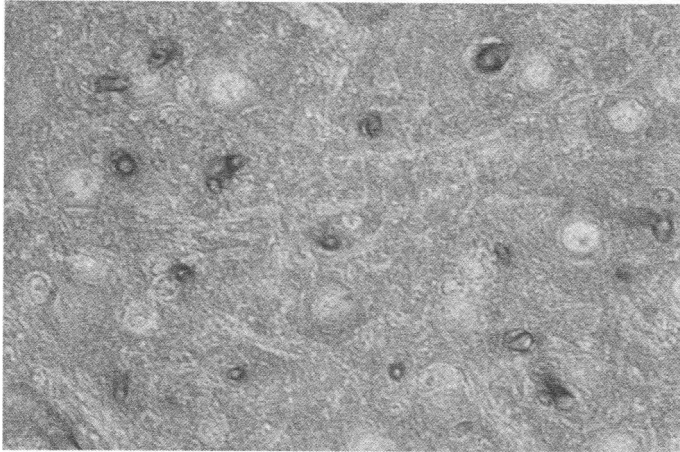


Fig. 3. TL histochemistry: tissue sections from the hamster cerebellum demonstrate convincingly that non-cellular TL(+) objects in CNS are microvessels, $\times 400$

cedure) shows very peculiar forms of the marked structures (Fig. 2). Big rounded or prolonged positive to TL objects are situated abundantly everywhere in the brain tissue and they are very often localized closely to groups of unlabelled cells. Assuming the abundance of these non-cellular structures, their morphologic characteristics and their distribution as loose-textured network everywhere in studied zones, we determine that these objects are components of the brain microvasculature – transversally or longitudinally cut. On the other hand, all obtained by us Nomarski optics images in the hamster cerebellum demonstrate convincingly that non-cellular TL(+) objects in CNS are microvessels (Fig. 3).

Discussion

The morphologic analysis of the brain microanatomy via *Lycopersicon esculentum* histochemistry made by us aims to help and perfect the brain mapping in vertebrate species. In this mapping the markers are crucial for the identification of cells and non-cellular components of the CNS structure. In this study we show various morphological signatures of the brain microanatomy using a simple histochemical method for visualization of these objects in CNS. The studies on vertebrate brain structure and especially the construction of the CNS map of this system are full for many years of historical controversies surrounding their achievement. A clear retardation in this field could be explained by the slower introduction of many new histochemical and immunohistochemical markers and procedures.

Our investigations of the brain microanatomy by *Lycopersicon esculentum* lectin in the healthy adult hamster contribute to this mapping. Brain TL labelling now reveals readily specific distribution, morphology and morphometry of the microglial population [5]. On the other hand, the use of this marker in neuromorphology represents a suitable methodology for generation of structural and even 3D maps of vascularized brain parenchyma [7]. As evidenced scientific publication from the last five years the dualism in the specificity of the TL histochemistry in CNS persists till now but many authors

continue to use *Lycopersicon esculentum* lectin histochemistry as specific microglial marker [2, 3].

The final result of our study is a new specific light microscopic image of the brain microanatomy suitable for early registration of the morphological signs in CNS during the development and in some pathology of the brain.

References

1. Acarin, L., J. Vela, B. Gonzales, B. Castellano. Demonstration of poly-N-acetyl lactosamin residues in amoeboid and ramified microglial cells in rat brain by tomato lectin binding. – *J. Histochem. Cytochem.*, **42**(8), 1994, 1033-1041.
2. Billards, S. S., R. L. Haynes, R. D. Folkerth, F. L. Trachtenberg, L. G. Liu, J. J. Volpe, H. C. Kinney. Development of microglia in the cerebral white matter of the human fetus and infant. – *J. Comp. Neurol.*, **497** (2), 2006, 199-208.
3. Caltana, L., A. Merelli, A. Lazarowski, A. Brusco. Neuronal and glial alteration due to focal cortical hypoxia induced by direct cobalt chloride (CoCl₂) injection. – *Neurotox Res.*, **15** (4), 2009, 348-358.
4. Graeber, M. B. W. J. Streit. Microglia: biology and pathology. – *Acta Neuropathol.*, **119**, 2010, 89-105.
5. Ignacio, A. R., M. Y. Muller, M. S. Carvalho, E. M. Nazari. Distribution of microglial cells in the cerebral hemispheres of embryonic and neonatal chicks. – *Braz. J. Med. Biol. Res.*, **38** (11), 2005, 1615-1621.
6. Kadiysky, D., M. Svetoslava. Distribution of the tomato lectin-reactive objects in healthy and degenerative hamster brain. – *Acta morphologica and anthropologica*, **15**, 2010, 31-35.
7. Manning, H. C., S. D. Shay, R. A. Mericle. Multispectral molecular imaging of capillary endothelium to facilitate preoperative endovascular brain mapping. – *J. Neurosurg.*, **110** (5), 2009, 975-980.
8. Schmid, C. D., B. Melchir, K. Masek, S. S. Puntambekar, P. E. Danielson, D. D. Lo, M. J. Carson. Differential gene expression in LPS/IFN gamma activated microglia and macrophages: in vitro versus in vivo. – *J. Neurochem.*, **109**(Suppl. 1), 2009, 117-125.
9. Streit, W. J., C. A. Kincaid-Colton. The brain's immune system. – *Sci. Am.* **273**(5), 2006, 58-61.
10. Totosa, R., E. Vidal, C. Costa, E. Alamillo, J. M. Torres, I. Ferrer, M. Pumarolla. Stress response in the central nervous system of a transgenic mouse model of BSE. – *The Vet. J.*, **178**, 2008, 126-129.
11. Zhu, BC-R., R. Laine. Purification of acetyllactosamine specific tomato lectin by erythroglucan-sepharose affinity chromatography. – *Prep. Biochem.*, **19**(4), 1989, 341-350

Orexinergic Innervation of the Rat Extended Amygdala

N. Lazarov^{1,2}, K. Usunoff^{1,2,3}, D. Itzev², A. Rolfs⁴, A. Wree³, O. Schmitt³

¹*Department of Anatomy and Histology, Medical University – Sofia, Sofia, Bulgaria*

²*Institute of Neurobiology, Bulgarian Academy of Sciences, Sofia, Bulgaria*

³*Institute of Anatomy, University of Rostock, Rostock, Germany*

⁴*Albrecht Kossel Institute for Neuroregeneration, University of Rostock, Rostock, Germany*

The orexinergic system participates in the regulation of emotions, stress, hunger, wakefulness and behavioral arousal. Despite their limited number and restricted origin from the lateral hypothalamus, orexin-containing neurons give out vast projections that innervate the entire neuraxis. To identify the orexinergic innervation of the amygdala, which is substantially involved in the hypothalamic output, the distribution of orexin A- and orexin B-containing fibers and terminals was mapped in the rat amygdaloid nuclear complex by using immunohistochemistry. We observed the most prominent axonal immunolabelling in the nuclei of the corticomедial group. The orexin-immunoreactive axons were dense in the basolateral amygdaloid nucleus while the basomedial nucleus contained moderately labelled axons in its all subdivisions. Besides, our results showed that subdivisions and subnuclei of the extended amygdala were specific targets of the orexinergic system as well. The present data suggest that the orexinergic amygdala projections may exert excitatory modulatory effects on the expression of emotional behavior.

Key words: amygdaloid nuclear complex, hypothalamus, immunohistochemistry, orexin, rat.

Introduction

Orexin A and B, also named hypocretin 1 and 2, are two recently described excitatory hypothalamic neuropeptides shown to influence a wide range of physiological and behavioral processes. Orexins are solely synthesized in a restricted population of neurons located in the caudal aspects of the lateral hypothalamus (LH) and the adjacent areas. These neurons project extensively to multiple cerebral regions throughout the entire neuraxis by four major pathways [13]. It has been proposed that orexin (OX) serves as a master switch within multiple efferent pathways that mediate the defense response [15]. Thus, we focused on the amygdala (Am) orexinergic target that is substantially involved in the LH output and contributes most to the functional outcome of the defense responses closely related to emotional behavior.

The amygdaloid nuclear complex in rats consists of several structurally and functionally distinct nuclear groups located deeply in the temporal lobe [6]. It is traditionally divided, on the basis of cytoarchitectonic, hodological, histochemical, and immunohistochemical studies, into a corticomедial division and a basolateral division. The former is evolutionarily newer and encompasses the centromedial and cortical nuclei, while the latter is phylogenetically older and comprises the lateral, basolateral and basomedial amygdaloid nuclei [reviewed in 3]. The rat Am has a wide variety of afferent and efferent connections throughout the central nervous system (CNS) and is involved in a vast range of normal behavioral functions (for a recent comprehensive review see [14]. Furthermore, the extended Am, which includes the bed nucleus of the stria terminalis (BST) and its sublenticular extension into the centromedial Am, is implicated in complex motivational responses [1].

Not long ago, it has been shown that OX neurons in the LH mediate cardiorespiratory responses induced by disinhibition of the Am and BST [15]. More recently, it has been suggested that the OX system is one of the essential modulators required for orchestrating the neural circuits controlling autonomic functions and emotional behaviors [8].

From these backgrounds, we have paid in this study special attention to the orexinergic innervation of the rat extended Am, with a particular focus on the excitatory modulatory role of orexins in autonomic and emotional functions.

Materials and Methods

The experiments were carried out on adult male rats of both sexes, weighing 250-300 g. All housing facilities were supervised and approved by the Ethic Commissions at the Medical University-Sofia, Bulgaria, and the University of Rostock, Germany. The animals were transcardially perfused with 4% paraformaldehyde in 0.1 M phosphate buffer (PB), pH 7.4, the brains were removed, cut on a Reichert Jung freezing microtome at 30 μ m thick sections and they were subsequently processed for ABC (avidin-biotin-horseradish peroxidase complex) immunohistochemistry. Briefly, the tissue sections were treated with hydrogen peroxide (1.2% in absolute methanol; 30 min) to inactivate endogenous peroxidase, and the background staining was blocked with 2% normal goat serum (NGS) in PBS for 30 min. Thereafter, the sections were incubated for 24 h at room temperature with the respective primary antibodies, rabbit anti-OX-A (diluted 1:2000) and rabbit anti-OX-B (1:500; both from Oncogene, Cambridge, MA, USA). After rinsing in 0.1 M PBS, the sections were incubated with the secondary antibody, biotinylated goat anti-rabbit IgG (Dianova, Hamburg, Germany) at a dilution of 1:500 for 2 h at room temperature and finally the ABC complex (Vector Laboratories, Burlingame, CA, USA) was applied for 2 h at room temperature. The peroxidase activity was visualized using 2.4% SG substrate kit (Vector) for 5 min. The sections were then mounted on chrome-gelatin slides, air dried, dehydrated in a graded series of ethanols, cleared in xylene, and coverslipped with Entellan (Merck, Darmstadt, Germany). Each third from the immunostained sections was counterstained with 1% Neutral Red (Sigma, St. Louis, MO, USA) to reveal the precise cytoarchitectonic orientation of the stained neuronal population. The delineation of the investigated structures was made according to the stereotaxic atlas of the rat brain [Paxinos and Watson, 2007]. The specimens were examined and photographed with a Zeiss Axioplan 2 research microscope, and the digital images were saved in a TIF format. Negative controls included an omission of the primary antibody and/or its replacement with a non-immune normal serum as well as antigen-antibody preabsorption experiments with the respective native antigens.

Results

In general, the distribution of OX-A and OX-B immunoreactive cell bodies and fibers was almost identical. The OX-containing perikarya were distributed exclusively in the tuberal part of the hypothalamus. A prominent group of orexinergic neurons was symmetrically located on both sides in the central portion of the LH (Fig. 1A). Most of the immunostained cells were medium in size ($25.4 \pm 2.3 \mu\text{m}$ maximal diameter and $16.2 \pm 1.6 \mu\text{m}$ minimal diameter, mean \pm S.E.M., $n=120$) and fusiform or multipolar in shape. A considerably lower number of OX-immunopositive neurons were located immediately ventral to the fornix. In rostral and caudal directions the number of OX neurons gradually diminished.

The rat Am was richly supplied with intensely stained OX fibers. Numerous labelled axons entered the Am through the central amygdaloid nucleus. All its three subdivisions, central medial, central lateral and central capsular, contained a substantial to moderate number of thin varicose OX-immunostained axons (Fig. 1B). Prominent labelling was also observed in the medial amygdaloid nucleus, with a decreasing density from its posterodorsal to posteroventral parts. In the cortical amygdaloid nuclei, anterior, posteromedial and posterolateral, the density of OX axons was moderate (Fig. 1C). In the basolateral group the number of OX-positive axons was lower than in the corticomедial group. Somewhat larger was the number of OX axons in the basolateral nucleus while the lateral

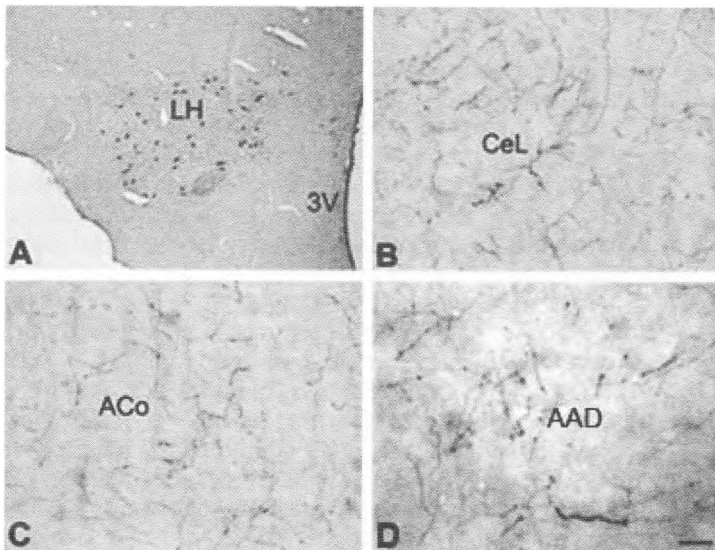


Fig. 1. (A) Distribution of orexin-containing cells bodies in the tuberal part of the rat lateral hypothalamus (LH). Note that the immunoreactive perikarya are mostly medium in size with multipolar or fusiform morphology. 3V, 3rd ventricle. (B) Dense orexinergic innervation of the central amygdaloid nucleus, lateral division (CeL). Thin varicose axons are also seen in the other subdivisions of this nucleus. (C) OX immunoreactive fibers in the anterior cortical amygdaloid nucleus (ACo). Note that their density is comparable to those of the central amygdaloid nucleus. (D) Distribution of OX-immunoreactive fibers in the extended amygdala. Numerous densely arranged axonal varicosities and their terminals are observed in the anterior amygdaloid area, dorsal part (AAD). Scale bars = $100 \mu\text{m}$ (A); $50 \mu\text{m}$ (B-D)

nucleus contained the smallest number of OX axons in the amygdaloid nuclear complex. Conversely, the anterior amygdaloid area was the most heavily innervated by OX axons component of the Am (Fig. 1D).

In the extended Am many new orexinergic targets were found in the anterior cortical nucleus (moderate), amygdalostriatal transition region (moderate) and BST (significant).

Discussion

Despite the low number of OX-containing neurons in the hypothalamus, orexinergic fibers project widely in the CNS. Our previous research has shown that the whole sub-cortical motor network from motor regions over the basal ganglia and back over the thalamus to the motor cortex receives orexinergic afferents (unpublished data). In this study we confirm and further extend the data of Nambu et al. [11] on the distribution of OX neurons in the adult rat brain. More specifically, the present results provide evidence that the rat amygdaloid nuclear complex is a specific target of orexinergic projections.

The orexinergic input appears to be involved in the modulation of different functional responses that have been attributed to Am, including behavioral and autonomic responses to stressors such as fear and anxiety, assigned to the extended Am. It has recently been reported by Bisetti et al. [2] that the OX system exerts a direct action on neurons in the central medial nucleus, the major output structure of the Am. The authors also demonstrated that Am neurons are depolarized by OX through the activation of postsynaptic OX-2 receptors, which are also excited by vasopressin. Thus, it seems likely that the orexinergic innervation may modulate emotionality and memory consolidation through the excitatory action it exerts on several neurotransmitter and neuromodulatory systems affecting the Am neurons. Besides, we found OX-fibers in the amygdalostriatal transition area that may act as a relay with functions of positive enhancement or negative filtering for the inhibition of specific signal patterns.

On the other hand, it is proposed that the Am is implicated in various aspects of emotional behavior through an extensive network of projections to other brain regions [reviewed in 9]. Specifically, the direct projections from the central nucleus of the Am to the LH [7] appear to be involved in the activation of the autonomic concomitants of conditioned fear and anxiety [cf. 10]. Moreover, there are dense connections from the amygdala to the BST [5] and vice versa [4]. Therefore, input from the Am and BST might be important in modulating the activity of orexin neurons upon emotional stimuli and thus could participate in evoking emotional arousal or fear-related responses [15].

In conclusion, combined with our previous data, it can be inferred that the hypothalamic orexinergic projections may act as an excitatory modulator of motor signals in the Am. In turn, the Am contributes most to the functional outcome of the OX system.

Acknowledgements. This work was supported by National Science Fund of the Bulgarian Ministry of Education, Youth and Science (grant VU-L-306/2007). Dr. Kamen Usunoff passed away unexpectedly on February 28, 2009 while working on this study.

References

1. Alheid, G., J. S. De Olmos, C. A. Beltramino. Amygdala and extended amygdala. – In: The rat nervous system (Ed. G. Paxinos). New York, Academic Press, 1995, 495-578.
2. Bisetti, A., V. Cvetkovic, M. Serafin, L. Bayer, D. Machard, B. E. Jones, M. Mühlethaler. Excitatory action of hypocretin/orexin on neurons of the central medial amygdala. – *Neuroscience*, **142**, 2006, 999-1004.

3. De Olmos, J. S., C. A. Beltramo, G. Alheid. Amygdala and extended amygdala of the rat: a cytoarchitectonical, fibroarchitectonical, and chemoarchitectonical survey. – In: *The rat nervous system* (Ed. G. Paxinos). 3rd edition, San Diego, Elsevier, 2004, 509-603.
4. Dong, H.-W., L.W. Swanson. Projections from bed nuclei of the stria terminalis, anteromedial area: cerebral hemisphere integration of neuroendocrine, autonomic, and behavioral aspects of energy balance. – *J. Comp. Neurol.*, **494**, 2006, 142-178.
5. Dong, H.-W., G. D. Petrovich, L.W. Swanson. Topography of projections from amygdala to bed nuclei of the stria terminalis. – *Brain Res. Rev.*, **38**, 2001, 192-246.
6. Johnston, J. B. Further contributions to the study of the evolution of the forebrain. – *J. Comp. Neurol.*, **35**, 1923, 337-481.
7. Krettek, J. E., J. L. Price. Amygdaloid projections to subcortical structures within the basal forebrain and brainstem in the rat and cat. – *J. Comp. Neurol.*, **178**, 1978, 225-254.
8. Kuwaki, T. Orexin links emotional stress to autonomic functions. – *Auton. Neurosci.*, 2010, doi:10.1016/j.autneu.2010.08.004.
9. LeDoux, J. The amygdala. – *Curr. Biol.*, **17**, 2007, R868-R874.
10. LeDoux, J. E., J. Iwata, P. Cicchetti, D. J. Reis. Different projections of the central amygdaloid nucleus mediate autonomic and behavioral correlates of conditioned fear. – *J. Neurosci.*, **8**, 1988, 2517-2529.
11. Nambu, T., T. Sakurai, K. Mizukami, Y. Hosoya, M. Yanagisawa, K. Goto. Distribution of orexin neurons in the adult rat brain. – *Brain Res.*, **827**, 1999, 243-260.
12. Paxinos, G., C. Watson. *The rat brain in stereotaxic coordinates*. 6th edition. Amsterdam, Elsevier, 2007.
13. Peyron, C., D. K. Tighe, A. N. van den Pol, L. de Lecea, H.C. Heller, J. G. Sutcliffe, T. S. Kilduff. Neurons containing hypocretin (orexin) project to multiple neuronal systems. – *J. Neurosci.*, **18**, 1998, 9996-10015.
14. Pitkänen, A. Connectivity of the rat amygdaloid complex. – In: *The amygdala: a functional analysis* (Ed. J.P. Aggleton). Oxford, Oxford University Press, 2000, 31-115.
15. Zhang, W., N. Zhang, T. Sakurai, T. Kuwaki. Orexin neurons in the hypothalamus mediate cardiorespiratory responses induced by disinhibition of the amygdala and bed nucleus of the stria terminalis. – *Brain Res.*, **1262**, 2009, 25-37.

Effect of Hypoxia on Glycolipids in Rat Brain Myelin

E. Petrova, A. Dishkelov, E. Vasileva

*Bulgarian Academy of Sciences, Institute of Experimental Morphology,
Pathology and Anthropology with Museum, Department of Experimental Morphology
Sofia 1113*

In this study we present data from our examinations of the changes in myelin glycolipid content in a rat model of sodium nitrite-induced hypoxia. Twenty male Wistar rats at the age of three months were used in the experiment. The myelin fraction was isolated and lipids were extracted. The glycolipid content was measured by spectrophotometry and thin-layer chromatography.

In the myelin of hypoxic brains, we found increased levels of total glycolipids (2.4-fold), gangliosides (2.1-fold), and cerebroside (2.7-fold). These changes indicate a disturbance of lipid metabolism. The accumulation of glycolipids may be interpreted as a physiological adaptive response to hypoxia.

Key words: gangliosides, cerebroside, sodium nitrite, hypoxia, myelin, rat brain.

Introduction

Brain is of special interest for hypoxia studies as it is critically dependent on its oxygen supply. Hypoxia, as well as ischemia, provokes alterations in the lipid metabolism. Although considerable efforts have been directed at evaluating alterations in hypoxia, lipid metabolism at brain subcellular level has not been fully evaluated.

It is well recognized that the myelin sheath of the brain is a structure which is highly sensitive to hypoxic injury. Glycolipids are a dominant class of lipids in the myelin bilayer. Therefore, the present investigation was undertaken to evaluate the level of glycolipids in rat brain myelin in a model of sodium nitrite-induced hypoxia.

Materials and Methods

Twenty male Wistar rats at the age of three months, each weighing 190-220 g, were subjected to sodium nitrite-induced hypoxia. Sodium nitrite was administered intravenously at 20 mg/kg body weight (2 ml/kg dosing volume). Hypoxic rats were killed by decapitation.

Myelin was isolated according to the method described by Venkov [12] using two-step sucrose gradient. Lipids were extracted according to the method of Kates [13] using the following eluates: chloroform:methanol 1:2 (v/v) and chloroform:methanol:water 1:2:0.8 (v/v/v). The content of total glycolipids was determined according to Hamilton et al. [5]. Glycolipid classes were separated by thin-layer chromatography.

The data were analyzed with Student's t-test.

The animal experiments were performed in accordance with animal protection guidelines approved by the Ethics Committee for experimental animal use at IEMPAM – BAS.

Results and Discussion

In the present study, we examined the changes in myelin glycolipids in a rat model of sodium nitrite-induced hypoxia.

It is well known that the lipid bilayer of myelin membranes has highly specialized properties as a result of its unique lipid composition [10]. A dominant class of lipids in the myelin bilayer are the glycolipids, which include cerebrosides, sulfatides and gangliosides. Cerebrosides are the predominant component and they together with the polar head groups of phosphatidylserine and phosphatidylinositol provide a polyanionic surface array. Strong interactions with both the positively charged myelin basic protein at the cytosolic and hydrophobic domains of proteolipid protein at the extracytoplasmic surface might contribute to the tight compaction of the multilayer membrane system [2]. Our observations in control rats are in good agreement with the literature data. We found gangliosides and cerebrosides and they accounted for 47.5% (0.107 ± 0.03 mg/g dry lipid residue/ml; mg/g/ml) and for 52.5% (0.118 ± 0.03 mg/g/ml) of total glycolipids, respectively.

Hypoxia is one of the major pathological conditions causing neuronal cell injury. The brain is the most hypoxic vulnerable of all vertebrate tissues because of its high rate of aerobic metabolism. In our experiments we applied a model of sodium nitrite-induced chemical hypoxia. This model is convenient because no restraint of the animal or special enclosure is required [3]. It refers to anemic hypoxia – a condition in which there is a reduction in hemoglobin's ability to transport oxygen. Sodium nitrite converts hemoglobin to methemoglobin and unlike ferrous form of hemoglobin, methemoglobin does not bind oxygen strongly. Thus the oxygen-carrying capacity of the blood is reduced. It is reported that the oxidation of oxyhemoglobin by nitrite to produce methemoglobin is a complex process that has been characterized by a lag phase followed by an autocatalytic phase [7].

In hypoxic brains we found increased levels of total glycolipids (2.4-fold), gangliosides (2.1-fold), and cerebrosides (2.7-fold) (Fig. 1). Gangliosides and cerebrosides accounted for 41% (0.224 ± 0.01 mg/g/ml) and for 59% (0.317 ± 0.03 mg/g/ml) of the total glycolipids, respectively. The high concentration of glycolipids and especially gangliosides can apparently be explained by their neuroprotective effect. It is supposed that gangliosides can acutely reduce the extent of central nervous system injury by protection of membrane structure and function [8]. Another hypothesis supports the view that gangliosides may promote neuronal regeneration through modulation of trophic factors.

Probably the high content of cerebrosides makes the membrane steadier because cerebrosides contribute to a dense network of H-bonding between three hydroxy groups of cholesterol, the hydroxy group of the sphingosine, the hydroxy groups of the acyl chains and the amide bond of the sphingolipids [2]. Considering gangliosides as neu-

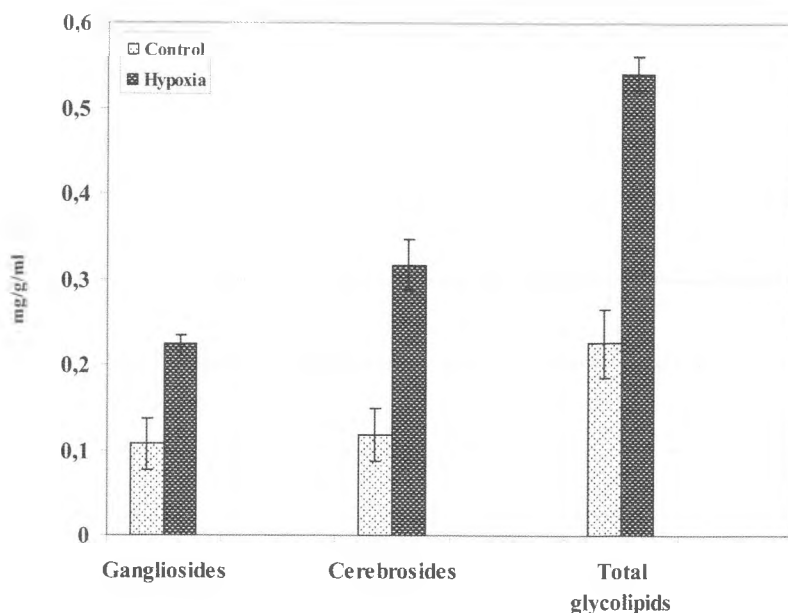


Fig. 1. Changes of the gangliosides, cerebrosides and total glycolipids in hypoxic rat brain myelin. Values are expressed in mg/g dry lipid residue/ml, $p < 0.001$

roprotectors [8], these changes may be interpreted as a defensive and compensatory mechanism against hypoxic damage.

There are few reports in the literature on glycolipid changes in hypoxic rat brain. To our knowledge, only the study of Baev et al. [1] refers to sodium nitrite-induced hypoxia although performed on total brain homogenate. Our data are in good agreement with the latter as it demonstrates elevated content of rat brain gangliosides. In contrast, earlier studies of Domanska-Janik et al. [4] show moderate decreases in cerebrosides and gangliosides of brain homogenate in three different experimental models of oxygen deficiency. A decrease in the myelin cerebrosides in moderate hypoxia is documented by Kapelusiak-Pielok et al. [6], too. Similar results are demonstrated by Ramirez et al. [9] in neonatal hypoxia-ischemia in the rat hippocampus. Their findings indicate reduced ganglioside content. Besides, no effect of hypoxia on the content of myelin cerebrosides is observed by Wender et al. [11]. As we demonstrate the opposite pattern of changes in the glycolipid content, our results differ from the above literature data. Most probably it is due to the different types of hypoxia, degree and duration of hypoxia, the time interval after which the studies are performed, the regional and subcellular fractions studied, etc.

Conclusion

Our data provide evidence that sodium nitrite-induced hypoxia influences glycolipid metabolism in rat brain myelin. They also show that myelin responds to hypoxia by synthesizing a high amount of cerebrosides and gangliosides and this is probably involved in the cell survival pathways.

References

1. Baev, V. I., I. V. Vasil'eva, N. N. Nalivaeva. Rat brain gangliosides during hypoxia. – Bull. Exp. Biol. Med., **118**, 1994, No 1, 698-700.
2. Bosio, A., E. Binczek, W. Stoffel. Functional breakdown of the lipid bilayers of the myelin membrane in central and peripheral nervous system by disrupted galactocerebroside synthesis. – Proc. Natl. Acad. Sci. U. S. A., **93**, 1996, 13280-13285.
3. Boulton, A., G. Baker, R. Butterworth. Animal models of neurological disease, II: Metabolic encephalopathies and the epilepsies. Totowa, New Jersey, Humana Press, 1992, 1- 373.
4. Domańska-Janik, K., J. Strosznajder, T. Zalewska. Effect of ischemia and hypoxia on rat brain glycolipids. – J. Neurosci. Res., **7**, 1982, No 4, 363-370.
5. Hamilton, P. B. A spectrometric determination of glycolipids. – Anal. Chem., **28**, 1956, 557-565.
6. Kapelusiak-Pielok, M., Z. Adamczewska-Goncerzewicz, J. Dorszewska, A. Grochowalska. The protective role of alpha-tocopherol on the white matter lipids during moderate hypoxia in rats. – Folia Neuropathol., **43**, 2005, No 2, 103-108.
7. Kosaka, H., I. Tyuma. Mechanism of autocatalytic oxidation of oxyhemoglobin by nitrite. – Environ. Health Perspect., **73**, 1987, 147-151.
8. Mahadik, S. P., S. K. Karpik. Gangliosides in treatment of neural injury and disease. – Curr. Trends Rev., **15**, 2004, No 4, 337-360.
9. Ramirez, R. M., F. Muraro, D. S. Zylbersztein, C. R. Abel, N. S. Arteni, D. Lavinsky, C. A. Netto, V. M. T. Trindade. Neonatal hypoxia-ischemia reduces ganglioside, phospholipid and cholesterol contents in the rat hippocampus. – Neurosci. Res., **46**, 2003, 339-347.
10. Stoffel, W., A. Bosio. Myelin glycolipids and their functions. – Curr. Opin. Neurobiol., **7**, 1997, 654-661.
11. Wender, M., Z. Adamczewska-Goncerzewicz, J. Stanisławska, J. Pankrac, D. Talkowska, A. Grochowalska. Myelin lipids of the rat brain in experimental hypoxia. – Exp. Pathol., **33**, 1988, 59-63.
12. Венков, Л. Получаване на обогатени фракции на елементи, изграждащи нервната тъкан. – Сърв. пробл. невроморфол., **11**, 1983, 1-60.
13. Кейтс, М. Техника липидологии. Москва, Мир, 1975, с. 322.

Clinical Significance of Serum Anti-Ganglioside Antibodies in Multiple Sclerosis

E. Zaprianova, D. Deleva, V. Kolyovska, B. Sultanov

*Institute of Experimental Morphology, Pathology and Anthropology with Museum,
Bulgarian Academy of Sciences, Sofia*

Recently it has become clear that multiple sclerosis (MS) is an immune-mediated neurodegenerative disease. The neuronal damage begins at the earliest stages of the disease. Therapeutic interventions directed toward this neuronal injury need the discovery of serum markers for its early detection. In this investigation the diagnostic value of IgG and IgM anti- GM1 and anti- GD1a antibodies was determined by a standardized ELISA method in the serum of patients with relapsing-remitting MS (RRMS). Significantly elevated serum IgM and IgG titers were detected in patients with their first attacks of RRMS. Patients with more advanced RRMS had higher titers of IgG antibodies than IgM antibodies to GM1. The elevated serum IgM titers to GD1a antibodies suggest the immune-mediated neurodegeneration. Therefore, IgM anti-GD1a antibodies can serve as a marker of neuronal damage in MS.

Key words: multiple sclerosis, serum, ganglioside GM1 antibodies, ganglioside GD1a antibodies.

Introduction

For many years multiple sclerosis (MS) was considered to be primary demyelinating central nervous system (CNS) disease with preserved neuronal and axonal integrity at the onset of the disease. In recent years, several lines of evidence from imaging and morphological studies demonstrate that neuronal degeneration and axonal injury occur early in MS pathogenesis [2, 5, 7]. At present, multiple sclerosis is characterized as an immune-mediated progressive neurodegenerative disease of the CNS [1]. The neuronal damage begins at the earliest stages of the disease and underlies the accumulation of clinical disability. Therefore, it is of great importance to detect in the serum the early injury of brain neurons.

Considerable changes of GM1 and GD1a gangliosides were detected in the central nervous system of Lewis rats with chronic relapsing experimental allergic encephalomyelitis (CREAE), an animal model of relapsing-remitting MS, just before the onset of the first clinical signs of the disease [10]. Gangliosides are a family of acidic glycosphingolipids highly concentrated in the nervous system, where they represent about

10% of the total lipid content [9]. GM1 is one of the main ganglioside in human CNS myelin, while GD1a is one of the major ganglioside in human brain neurons.

Our finding of an increase of serum GM1 and GD1a gangliosides during the first MS attack confirms previous evidence for the involvement of gangliosides in the early pathogenesis of MS [12].

The objective of this study was to estimate the clinical significance of IgG and IgM antibodies to GM1 and GD1a gangliosides in the serum of patients with relapsing-remitting MS (RRMS) during the different phases of the disease.

Materials and Methods

Serum samples were obtained from 20 healthy subjects, from 42 patients with longer duration of relapsing-remitting multiple sclerosis (RRMS), more attacks and higher invalidization, and from 7 patients during their first attack of the disease of what later was definitely diagnosed as RRMS (FARRMS).

Sera were also obtained from one and the same RRMS patient before, during and after her pregnancy, during a treated relapse and in remission after the treatment with Copaxon (neuron-protective therapy).

ELISA protocol

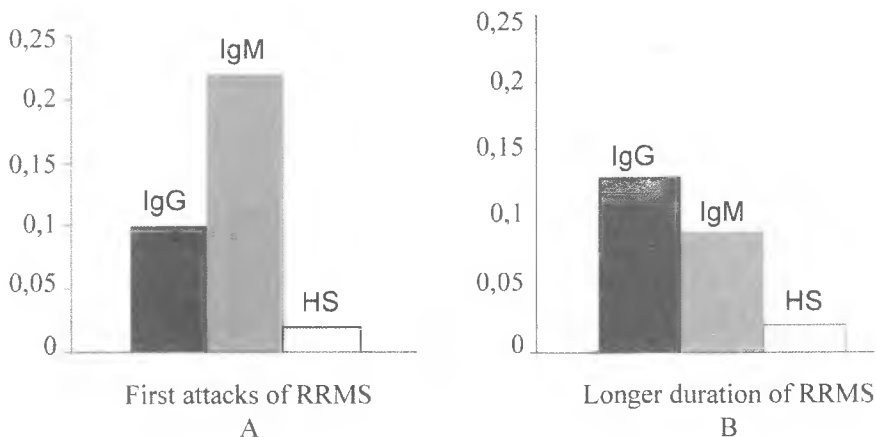
The presence of anti-GM1 and anti-GD1a antibodies in the serum was measured by the enzyme-linked immunosorbent assay (ELISA). The ELISA protocol was selected according to the recommendations of the workshop "Measurement and significance of antibodies against GM1 ganglioside". Finally we made slight modifications of the method of Mitzutamari et al. [4]. We determined antiganglioside antibodies (AGA) of the IgM and IgG class against GM1 ganglioside and IgM class against GD1a ganglioside [11]. As AGA were found in low titers in some healthy subjects we estimated a reference range for the healthy controls. MS patients were considered strongly positive only if the optical density of their sera exceeded $\bar{x} \pm 2$ SD of the healthy controls. The optical density was measured and read spectrometrically at 490 nm in a ELISA reader (TECAN, Sunrise TM, Austria). The Student test was used to determine statistical differences between the groups using $p < 0.05$ as the level of confidence.

Results

Significantly elevated serum IgM antibodies titers to GM1 were found in comparison with healthy subjects in patients with their first attacks of RRMS (Fig. 1A).

Patients with longer duration of the disease (LDRRMS), more attacks and higher invalidization had higher serum IgG antibodies titers than serum IgM antibodies titers to GM1 (Fig.1B).

The difference of optical density of serum IgG and IgM anti-GM1 antibodies between healthy subjects, RRMS patients and FARRMS patients was statistically significant (Table 1).



OD – optical density
 RRMS – patients with relapsing – remitting form of multiple sclerosis
 FARRMS – first attacks of RRMS patients
 HS – healthy subjects

Fig. 1. Serum IgG and IgM antibodies to GM1 in patients with RRMS

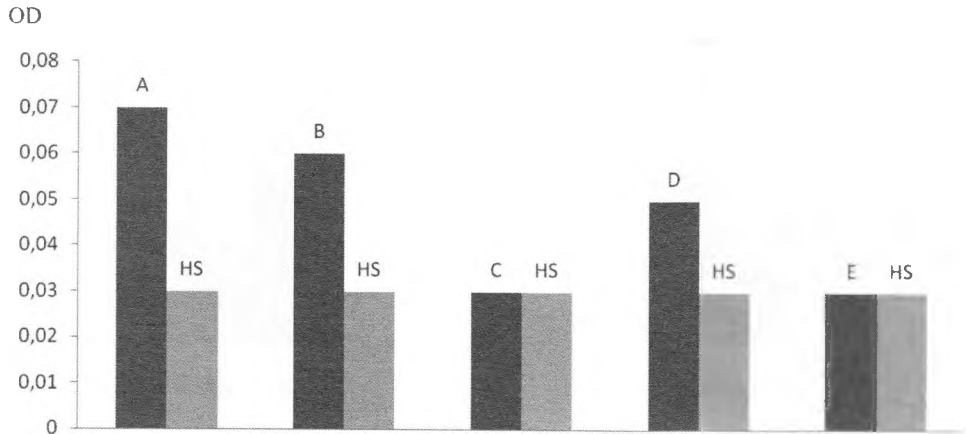
Table 1. Optical density of serum IgG and IgM anti-GM1 antibodies of RRMS patients and of healthy subjects

Group	n	IgG anti-GM1 antibodies mean ± SEM	IgM anti-GM1 antibodies mean ± SEM
HS	20	0,03 ± 0,01	0,02 ± 0,01
LDRRMS	42	0,13 ± 0,04	0,09 ± 0,02
FARRMS	7	0,10 ± 0,06	0,22 ± 0,07

HS – healthy subjects
 LDRRMS – longer duration of RRMS
 FARRMS – first attacks of RRMS patients
 n – number of patients
 SEM – standard error of mean

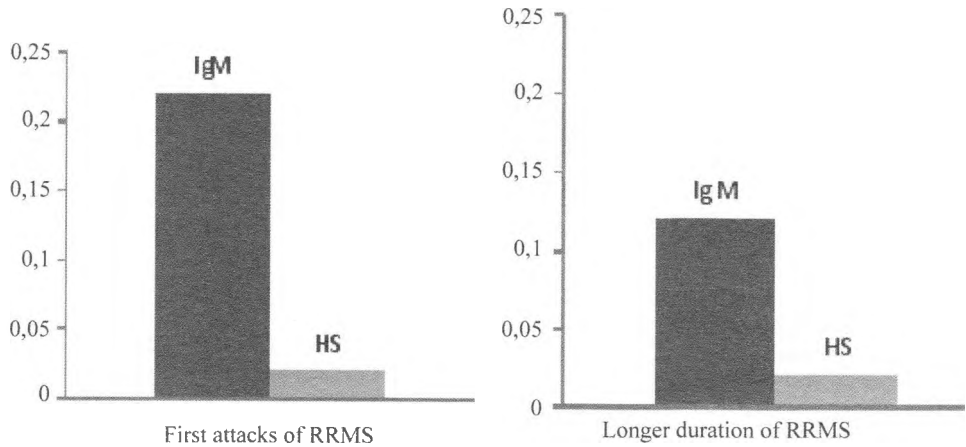
Results of estimation of IgM antibodies to GM1 in the serum of one and the same RRMS patient before, during and after her pregnancy, during a treated relapse and after the treatment with Copaxon are presented in Fig. 2.

Statistically significant higher IgM titers of serum anti-GD1a antibodies were detected in patients with their first attacks of RRMS in comparison of healthy subjects and RRMS patients with longer duration of the disease (Fig.3).



OD – optical density
 A – before the pregnancy
 B – 8 month of pregnancy
 C – 7 months after the delivery
 D – during a treated relapse
 E – in remission after treatment
 HS – healthy subjects

Fig. 2. Estimation of IgM antibodies to GM1 in the serum of one and the same RRMS patient



OD – optical density
 RRMS – patients with relapsing-remitting form of multiple sclerosis
 FARRMS – first attacks of RRMS patients
 HS – healthy subjects

Fig. 3. Serum IgM antibodies to GD1a in RRMS patients

Discussion

The main result of this investigation is the detection of elevated IgM titers of serum anti-GD1a antibodies in patients with their first attacks of relapsing-remitting MS in comparison with patients with more attacks and longer duration of RRMS. These findings are in full concordance with our previous studies which have demonstrated a considerable increase of GD1a in the serum of FARRMS connected with the early neuronal damage in MS [13, 14]. In humans gangliosides elicit a T-cell independent IgM response. Antiganglioside IgM antibodies can serve as a marker of axonal damage in neuropathies as multiple sclerosis [6]. This study revealed also significantly higher IgM and IgG titers to GM1 antibodies in patients with their first attacks of RRMS. Patients with more advanced RRMS, that is, those with more attacks and higher invalidization, had elevated levels of IgG antibodies to GM1 than IgM antibodies. High IgG titers of anti-GM1 antibodies were found in Guillian-Barré syndrome [3]. The elevated serum anti-GM1 antibodies suggest the immune-mediated demyelination and they do not represent a marker of axonal damage in patients with RRMS [8].

In conclusion, the estimation of IgM antibodies to GD1a in the serum can detect the early neuronal damage in multiple sclerosis, a very important indication for immediate neuroprotective treatment and its efficacy.

References

1. Borazanci, A. P., M. K. Harris, R. N. Schwendimann, E. Gonzalez-Toledo, A.H. Maghzi, N. Alekseeva, J. Pinkston, R. E. Kelley, A. Minagar. Multiple Sclerosis: Clinical Features, Pathophysiology, Neuroimaging and Future Therapies. – *Future Neurology*, **4** (2): 2009, 229-246.
2. De Stefano, N., M. Bartolozzi, L. Guidi, M. Stromillo, A. Federico. Magnetic resonance spectroscopy as a measure of brain damage in multiple sclerosis. – *J. Neurol. Sci.*, **233** (1-2), 2005, 203-208.
3. Kuijf, M. L., P. A. van Doorn, A. P. Tio-Gillen, K. Geleijns, C. W. Ang, H. Hooijkaas, W. C. Hop, B. C. Jacobs. Diagnostic value of anti-GM1 ganglioside serology and validation of the INCAT-ELISA. – *J Neurol Sci.*, **239** (1), 2005, 37-44.
4. Mizutamari, R. K., H. Wiegandt, G. N. Ores. Characterization of antiganglioside antibodies present in normal human plasma. – *J. Neuroimmunol.*, **50** (2), 1994, 215-220.
5. Narayana, P. A. Magnetic resonance spectroscopy in the monitoring of multiple sclerosis. – *J. Neuroimaging*, **15**, 2005, (Suppl. 4), 46S-57S.
6. Ravindranath, M. H., S. Muthugounder. Human antiganglioside autoantibodies: validation of ELISA. – *Ann NY Acad Sci.*, **1050**, 2005, 229-242.
7. Trapp, B.D. Pathogenesis of neurological disability in multiple sclerosis. – *Int. J. of MS care*, 2007, Suppl., 4-7.
8. Valentino, P, A. Labate, R. Nistico, D. Pirritano, A. Cerasa, M. Liguori, L. Bastone, L. Crescibene, A. Quattrone. Anti-GM1 antibodies are not associated with cerebral atrophy in patients with multiple sclerosis. – *Mult. Scler.*, **15** (1), 2009, 114-115.
9. Wiegandt, H. Gangliosides: a review with 677 references. – *New Compr. Biochem.*, **10**, 1985, 199.
10. Zaprianova, E., D. Deleva, B. Hauttecoeur, M. Bakalska, A. Filchev. Ganglioside spinal cord changes in chronic relapsing experimental allergic encephalomyelitis induced in the Lewis rats. – *Neurochem. Res.*, **22** (2), 1997, 175-179.
11. Zaprianova, E., O. Mikova, D. Deleva, A. Filchev, X. Kmetska, I. Karaivanova, K. Milanov, D. Georgiev. Serum antibodies to GM1 ganglioside in patterns with multiple sclerosis. – *Abstr. Second Balkan Immunology Conference, Varna*, **119**, 1998.

12. Zaprianova, E., D. Deleva, P. Ilinov, E. Sultanov, A. Filchev, L. Christova, B. Sultanov. Serum ganglioside patterns in multiple sclerosis. – *Neurochem. Res.*, **26** (2), 2001, 95-100.
13. Zaprianova, E, D. Deleva, B. Sultanov, V. Kolyovska. Current knowledge of multiple sclerosis pathogenesis. – *Acta morphol. et anthropol.*, **14**, 2009, 136-140.
14. Zaprianova, E, S. S. Sergeeva, O. S. Sotnikov, D. Deleva, B. Sultanov, V. Kolyovska, T. V. Krasnova. Evidence of early neuronal damage in the serum of multiple sclerosis patients. – *Compt. rend. Acad. bulg. Sci.*, **63** (3), 2010, 447-454.

Quantitative Assessment of a Peripheral Nerve in Chronic Constriction Injury Model of Neuropathic Pain

*L. Surchev, S. Surcheva**

Department of Anatomy, Histology and Embryology, Medical University of Sofia, Sofia

**Department of Pharmacology and Toxicology, Medical Faculty, Medical University of Sofia, Sofia*

Neuropathic pain is a result from damage to the nervous system caused by many diverse processes, rather than stimulation of pain receptors. Chronic constriction injury model (CCI) is a classical model of neuropathic pain based on a loose ligation of the rat sciatic nerve. Here this animal model is used to derive quantitative data. Image analyzer with a motorized stage was applied to analyze the very large light microscopy images from nerve transverse sections. Three weeks after CCI the mean axon size of the injured nerve appears almost the same as in intact nerve. The sphericity and the mean myelin width of the damaged nerve also do not show significant differences as compared to the intact ones. However, the mean axon density in an injured nerve is diminished to 64% of the value from the intact nerve. The connection of these data with pain pathogenesis is discussed.

Key words: CCI, sciatic nerve, axon, myelin, density.

Introduction

Neuropathic pain is defined as pain initiated or caused by a primary lesion or dysfunction in the nervous system [4]. Neuropathic pain results from damage to the nervous system due to many diverse processes, rather than stimulation of pain receptors. Notwithstanding the steady efforts in many laboratories to unravel the mechanisms underlying the existence of neuropathic pain, they are still unclear. Therefore different animal models are continuously developed to study the pathophysiology of this type of pain [1, 5]. Chronic constriction injury (CCI) model [1] of neuropathic pain is used to investigate the underlying mechanisms of pain associated with damage to the peripheral nervous system and can spur development of novel therapy approaches.

CCI model was proposed in 1988 by Bennett and Xie and is based on a loose ligation of a peripheral nerve that in the rat produces hyperalgesia and allodynia in the sciatic distribution of one hindlimb [1]. Morphological analysis of the damaged nerve has shown that the intact myelinated nerve fibers were reduced and the few surviving myelinated fibers were in the small to medium size range [6]. In the recently proposed mouse model of neuropathic cancer pain the severity of damage to the myelinated fibers was considerably less expressed and the pain characteristics are somewhat different [5].

All these data suggest that the size and density of axons in the damaged nerve could be of importance for the pathogenesis and manifestation of neuropathic pain. Therefore, the aim of the present investigation was to study the light microscopic morphology of sciatic nerve in CCI model of neuropathic pain quantitatively by means of computer assisted image analyzer of high resolution multiple images (Figs. 1-3).

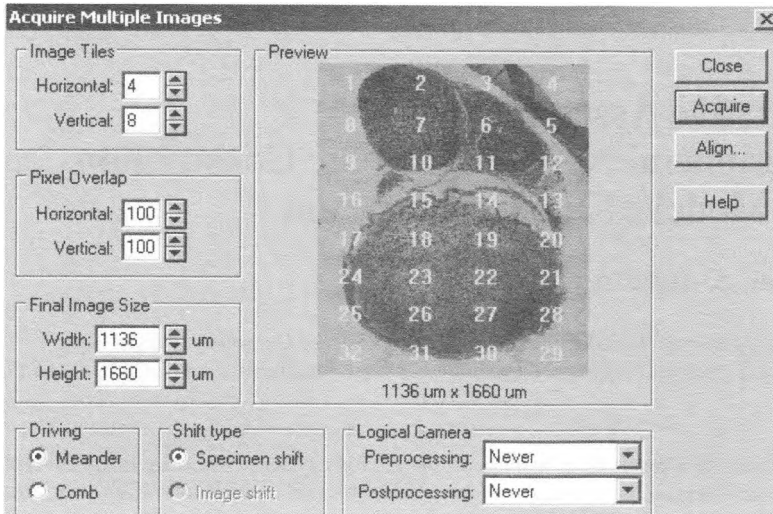


Fig. 1. "Print Screen" from the desktop of the Olympus image analyzer presents the division of a large image of sciatic nerve in 32 individual images

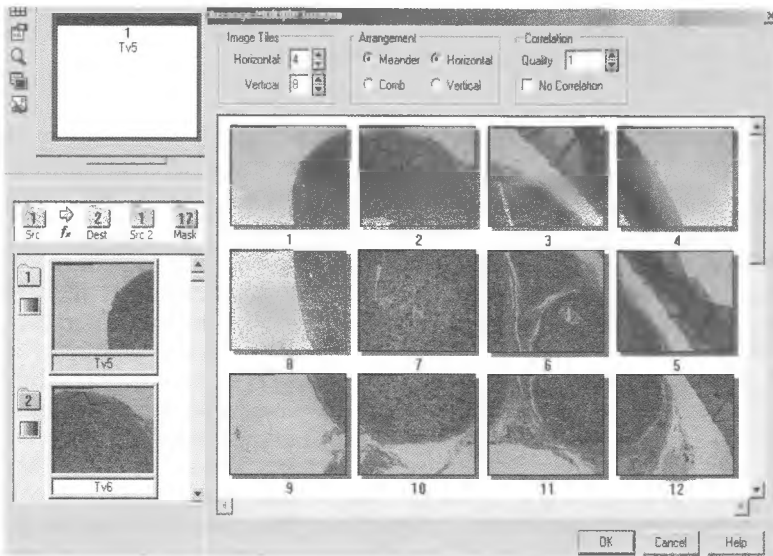


Fig. 2. "Print Screen" from the desktop of the Olympus image analyzer presents at higher magnification 12 from the total 32 individual images

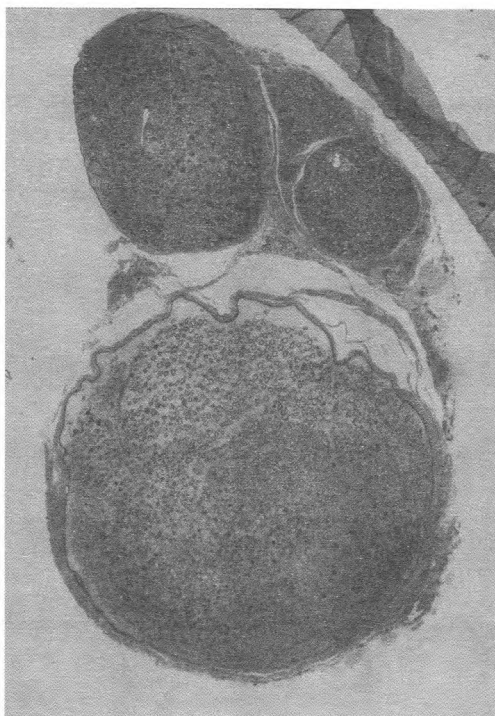


Fig. 3. "Print Screen" from the desktop of the Olympus image analyzer presents the total final image after image alignment

Materials and Methods

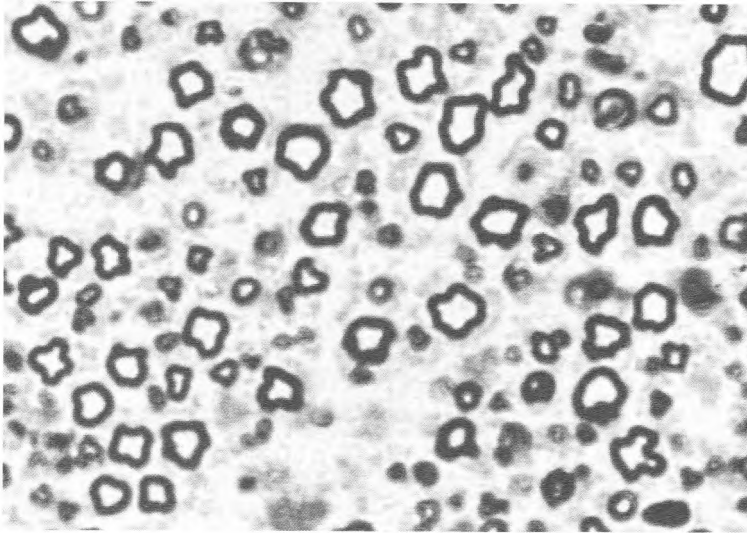
Adult female Wistar albino rats (200-250 g) were used in this study. Animals were provided ad libitum access to food and water until the day of death. The experimental protocols were approved by the Ethics Committee of the Medical University of Sofia.

CCI of the sciatic nerve of the rats was induced over the right hind limb (Bennett and Xie, 1988) [1]. Control animals were sham operated. All animals were operated under general anesthesia (thiopental 40 mg/kg, i.p.). The rats were allowed to recover and survive. During the postoperative period the nociceptive thresholds were determined by paw pressure, hot plate, plantar heat, dynamic plantar and incapitance analgesia tests.

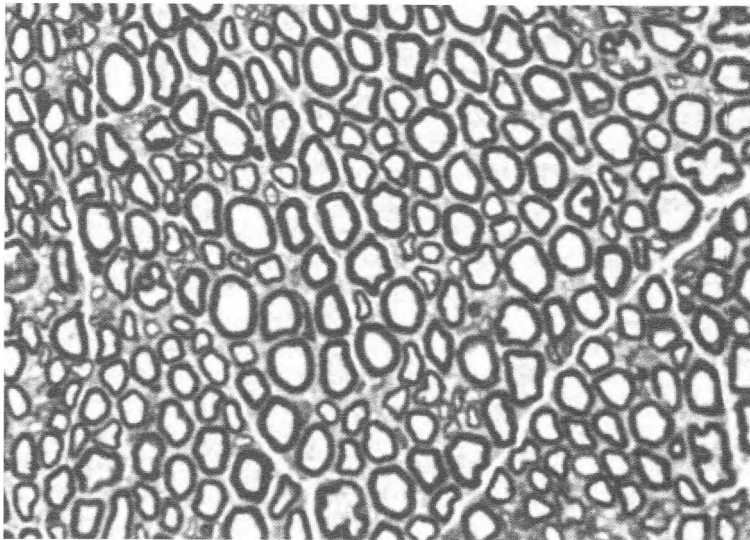
Three weeks after CCI, 3 animals per group were anesthetized with sodium pentobarbital (40 mg/kg). The rats were perfused intracardially with half-strength Karnovsky solution (2% paraformaldehyde and 2.5% glutaraldehyde) in 0,1M phosphate buffer pH 7,4 for 20 min. Small tissue samples of the sciatic nerve distal to the ligatures were post-fixed for several hours in the same fixative at 4°C. They were then rinsed in buffer and post-fixed with 1% osmium tetroxide for 1 hour. Following a second wash the tissue pieces were dehydrated in graded ethanols and embedded in durcupan. Semithin transverse sections of the sciatic nerve were cut on a Reichert-Jung ultramicrotome, stained with toluidine blue and photographed ($\times 40$ objective) in an Olympus image analyzer. It was equipped with automatic stage unit and image analysis system AnalySIS. The results were statistically evaluated using the Student's t-test. $P < 0,05$ was considered significant.

Results

Under the light microscope the transverse sections of the loosely ligated and the control (intact) sciatic nerves show very different images (Figs. 4a, b). The characteristic view of an intact sciatic nerve comprising of many fascicles separated from one another by thin laminae of connective tissue is not present in a CCI nerve. The connective tissue appears as a common background in which the individual axons are distributed. Distal to the ligature the exposed axonal profiles are obviously fewer than the ones in the in-



a)



b)

Fig. 4. Light micrographs of transverse sections of sciatic nerve of female rat: a) CCI, b) Intact rat. $\times 400$

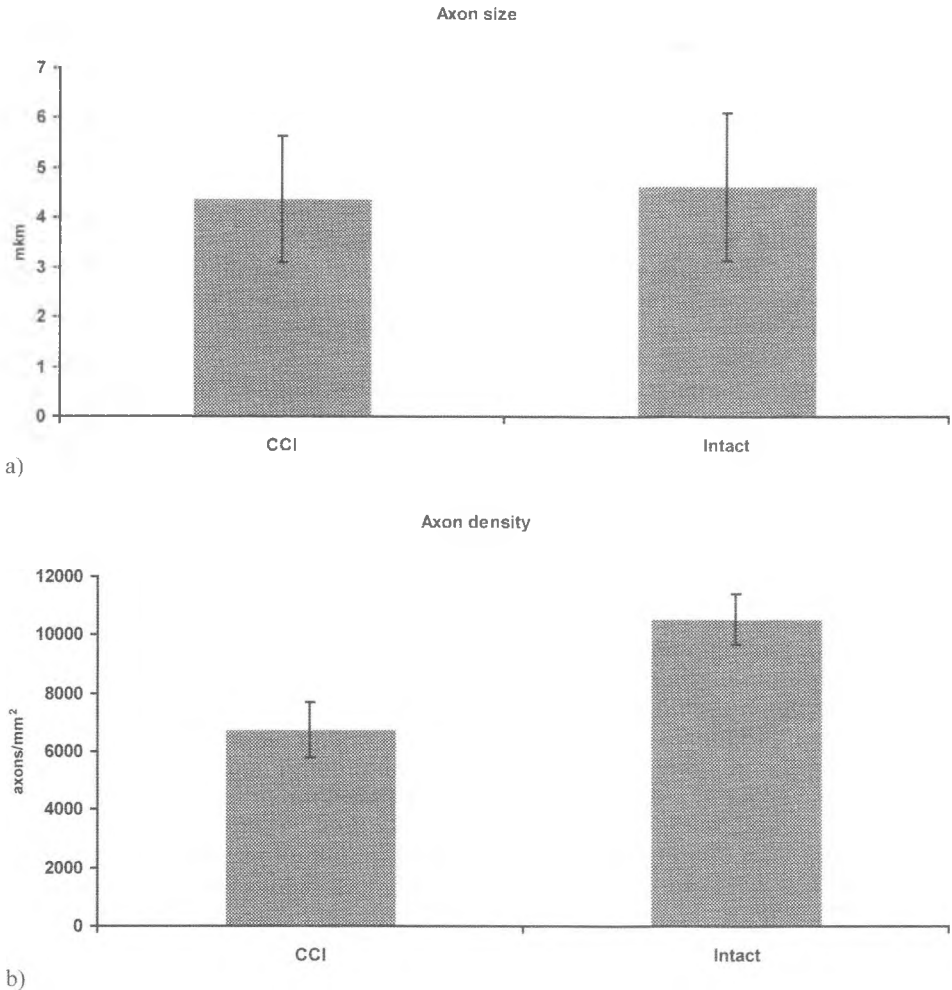


Fig. 5. Quantitative parameters of axons in the sciatic nerve after CCI and in intact rat: a) Mean axon size, b) Mean axon density

tact nerve. They are distantly located from the preserved neighboring ones as compared with the relatively tightly packed axons in the control sciatic nerve. Moreover, the contours of the axonal profiles in the CCI nerve are indented and more irregular whereas the intact nerves display approximately oval profiles. The myelin sheath of the axons in the injured nerve is unevenly thick along their circumference. Additionally, all myelin sheaths in a CCI nerve appear to be almost equally thick regardless of the caliber of the axon they ensheath. Therefore, in cases with very small axon profiles the impression is that they comprise of only myelin sheath. Some of these are very pale. On the contrary, in an intact sciatic nerve the thickness of the myelin sheath is dependent on the axon caliber – larger axons have usually thicker sheaths and vice versa.

The quantitative analysis of the images exposed gives additional information. The mean axon sizes in CCI and intact sciatic nerves are very close (Fig. 5a). The sphericity

of the axon profiles and the mean width of the myelin sheaths do not display significant differences as well (data not shown). However, the axon density in CCI sciatic nerve – 6743 ± 965 axons/mm² is significantly diminished as compared to the density in intact nerve – 10542 ± 874 axons/mm², i.e. the difference is very significant at $p < 0,01$ (Fig. 5b).

Discussion

CCI is a peripheral neuropathic pain model that is caused by an injury to the peripheral nervous system and refractory to available conventional treatment [3]. The last circumstance makes the neuropathic pain a serious clinical problem. Therefore, any information derived by using the CCI model could add to elucidating the yet unknown pathogenesis of this problematic pain.

The results of the present study are very interesting. Here for the first time the density of the axons in a sciatic nerve in CCI model of neuropathic pain is quantitatively determined. This is carried out by using a motorized stage with automatic stage control unit. This progressive approach makes it possible to analyze simultaneously the entire area of nerve transverse sections, which in rat sciatic nerve are very large. Using this approach the transverse section is divided in smaller individual images with their subsequent multiple image alignment. The resulting overview image shows a high resolution previously not possible. Our results indicate that three weeks after the CCI the axon density in the sciatic nerve is 64 % of the respective value in intact rats. This is in accordance with the fact reported by others that the pathogenesis of the extended hyperalgesia following chronic constrictive nerve injury is temporally linked with Wallerian-like degeneration [6]. It should be pointed out that the persistence of the usual mean axon size value after CCI means that not the large [2] but also the small axons are affected by the loss of myelinated nerve fibers. This fact could be connected with the pathogenesis of neuropathic pain and therefore it deserves more attention in future investigations.

The lack of significant difference between the mean myelin width values in CCI and intact rats must also be born in mind. Whereas in the intact nerve the mean myelin width is derived from myelin sheaths with very different widths, in CCI nerve it results from sheaths with nearly the same thickness. This is very characteristic and therefore, may be also of importance for generating the neuropathic pain. Additional studies are needed to solve this problem.

References

1. Bennett, G. J., Y. K. Xie. A peripheral mononeuropathy in rat that produces disorders of pain sensation like those seen in man. – *Pain*, **33**, 1988, 87-107.
2. Gabay, E., M. Tal. Pain behavior and nerve electrophysiology in the CCI model of neuropathic pain. – *Pain*, **110**, 2004, 354-360.
3. Gilron, I., C. P. N. Watson, C. M. Cahill, D. E. Moulins. Neuropathic pain: a practical guide for the clinician. – *CMAJ*, **175**, 2006, 265-275.
4. Merskey, H., N. Bogduk. Classification of chronic pain: description of chronic pain syndromes and definitions of pain terms. 2nd edn., Seattle, IASP Press, 1994, p. 212.
5. Shimoyama, M., K. Tanaka, F. Hasue, N. Shimoyama. A mouse model of neuropathic cancer pain. – *Pain*, **99**, 2002, 167-174.
6. Sommer, C., A. Lalonde, H. M. Heckman, M. Rodriguez, R. R. Myers. Quantitative neuropathology of a focal nerve injury causing hyperalgesia. – *J. Neuropathol. Exp. Neurol.*, **54**, 1995, 635-643.

Effect of Gender and Sex Hormones on Chronically Injured Nerve as a Model of Neuropathic Pain

L. Surchev, S. Surcheva, M. Vlaskovska*, L. Kasakov***

Department of Anatomy, Histology and Embryology, Medical University of Sofia, Sofia

**Department of Pharmacology and Toxicology, Medical Faculty, Medical University of Sofia, Sofia*

*** Institute of Neurobiology, Bulgarian Academy of Sciences, Sofia*

Gender differences in pain perception are caused by differential modulating effects of estrogens and androgens. The aim of this study was to disclose any possible relation between the microscopical changes and the sex following chronic constriction injury (CCI) of the sciatic nerve. CCI model of neuropathic pain was induced in male and female Wistar rats (200-250 g) three weeks after gonadectomy. The animals were randomly assigned into groups: (1) ovariectomized females; (2) ovariectomized, estradiol treated (0.5 mg/kg, p.o. in 11 doses for 21 days) females; (3) gonadally intact males and (4) castrated males. Light microscopy and computer assisted image analysis were applied to reveal the morphological changes. The axonal and myelin injuries are more heavily expressed in castrated males than in ovariectomized females. However, ovariectomized and estrogen treated females show greater changes than gonadally intact males. Results show clearly that there are sex differences in the morphological changes after CCI.

Key words: chronic constriction injury, androgens, estrogens, axons, sciatic nerve.

Introduction

Pain perception is characterized by sex differences according to its differential modulation by estrogens and androgens with females typically presenting higher sensitivity to noxious stimuli and higher incidence of various painful conditions [3-5]. Gonadal hormones are thought as one of the most important factors causing the gender differences in response to pain and analgesia [1, 5]. Such differences suggest that gonadal steroid hormones – estradiol and testosterone could modulate drug induced analgesia. A large number of experimental and clinical investigations imply the role of estrogens in pain sensitivity, endogenous pain modulation and analgesia [11, 14, 16]. Depending on the stimuli, lower pain thresholds have been reported in female animals compared to males, and variability in pain perception is established across menstrual cycle in women [7, 15]. Androgens are also discussed as possible modulators of nociception [2]. However, little is known about influence of sex hormones on the microscopic structure of peripheral nerves affected by neuropathic pain.

The role of sex hormones in neuropathic pain remains elusive. According to some investigators, gender and hormonal status play a key role in experimental neuropathic pain [9]. Simultaneously, there are no corresponding morphological studies on animal models for neuropathic pain. However, some other researchers suggest that sex or sex hormones can influence the nerve injury and/or subsequent recovery [12, 17].

Therefore, the aim of this investigation was to study differences in the light microscopic structure of the sciatic nerve following chronic constriction injury (CCI), a rodent model of neuropathic pain, in relation to gender and sex hormones.

Material and Methods

Adult male and female Wistar rats (200-250 g) were raised under standard laboratory conditions with food and water available ad libitum. All experimental protocols were approved by the Ethics Committee of the Medical University of Sofia. Some of the animals were gonadectomised under anesthesia with ketamine (50 mg/kg, i.p.) and nembutal (12 mg/kg, i.p.). A single dose of gentamycin (8 mg/kg, i.m.) was applied postoperatively.

CCI of the sciatic nerve was induced three weeks after gonadectomy through the following procedure. The animals were anesthetized (ketamine, 50 mg/kg, i.p. and nembutal 12 mg/kg, i.p.). The right sciatic nerve was exposed at mid-thigh level through a small incision, and one-third to one-half of the nerve thickness was loosely ligated with 2 silk threads. The wound was closed with muscle and skin suture. The rats were allowed to survive and were divided into following treatment groups: (1) ovariectomized females, (2) ovariectomized, 17- β -estradiol treated females (0.5 mg/kg, 11 s.c. injections through 21 days), (3) gonadally intact males, (4) castrated males. The nociceptive thresholds were determined by paw pressure, hot plate, plantar heat, dynamic plantar and incapitance analgesia tests.

Thirty days after CCI, 3 animals per group were anesthetized with sodium pentobarbital (40 mg/kg). The rats were perfused intracardially with half-strength Karnovsky solution (2% paraformaldehyde and 2.5% glutaraldehyde) in 0,1M phosphate buffer pH 7,4 for 20 min. Small tissue samples of the sciatic nerve distal to the ligatures were post-fixed for several hours in the same fixative at 4°C. They were then rinsed in buffer and post-fixed with 1% osmium tetroxide for 1 hour. Following a second wash the tissue pieces were dehydrated in graded ethanols and embedded in durcupan. Semithin transverse sections of the sciatic nerve were cut on a Reichert-Jung ultramicrotome, stained with toluidine blue and photographed (x40 objective) in an Olympus image analyzer, which was equipped with automatic stage unit and image analysis system AnalySIS. The obtained data were evaluated by the one-way analysis of variance (ANOVA), followed by two-tail P value or Dunnett's multiple comparison test; $p < 0.05$ was considered significant.

Results

Under the light microscope the transverse sections of the CCI sciatic nerves of rats from the four experimental groups show different images (Figs. 1-4). The nerve sections from ovariectomized rats show reduced number of mainly small to medium sized axonal profiles with relatively thickened myelin sheaths. The sections from ovariectomized and estradiol treated rats display almost the same images with the obvious distinction that the axonal profiles persisted are fewer in number and smaller as compared to the former

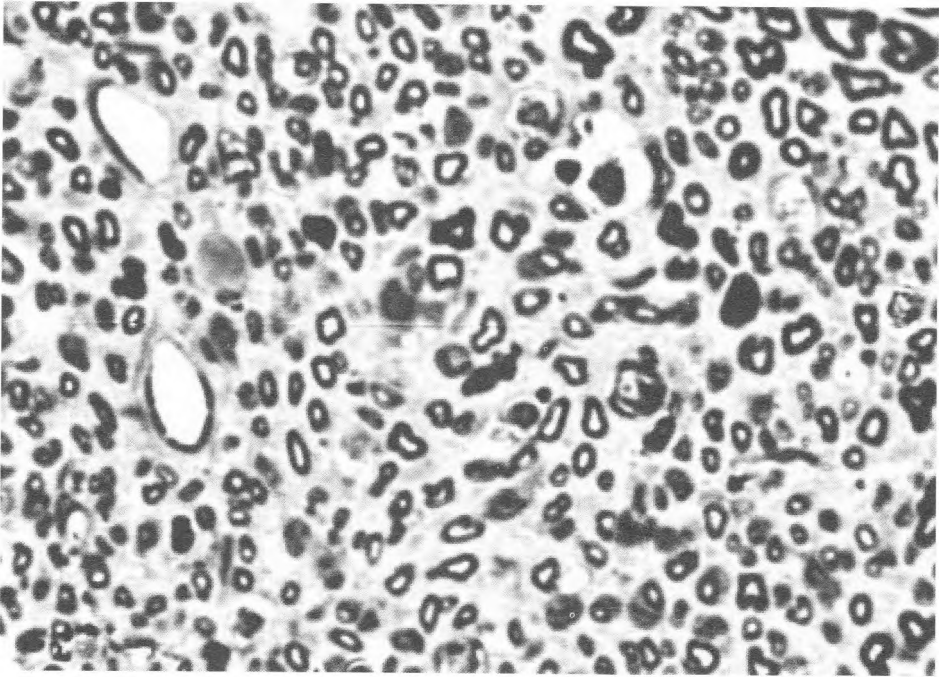


Fig. 1. CCI of sciatic nerve, ovariectomized rat. Light micrograph of transverse section. $\times 400$

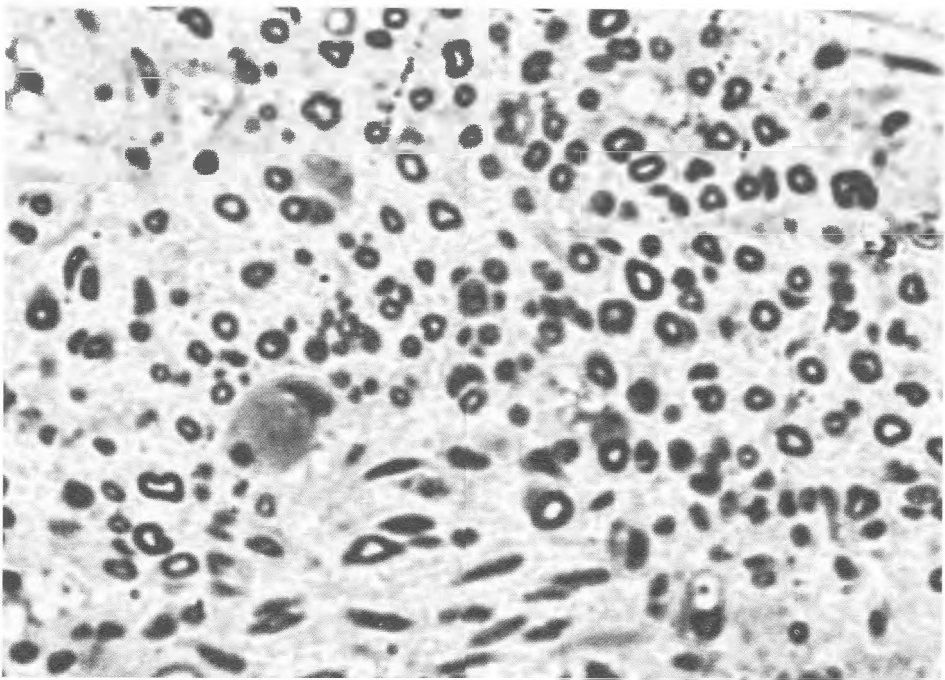


Fig. 2. CCI of sciatic nerve, ovariectomized and estradiol treated rat. Light micrograph of transverse section. $\times 400$

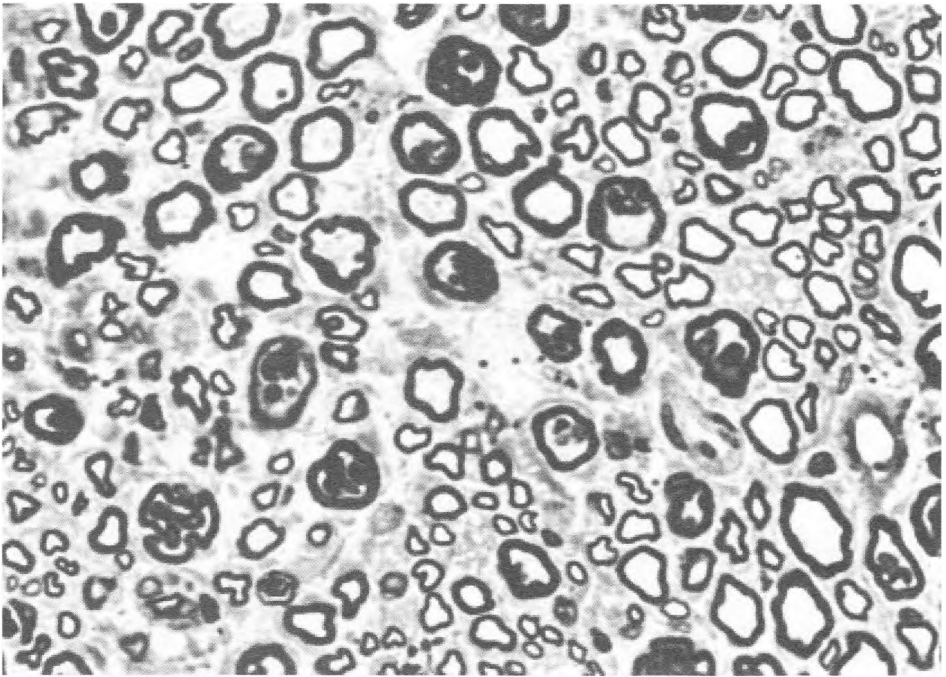


Fig. 3. CCI of sciatic nerve, intact male rat. Light micrograph of transverse section. $\times 400$

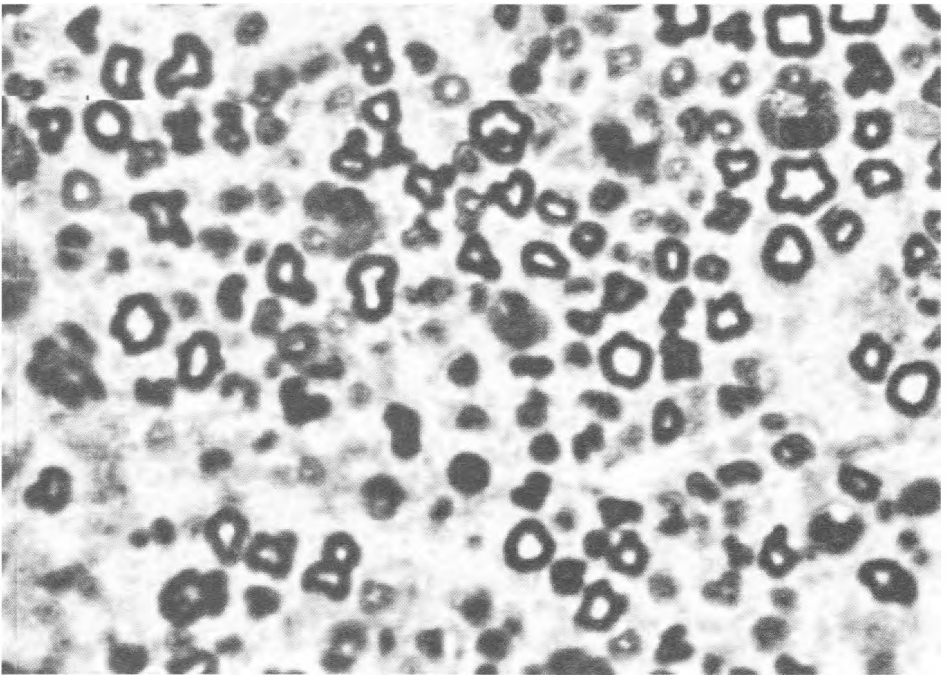


Fig. 4. CCI of sciatic nerve, castrated male rat. Light micrograph of transverse section. $\times 400$

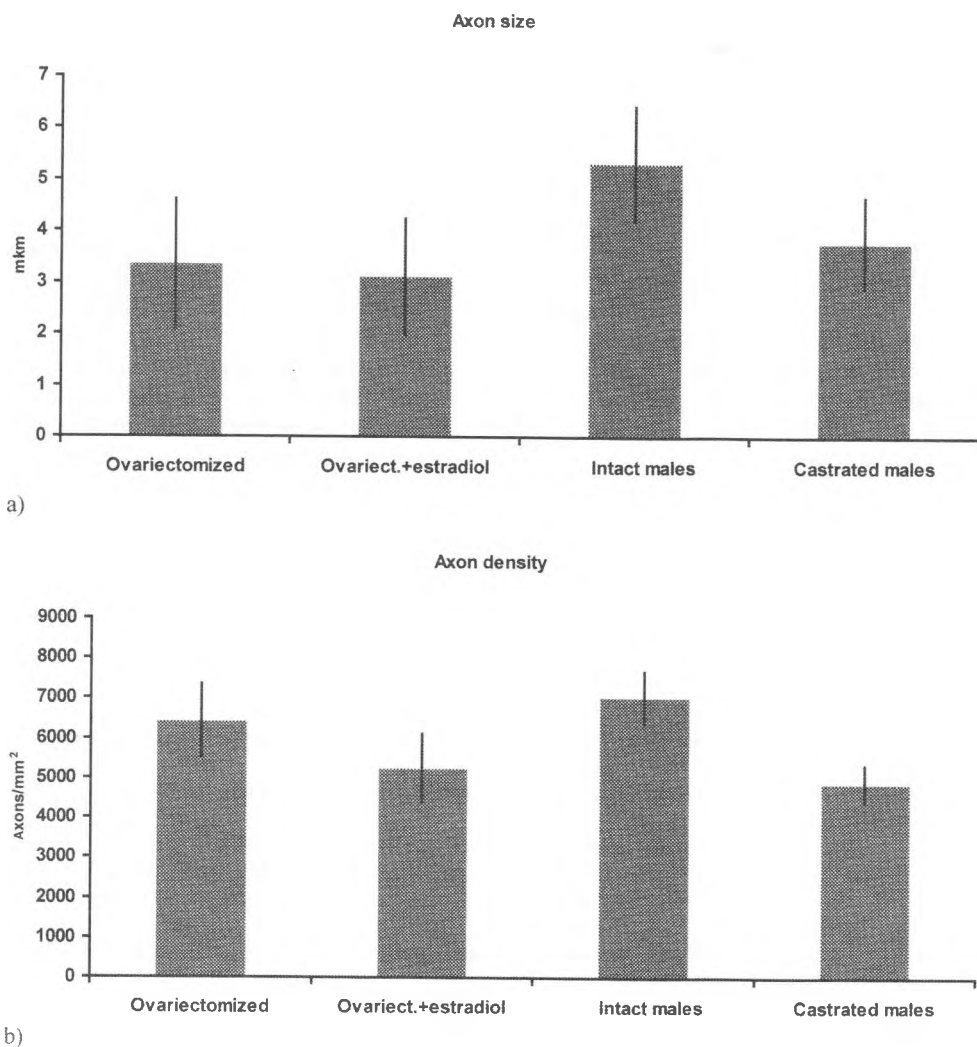


Fig. 5. Quantitative parameters of axons in the sciatic nerve after CCI: a) Mean axon size, b) Mean axon density

group. The sciatic nerve sections from intact male rats expose many and relatively large axon profiles. They also show some signs of deformation but it is comparatively light and the myelin sheaths are not thickened. The nerve sections from castrated rats show reduced number of mainly small axonal profiles, showing signs of severe deformation.

The quantitative image analysis indicates that the mean axon size in the group of intact male rats is larger than the means from all other groups, although this difference is not significant (Fig. 5a). The mean axon density values of the four groups investigated differ from one to another with the greatest value for the group of intact male rats (Fig. 5b). These differences are again not statistically significant.

Discussion

A considerable body of evidence has been collected indicating that sex-related differences exist in nociception and gonadal steroids influence the analgesic response in animals and humans [10].

The effects of estrogens on pain perception remain controversial [e.g. 13]. About the effect of androgens on pain, the literature data are not so plentiful. Experimental and clinical evidence exists for an analgesic effect of testosterone [2, 6].

The reported here morphological data are of special interest. In the present study for the first time light microscopic changes in the CCI model of neuropathic pain are described separately in different experimental groups of males and females. These changes show clear sex differences. The axonal and myelin destruction are more expressed in castrated males than in ovariectomized females. Surprisingly, the destructive changes are lightly more severe in ovariectomized and estradiol treated animals than in solely ovariectomized rats. This could mean that the artificially applied estradiol cannot replace and is not fully identical with its naturally produced hormone in the animal. The ovariectomized and estrogen treated females display greater injuries than the gonadally intact males. Taken together all these findings outline the stronger action of testosterone as compared to estrogens in relation to the microscopic changes in the CCI model of neuropathic pain. This fact corresponds with the protective role of testosterone on the nerve injuries [8].

References

1. Aloisi, A. M. Gonadal hormones and sex differences in pain reactivity. – *Clin. J. Pain*, **19**, 2003, 168-174.
2. Aloisi, A. M., M. Bonifazi. Sex hormones, central nervous system and pain. – *Horm. Behav.*, **50**, 2006, 1-7.
3. Berkley, K. J. Sex differences in pain. – *Behav. Brain Sci.*, **20**, 1997, 473-479.
4. Ceccarelli, I., P. Fiorenzani, C. Massafra, A. M. Aloisi. Repeated nociceptive stimulation induces different behavioral and neuronal responses in intact and gonadectomized female rats. – *Brain Res.*, **1106**, 2006, 142-149.
5. Fillingim, R. B., T. J. Nesses. Sex-related hormonal influences on pain and analgesic response. – *Neurosci. Biobehav. Rev.*, **24**, 2000, 485-501.
6. Fischer, L., J. T. Clemente, C. H. Tambelli. The protective role of testosterone in the development of temporomandibular joint pain. – *J. Pain*, **8**, 2007, 437-442.
7. Giles, B. E., J. S. Walker. Gender differences in pain. – *Curr. Opin. Anaesthesiol.*, **12**, 1999, 591-595.
8. Kinderman, N. B., K. J. Jones. Axotomy-induced changes in ribosomal RNA levels in female hamster facial motoneurons: differential effects of gender and androgen exposure. – *Exp. Neurol.*, **126**, 1994, 144-148.
9. LaCroix-Fralish, M. L., V. L. Tawfik, J. A. DeLeo. The organizational and activational effects of sex hormones on tactile and thermal hypersensitivity following lumbar nerve root injury in male and female rats. – *Pain*, **114**, 2005, 71-80.
10. Lin, S. M., C. M. Tsao, S. K. Tsai, M. S. Mok. Influence of testosterone on autotomy in castrated male rats. – *Life Sci.*, **70**, 2002, 2335-2340.
11. Mannino, C. A., S. M. South, V. Quinones-Jenab, C. E. Inturrisi. Estradiol replacement in ovariectomized rats is antihyperalgesic in the formalin test. – *J. Pain*, **8**, 2007, 334-342.
12. Morell, R. C., R. C. Prielipp, T. N. Harwood, R. L. James, J. F. Butterworth. Men are more susceptible than women to direct pressure on unmyelinated ulnar nerve fibers. – *Anesth. Analg.*, **97**, 2003, 1183-1188.

13. Pju F, C. Cheevers, L. Hyldtoft, L. R. Gardell, A. L. DelTredici, C. B. Andersen, L. C. Fairbairn, B.W. Lund, M. Gustafsson, H. H. Schiffer, J. E. Donello, R. Olsson, D. W. Gil, M. R. Brann. Broad modulation of neuropathic pain states by a selective estrogen receptor beta agonist. – *Eur. J. Pharmacol.*, **590**, 2008, 423-429.
14. Spooner, M. F., P. Robichaud, J. C. Carrier, S. Marchand. Endogenous pain modulation during the formalin test in estrogen receptor beta knockout mice. – *Neuroscience*, **150**, 2007, 675-680.
15. Stening, K., O. Eriksson, L. Wahren, G. Berg, M. Hammar, A. Blomqvist. Pain sensations to the cold pressor test in normally menstruating women: comparison with men and relation to menstrual phase and serum sex steroid levels. – *Am. J. Physiol. Regul. Integr. Comp. Physiol.*, **293**, 2007, R1711-R1716.
16. Stoffel, E. C., C. M. Ulibarri, J. E. Folk, K. C. Rice, R. M. Craft. Gonadal hormone modulation of mu, kappa, and delta opioid antinociception in male and female rats. – *J. Pain*, **6**, 2005, 261-274.
17. Yu, W. H., M.Y. McGinnis. Androgen receptors in cranial nerve motor nuclei of male and female rats. – *J. Neurobiol.*, **46**, 2001, 1-10.

Livedo Vasculitis

M. Gantcheva

*Institute of Experimental Morphology, Pathology and Anthropology with Museum,
Bulgarian Academy of Sciences, Sofia*

We report twenty-two patients with persistent livedo racemosa and recurrent ulcerations on the lower extremities with biopsy-proved livedoid vasculopathy. The clinical presentation, together with histopathological findings of vascular occlusion without overt vasculitis in the dermis, confirm the diagnosis of livedo vasculitis. The pathogenesis of livedo vasculitis is still unclear, but the disease is considered an occlusive thrombotic process due to a hypercoagulable state and appears on the basis of prothrombotic and procoagulant processes rather than vascular inflammation. Following the clinical evolution of the disease we resume that even discrete cutaneous finding like atrophie blanche could be a marker and first clinical sign of a thrombotic disease, which could lead to extensive skin disorders. Our cases also confirm the hypothesis that livedo vasculitis may represent a clinical sign of a sole entity or could be a clinical manifestation of heterogeneous group of diseases.

Key words: livedo vasculitis, thrombosis, atrophie blanche, histopathology.

Introduction

Livedo vasculitis (LV) is a chronic cutaneous disease characterized by painful purpuric eruptions on the legs and feet, which often ulcerate and leave atrophic, stellate, ivory to white, scarlike plaques stippled with telangiectasia and surrounded by hyperpigmentation after healing. Histologic features include hyalinizing vascular changes of the subintimal layer of dermal blood vessels, typically with minimal inflammation, endothelial proliferation, and thrombosis of the upper and middermal blood vessels.

Originally described as atrophie blanche en plaque by Milian in 1929 [10], synonyms for this disease have included “livedo reticularis with ulcerations” [4], “segmental hyalinizing vasculitis” [1], “livedo vasculitis” and “livedoid vasculitis” and more recently “PURPLE – painful purpuric ulcers with reticular pattern of the lower extremities” [12].

The pathogenesis of the disease is still not fully understood. The multifactorial nature of cutaneous ulcerations, which are the clinical sign of LV and the variable nomenclature complicate its classification. It has been described as idiopathic [13] and with immune complex-associated diseases [14]. However, there is accumulating evidence that livedoid vasculopathy is caused by increased prothrombotic and procoagulant processes rather than by vascular inflammation [8, 11]. There is still no defined therapy of

choice for this difficult-to-manage disorder may be because of its chronic or recurrent nature and its often debilitating clinical course. A lot of therapies have been attempted, including nicotinic acid, sulfapyridine, minidose heparin, aspirin and dipyridamole, and nifedipine. Recent reports have shown that warfarin therapy alone improves clinical manifestations of livedoid vasculopathy [2, 3, 9].

Herein, we report twenty-two patients with this rare diagnosis LV. The purpose of study is to further characterize the clinical features, disease associations and laboratory test result abnormalities, including coagulation markers. Based on the histopathological findings of skin efflorescence to maintain the hypothesis that LV is not a vasculitis but rather vascular coagulopathy.

Materials and Methods

We have studied the clinical, histopathological and laboratory findings in 22 patients with LV. They were 14 women and 8 men, aged between 18 and 72, mean age 46 years. We followed the evolution of clinical signs and associated symptoms (in some of the cases due to internal diseases) on the first visit, after 1 month and after 6 months. Laboratory and immunological studies, including determinations of antinuclear antibodies, antibodies to DNA, antiendothelial antibodies, antineutrophil cytoplasmic autoantibodies, anticardiolipin antibodies (ACL), lupus anticoagulant, serum complement levels (C3, C4), circulating immune complexes, cryoglobulins, cryofibrinogen and rheumatoid factor were routinely performed in all patients. ACL of IgG, IgM, IgA and beta 2-glycoprotein IgG were controlled in the beginning and at the end of the study. Biopsy specimens were obtained from active skin lesions from the edge of the livedoid vasculitis like-ulcers located on the lower portion of the legs with punch 4-mm technique. All the histological findings were studied of hematoxylin-eosin staining.

Results

All twenty-two patients included in this study were diagnosed as LV according to their clinical and histopathological findings. The distribution of the cutaneous lesions was predominantly bilateral, but three of the cases were unilateral. The skin around the ankle was the most common site, followed by the leg. The dorsal surface of the foot was the least common. Most patients had efflorescence in a combination of these locations. Morphologic lesions beginning as macular purpura 1 to 2 mm in diameter, enlarging to an irregular purpuric papule 2 to 5 mm in diameter, eventuating in ulceration in the center, and a purpuric border. Fourteen patients were with painful ulcerations on the background of persistent cyanotic discoloration. Seventeen patients were with persistent violaceous reticulated skin pattern, called livedo reticularis that is a main clinical sign of atheromatous vascular disease and occlusive vasculopathies, such as livedo vasculitis [5,12]. Some of the lesions healed with a stellate-shaped depressed white scar with a slightly elevated border characterized by tiny telangiectatic vessels. This is so called atrophie blanche and it was seen in eight of our patients. This clinical pattern was noted to follow a painful ulcerative stage but was also seen in the absence of previous ulceration in four of our cases. Of the all patients, 15 had livedoid vasculopathy in association with other diseases, 8 of whom had antiphospholipid syndrome(APS), 4 were with rheumatoid arthritis, 2 were with associated venous insufficiency and 1 with idiopathic thrombocytopenia.

Laboratory findings, including complete blood cell count, erythrocyte sedimentation rate, antinuclear antibody, antiphospholipid antibody, cryoglobulin levels, prothrombin time, partial thromboplastin time, international normalized ratio, proteins C and S levels, were all within normal limits in the other seventh patients who we diagnosed as idiopathic LV. A deep skin biopsy specimen showed the presence of focal hyalinizing regions in the mid and deep dermis with the evidence of a hyalinizing vasculitis with fibrinoid deposits around the vessels without thrombosis (Fig. 1, Fig. 2).

In eight of the patients we found elevated ACL, detected twice in 3-month period. According to clinical and laboratory criteria, they were diagnosed as having APS and histologically, skin lesions showed microvascular thromboses, which is typical for this kind of pathology, but also mild lymphocytic perivascular infiltrate and hyalinization of dermal vessels (Fig. 3). Leukocytoclastic vasculitis was not detected, although moderate perivascular infiltration of lymphocytes was seen.

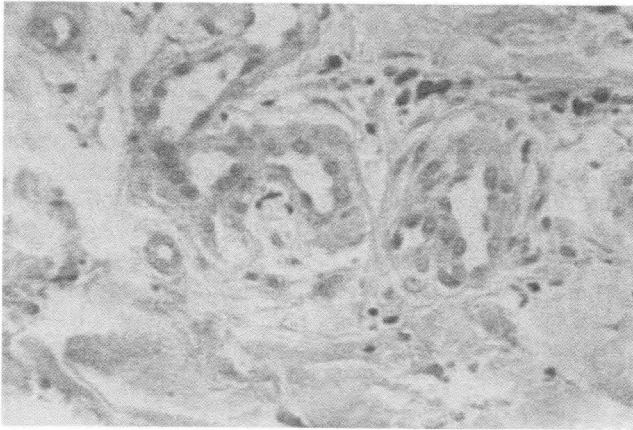


Fig. 1. Hyalinizing segmental vasculitis in the wall of dermal vessels (HE, $\times 20$)

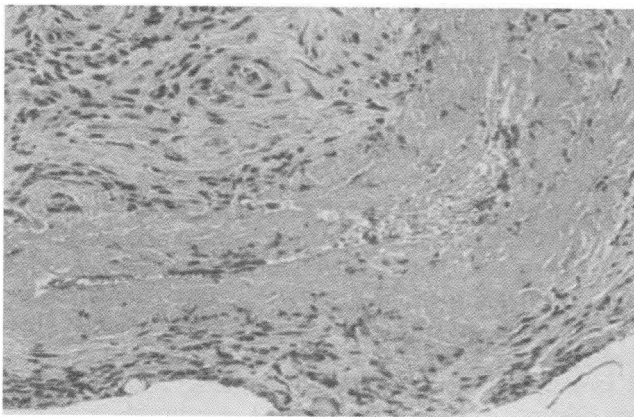


Fig. 2. Deposition of fibrin materials in the wall and lumen of a vessel in the deep dermis (HE, $\times 40$)

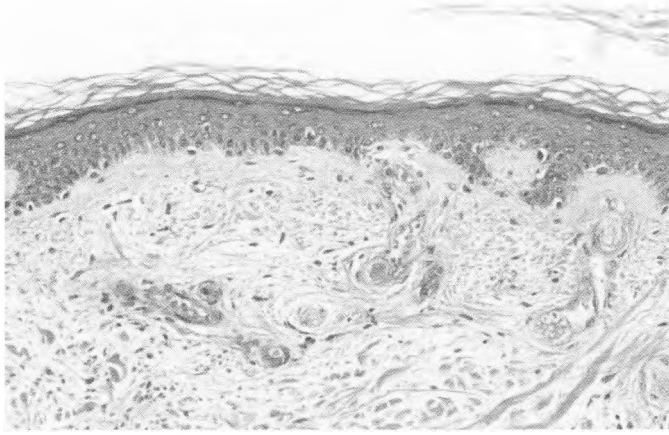


Fig. 3. Microvascular thromboses, mild lymphocytic perivascular infiltrate, and hyalinization of dermal vessels (HE, $\times 10$)

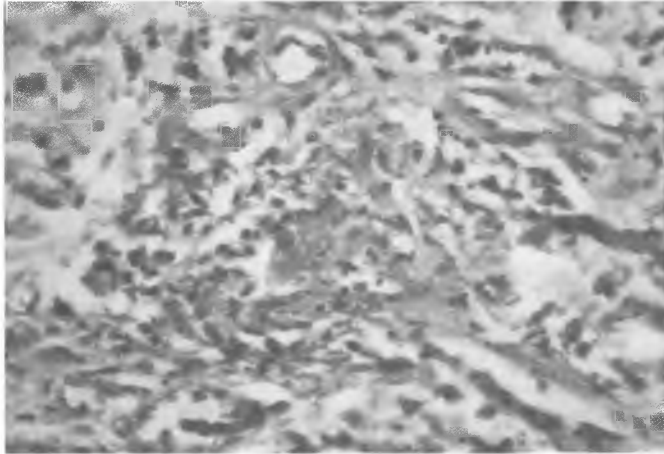


Fig. 4. Hyper and parakeratosis, acanthosis, endothelial swelling and fibrinoid deposition in the lumen of dermal vessels, erythrocyte extravasation (HE, $\times 20$)

The fourth patients with LV in association with venous insufficiency showed mild superficial and deep perivascular infiltrates of neutrophils and lymphocytes, fibrin in the vessel walls and microthromboses.

One of the patients was with idiopathic thrombocytopenia, based on the low levels of the platelets, anisocytosis with hypochromia and anti- Ro antibodies. The skin biopsy specimen showed hyper and parakeratosis, acanthosis, endothelial swelling and fibrinoid deposition in the lumen of dermal vessels (Fig. 4).

Discussion

LV was first described in 1967 by Bard and Winkelmann [1]. Livedoid vasculopathy is an uncommon skin condition that poses a diagnostic and therapeutic challenge for dermatologists and dermatopathologists.

All our patients were assessed clinically for the characteristic aspect of painful, reticulated, ulcerative lesions of the legs, which result in ivory atrophic areas, and histologically for the typical focal thrombi, segmental hyalinization, and a mild lymphocyte infiltration around the dermal vessels. No sign of fibrinoid necrosis of the dermal vessels was seen. Nuclear dust were also absent in the infiltrate. We did not detect any significant sign of leukocytoclastic vasculitis. From this point of view we support the thrombo-occlusive pathogenesis rather than a vasculitis. For some time, LV has been considered a vasculitic process and probably was misdiagnosed as vasculitis. However, it is a common observation that, at histopathologic examination, most lesions of LV lack neutrophilic infiltrate of the blood vessel walls and fibrinoid necrosis, hallmark features of true vasculitis. Many studies favoured this theory, demonstrated that in cutaneous small vessel vasculitis, the serum levels of proinflammatory cytokines are high, whereas in LV, the levels of inflammatory mediators are in the normal range [11]. Although the pathogenesis of LV is still unclear, most authors consider a hypercoagulable state as the primary pathogenic mechanism.

Livedo racemosa and livedoid vasculopathy are often associated with APS [7,12]. LV and APS are suggested to be interconnected diseases as elevated ACL in patients with LV have a predictive importance for development of thrombosis [6]. Occlusion of the smaller dermal vessels in APS may result in the clinical picture of LV. Consequently LV may represent only a clinical manifestation of APS and LV-like ulcers are considered to be very important skin feature of the disease.

In summary, we may conclude that LV arises on the basis of procoagulant and prothrombotic processes rather than a vascular inflammation. Hyalinization of the vessels must be included in the interpretation of the occlusive vasculopathy. Thrombosis is one and the same process which is seen histopathologically both in biopsy specimens from minimal skin lesions and from life-threatening conditions as APS. Discrete cutaneous findings like atrophie blanche could be a marker and a first clinical sign of a thrombotic disorder which may lead to extensive skin efflorescence.

Livedo vasculitis may represent a clinical manifestation of a heterogeneous group of diseases that cause an occlusive vasculopathy or that it may occur as a sole entity.

References

1. Bard, J. W., R. K. Winkelmann. Livedo vasculitis: segmental hyalinizing vasculitis of the dermis. – Arch. Dermatol., **96**, 1967, 489-499
2. Browning, C. E., J. P. Callen. Warfarin therapy for livedoid vasculopathy associated with cryofibrinogenemia and hyperhomocysteinemia. – Arch. Dermatol., **142**, 2006, 75-78.
3. Davis, M. D., W. E. Wysokinski. Ulcerations caused by livedoid vasculopathy associated with a prothrombotic state: response to warfarin. – J. Am. Acad. Dermatol., **58**, 2008, 512-515.
4. Feldaker, M., E. A. Jr Hines, R. R. Kierland. Livedo reticularis with ulcerations. – Circulation., **13**, 1956, 196-216.
5. Fritsch, P., B. Zelger. Livedo vasculitis. – Hautartz., **46**, 1995, 215-224.
6. Gantcheva, M. Dermatological aspects in antiphospholipid syndrome. – Int. J. Dermatol., **36**, 1998, 173-180.
7. Gantcheva, M., I. Anguelova. Antiphospholipids in vasculitic patients. – Clinics Dermatol., **17**, 1999, 619-624.

8. Hairston, B. R., M. D. Davis, M. R. Pittelkow, I. Ahmed. Livedoid vasculopathy: further evidence for procoagulant pathogenesis. – Arch. Dermatol., **142**, 2006, 1413-1418.
9. Kavala, M., E. Kocaturk, I. Zindanci, Z. Turkoglu, S. Altintas. A case of livedoid vasculopathy associated with factor V Leiden mutation: successful treatment with oral warfarin. – J. Dermatolog. Treat., **19**, 2008, 121–123.
10. Milian, G. Les atrophies cutane'es syphilitiques. – Bull. Soc. Franc. Derm. Syph., **36**, 1929, 865-871
11. Papi, M., B. Didona, O. De Pita et al. Livedo vasculopathy vs small vessel cutaneous vasculitis: cytokine and platelet P-selectin studies. – Arch. Dermatol., **134**, 1998, 447-452.
12. Papi, M., B. Didona, O. De Pita, M. Gantcheva, L. Chinni. Purple (atrophie blanche): clinical histological and immunological study of twelve patients. – J. Europ. Acad. Dermatol. Venerol., **9**, 1997, 129-133.
13. Shornick, J. K., B. K. Nicholes, P. R. Bergstresser, J. N. Gilliam. Idiopathic atrophie blanche. – J. Am. Acad. Dermatol., **8**, 1983, 792-798.
14. Winkelmann, R. K., A. L. Schroeter, R. R. Kierland, T. M. Ryan. Clinical studies of livedoid vasculitis (segmental hyalinizing vasculitis). – Mayo Clin. Proc., **49**, 1974, 746-750.

Ultrastructure Studies of Abnormal Sperm in the Pathology of the Male Reproductive System. Deviations in Sperm Head

I. Ilieva, S. Ivanova, P. Tzvetkova, B. Nikolov

*Institute of Experimental Morphology, Pathology and Anthropology with Museum,
Bulgarian Academy of Sciences, Sofia, Bulgaria*

Ultrastructure studies of sperm of patients with various diseases of the reproductive system showed a wide range of distortions in the morphology of the sperm, leading to severe reduction of the fertilizing capacity of germ cells. Morphological studies of sperm of 664 patients (mean age 32.6 ± 3.59 years) with congenital, vascular, specific and unspecific inflammatory diseases of the male reproductive system are carried out according to the WHO criteria. The results of the morphological study on the ultrastructure changes in sperm cell can be combined into three major groups: deviations in the sperm head (a form of chromatin state and acrosome), deviations in the structure of the neck and middle piece and deviations in the tail of the spermatozoa.

Data from these studies contributes to better understanding of the etiology of male infertility, the selection of appropriate therapy and techniques for in vitro fertilization.

Key words: abnormalities spermatozoa, transmission electron microscopy, male infertility.

Introduction

Light microscopic (LM) studies show different changes in the morphology of spermatozoa of ejaculate of men with diseases of the reproductive system. These changes can affect every part of the structure of the sperm cell – head, tail, and combinations of alterations. As a result of abnormalities, changes in the functional properties of the germ cells occur – e.g. their mobility and fertility. Better understanding and insight into the subcellular organization of sperm and organelle complex system can be achieved by transmission electron microscopy (TEM). An in-depth evaluation of semen quality by TEM provides substantial information about motility and the fertilizing competence of spermatozoa [10, 15, 12].

The *aim* of this study has been to determine characteristic malformations of sperm ultrastructure in patients with pathology of the male germ system.

Material and Methods

Morphological studies of ejaculates of 664 patients (mean age 32.6 ± 3.59 years) with congenital, vascular, specific and unspecific inflammatory diseases of the male reproductive system are carried out according to the WHO criteria (1996). The results are compared with those of 20 healthy men (mean age 30.6 ± 3.59 years) (Table 1).

The following methods are used:

- *Anamnesis and local andrologic status*
- *Transmission electron microscopy /“Opton” EM 109/ for evaluation of ultra-structure changes in the sperm cells.*

Table 1. Distribution of the surveyed patients

Patients with:	Number	Patients with:	Number
Congenital diseases of male sexual system	118	Epididymitis chronica	94
Kryptorchism	148		
Kysta epididymis	23	Sexually transmitted infections – STI	55
Inflammatory diseases of male sexual system	431	Vascular diseases	60
Specific inflammatory diseases	152	Varicocele	56
Tuberculosis of epididymis – EPID. TBC	9	Torsio testis	4
Mumps orchitis – MO	143		
Nonspecific inflammatory diseases	379	Total number of patients	664
Prostatitis chronica	285	Control group healthy men	20

Results and Discussion

The results of the morphological study on the ultrastructure changes sperm cell can be combined into three major groups: deviations in the sperm head (a form of chromatin state and acrosome), deviations in the structure of the neck and middle piece and deviations in the tail of the spermatozoa.

I. Sperm head morphological deviations. Abnormal cells with irregular shaped head – “amorphous head” was observed by TEM (Fig. 1) Diversity of this anomalies was found and they were related to irregular surface in equatorial region of head or with abnormal location of acrosome. Expanded subacrosomale layer at different places was observed (Fig. 1-G, H) which defected snug fit of acrosome toward nuclear envelope. Often typical teratological spherical and elongated sperm head were seen in ejaculate of patients with nonspecific inflammatory and vascular diseases (Fig.1-B, C, E).

Elongated head revealed sharpening of posterior nuclear end and decreased transversal diameter. The head shape changed of oval to lake lance form (Fig. 2-C). The spherical head was illustrated with uncompleted acrosome development or absence of it (see Fig. 1). Morphological assessment of nuclear substance was presented by coarse granular appearance of inhomogeneous chromatin and presence of vacuoles with larger then normal dimensions. The heads with such chromatin are more often large with spherical shape (see Fig. 1-B).



Fig. 1. Sperm heads: (A) normal sperm head, (B)-(H) different sperm head deviation – (B) Round sperm head with incomplete chromatin condensation, (C) round sperm head with vacuole and lost acrosome, (D)-(F) amorphous sperm heads – (D) with cytoplasmic droplet, (F) with invagination of the acrosome into nucleus, (G) with detached acrosome, (H) spear-like sperm head. TEM, $\times 20\ 000$

In fact, morphological deviations of the spermatozoa head seems to be the frequent cause of the male infertility [8]. The structural elements that conferred upon spermatozoa the ability both to penetrate the oocyte's vestments and to fuse with the oolemma reside in the head. They are the acrosome and the sperm plasma membrane, which covers the equatorial segment of the acrosome and the post-acrosomal region of the head.

Defects in the sperm head itself may concern size and form of the nucleus or chromatin condensation. Giant and dwarf heads, deformed heads and double heads are already to be identified in LM. Giant heads are often diploid or even triad- or tetraploid [5]. Another abnormality is the round-head-syndrome (globozoospermia) known in man [6, 11], when the sperm head is untypically rounded. Globozoospermia correlates with defective acrosome biogenesis and tail defects that have a disruption in the intramanchette [7] and intraflagellar transport systems of molecules to the centrosome and the developing tail [13].

Abnormalities of the acrosome are often associated with abnormal spermiogenesis, sub- or even infertility in man [14]. Detached acrosomes, partially or totally lost acrosomes are identified regularly. In infertile patients, Yu and Xu [14] found acrosomes covering a bigger proportion of the sperm head and an acrosome less smooth and less intact. Asymmetric thickening of the acrosome cap is described by Holstein [6]. Droplets attached to the acrosome membrane were also shown [14]. Zamboni [15] and Latini et al. [8] mentioned "miniacrosomes". Vacuoles in the acrosome and in the nucleus reported by us have also been described in man [6]. Cavities filled with amorphous material and surrounded by two membranes are also known [15] and are similar to cytoplasmic droplets. The vesicles are formed by separation and expansion of the plasma membrane away from the underlying structure. Differential diagnoses to these vesicles are proximal cytoplasmic droplets with electron-dense material and organelles similar to the Golgi apparatus. Furthermore, swollen acrosomes, sometimes together with swollen mitochondria at the midpiece and a coiled axonema in a cytoplasmic droplet are thought to be indicative of apoptosis [1].

Local defects in chromatin condensation are observed regularly as small vacuoles, but sometimes the vacuoles are big or chromatin condensation is incomplete what results in an inhomogeneous structure. Nuclear vacuoles have been reported in spermatozoa from individuals with seminal infections, varicocele, fever, testicular tumors and inflammatory bowel disease [15, 9]. Incomplete condensation is a sign of immaturity what was already discussed by Fawcett [5]. Furthermore, it is associated with low chromatin stability and teratozoospermia of the sperm head. Some authors suggest that the spermatozoa with incomplete chromatin condensation apparently more often display single-stranded rather than double-stranded DNA or possess chromosomal abnormalities [11] than evidence suggests that living spermatozoa with abnormal chromatin have a sharply reduced capacity to fertilize oocytes or may be responsible for defective early development. This might be caused by chromatin fragmentation or defects in histone-protamine exchange [3].

Ultrastructure studies of sperm of patients with diseases of the reproductive system showed a wide range of various distortions in the morphology of the sperm. Of most importance on the fertility of the sperm cells are disabilities in a head, were observed by us predominantly in infertile men. Data from these studies contribute to better understanding of the etiology of male infertility, the selection of appropriate therapy and techniques for *in vitro* fertilization.

References

1. Baccetti, B., S. Capitani, G. Collo del, E. Strehler, P. Piomboni. Recent advances in human sperm pathology. – *Contraception*, **65**, 2002, 283-287.
2. Bragina, E., R. Abdumalikov, L. Kurilo, L. Shilejko. Electron microscopic study of human spermatozoa. – *Problems of Reproduction*, **6**, 2000, 62-71.
3. Chenoweth, P. Genetic sperm defects. – *Theriogenology*, **64**, 2005, 457-468.
4. Escalier, D. Arrest of flagellum morphogenesis with fibrous sheath immaturity of human spermatozoa. *Andrologia*, **38**, 2006, No 2, 54-60.
5. Fawcett, D. The mammalian spermatozoon. – *Dev. Biol.*, **44**, 1975, 394-436.
6. Holstein, A., E. Roosen-Runge, C. Schirren. Illustrated pathology of human spermatogenesis. Grosse Verlag, Berlin., 1988
7. Kierszenbaum, A. Intramanchette transport (IMT): managing the making of the spermatid head, centrosome, and tail. – *Mol. Reprod. Dev.*, **63**, 2002, 1-4.
8. K pker, W., W. Schulze, K. Diedrich. Ultrastructure of gametes and intracytoplasmic sperm injection: the significance of sperm morphology. – *Hum. Reprod.*, **13**, 1998, No 1, 99-106
9. Latini Latini, M., L. Gandini, A. Lenzi, F. Romaneli. Sperm tail agenesis in a case of consanguinity. – *Fertil. Steril.*, **81**, 2004, 1688-1691.
10. Mashiach, R., B. Fisch, F. Eltes, Y. Tadir, J. Ovadia, B. Bartoov. The relationship between sperm ultrastructural features and fertilizing capacity *in vitro*. – *Fertil. Steril.*, **57**, 1992, 1052-1057.
11. Pesch, S., M. Bergmann. Structure of mammalian spermatozoa in respect to viability, fertility and cryopreservation. – *Micron*, **37**, 2006, 597-612
12. Rawe, V., Y. Terada, S. Nakamura, C. Chillik, S. B. Olmedo, H. Chemes. A pathology of the sperm centriole responsible for defective sperm aster formation, syngamy and cleavage. – *Hum. Reprod.*, **17**, 2002, No 9, 2344-2349.
13. Rosenbaum, J., G. Witman. Intraflagellar transport. – *Nat. Mol. Cell Biol.*, **3**, 2002, 813-825.
14. Yu, J., Y. Xu. Ultrastructural defects of the acrosome in infertile men. – *Arch. Androl.*, **50**, 2004, 405-409.
15. Zamboni, L. Sperm structure and its relevance to infertility. An electron microscopic study. – *Arch. Pathol. Lab. Med.*, **116**, 1992, 325-344.

Azoospermia – Clinical and Cytological Manifestations

S. Ivanova, I. Ilieva, P. Tzvetkova

*Department of Experimental Morphology, Institute of Experimental Morphology,
Pathology and Anthropology with Museum, BAS, Sofia, Bulgaria*

Several clinical factors for azoospermia exist. Records of semen analyses frequently contain the item “round cells” without further specification of the type of cells. **Material and Methods:** We investigated 1333 patients (average 24.81 ± 1.90 years old) with congenital ($n=299$), specific ($n=226$) and non-specific inflammatory ($n=390$), and vascular diseases ($n=363$) of male genital system and 129 (average 25.63 ± 2.15 years old) healthy men as a control group. The following methods were used: andrological anamnesis and status; spermatological analysis of the ejaculate and sperm morphology according to WHO (1996); cytological analysis of round cells using Papanicolaou staining technique; statistical significance was verified with Student’s t-test and SPSS computer program. **Results:** Azoospermia was proved in 20.18% in all male genital pathology. Cytological analysis of type round sperm cells was determined the following “round cells” of spermatogenic origin: spermatides – 79%, spermatocyte – 7%. The “round cells” of non-spermatogenic origin were counted: monocyte – 2%, granulocyte – 1%, macrophage – 3%, abnormal form cells – 8%. **Conclusion:** A knowledge of clinical features and cytological sight of azoospermia open new horizons in the treatment of infertility in some forms of azoospermia, and therefore knowledge of the specific degree of testicular damage is a necessary step in the evaluation of azoospermic men.

Key words: azoospermia, frequency, round cells, men.

Introduction

Several aetiologies for azoospermia exist, but the prospects of fertility in every case are very poor [11, 12, 5].

Azoospermia is found in approximately 5-20% of men evaluate for infertility [8, 6].

Records of semen analyses frequently contain the item “round cells” [10] without further specification of the type of cells. The “round cells” observed in the semen samples could be either of spermatogenic origin [3, 7, 1] or varying types of cells of non-spermatogenic origin [4, 14].

The purpose of this report was to provide an update on the clinical manifestation and frequency of azoospermia, also to investigate the cytological manifestation of such seminal plasma.

Material and Methods

We investigated 1333 patients (average 24.81 ± 1.90 years old) with congenital ($n=299$), inflammatory ($n=671$) and vascular ($n=363$) diseases of male genital system and 129 (25.63 ± 2.15 years old) healthy men as a control group.

The fellow **methods** were used:

- Andrological anamnesis and status;
- Spermatological analysis of the ejaculate and sperm morphology according WHO (1996);
- Cytological analysis of seminal plasma, used the Papanicolaou staining to distinguish "round cells" of spermatogenic and non-spermatogenic origin.

The following forms were identified: spermatopoetic – spermatogonia (dark and pale), primary spermatocytes, secondary spermatocytes, early and late spermatids (corresponding to Sa-Sb and Sc-Sd steps of spermatogenesis; non-spermatopoetic round cells.

- Statistical significance was verified with Student's *t*-test. The results are given as mean \pm SD.

Results

I. Clinical Manifestation

Congenital diseases of male reproductive system and azoospermia

Quite natural and understandable data are complete lack of spermatogenesis in congenital diseases of male reproductive system (Fig. 1) in the cases of Del-Castilo and Klinefelter's syndrome (100%).

Interesting tracking were two other pathologies of the male reproductive system – Monorchism and Criptorchidism. In Monorchism, accompanying disease testis only

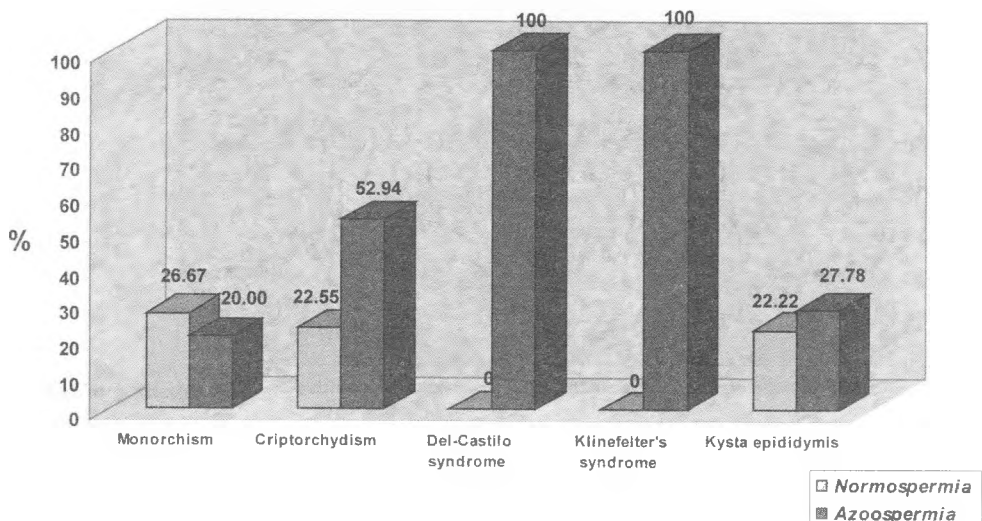


Fig. 1 Percent of azoospermia and congenital pathology

(egs. inflammation) may lead to azoospermia. As to Cryptorchidism, in 52% of cases leads to lack of spermatogenesis.

Specific inflammatory diseases of male genital system and azoospermia

Disturbing fact which is clear was that in inflammatory diseases of the male reproductive system, whether specific (16.95%) or nonspecific (29.26%), surveyed in 1333 on 50.34% in the patients establishes existing impaired fertility, respectively azoospermia (Fig. 2).

In non-specific inflammatory diseases of male genital system we proved azoospermia in 5.35 and 3.29% on cases with Prostatitis and Epididymitis chronica, respectively (see Fig. 2).

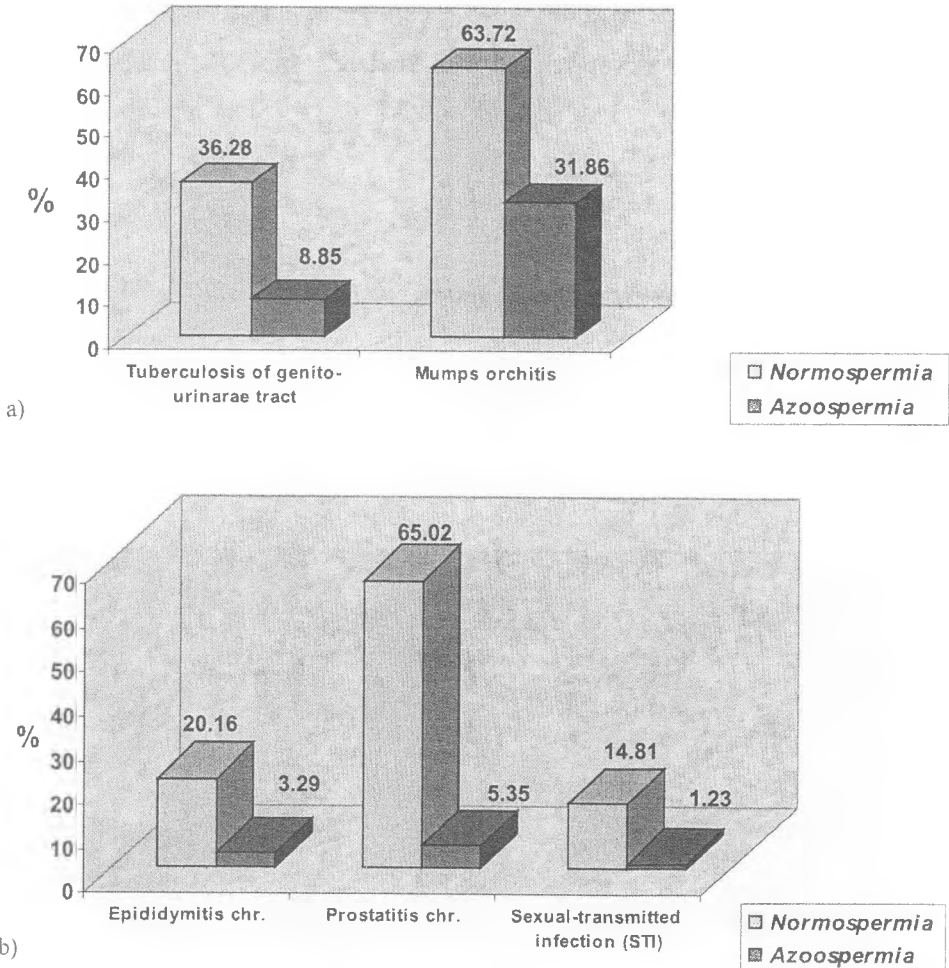


Fig. 2. Percent of azoospermia and inflammatory pathology of male genital tract: a) Specific inflammatory diseases; b) Non-specific inflammatory diseases

Vascular pathology of male genital system and frequency of azoospermia

Not least is the proportion of azoospermia (27.23%) in cases with vascular pathology of male genital system (Fig. 3).

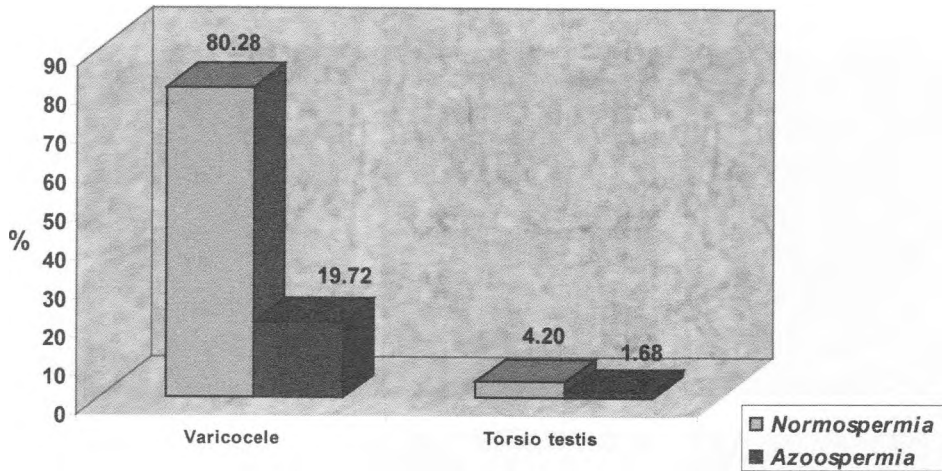


Fig. 3. Percent of azoospermia and vascular pathology of male genital tract

II. Cytological manifestations

Cytological examination of seminal plasma in cases with azoospermia were studied. Conditional observed cell divided into two groups (Fig. 4) – of spermatogenic and non-spermatogenic round cells (Fig. 5) origin.

The cells of spermatogenic origin, most common are spermatidite (79%). As for those of non-spermatogenic origin, most common are monocytes (2%) and macrophages (3%) (Fig. 6).

Discussion

Clinical manifestation and frequency of azoospermia – 20.18%, described by us are not different from the data by other authors [9, 13, 15, 12, 5].

Inflammatory and vascular diseases of male reproductive system were very often genital pathology attended with disturbances of sperm fertilizing ability. Azoospermia was found in 20.35% on specific, 5.38% in non-specific inflammatory diseases. Sexually-transmitted inflammation of male system led in to 1.23% absence of spermatozoa. Varicocele and azoospermia we proved in 19.72%.

In our study we conducted cytological examination of seminal plasma in cases with azoospermia. We made a comparison between the different types of round cells and the normal spermatogenesis. Spermatids were frequently counted – 79% of all type of cells. A number of spermatocytes in the semen is seldom accompanied by a large number of mature spermatozoa and severe disturbances of the spermatogenesis can be expected in such cases. On the other hand, degenerated spermatids are frequently

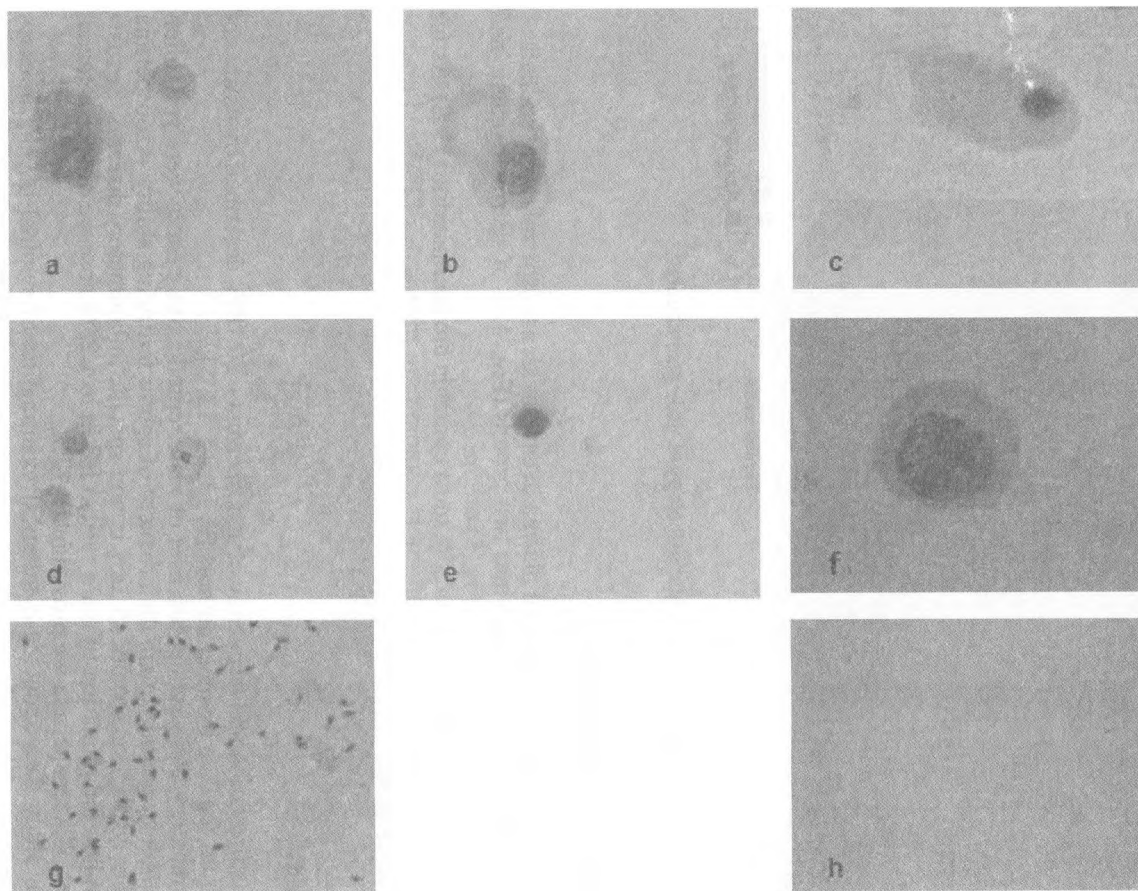


Fig. 4 Spermatic cells in the seminal plasma on azoospermic men. (a-e) spermatid cells; (f-h) spermatocytes. Papanicolau, $\times 600$

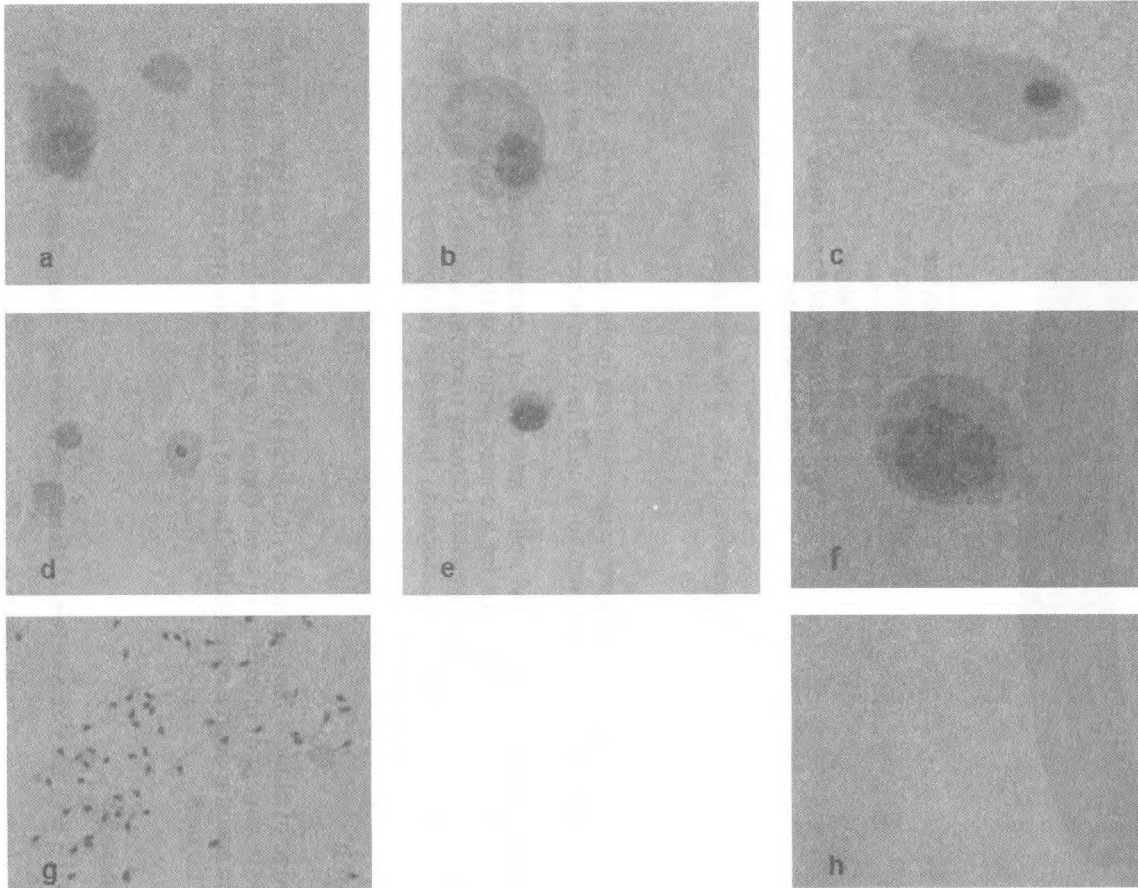


Fig. 5 Non- spermatogenic cells in the seminal plasma on azoospermic men. (a) degenerating monocyte, (b) monocyte, (c-d) epithelial cells, (e) lymphocyte, (f) macrophage, (h) seminal plasma (azoospermia), (g) seminal plasma (normal, X400). Papanicolau, $\times 600$

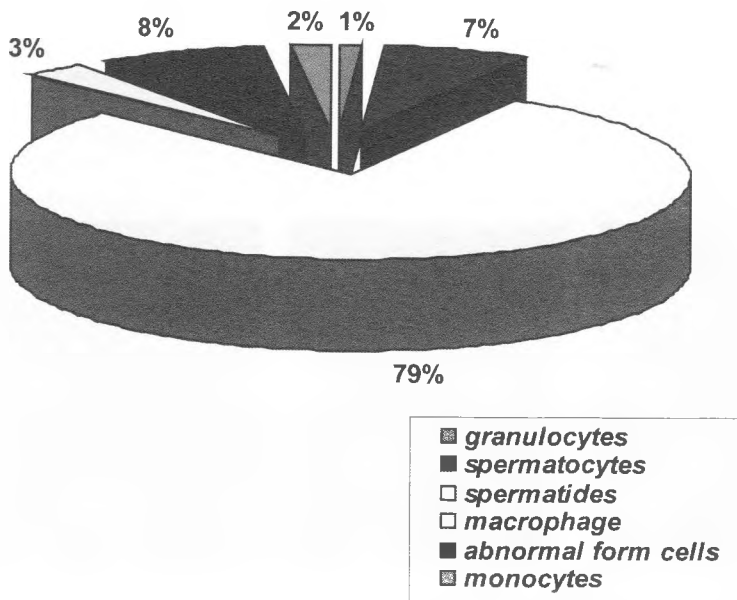


Fig. 6. Frequency of non-spermatogenic cells in the seminal plasma on azoospermic men

observed also in the presence of mature spermatozoa in the semen [2, 10]. According Holstein and Schirren (1979) abnormal form cells has been detected in 50% of all cases studied. We founded 8%.

A differentiation of the “round cells” into cells of spermatogenic and non-spermatogenic origin is very important for a correct semen analysis. The lumping of all “round cells” into one group (as suggested in many recommendations for semen analysis) highly increases the risk of misinforming the treating clinicians.

Conclusion

A knowledge of clinical features and cytological sight of azoospermia open new horizons in the treatment of infertility in some forms of azoospermia, and therefore knowledge of the specific degree of testicular damage is a necessary step in the evaluation of azoospermic men.

References

1. Comhaire, F. C. and Vermeulen, L. Humansemen analysis. – Hum. Reprod., Update, **1**, 1995, 343-362.
2. Dym, M. and Fawcett, D. W. (1971) Further observations on the number of spermatogonia, spermatocytes, and spermatids, joined by intercellular bridges in mammalian spermatogenesis. – Boil. Reprod., **4**, 195-215.
3. Fawcett, D.W. (1975) Gametogenesis in the male: prospects for its control. – In: Marhert, C.L. and Papanconstantinou, J. (eds), The Developmental Biology of Reproduction. Academic Press, New York, USA, pp. 25-54.

4. Fedder, J (1996) Nonsperm cells in human semen with special reference to seminal leukocytes and their possible influence on fertility. – *Arch. Androl.*, **36**, 41-65.
5. Ferhi, K., Avakian, R., Griveau, JF, Guille, F. Age as only predictive factor for successful sperm recovery in patients with Klinefelter's syndrome. – *Andrologia*. **41**(2):84-7, 2009 Apr.
6. Foresta, C., Zorzi, M., Galeazzi, C. & Rossato, M. Functional and structural characteristics of human epididymal sperm retrieved by transcutaneous aspiration. – *International Journal of Andrology*, 1995, **18**, 197-202.
7. Holstein, A.F. and Schirren, C. (1979) Classification of abnormalities in human spermatids based on recent advances in ultrastructure research on spermatids differentiation. – In: Fawcett, D.W. and Bedford, J.M. (eds), *The Spermatozoon: Maturation, Motility, Surfaces, Properties and Comparative Aspects*. Urban and Schwarzenberg, Baltimore, USA, pp. 341-353.
8. Jarow, JP, Oates, RD, Buch, JP, Shaban, SF, Sigman, M. Effect of level of anastomosis and quality of intraepididymal sperm on the outcome of end-to-side epididymovasostomy. – *Urology*. 1992, **49**:590-595.
9. Johannisson, E. and Eliasson, R. (1978) Cytological studies of prostatic fluids from men with and without abnormal palpatory finding of the prostate. – *Int. J. Androl.*, **7**, 201-212.
10. Johannisson, E., Campana, A., Luthi, R., A gostini, A. de. Evaluation of "round cells" in semen analysis: a comparative study. – *Human Reproduction*, Vol. 6, 2000, No 4, 404-412.
11. Matsumiya, K., Namiki, M., Takahara, S. Clinical study of azoospermia. – *International Journal of Andrology*, 1994, **17**, 140-142.
12. Popken, G. Schwarzer, J. U. Current aspects of surgical restoration of fertility. – *Urology*, **47**(12):1568-72, 2008 Dec.
13. Sousa, M., Barros, A., Takahashi, K. et al. (1999) Clinical efficacy of spermatid conception, analysis using a new spermatid classification scheme. – *Hum. Reprod.*, **14**, 1279-1286.
14. Thomas, J., Fishel, S. B., Hall, J. A. et al. (1997) Increase polymorphonuclear granulocytes in seminal plasma in relation to sperm morphology. – *Hum. Reprod.*, **12**, 1418-1421.
15. Uchechukwu, I.O. Ezech. Beyond the clinical classification of azoospermia: Opinion. – *Human Reproduction*, Vol. 15, 2000, No 11, 2356-2359.

Morphometric Parameters of the Rat Choroid Plexus Blood Vessels

V. Ormandzhieva

*Department of Experimental Morphology, Institute of Experimental Morphology, Pathology
and Anthropology with Museum, BAS, Sofia*

Background: The choroid plexus is an epithelial-endothelial vascular structure within the ventricular system of the vertebrate brain. It consists of epithelial cells, fenestrated blood vessels, and the stroma, dependent on various physiological or pathological conditions.

Methods: The blood vessels divided in four subgroups of the choroid plexus of young (1 month) and adult (10, 13 and 22 months) rats were morphometrically studied. The investigations were performed on semithin sections examined with the light microscope using a square grid system calibrated for semiautomatic image analysis.

Results: No significant changes were observed in the luminal diameter and cross-sectional area of capillaries (vessels $<15.0\ \mu\text{m}$ in diameter) and large vessels (vessels of $15.5 - 30.0\ \mu\text{m}$ and $>30.0\ \mu\text{m}$ in diameter) in the young (mean luminal diameter of capillaries $- 8.95 \pm 0.29\ \mu\text{m}$) and adult (mean luminal diameter of capillaries $- 9.15 \pm 0.58\ \mu\text{m}$ of 10 months, $9.08 \pm 0.26\ \mu\text{m}$ of 13 months, and $9.25 \pm 0.29\ \mu\text{m}$ of 22 months) rats.

Conclusion: These results indicate that the luminal diameter and cross-sectional area of the capillaries and large vessels of the plexus choroideus in the young and adult rat do not change. In young rats the blood vessels with luminal diameter $>30\ \mu\text{m}$ have not been found and this may be related with a larger number of the blood vessels with small luminal diameter, i.e. capillaries.

Key words: rat choroid plexus, blood vessels, morphometrical and ultrastructural study.

Introduction

The choroid plexuses are specialized highly vascular anatomical structure which protrude into the lateral ventricle, as well as in the third ventricle and fourth ventricle. The surface of the choroid plexus consists of numerous villi each covered with single layer of epithelial cells surrounded by vascular connective tissue cells [6, 2]. These cells are generally considered to be modified ependymal cells with epithelial cell characteristics and referred to as choroidal epithelial cells.

The choroid plexus is mainly involved in the production of cerebrospinal fluid (CSF) by using the free access to the blood compartment of the leaky vessels. In order to separate blood and CSF compartments, choroid plexus epithelial cells and tanycytes of circumventricular organs constitute the blood-CSF-brain barrier [12]. As a secretory

source of vitamins, peptides and hormones for neurons, the choroid plexus provides substances for brain homeostasis [3]. Most blood vessels in the plexus choroideus are wide-calibre (approximately 15 μm) capillaries with thin fenestrated endothelial walls and bridging diaphragms overlying the fenestrations [5].

Purpose of the present study is an investigation of the morphometrical characteristics of the rat choroid plexus blood vessels.

Materials and Methods

Wistar rats aged 1 (n=5), 10 (n=5), 13 (n=5) and 22 (n=5) months were used in the present study. The animals were anesthetized with sodium pentobarbital (40 ml/kg, i.p.) and perfused intracardially with 2.5% glutaraldehyde and 2% paraformaldehyde in 0.1 M cacodilate buffer [4]. Extracted choroid plexuses were postfixes in 1% OsO₄, dehydrated through graded ethanol and embedded in Durcupan and examined with JEOL JEM 1200EX transmission electron microscope. The semithin sections (1 μm) were stained with 1% toluidine blue for morphometric measurements and examined under Light microscope Carl Zeiss Jena.

Morphometric Analysis

Investigations were performed on semithin sections examined with the light microscope using a square grid system [11] calibrated for semiautomatic image analysis, described in our previous studies [6, 7].

In the present study the relative number of blood vessels and luminal diameter and cross-sectional area of the blood vessels divided in four subgroups were measured. The luminal diameter was measured as perpendicular distance across the maximum chord axis of each vessel.

Statistical Analysis

Results are reported as mean values \pm SEM and as relative part in percentage, and statistically analyzed by Student's t-test using statistical package (STATISTICA, ver.6, Stat-Soft Inc., 2001), and differences were regarded as significant at $p < 0.05$.

Results

Changes in luminal diameter, area of the luminal profile and relative part of the all blood vessels and vessels divided in four subgroups in young (1 month) and adult rats (10, 13 and 22 months) were determined. These findings are shown on Table 1 and in Figure 1. No significant changes were observed in the luminal diameter of capillaries (vessels $< 15.0 \mu\text{m}$ in diameter) and large vessels (vessels of $15.5 - 30.0 \mu\text{m}$ and $> 30.0 \mu\text{m}$ in diameter) in the young (mean luminal diameter of capillaries – $8.95 \pm 0.29 \mu\text{m}$) and adult (mean luminal diameter of capillaries – $9.15 \pm 0.58 \mu\text{m}$ of 10 months, $9.08 \pm 0.26 \mu\text{m}$ of 13 months, and $9.25 \pm 0.29 \mu\text{m}$ of 22 months) rats. Blood vessels with luminal diameter $> 30 \mu\text{m}$ have not been found in young rats.

The surface of the choroid plexus consists of small villi each covered with a single layer of large cuboidal epithelial cells, electron-dense epithelial cytoplasm, well diffe-

Table 1. Morphometric data of choroid plexus blood vessels of young and adult rats (luminal diameter in μm and cross-sectional area in μm^2)

Blood vessels Diameter	1 month		10 months		13 months		22 months	
	Luminal diameter \pm SEM	Luminal area \pm SEM	Luminal diameter \pm SEM	Luminal area \pm SEM	Luminal diameter \pm SEM	Luminal area \pm SEM	Luminal diameter \pm SEM	Luminal area \pm SEM
5.0 – 7.5 μm	6.54 \pm 0.29	72.82 \pm 3.74	6.77 \pm 0.80	76.48 \pm 4.08	7.06 \pm 0.22	74.95 \pm 4.37	7.18 \pm 0.25	79.85 \pm 3.88
8.0 – 15.0 μm	11.35 \pm 0.28	177.27 \pm 6.95	11.53 \pm 0.37	192.14 \pm 8.24	11.10 \pm 0.30	188.77 \pm 9.69	11.32 \pm 0.33	190.39 \pm 8.25
15.5 – 30.0 μm	19.03 \pm 1.07	412.15 \pm 53.10	35.52 \pm 3.34	437.45 \pm 34.78	18.79 \pm 0.69	364.52 \pm 35.99	19.73 \pm 0.74	403.36 \pm 32.66
>30 μm	-	-	35.52 \pm 3.34	741.11 \pm 40.68	32.18 \pm 1.98	774.08 \pm 27.99	37.54 \pm 2.45	774.56 \pm 18.35
Number of measurements	324	324	280	280	262	262	350	350

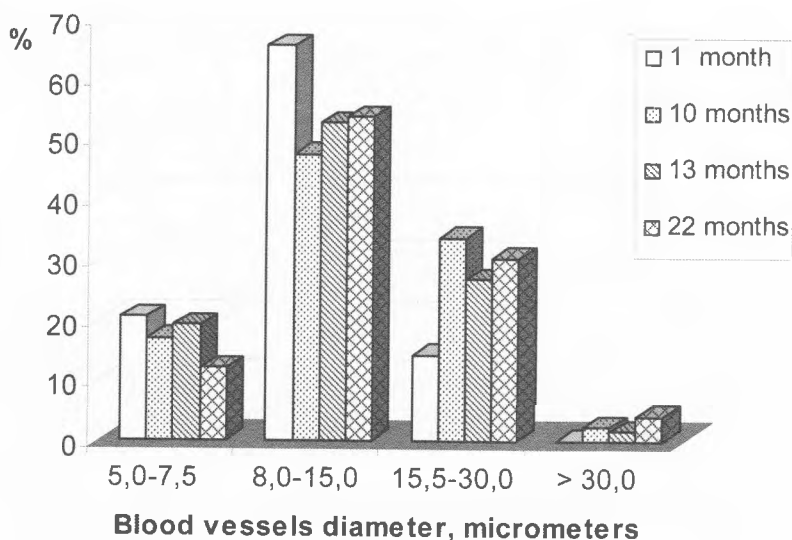


Fig. 1. Comparison of morphometric data of choroid plexus blood vessels in young and adult rats (relative part in %)

rentiated connective tissue elements and capillary with many fenestrations (1-month rat). The microvilli of the epithelial cells of the rat choroid plexus aged 10 and 13 months are fine, slender and dense, the nuclei of the epithelial cells are rounded, basally located and have relatively homogenous chromatin (Fig. 2). The cytoplasm of the dark epithelial cells contains more polyribosomes and endoplasmic reticulum. In the epithelial cytoplasm are seen many lipid droplets, imbibing mitochondria, dense bodies and electron-dense lysosome-like bodies with lamellar structures. These changes (22 months rats) might indicate a gradual change in function or at least a decrease in efficiency of the choroid plexus and may be evidence of slow degeneration of the rat choroid plexus.

Discussion

Up to present time little quantitative information has been available regarding the vessels of the brain, in particular, regarding the vessels of the rat choroid plexus. The capillaries of the plexuses had a large diameter and sinusoidal dilations, and showed the presence of occasional short, blind sprouts indicative of angiogenesis. Short anastomoses between arterioles supplying the plexuses and venules draining them were only rarely observed [13].

Statistical evaluation of data showed that the diameter and cross-sectional area of capillaries (vessels <15.0 μm in diameter) and that of large vessels (vessels of 15.5 – 30.0 μm and >30.0 μm in diameter) were statistically unchanged in the young and adult rats. The mean luminal diameter of blood vessels of 15.5-30.0 μm was $19.75 \pm 0.78 \mu\text{m}$ in the 10, 13 and 22 months rats. The mean cross-sectional area of capillaries (vessels <15.0 μm in diameter) in the young rats was $125.04 \pm 4.99 \mu\text{m}^2$ and the mean cross-sectional area of capillaries in adult rats was $133.76 \pm 6.41 \mu\text{m}^2$. Blood vessels with luminal diameter >30 μm have not been found in young rats and this may be related

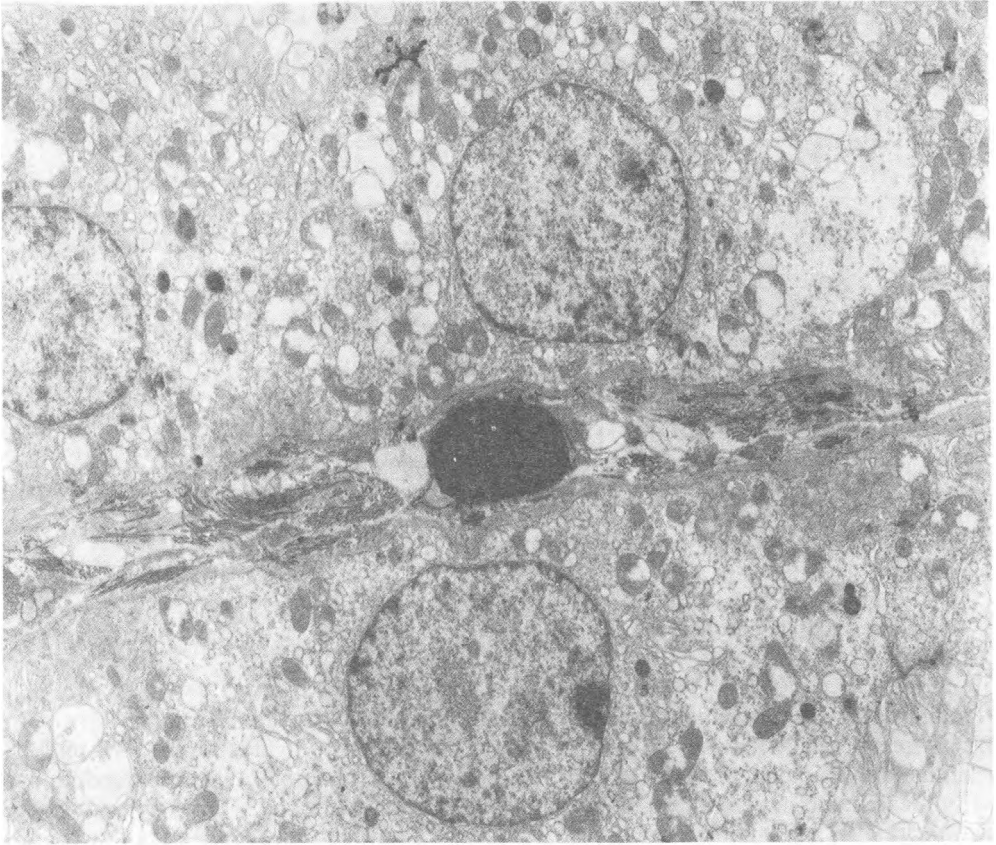


Fig. 2. Rat choroid plexus aged 13 months. The epithelial cells with a round nucleus, numerous microvilli, scanty connective tissue and blood vessel at the basal part of the epithelial cells. $\times 3\ 000$

with a larger number of the blood vessels with small luminal diameter, i.e. capillaries (85.80%) and blood vessels of 15.5 – 30.0 μm in diameter (14.20%).

The choroid plexus epithelium constitutes a physical barrier between blood and cerebrospinal fluid (the blood–CSF barrier – BCSFB) by virtue of the complexity of the tight junctions between adjacent epithelial cells. The age-related changes (22-month rats) might indicate a gradual change in function or at least a decrease in efficiency of the choroid plexus and may be evidence of slow degeneration of the rat choroid plexus [7, 9, 10].

The investigation of the age-related changes in choroid plexus indicate that normal ageing processes alter protein content in the CSF, CSF secretion and integrity of the BCSFB, which could impact on CSF homeostasis and turnover [1, 8].

Conclusion

These results indicate that the luminal diameter and cross-sectional area of the capillaries and large vessels of the plexus choroideus in the young and adult rat do not change. In young rats the blood vessels with luminal diameter $>30\ \mu\text{m}$ have not been found and

may be related with a larger number of the blood vessels with small luminal diameter, i.e. capillaries (85.80%). In adult rats the relative part of the capillaries is mean 67.25%. The ageing of choroid plexus in rats is morphologically characterized by atrophy of the epithelial cells and these functional changes could result in decreased choroid plexus functions of secretion, absorption and transport of substances and could play a part in normal homeostatic functions in CNS.

Acknowledgments: This study was supported by the project funded by the Bulgarian Academy of Sciences, Sofia, Bulgaria. The author is grateful to L. Voyvodova for excellent technical assistance at the TEM.

References

1. Chen, R. L., N. A. Kassem, Z. B. Redzic, C. P. C. Chen, M. B. Segal, J. E. Preston. Age-related changes in choroid plexus and blood–cerebrospinal fluid barrier function in the sheep. – *Experimental Gerontology*, **44**, 2009, No 4, 289-296.
2. Emerich, D. F., A. V. Vasconcellos, R. B. Elliott, S. J. M. Skinner, C. V. Borlongan. The choroid plexus: function, pathology and therapeutic potential of its transplantation. – *Expert. Opin. Biol. Ther.*, **4**, 2004, No 8, 1-11.
3. Johanson. C. E., J. A. Duncan, P. M. Klinge, T. Brinker, E. G. Stopa, G. D. Silverberg. Multiplicity of cerebrospinal fluid functions: New challenges in health and disease. – *Cerebrospinal Fluid Research*, 2008, **5**(1):10.
4. Karnovsky, M. J. A formaldehyde-glutaraldehyde fixative of high osmolarity for use in electron microscopy. – *J. Cell Biol.*, **27**, 1965. 137A.
5. Milhorat, T. H. Structure and function of the choroid plexus and other sites of cerebrospinal fluid formation. – *Intern. Rev. Cytol.*, **47**, 1976, 225-88.
6. Ormandzhieva, V. K. Morphometric analysis of epitheliocytes in the choroid plexus of brain ventricles in rat ontogenesis. – *Morfologija*, **124**, 2003, No 6, 30-33.
7. Ormandzhieva, V. K. Ageing choroid plexus and experimental models: morphometrical study. – *Compt. rend. Acad. bulg. Sci.*, **56**, 2003, No 7, 105-110.
8. Ormandzhieva, V. K. Morphometrical study of the nucleo-cytoplasmic index, cell height and width and nuclear localisation of the light and dark epithelial cells of the rat choroid plexus during development from 17 postconception days to 22 months postnatum. – *Compt. rend. Acad. bulg. Sci.*, **57**, 2004, No 8, 87-92.
9. Ormandzhieva, V. K., E. Petrova. Morphometrical and ultrastructural study of the choroid plexus blood vessels in young and adults rats. – *Compt. rend. Acad. bulg. Sci.*, **63**, 2010, No 2, 311-316.
10. Ormandzhieva, V. K. Rat choroid plexus: morphometric characteristics. – *Medical Data*, **2**, 2010, No 1, 47-50.
11. Weible E. R. Selection of the best method in stereology. – *J. Microsc.*, **100**, 1974, 261-269.
12. Wolburg, H., W. Paulus. Choroid plexus: biology and pathology. – *Acta Neuropathol.*, **119**, 2010, 75–88
13. Zagorska-Swiezy K., J. A. Litwin, J. Gorczyca, K. Pitynski, A. J. Miodonski. The microvascular architecture of the choroid plexus in fetal human brain lateral ventricle: a scanning electron microscopy study of corrosion casts. – *Journal of Anatomy*, **213**, 2008, No 3, 259-265.

Blood Supply of Canine Paranal Sinus

I. Stefanov, A. Vodenicharov, N. Tsandev

*Department of Veterinary Anatomy, Histology and Embryology, Faculty of Veterinary Medicine,
Trakia University, 6000 Stara Zagora, Bulgaria*

The investigations on macro- and microvascularization of the canine paranal sinus showed that the main vessels supplying it with blood were the dorsal perineal artery (from the caudal gluteal artery) and the caudal rectal artery – from the ventral perineal artery (a branch of the internal pudendal artery). From them, 1 or 2 Aa. sinus paranalisis are separated, that supply with blood the wall of the sinus. On their entry into the wall, they divide into branches that supply with blood the apocrine and sebaceous glands. These branches give rise to arterioles and capillaries forming a dense blood vessels network. The morphometric study showed that the size of arterioles and venules in the connective tissue between the basal membrane of the stratified squamous cornified epithelium and apocrine glands was smaller than that of arterioles and venules of connective tissue between apocrine glands and anal sphincters.

Key words: vascularization, sinus paranalisis, dog.

Introduction

By reason of the clinical importance of the paranal sinus in dogs [14] this organ has been subject to numerous histological and histochemical investigations [3, 7, 8, 9]. The information about the vascularization of canine paranal sinus is relatively scarce. According to Baker [1], the arteries supplying blood to the canine paranal sinus are the perineal artery, the caudal haemorrhoidal artery, branches of the internal pudendal artery and the caudal gluteal artery (the caudal branch of the internal iliac artery). These arteries are accompanied by the respective satellite veins. Gerisch and Neurand [5] demonstrated that in dogs, many capillaries were encountered in the vicinity of the sinus glands. From comparative point of view, the blood supply of anal sacs in cats are studied in detail. Godynicki et al. [6] reported that feline anal sac received blood from the ventral perineal artery and the caudal rectal artery, branches of the internal pudendal artery. In the view of the authors, the caudal rectal artery diverged in the anal sac wall and supplied it with blood, whereas the excretory duct of the anal sac receives blood mainly from the ventral perineal artery. Anal sac arteries ramify in its wall, giving rise to branches for apocrine glands (Rr. glandulae apocrine), sebaceous glands (Rr. glandulae holocrine) and the epithelium (Rr. epitheliales). These branches form small capillary networks. The venous drainage is performed by veins, oriented parallelly to arteries.

The scarce information about the blood supply of the paranal sinus in dogs motivated the present investigation aimed to clarify the macro- and microcirculation of the organ.

Material and Methods

Immediately after euthanasia of dogs with 5% Thiopental solution (Biochemie, Austria) i.v., the blood vessels of the pelvic cavity were washed with saline. For visualization, 5% solution of Indian ink-gelatin (37 °C) was injected [11] in the internal iliac artery of three male and two female mixed breed dogs at the age of 3-6 years.

Micrometric investigations were performed on permanent histological preparations stained with Erlich eosin made from material obtained from the paranal sinus of 8 healthy mixed-breed dogs euthanized with 5% Thiopental solution (Biochemie, Austria) i.v. and fixed in 10% formalin. The sized of blood vessels in the paranal sinus wall was measured by means of light microscope ZEISS Primo Star, Germany, camera Progres, Capture 2.6 – JENOPTIK Laser, Optic, and analysis programme of Soft Imaging Sistem GmbH.

Investigation of the microcirculatory bed

The blood vessels from the microcirculatory bed in the paranal sinus wall were visualized by the reaction of Sherer-Singler et al. [10], used to detect the enzyme histochemical expression of endothelial NADPH-diaphorase.

Immediately after the euthanasia, pieces of 1 cm³ were obtained from different parts of the organ and put immediately in 4% paraformaldehyde (Sigma Aldrich Chemie, Switzerland) in phosphate-buffered saline (PBS), pH 6.9, for 24 h at 4°C. Cross-sections of 10–20 µm were prepared on a freezing microtome (Slee, Mainz, Germany) and then, they were processed by the technique of Sherer-Singler et al. (1983) as free-floating sections by incubation in a solution containing nitro blue tetrazolium (0.2 mg/ml, Sigma Aldrich Chemie GmbH, Germany), β-NADPH (Santa Cruz Biotech, Santa Cruz, CA, USA) Triton X-100 (0.5%) (Merck Belgalabo, Overisje, Belgium) in PBS (0.1 M, pH 7.4) for 1-2 h at 37°C. This technique was chosen as the Indian ink-gelatin contrasting did not give a satisfactory result.

Cryostat cross-sections of 6–7 µm were prepared from the same areas. They were slide-mounted, fixed for 1 h in Carnoy's fixative, dehydrated in ascending alcohol series and stained with 0.1% solution of toluidine blue in McIlvane's buffer, pH 3 [12].

Histochemical detection of collagen and elastin fibres in blood vessels' wall

Material from the paranal sinus wall was fixed in 10% neutral formalin, dehydrated in alcohol series, cleared in xylene and embedded in paraffin. Paraffin cross sections of 5–7 µm were stained with Elastica Van Gieson Staining Kit (MERK, Germany); collagen fibres were stained in red and elastic fibres – in black.

Data were statistically processed by the *t*-test, StatMost for Windows, at a level of significance $P < 0.05$.

Results

Using carcasses filled in situ with Indian ink-gelatin through the iliac artery, we demonstrated that the vascularization of the canine paranal sinus was performed by the dorsal perineal artery, a branch of the caudal gluteal artery and by the caudal rectal

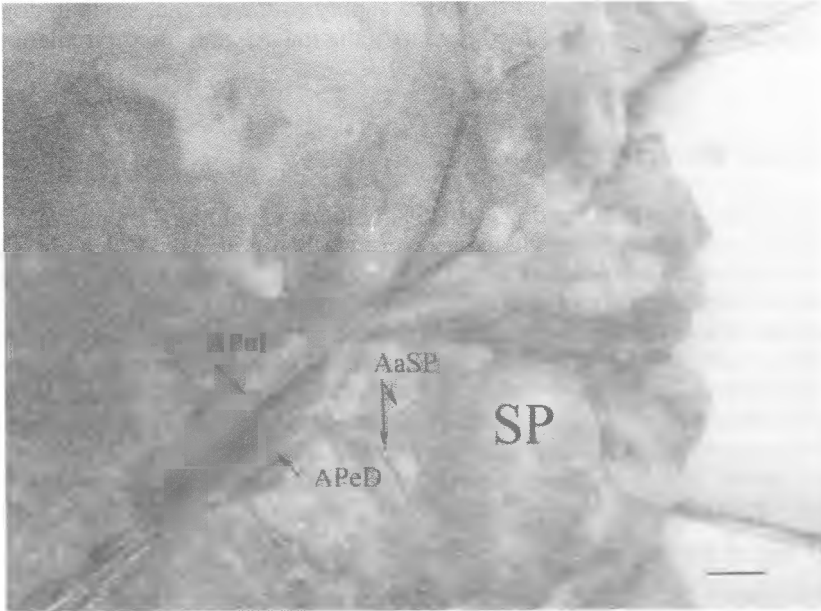


Fig. 1. Both Aa. Sinus Paranalis (ASP) Separate with a Common Trunk from A. Perinealis Dorsalis (ApeD), a Branch of A. Glutea Caudalis. APuI – A. Pudenda Interna ; SP – Sinus Paranalis. Blood Vessels Filled with Indian Ink-Gelatin. Bar=1cm

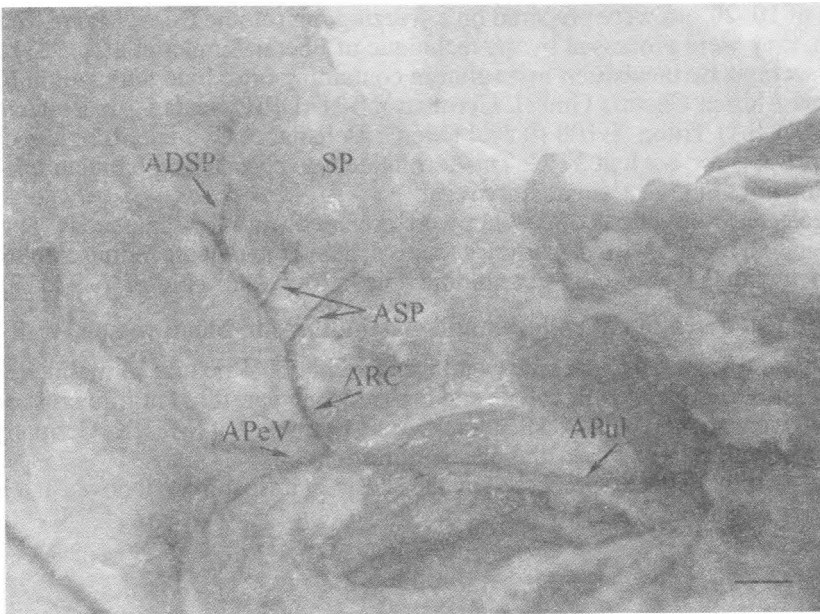


Fig. 2. Both Aa. Sinus Paranalis (ASP) Separate Individually from A. Rectalis Caudalis (ARC), a Branch of A. Perinealis Ventralis (APeV) (Branch of A. Pudenda Interna: APuI). A. Ductus Sinus Paranalis (ADSP) also Separates from ARC. SP – Sinus Paranalis. Blood Vessels Filled with Indian Ink-Gelatin. Bar=1cm

artery – branch of the ventral perineal artery (branch of the internal pudendal artery). In the different subjects, the dorsal perineal artery ramifies in 1 or 2 branches near to the paranal sinus, which represent Aa. sinus paranalisis (Fig. 1). One or two anal sac arteries also diverged from the caudal rectal artery, either independently or from a common trunk (Fig. 2). After reaching the sinuses, Aa. sinus paranalisis give branches for the external anal sphincter, the apocrine and holocrine glands, and further ramify in the sub epithelial connective tissue, forming a dense network in the sinus wall. The branches for apocrine glands formed a glandular vascular network, some vessels from which penetrated among the acini and formed a periacinar vascular network. The veins accompany the respective arteries and joined the veins of the sinus. The blood supply of paranal sinus apocrine glands was done by branches for apocrine glands, originating from the arteries of the sinus. Adjacently to tubules, they continued into a periglandular capillary network, from where the blood passed into a peritubular capillary network, visualized by both toluidine blue staining and by detection of a moderate expression of NADPH-d activity in the vascular endothelium. The branches directed onto the basal membrane of the epithelium formed a subepithelial capillary network.

The light microscopy of microcirculatory bed vessels showed that the tunica interna of arterioles was composed of an endothelial layer, a thin subendothelial layer and an inner elastic membrane. This membrane was absent or only some segments of it were preserved in the smallest arterioles of a size $< 12 \mu\text{m}$. The tunica media contained 1-3 layers of smooth muscle cells. The external elastic membrane was absent. The tunica externa consisted of loose connective tissue where collagen fibres prevailed. The size of arterioles ($33.9 \pm 14.1 \mu\text{m}$, mean \pm SD) in the subglandular connective tissue (SGC) and in the interstitial tissue (IS) between the tubular apocrine glands was statistically significantly bigger than that of arterioles ($12.8 \pm 4.5 \mu\text{m}$, mean \pm SD) in the subepithelial connective tissue (SEC). Arterioles arborized into dense capillary networks. The wall of capillaries was represented by the tunica interna, that contained an endothelial layer with 1-3 endothelial cells, basal lamina and pericytes. The size of venules was also variable: from $13.7 \pm 2.9 \mu\text{m}$ (mean \pm SD) in the subepithelial connective tissue to $53.6 \pm 19.2 \mu\text{m}$ (mean \pm SD) in the subglandular connective tissue. Postcapillary venules had a structure similar to that of capillaries, but with larger lumens. They passed into venules of a larger size with a continuous pericyte layer. With increase in venules' size, a smooth muscle cell layer (muscle venules) was formed. Although thin, the tunica externa was also observed.

The excretory duct of the paranal sinus in this investigation was found to be vascularized by A. ductus sinus paranalisis, originating from the caudal rectal artery (Fig. 2). The size of arterioles and venules in the excretory duct stroma also decreased towards the stratified squamous cornified epithelium.

Discussion

The vascularization of canine paranal sinus through the dorsal perineal artery, observed in this study, was similar to data reported by Baker [1]. In our investigation, however, we describe for the first time the blood vessels that enter and ramify into the wall of the sinus. These vessels were called by us Aa. sinus paranalisis by analogy to the vessels in cats illustrated by Godynicki et al. [6]. With regard to the way Aa. sinus paranalisis separate, our results support the findings of Godynicki et al. [6] that feline sinus arteries were more numerous (2-5). The data from our observations on intraorgan vessels and microcirculatory bed allowed us to assume that the vascularization in the dog was similar to that described by Godynicki et al. [6] in the cat. The names of branches as

suggested by these authors, could be also used for the respective branches in dogs. For example, after reaching the sinuses, Aa. sinus paranalisis give rise to branches for the external anal sphincter muscle, for apocrine glandular tubules and holocrine glands, termed as Rr. glandulae apocrinae and Rami glandulae holocrinae in the cat, and then arborize in the subepithelial connective tissue (R. mucosae) and form a blood vessels network in the sinus wall. Rami glandulae holocrinae form a periglandular blood vessel network, from where blood vessels penetrate among the acini to form a periacinar capillary network. Venous vessels accompany the respective arterioles and join the sinus veins. The blood supply of apocrine sinus glands is performed by Rami glandulae apocrinae, originating from the sinus arteries or from Rami glandulae holocrinae [6]. In the vicinity of tubules, they go on in a periglandular vascular network that was visualized by toluidine blue staining and by the moderate degree of NADPH-d expression in the vascular endothelium. The expression of NADPH-d activity in paranal sinus vascular endothelium assisted for their visualization and also, provided evidence for confirming the conclusion of Bull et al. [2] about the influence of nitric oxide on skin blood vessels. By the measurements of the size of blood vessels from the microcirculatory bed, we add to the information of Godynicki et al. [6] about the vascularization of feline paranal sinus. The size of capillaries in the subglandular, interstitial and subepithelial connective tissue varied from 2.9 to 8.1 μm [4]. The size of arterioles and venules was statistically significantly bigger in the subglandular and interstitial connective tissue as compared to the size of these vessels in the subepithelial connective tissue ($p < 0.001$). The Van Gieson staining showed that the inner elastic membrane was absent in arterioles of a size under 12 μm or only some segments were preserved. This confirmed the findings of Dellmann and Eurell [4], about the disappearance of the inner membrane or presence of some segments only from the smallest arterioles.

The excretory duct of the canine paranal sinus was vascularized by A. ductus sinus paranalisis, originating from the caudal rectal artery – branch of the ventral perineal artery, dissimilar to cats where the A. ductus sinus paranalisis comes from the ventral perineal artery [6]. The size of arterioles and venules in the excretory duct stroma also found to decrease towards the stratified squamous cornified epithelium, thus adding to the available information about canine paranal sinus vascularization.

In conclusion, this study showed that the wall of the paranal sinus, including its excretory duct in dogs was richly vascularized, determining an enhanced production of secretion from apocrine glandular tubules and holocrine acini.

References

1. Baker, E. Diseases and therapy of the anal sacs of the dog. – Journal of the American Veterinary Medical Association, **141**, 1962, 134-1350.
2. Bull, H., J. Hotherhall, N. Chowdhury, J. Cohen, P. Dowd. – Neuropeptides induce release of nitric oxide from human dermal microvascular endothelial cells. Journal of Investigative Dermatology, **106**. 1996, 655-660.
3. Coquot, A., C. Bresson, M. Monet. Glandes anales du chien. – Recueil Med. Vet., **109**, 1933, 385-393.
4. Dellmann, H., J. Eurell, 1998. Textbook of Veterinary Histology. Lippincott Williams & Wilkins, Baltimore, 115-120.
5. Gerisch, D., K. Neurand. Topographie und Histologie der Drüsen der Regio analis der Hundes. – Anatom. Histolog. Embryol., **2**, 1973, 280-294.
6. Godynicki, S., M. Flachsbarth, R. Schwarz. Die Gefäßversorgung der Analbeutel der Hauskatze. – Annals of Anatomy, **177**, 1995, 421-426.
7. Montagna, W., H. Parks. A histochemical study of the glands of the anal sac of the dog. – Anat. Rec., **100**, 1948, 297-315.

8. Sokolov, V., S. Shabadash, A. Zelikina. Alkaline phosphatase in the cutaneous glands and vessels in the rat and mouse. – Doklady Akademii Nauki SSSR, **281**, No 6, 1985, 1450–1454.
9. Salazar, I., P. Fdez de Troconiz, M. Prieto, J. Cifuentes, P. Quinteiro. Anatomy and cholinergic innervation of the sinus paranasalis in dogs. – Anatomia, Histologia, Embryologia, **25**, 1996, 49-53.
10. Sherer-Singler, U., S. R., Vincent, H. Kimura et al. Demonstration of a unique population of neurons with NADPH-diaphorase histochemistry. – Journal of Neuroscience Methods **9**, 1983, 229-234.
11. Simoens, P., A. Vodenicharov, D. Dimitrov, W. Van den Broeck, H. Lauwers. Arteriolar and glomerular dimensions in the porcine renal cortex: a morphometric study on corrosion casts and histological sections. – Bulgarian Journal of Veterinary Medicine, **3**, 2000, No 1, 1-12.
12. Pearce, A. Histochemistry, 2nd edn. London: J. & A. Churchill Ltd., 1960: 692.
14. Van Duijkeren, E. Disease conditions of canine anal canal. – Journal of Small Animal Practice, **36**, 1995, 12-16.

Morphogenesis of the Hip Joint. Plastination-Histological and Electron Microscopic Studies

I. Vasilev, V. Vasilev**, D. Andreev***

** Center of Sport Traumatology, Uhingen, Germany*

*** Department of Anatomy and Histology, Medical University Sofia*

Hip joints of 4-6 months old human fetuses were examined with the plastination histological technique. In addition, transmission and scanning electron microscopic analysis of the elements of hip joints of Wistar rat embryos was performed. Attention was paid to the structural changes taking place during the differentiation of the skeletal anlagen, the synovial membrane, the internal joint structures (i.e. the labrum acetabulare, the lig. transversum acetabuli, the lig. capitis femoris, the capsule) and the extra articular ligaments.

Key words: hip joint, morphogenesis, plastination-histological technique, electron microscopy.

Introduction

The hip joint is a leading link of the kinematic chain of the lower limb. Because of the erect posture of man, it also fulfils supportive functions. This has affected both its normal structure and its pathology – coxarthrosis for instance is one of the most frequent diseases of the locomotory apparatus. Also very frequent are the congenital dysplasia and luxation of the hip joint. For their clarification, information on the morphogenesis of this joint is necessary.

The morphogenetic studies available of the hip joint have been carried out with routine histological techniques and concern mainly the skeletal elements (Gardner and Gray, 1950; Strayer, 1971; Dorskocil, 1984; Tillmann, 1990). In our study the plastination histological technique was used, for it preserves the relationships between tissues possessing different density and thus provides the opportunity for the differentiation not only of the skeletal elements but also of the other joint structures to be investigated (Fritsch, 1989; Fritsch and Hegemann, 1991; Vassilev I., 1997). In addition, transmission and scanning electron microscopic (TEM and SEM) analysis of hind limb anlagen of animal embryos was performed, for it provides information on the ultrastructural changes of the cell populations and the extracellular matrix during the development of joints (Roy and Ghadially, 1964; Wassilev W, 1972; Vidinov, 1979).

Materials and Methods

With the plastination-histological technique, hip joints of 3-6 months old human fetuses of the two sexes were examined. After fixation and dehydration in toto, the pelvises were impregnated in vacuum with epoxy resin (Biodur R E12, E6 and E600) and cut with diamond saw (Well, Manheim) in 300-600 μm thick cross, saggital and frontal sections. The sections were polished and then stained with Azur II-Methylene blue (Fritsch and Hegemann, 1991).

The electron microscopic analysis of the developing hip joint structures was performed on 14-21 days old Wistar rat embryos. The samples were processed according to the routine TEM and SEM technique and examined with electron microscopes Hitachi 11 A (60 kV) and Philips SEM 505 (10-30 kV).

Results

The limb anlagen are made up of mesenchymal cells interconnected through their outgrowths. The intercellular spaces are optically empty (Fig. 1). Later, the cells differentiate in chondroblasts rich of organelles. In addition, matrix with collagen fibers is formed, and the cartilaginous skeletal anlagen occur. Between them the joint intermediate cleft is situated, in which the joint cavity, outlined by the joint capsule, is formed (Fig. 2). From the internal part of the capsule an abundantly vascularized synovial membrane differentiates (Fig. 3).

The skeletal elements of the joint occur after birth and are at first cartilaginous. The femur possesses a round head and a short neck with numerous vascular canals in them (Fig.4). At first the acetabulum is shallow. In the hipbone quick mineralization takes place. The acetabular labrum differentiates as a fibrous ring with a wide basal portion

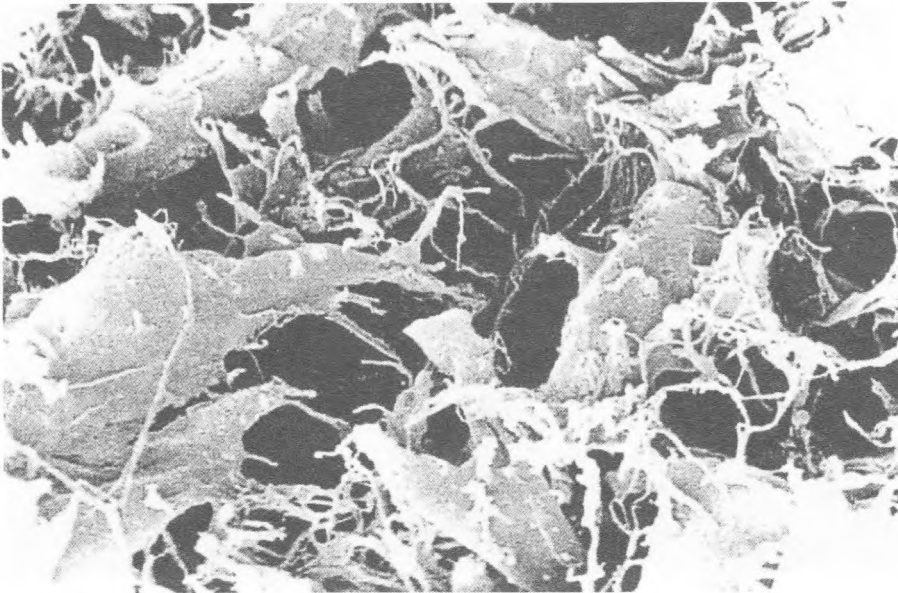


Fig. 1. Mesenchymal cells of a limb anlage of a 15 days old rat embryo. SEM

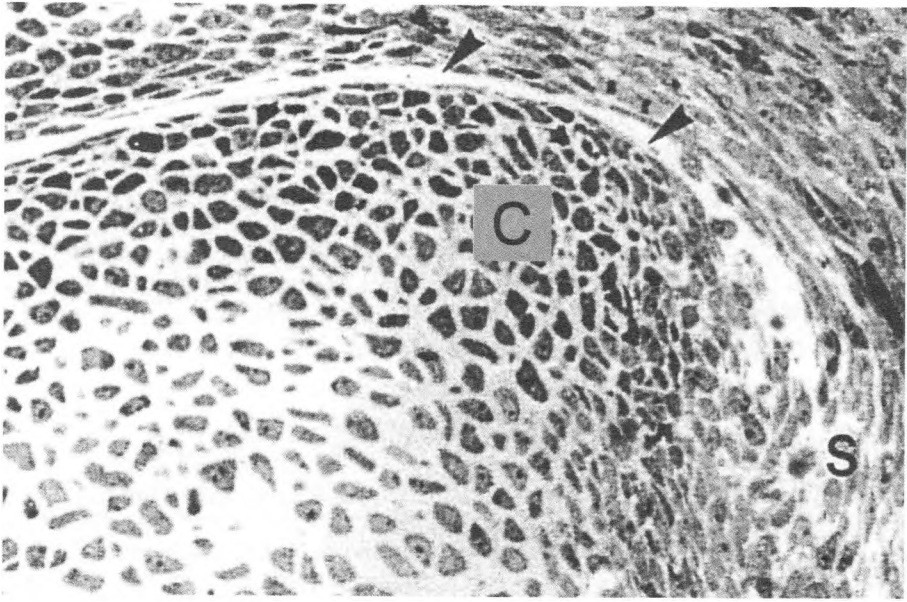


Fig. 2. Cartilaginous skeletal anlage (C), joint cleft (arrowheads) and joint capsule with synovial membrane (S) of an 18 days old rat embryo

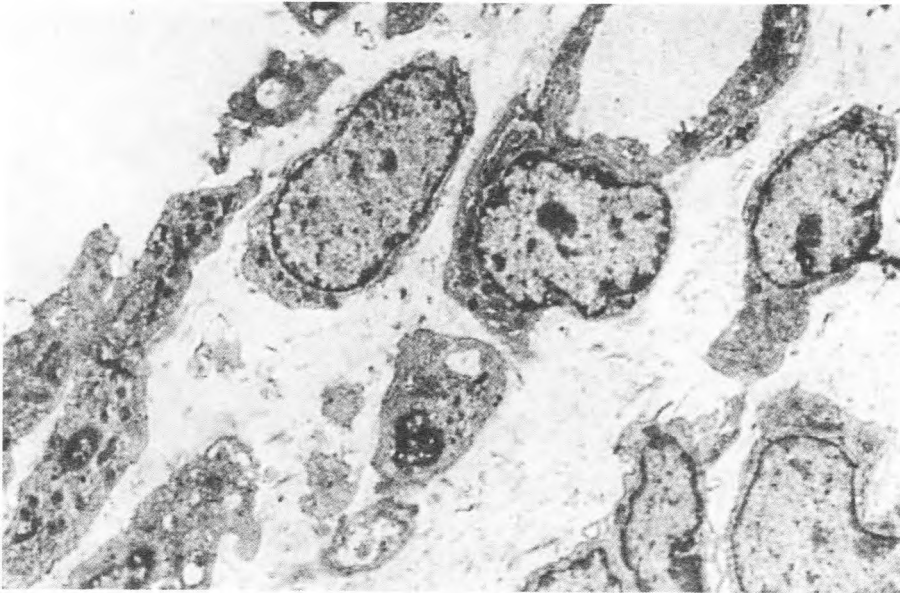


Fig. 3. Synovial membrane of the capsule of the hip joint of a 20 days old rat embryo. TEM



Fig. 4. Hip joints of a 4 months old human fetus. Plastination section

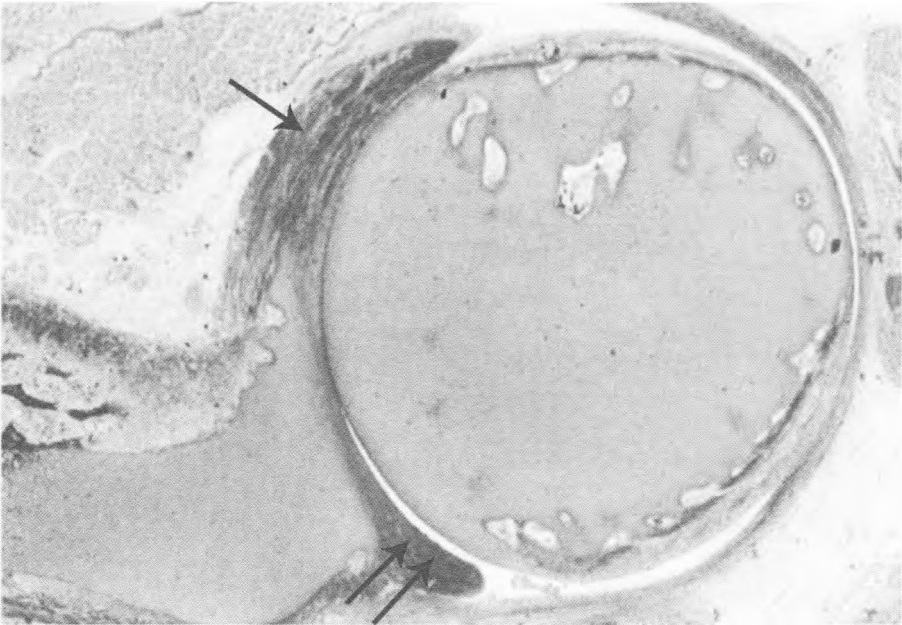


Fig. 5. Cranial (single arrow) and caudal (double arrows) portion of the labrum acetabulare of a 4 months old human fetus

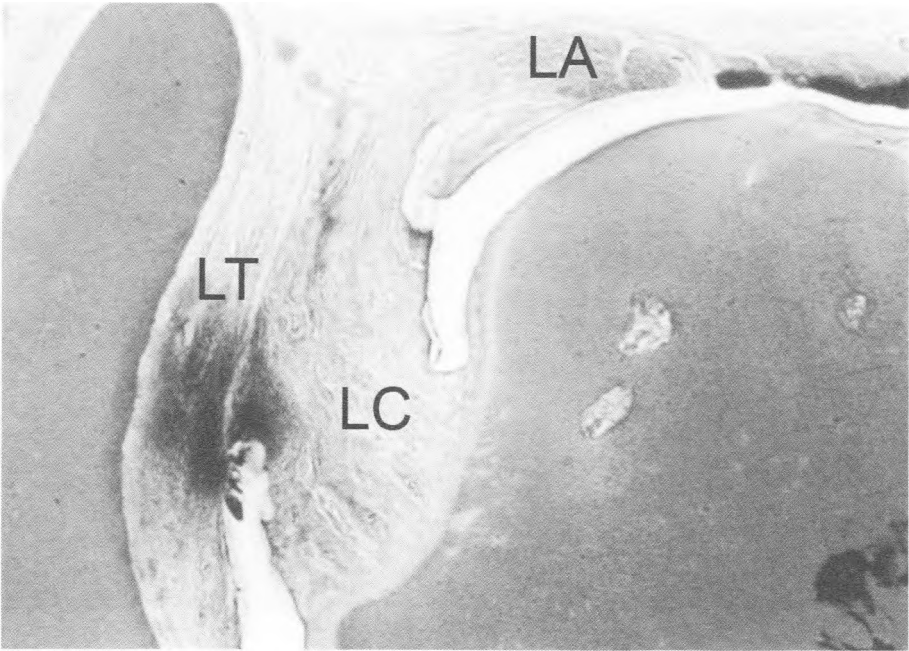


Fig. 6. Lig. transversum acetabuli (LT), lig. capitis femoris (LC) and labrum acetabulare (LA) of a 5 months old human fetus

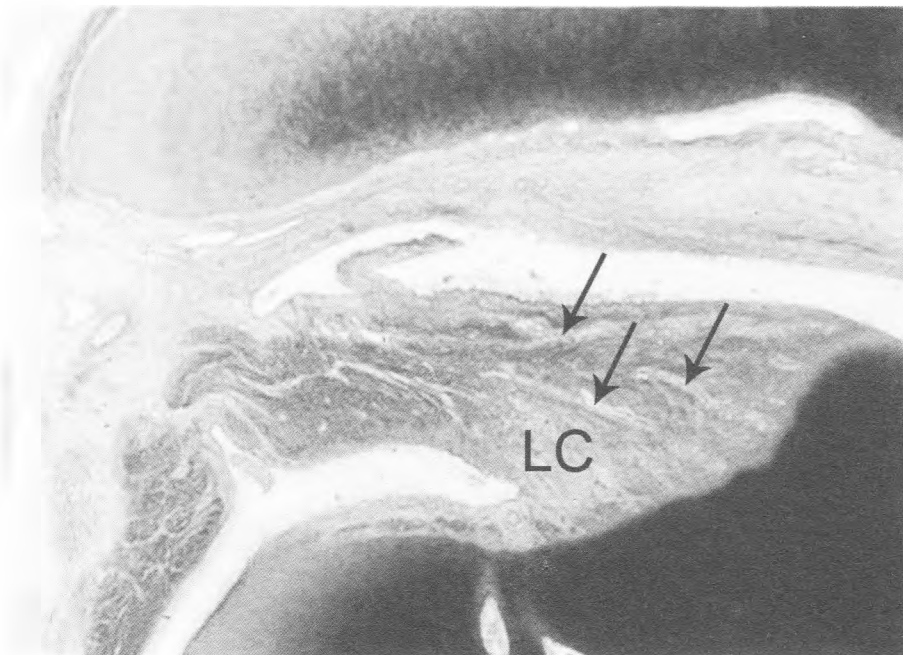


Fig. 7. Lig. capitis femoris (LC) of a 5 months old human fetus with vascular canals (arrows)

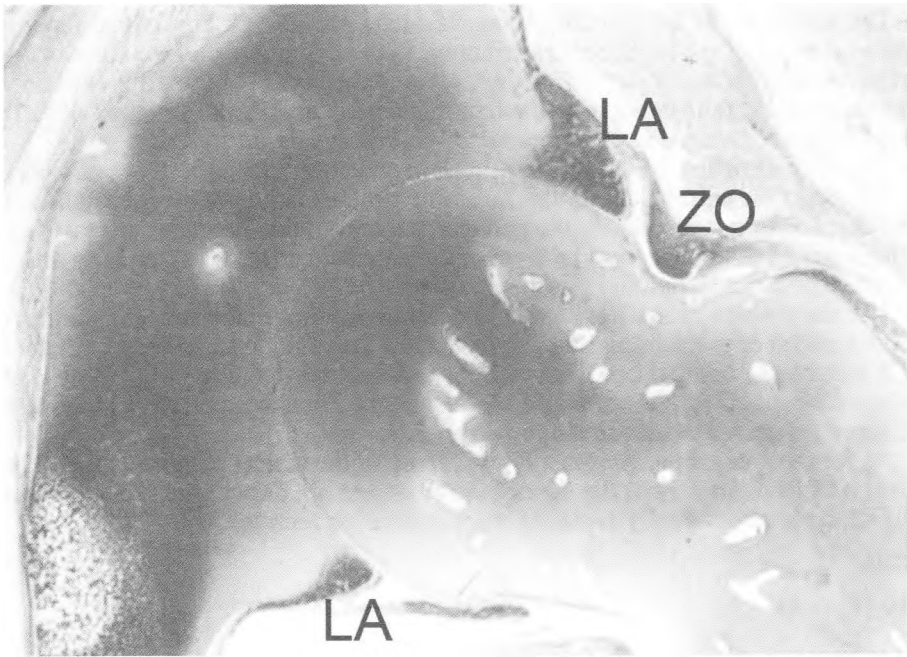


Fig. 8. Zona orbicularis (ZO) and labrum acetabulare (LA) of a 5 months old human fetus

(caudal labrum) whose collagen fibers penetrate the embryonic cartilage. The ring is abundantly vascularized during all the stages of development. Its upper portion (cranial labrum) is much more prominent and covers the femoral head (Fig. 5).

The internal joint structures differentiate in parallel with the articulating surfaces, and at first look like mesenchymal condensations. With advancing time, the amount of collagen fibers in them gradually increases. The lig. transversum acetabuli and the lig. capitis femoris are formed together with the caudal labrum (Fig. 6). The lig. capitis femoris occurs in the intermediate zone of the joint and retains its location between the skeletal anlagen. Between the collagen bundles making it up, numerous vascular canals are present (Fig. 7).

The joint capsule, the zona orbicularis and the extra articular ligaments appear as accumulations of collagen fibers (Fig.8).

Discussion

The study corroborates the data of other authors (Gray and Gardner, 1950) about absence of essential differences in the main stages of the development of the hip and other joints. An important stage of the formation of the skeletal elements is the occurrence of chondroblasts, that produce precursors of the extracellular matrix.

The hip joint structures originate from the joint intermediate zone. Together with the chondrification of the skeletal anlagen, differentiation of the synovial membrane takes place. It includes differentiation of functionally different synovial fibroblasts and synovial macrophages that provide the homeostasis of the joint (Wassilev, 1981).

The formation of the chondrogenous skeletal anlage of the proximal femur gets ahead of the one of the hipbone. Contributing to the congruency of the joint is the acetabular labrum. Its upper portion predominates in the course of the differentiation and undertakes a part of the pressure of the femoral head. The internal structure of this portion is the one of an abundantly vascularised connective tissue complex.

The differentiation of the lig. transversum acetabuli lags behind when compared with the one of the acetabular labrum. As a result of the loading of the joint and because of the absence of a skeletal pad, the collagen content in this ligament increases, and a cartilaginous covering occurs. The latter complements the facies lunata as an articulating surface of the acetabulum.

The importance of the lig. capitis femoris to the hip joint biomechanics and trophics is a matter of great discussion. Given that the articulating surfaces at birth are only in part congruent, the ligament most probably contributes to the stability of the joint. In addition, by containing a lot of blood vessels (as the ultrastructural analysis reveals) it undoubtedly contributes also to the joint trophics.

As for the congenital dysplasia of the hip joint, the results obtained suggest that it is a result of deviations from the normal development not only of the skeletal elements but of all the joint structures including the surrounding muscles.

References

1. Doskocil, M. Contributions to the study of human hip joint development – Acta Univ. Carol. Med. Praha, **30**, 1984, 529-544.
2. Fritsch, H. Staining of differential tissue in thick epoxy resin impregnated sections in human fetusses – Stain Technol., **64**, 1984, 75-79.
3. Fritsch, H., Hegemann, L. Entwicklung des Ligamentum capitis femoris und der gleichnamigen Arterie – Z. Orthop., **129**, 1991, 447-452.
4. Gardner, E., Gray, D. Y. Prenatal development of the human hip joint – Am. J. Anat., **87**, 1950, 163-192.
5. Roy, S., Ghadially, F. Ultrastructure of normal rat synovial membrane – Ann. Rheum. Dis., **26**, 1964, 26-38.
6. Strayer, L. Embryology of the human hip joint – Clin. Orthop., **74**, 1971, 21-26.
7. Tillmann, B. Entwicklung des Hüftgelenks – Z. Orthop., **128**, 1990, 338-340.
8. Vassilev, I. Morphologische Untersuchungen des Hüftgelenks während der pränatalen Entwicklung und bei angeborener Hüftdysplasie – Diss. Med. Universität Luebeck, 1997.
9. Vidinov, N. Electron microscopic investigation on the articular cartilage of rats during early prenatal morphogenesis – Compt. rend. Acad. bulg. Sci., **32**, 1979, 989-992.
10. Vassilev, W. Elektronenmikroskopische und histochemische Untersuchungen zur Entwicklung des Kniegelenks der Ratte – Z. Anat. Entw.-Gesch., **137**, 1972, 221-238
11. Vassilev, W. Funktionelle Struktur der Synovialmembran – Verh. Anat. Ges. (Anat. Anz. Suppl.), **75**, 1981, 221-234.

Ultrastructural Characteristics of the Layer Stratum Compactum in Feline Stomach Mucosa

P. Zahariev

*Faculty of Veterinary Medicine, University of Forestry, 1756 Sofia,
10 Kl. Ohridski Str., Bulgaria*

The aim of the present study was to determine the ultrastructural arrangement of the specific layer stratum compactum at the cat stomach mucosa using electronmicroscopic technics.

The ultrastructure of the layer stratum compactum from the lamina propria mucosae of the feline stomach was investigated by transmitted electron microscope. The specific characteristic of the reticular disposition of the bundles of collagen fibres building the layer stratum compactum were established. The collagen fibres are associated with fibroblasts as well as with muscle cells from the lamina muscularis mucosae. Thus the collagen structure has determinant importance for the stomach wall solidity.

Key words: feline, stomach, mucosa, stratum compactum.

Introduction

The layer stratum compactum from the stomach mucous structure in carnivores is specific structure of the stomach wall in comparison with other mammals [2, 6]. It is located between the bases of the mucous glands and the muscle lamina of the stomach mucous membrane. Earlier it was called lamina subglandularis and it was considered that present into the stomachs of the all carnivorous [1, 8, 9, 11, 12]. The information about its designation and compound is poor. We established the presence of the layer stratum compactum in stomachs from domestic and wild cats but it was absent from the canine and fox stomachs [7]. The investigations by immunohistochemical methods showed the very high expression of collagen type IV and fibronectin, moderate positive reaction of collagen type III, and a comparatively weakest expression of collagen types I and V in the structure of stratum compactum from cat stomach mucosa [10].

The aim of the present study was to determine the ultrastructural arrangement of the specific layer stratum compactum at the cat stomach mucosa using electronmicroscopic technics.

Materials and Methods

Two cats (*Felis silvestris catus*), were included for electronmicroscopic investigations. The pets were under general narcosis by treatment with sodium pentobarbital (40 mg/kg) by intraperitoneal injection and the ethical principles and legal requirements for the welfare of the animals were kept. Then the animals were perfused transcardially with 500 ml phosphat buffered saline (PBS) with pH 7.4 containing 2.5 % glutaraldehyde and 4 % paraformaldehyde. After the perfusion and laparotomy the biopsy material was stored in the same fixative for 2 h. Biopsy was taken by partial gastrotomies from the stomach anatomic regions pars cardiaca, pars fundica and pars pylorica. Sections were postfixed with 1 % OsO₄ in PBS for 1 h dehydrated in graded series of ethanol and flat embedded in Durcupan (Fluka, Buchs, Switzerland) between acetate sheets. Blocks were trimmed out under a dissecting microscope and glued to epoxy blanks. Thin sections were cut with ultramicrotome (LKB, Stockholm-Bromba, Sweden). Sections were counterstained with uranyl acetate and lead citrate. Observation and fotodocumentation on magnification 10000× and 16000× were performed by electron microscope (500 Hitachi, Tokio, Japan).

Results and Discussion

In the mucosa layer in all areas of the cat stomach there are exocrinocytes and endocrinocytes from the gland tubules and between them the fascicles of collagen fibers filling the intercellular matrix. The ultrastructure of the cells shows characteristic features described in other publications [4, 7, 10].

In the deep part of the lamina propria mucosae under the gastric glands various sections through the fascicles of collagen fibers are found (Fig. 1). The collagen fas-

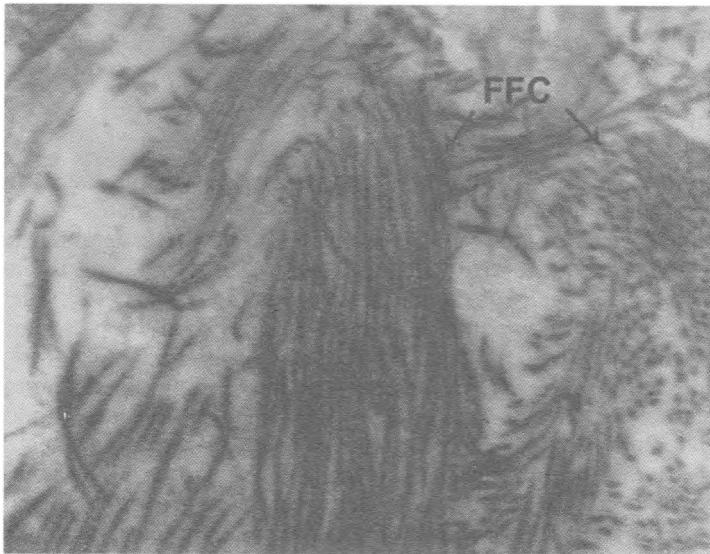


Fig. 1. Electronograma of reticular interweaved bundles of collagen fibres from the stratum compactum of the fundic region of the feline stomach. FFC – fasciculus fibrae collagenosae. 16000×

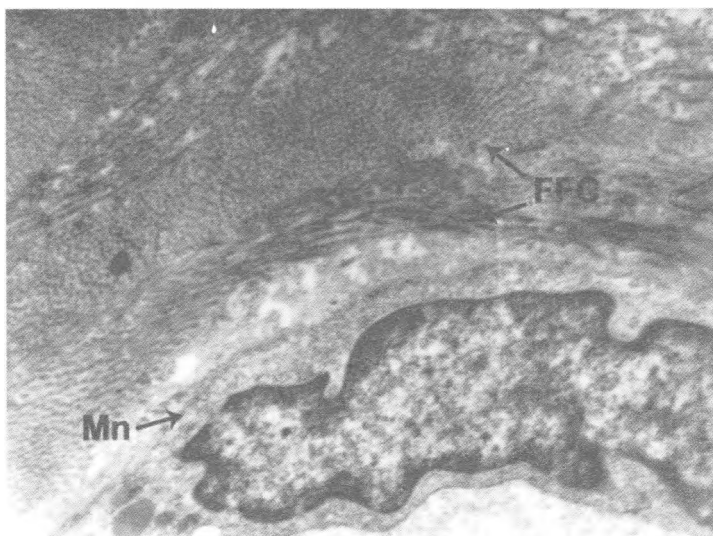


Fig. 2. Electronograma of myocytus nonstriatus from lamina muscularis mucosae associated with collagen fibres bundles of the layer stratum compactum. FFC – fasciculus fibrae collagenosae, Mn – myocytus nonstriatus. 10000×

cicles that build up the dense layer – stratum compactum of the cat stomach are cut at various angles. This determines the meshwork location of the fascicles that ensures their strength and elasticity. The longitudinal sections of the fascicles of collagen fibers show the cross lines of the collagen fibers and the lines are succeed in 640 Å [3]. The collagen fibers cross sections have oval sectional surface, which determines their trend to form fascicles of certain thickness and compactness. The collagen secreting fibroblasts are found on the fascicles surface bordering the gastric glands bottoms. They have specific heterochromatic nuclei and the chromatin is mainly located on the inner surface of the nuclear membrane. Its amount is smaller in the central part of the nucleus. On the collagen fascicles surface, from the side of lamina muscularis mucosae, a smooth muscle cells that seem associated with the collagen fibers are seen. Their heterochromatic nuclei are extended with deep invaginations of the nucleolema and typical position of the chromatin (Fig. 2). The opinion that smooth muscle cells secrete collagen like fibroblasts [5], support the hypothesis that they also contributed the construction of the stratum compactum layer by consolidation of its compound. All this data, as well as the increased presence of collagen fibers into the cat stomach wall mucosa, ensure its firmness when stretched, which is related to the increasing pressure when carnivorous animals are eating bones.

Conclusion

The electron microscopic observations of the subglandular layer stratum compactum show the expressive network formation of the collagen fascicles.

The layer stratum compactum is located just above to the lamina muscularis mucosae and these smooth muscle cells are probably related to its formation.

Acknowledgements. The investigation was financially supported by the Grant 118/2008 of the University of Forestry, Sofia

References

1. Bacha, W. Jr., L. M. Wood. Digestive system. – In: Color Atlas of Veterinary Histology (Ed. W. Bacha) Williams and Wilkins, Media, USA, 1990, 112-135.
2. Farppier, B. L. Digestive system. – In: Textbook of Veterinary Histology (Ed. H.-Dieter Dellmann and J. Eurell) Williams & Wilkins, USA, 1998, 164-180.
3. Hulmes, D.J. Building collagen molecules, fibrils, and suprafibrillar structures. – J. Struct. Biol., **137** (1-2), 2002, 2-10.
4. Lentz, Th. L. Cell fine structure. – In: An atlas of drawings of whole-cell structure. (Ed. T. L. Lentz) W. B. Saunders company, Philadelphia, London, Toronto. 1971, 64, 164-175.
5. Stevens, A., J. Lowe. – In: Histology (Ed. Stevens, A., J. Lowe) Mosby, England, 1992, 42-51.
6. Nomina histologica. Histologia generalis. International Committee on Veterinary Histological Nomenclature, Gent, 1992, 15, 37.
7. Sapundzhiev, E., P. Zahariev, D. Pupaki. Morphologic investigation of the stomach mucosa characteristics in dogs and cats. Suppl. XVII Europ. Congress Vet. Anat., Budapest, **3**, 2008, 32.
8. Smollich, A. Verdauungssystem. – In: Mikroskopische Anatomie (Ed. H. Sajonski and A. Smollich) S. Hirzel Verlag, Leipzig, 1972, 125-233.
9. Stinson, Al. W. M. Lois Calhoun. Digestive system. – In: Textbook of Veterinary Histology (Ed. H.-Dieter Dellmann) Lea & Febiger, Philadelphia, 1993, 153-193.
10. Zahariev P., E. Sapundzhiev, D. Pupaki, P. Rashev. Morphologic characteristics of the stomach mucosa in carnivores. – J. Biomedical and Clinical Res. **1**, 2009, 1, 27-31.
11. Витанов, С., Д. Димитров, А. Бочуков. Храносмилателна система – В: Ръководство за упражнения по цитология и хистология, София, Земиздат, 1995, 89-90.
12. Кръстев, Х., С. Витанов. Храносмилателна система – В: Учебник по цитология и хистология, София, Земиздат, 1993, 251-255.

Expression of Testicular Angiotensin I – Converting Enzyme in Ageing Spontaneously Hypertensive Rats

N. Atanassova[#], E. Lakova^{#}, S. Popovska^{*}, M. Donchev^{*},
G. Krasteva^{*}, V. Nikolov^{*}*

*Institute of Experimental Morphology, Pathology and Anthropology with Museum, Bulg. Acad. Sci, Sofia,
Medical Faculty, Medical University, Pleven

[#]N.A. and E.L. contributed equally to this study and should be considered as joint first authors

Recent studies demonstrated that testicular angiotensin-converting enzyme (tACE) is essential for fertilizing ability of spermatozoa and the enzyme is regulated by androgens. Relationship between hypertension, disturbance of spermatogenesis and androgen production is suggested. Dramatic changes occurred in the testis during ageing resulting in declined testosterone and sperm production. The aim of the present paper is to investigate the effect of both ageing and spontaneous hypertension on the expression of tACE. The normal stage-specific pattern of ACE immunoreactivity was seen in ageing spontaneously hypertensive rats (SHR) but lack of expression was found due to depletion of corresponding stages of spermatid maturation. Values of gonado-somatic index, blood pressure and serum testosterone levels are significantly elevated. Testicular ACE also could serve as a marker for germ cell depletion during aging and pathological conditions.

Key words: angiotensin-converting enzyme, ageing testis, SHR, androgens.

Introduction

ACE is an important component of renin-angiotensin system. Two isoforms – somatic (sACE) and testicular (tACE) are known. Substrate of tACE is not known. In contrast to sACE, tACE does not generate vasoconstrictor peptide Angiotensin II and it is not blocked by ACE inhibitors [4]. tACE is localized in developing male germ cells during elongation of spermatids. tACE plays an important role in the control of the male reproduction [5], being essential for fertilizing ability of spermatozoa [7]. Mice lacking ACE gene exhibited reduced fertility [3].

Androgens (A) are especially important for the maintenance of spermatogenesis and fertility in adulthood proved by experimental models of hormone manipulation and transgenic mice [12]. During ageing dramatic changes in the testis occurred at structural and functional levels manifested by germ cell loss, suppression of steroidogenesis, respectively testosterone (T) production in Leydig cells (LCs) and reduced responsiveness of Sertoli cells (SCs) to androgens (expression of androgen receptor) [2]. Andro-

gen regulation of tACE in germ cells is suggested using experimental ablation of LCs and hence withdrawal of testosterone production by ethane dimethanesulfoate (EDS) (our unpublished data).

Hypertension in spontaneously hypertensive rats (SHR) is androgen-dependent [11] and germ cell depletion accompanied by altered immunoexpression of tACE and elevated T levels was reported in our recent study [1]. The complex relationship between ageing and hypertension in action on spermatogenesis, both influencing androgen production and action, is not studied. In this respect the aim of present study was to investigate effect of both ageing and spontaneous hypertension on the expression of tACE.

Materials and Methods

Male Wistar rats (n=9) and SHR (n=14) at 8 months of age were used in this study. Blood pressure was measured by the tail-cuff method in conscious animals. Total serum testosterone concentrations were measured by RIA as reported previously [1]. Gonado-somatic index was calculated as ration of testis weight/body weight [8].

Immunohistochemistry for tACE: Dewaxed and rehydrated 5 µm testicular sections were subjected to antigen retrieval in 0.01 M Citrate buffer, pH 6 at 95 °C for 5 min water bath. For endogenous peroxidase block, slides were incubated in 3% H₂O₂ in methanol for 5 min at RT. Then, they were blocked for 1 hour in 1.5% donkey serum in PBS. Primary antibody against ACE (1:500) was applied for 30 min at 37 °C. After that goat biotinylated secondary antibody-ABC staining system was applied and liquid DAB was used as chromogen.

Results

The systolic blood pressure of the male SHR at age of 8 months was higher than in age- and sex-matched normotensive Wistar rats (Table 1). Testosterone level was significantly increased in serum of SHR compared to Wistar rats ($p < 0,001$). SHR displayed significantly lower body weight ($p < 0,001$) than control Wistar rats whereas absolute and relative testes weights (expressed as gonado-somatic index) in SHR were significantly higher ($p < 0,05$, resp. $p < 0,001$)

Table 1. Systolic blood pressure, mean serum testosterone level, mean body weight, mean absolute weight of the testes (right and left) and gonado-somatic index in Wistar rats and SHR

Parameters	Wistar rats (n = 9)	SHR (n = 14)	p – value
RR (mmHg)	115,6 ± 4,6	171,8 ± 3,8	$p < 0,001$
Serum testosterone(ng/ml)	0,55 ± 0,28	1,76 ± 0,79	$p < 0,001$
Body weight (g)	411,67 ± 26,92	330,71 ± 36,26	$p < 0,001$
Absolute weight of the testes (g)	3,06 ± 0,28	3,34 ± 0,39	$p < 0,05$
Gonado-somatic index	0,37 ± 0,03	0,52 ± 0,07	$p < 0,001$

Values are expressed as mean ± SD. n= number of rats.

Immunohistochemical analysis of control 8 month rats revealed stage-specific pattern of tACE expression in postmeiotic germ cells in particular elongating spermatids steps 8-19 (Fig. 1A). Spermatogenesis and ACE expression looks as normal as in con-

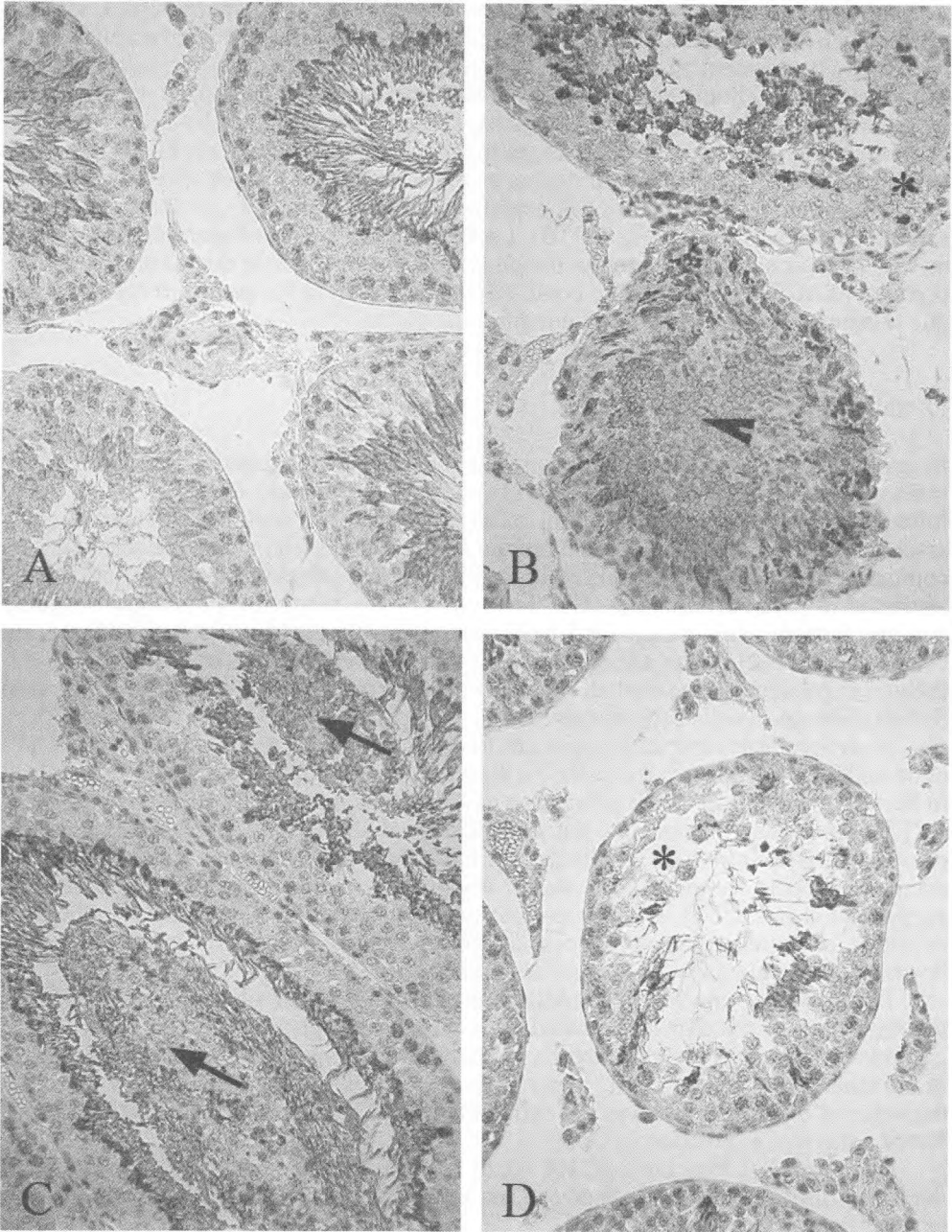


Fig. 1. Stage-specific immunoexpression of tACE in the cytoplasm of differentiating spermatids in ageing 8-month-old rat control (A) and SHR testis (B-D). **A:** Note the weaker intensity in the cytoplasm of elongating spermatids at step 10-11 in stage X-XI of the spermatogenic cycle; stronger intensity in early stages I-VI, step 15-17 and maximal intensity in middle stage VII-VIII step 19. **B-D:** Note lack of tubular lumen due to germ cells occupied its space (arrowhead); germ cells sloughed off into the lumen (arrows); germ cell depletion from the seminiferous epithelium (asterisks). $\times 400$

trols aged of 2 months. In 8 months SHR rats the stage specific pattern of ACE was not affected (1B-C). Structural changes in the seminiferous epithelium were manifested by abnormal arrangement of germ cell type, respectively abnormal position/topography of the germ cells. Some seminiferous tubules lack lumen and its space was occupied by germ cells. Most of them were elongating spermatids recognized by strong ACE immunoreactivity (Fig. 1B). In other cases tubular lumen is formed but filled with germ cells that were sloughed off seminiferous epithelium (Fig. 1C). More severe changes involved different degree of germ cell depletion and loss of mainly spermatids and some spermatocytes was found (Fig. 1B, D). Lack of defined stages of spermatid elongation as well as their slough off into the lumen is well distinguishable due to prominent expression of ACE. Therefore ACE could be used as a marker for germ cell type depleted due to aging or other pathological condition.

Discussion

In several recent papers we reported profound structural and functional changes in the main cell types of the testicular interstitium (perirubular and Leydig cells) and seminiferous epithelium (germ and Sertoli cells) [2, 6]. Aging of seminiferous epithelium is associated with thickening of basal lamina and blood vessels, indicative for disturbed communication between Seminiferous epithelium and interstitium as well as altered testicular trophic during aging. The thickening of the basement membrane in ageing rats and humans was coincidental with changes in the blood-testis barrier and germ cells depletion [10]. In the present study we found disorganization of seminiferous epithelium in particular abnormal arrangement of germ cells probably due to disruption of Sertoli cells–germ cells communications.

Androgens are especially important for maintenance of spermatogenesis in adulthood and their effects on germ cells are mediated via androgen receptor (AR) localized in Sertoli cells [12]. Reduced expression of AR in SCs reported by us in previous studies [2, 6] is probably associated with the functional alterations (decreased responsiveness to androgens) in SCs. It is likely that SCs from aging testis are unable to provide adequate support for germ cells and to respond to selective signal from them. This suggestion is in concert with our current data for elevated serum T levels providing evidence for decreased responsiveness of central nervous system to T. In spite of high T levels in SHR male they show a low sexual behavior [9].

Recently we reported [1] mildly altered expression of tACE in adult SHR (4 month-aged) associated with elevated T levels and high gonado-somatic index. In the current study we found similar trends of changes in aging SHR testis (8 month-aged). In the latter experimental model hypertensive condition is long lasting of 6 months but the value of blood pressure was not extremely high. This could explain relatively unaffected pattern of expression of tACE.

In conclusion, long lasting SHR could be considered as a potential risk factor for male infertility. ACE could be used as a marker for germ cell type depleted due to aging or other pathological condition.

Acknowledgements. We thank Mrs Tereza Dineva and Valeri Ivanov for technical assistance. This study was supported by a grant 7/2009 from Medical University of Pleven.

References

1. Atanassova, N., E. Lakova, Y. Bratchkova, G. Krasteva, M. Donchev. Expression of testicular angiotensin-converting enzyme in adult spontaneously hypertensive rats. *Folia Histochem. – Cytobiol.*, 47, 2009, 117-122.
2. Bakaska, M., N. Atanassova, E. Pavlova, Y. Koeva, B. Nikolov. Morphological alterations in rat testis during aging. – *Acta morphol. anthropol.*, 13, 2008, 82-86.
3. Esther, C.R., T.E. Howard, E.M. Marino, J.M. Goddard, M.R. Capecchi, K.E. Bernstein. Mice lacking angiotensin-converting enzyme have low blood pressure, renal pathology, and reduced male fertility. – *Lab. Invest.*, 74, 1996, 953-965.
4. Franke, F.E., K. Pauls, R. Metzger, S. Danilov. Angiotensin I-converting enzyme and potential substrates in human testis and testicular tumors. – *APMIS*, 111, 2003, 234-244.
5. Hagaman, J.R., J.S. Moyer, E.S. Bachman, M. Sibony, J.E. Welch, O. Smithies, J.H. Krege, D.A. O'Brien. Angiotensin-converting enzyme and male fertility. – *PNAS*, 95, 1998, 2552-2557.
6. Koeva, Y., M. Bakalska, N. Atanassova, K. Georgieva, M. Davidoff. Age-related changes in the expression of 11 β Hydroxysteroid dehydrogenase type 2 rat Leydig cells. – *Folia Histochem. Cytobiol.*, 47/2, 2009, 281-287.
7. Kondoh, G., H. Tojo, Y. Nakatani, N. Komazawa, C. Murata, K. Yamagata, Y. Maeda, T. Kinoshita, M. Okabe, R. Taguchi, J. Takeda. Angiotensin-converting enzyme is a GPI-anchored protein releasing factor crucial for fertilization. – *Nature Medicine*, 11, 2005, 160-166.
8. Latif, R., G. M. Lodhi, M. Aslam. Effects of amlodipine on serum testosterone, testicular weight and gonado-somatic index in adult rats. – *J. Ayub. Med. Coll. Abbottabad*, 20 (4), 2008, 8-10
9. Magnusson, K, Wall, A, Meyerson BJ. Difference in testosterone sensitivity in male spontaneously hypertensive (SHR) and Wistar-Kyoto rats (WKY). – *Physiol Behav.*, 60 (3), 1996, 907-912.
10. Levy, S., V. Serre, L. Hermo, B. Robaire. The effects of aging on the seminiferous epithelium and the blood-testis barrier of the Brown Norway rat. – *J. Androl.*, 20, 1999, 356-365.
11. Reckelhoff, JF, Zhang H, Srivastava K, Granger JP. Gender differences in hypertension in spontaneously hypertensive rats: role of androgens and androgen receptor. – *Hypertension*. 1999;34:920-923.
12. Sharpe, R.M. Sertoli cell endocrinology and signal transduction: Androgen regulation. – In: *Sertoli cell biology* (Eds. M.S. Skinner and M.D. Griswold), San Diego, Elsevier Acad. Press, 2005, 199-216.

Effects of Cobalt(II) Compounds on Some Hematological Parameters in Developing Mice

*Y. Gluhcheva¹, M. Madzharova¹, V. Atanasov², R. Zhorova²,
J. Ivanova³, M. Mitewa²*

¹Institute of Experimental Morphology, Pathology and Anthropology with Museum – BAS

²Faculty of Chemistry, Sofia University “St. Kliment Ohridski”

³Faculty of Medicine, Sofia University “St. Kliment Ohridski”

The effect of chronic exposure to cobalt(II) depends on the type of compound used, dose, time duration as well as on the age of the experimental animals. Day 18 mice showed to be more sensitive to Co(II) treatment. Higher hemoglobin content was measured in samples treated with CoCl₂, compared to those with CoEDTA. Higher plasma Fe concentration was measured in samples of mice treated with Co-EDTA which corresponded to low hemoglobin content.

Key words: cobalt(II) compounds, mouse blood plasma, hemoglobin, iron.

Introduction

As inorganic and complex compounds (with organic ligand) cobalt(II) is used as nutritional supplement, preservative, in drinks, as therapeutic agent for treating different diseases, etc. Cobalt(II) accumulates in organs such as kidney, liver, spleen, heart, stomach, intestines, muscle, brain and testes [1]. Exposure to this metal also causes allergic contact dermatitis, diseases of the upper respiratory tract, etc. [7]. Young animals (rats and guinea pigs) have 3- to 15-fold greater absorption than adult animals (aged 200 days or more). Water-soluble cobalt compounds exhibit greater absorption than non-water-soluble forms but absorption is species dependent [9]. Cobalt(II) chloride (CoCl₂) is a water soluble, hypoxia-mimicking agent. Ethylenediamine tetraacetic acid (EDTA) is a widespread organic pollutant. It is a powerful antioxidant and due its ability to bind metals it is used in chelation therapy. CoCl₂ oral treatment of patients with refractory anemia increased bone marrow erythropoietic activity, hematocrit and mean cell volume [3]. Topashka-Ancheva et al. determined that consuming food containing industrial dust with cobalt induces changes in hemoglobin, hematocrit, in red and white blood cell counts [8]. Iron (II), on the other hand, is incorporated in the heme complex which is an essential component of the oxygen carrier proteins such as hemoglobin. The daily requirement of iron is about 25 mg. Approximately about 80% of total body Fe is

incorporated into hemoglobin. Studies show strong relationship between cobalt blood and serum concentrations and iron status, having low cobalt concentration in case of high body iron stores [2].

The *aim* of the present work is to study the effects of cobalt(II) compounds – CoCl_2 and Co-EDTA on some hematological parameters in developing mice.

Material and Methods

Animal model

Pregnant balb/c mice in late gestation were subjected to cobalt chloride ($\text{CoCl}_2 \cdot 6\text{H}_2\text{O}$) or Co-EDTA treatment at daily doses of 75 mg/kg or 125 mg/kg. Cobalt(II) compounds were dissolved and obtained from drinking tap water. Animals were fed a standard diet and had access to food *ad libitum*. Mice were maintained in the institute's animal house at $23^\circ\text{C} \pm 2^\circ\text{C}$ and 12:12 h light-dark cycle in individual standard hard bottom polypropylene cages to ensure that all experimental animals obtained the required dose CoCl_2 . The newborn pups were sacrificed on days 18, 25 and 30 which correspond to different stages of development. Mice were weighed weekly and the experimental cobalt concentration was adjusted accordingly. Whole blood samples were obtained, centrifuged and plasma was stored at -20°C until further analysis. Plasma samples were used for measuring hemoglobin (Hb) and iron (Fe) concentration. Hb concentration was determined by hemiglobincyanide method (HiCN). Plasma iron concentration (transferrin-bound iron) was measured using spectrophotometric bathophenanthroline method [5]. The Fe content was calculated using standard solution of iron (II) (Sentinel).

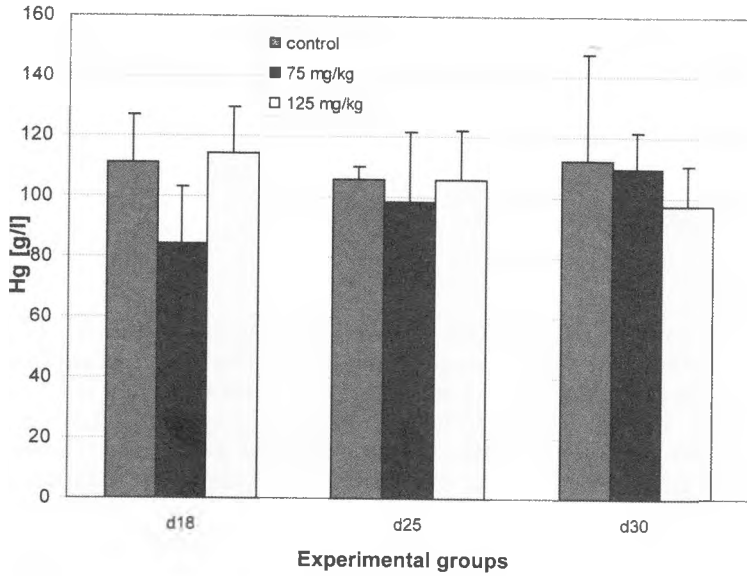
Statistical analysis

The obtained results are presented as mean value \pm SD. Statistical significance between the experimental groups was determined using Student's *t*-test. Difference was considered significant at $p < 0.05$.

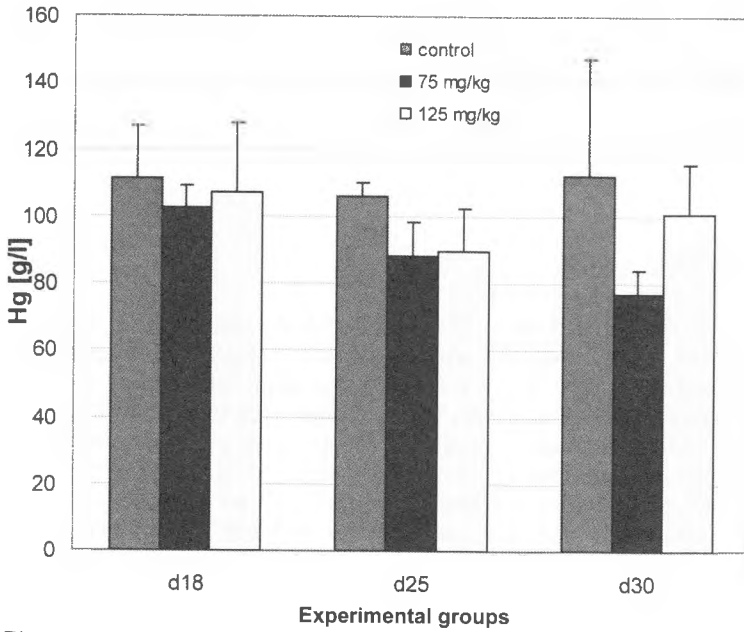
Results and Discussion

Results showed that high dose (125 mg/kg) of CoCl_2 induced an increase in Hb concentration in d18 mice. Treatment with low dose (75 mg/kg) reduced Hb concentration in all experimental groups. When CoEDTA was used Hb content was lower than the control samples in both cases – with low and high dose treatment. Results showed that high doses of CoCl_2 enhanced hemoglobin biosynthesis compared to CoEDTA.

Plasma Fe concentration was lower in samples of d18 and d25 mice treated with high dose CoCl_2 , compared to the same age mice treated with the low dose. Higher Fe content was measured in sampled treated either with low or high dose CoEDTA which corresponded to the lower Hb concentration measured. Elevated iron levels are also a sign for changes in the liver function, i.e. reduced levels of hepcidin, etc. Cobalt and iron are shown to compete with close affinity constant for transferrin [4]. Thus, cobalt competes with iron for incorporation in the heme moiety which may be a possible explanation for the increased plasma Fe content [6].

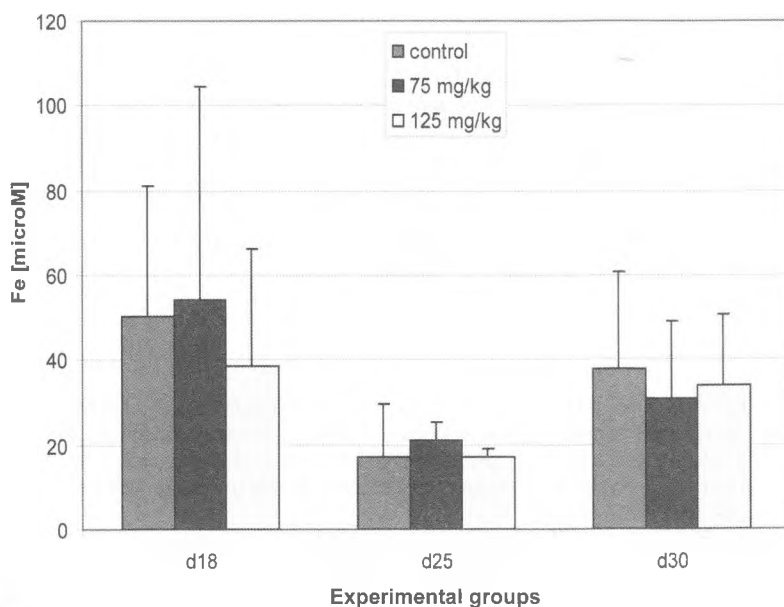


(A)

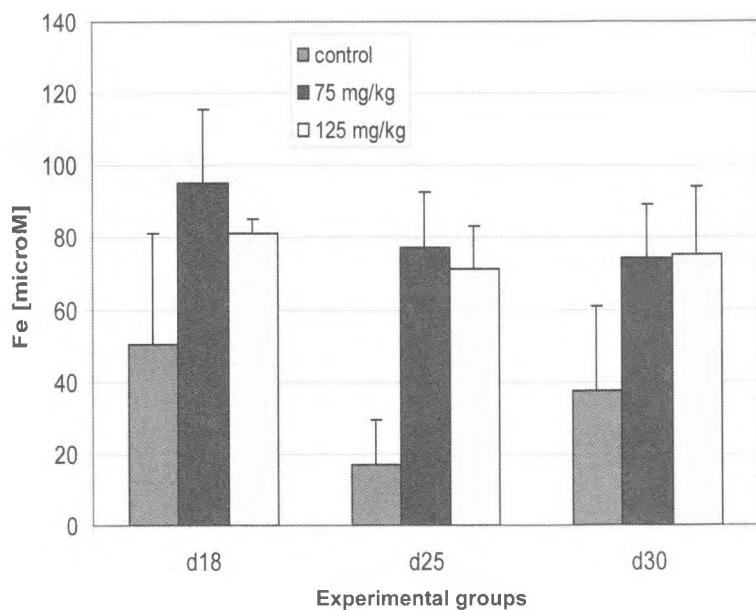


(B)

Fig. 1. Hemoglobin (Hb) content in blood plasma of mice treated with low or high daily doses of CoCl_2 (A), and CoEDTA (B)



(A)



(B)

Fig. 2. Iron (Fe) content in blood plasma of mice treated with low or high daily doses of CoCl_2 (A), and CoEDTA (B)

Conclusions

The effect of chronic exposure to cobalt(II) depends on the type of compound used, dose, time duration as well as on the age of the experimental animals. d18 mice are more sensitive to Co(II) treatment. High doses of CoCl_2 enhanced hemoglobin biosynthesis compared to CoEDTA. Higher plasma Fe concentration was measured in samples of mice treated with Co-EDTA which corresponded to low Hb concentration.

Acknowledgements. The work is supported by a grant No DOO2 – 351/2008 for Young scientists from the Bulgarian National Science Fund.

References

1. Ayala-Fierro, F., J. M. Firriolo, D. E. Carter. Disposition, toxicity, and intestinal absorption of cobaltous chloride in male Fischer 344 rats. – *J. Toxicol. Environ. Health A.*, **56**, 1999, 571-591.
2. Barány, E., I.A. Bergdahl, L.-E. Bratteby, T. Lundh, G. Samuelson, S. Skerfving, A. Oskarsson. Iron status influences trace element levels in human blood and serum. – *Environ. Res.*, **98**, 2005, 215–223.
3. Bowie, E. A., P. J. Hurley. Cobalt chloride in the treatment of refractory anaemia in patients undergoing long-term haemodialysis. – *Aust. N. Z. J. Med.*, **5**, 1975, 306-314.
4. Chikh, Z., M. Hémadi, G. Miquel, N.-T. Ha-Duong, J.-M. El Hage Chahine. Cobalt and the iron acquisition pathway: competition towards interaction with receptor 1. – *J. Mol. Biol.*, **380**, 2008, 900–916.
5. Dochev, D., K. Kolchakov, L. Sirakov. *Biochemistry and Clinical Chemistry*. 2nd ed, Bulvest – 2000, Sofia, 1993, pp. 337-339.
6. Ho, V. T., H. F. Bunn. Effects of transition metals on the expression of the erythropoietin gene: further evidence that the oxygen sensor is a heme protein. – *Biochem. Biophys. Res. Commun.*, **223**, 1996, 175-180.
7. Ortega, R., C. Bresson, A. Fraysse, C. Sandre, G. Deves, C. Gombert, M. Tabarrant, P. Bleuet, H. Seznec, A. Simionovici, P. Moretto, C. Moulin. Cobalt distribution in keratinocyte cells indicates nuclear and perinuclear accumulation and interaction with magnesium and zinc homeostasis. – *Toxicol. Lett.*, **188**, 2009, 26-32.
8. Topashka-Ancheva, M., E. Trakiiska, Zv. Pramatarova. Cytogenetical and haematological alterations in laboratory white mice ICR, caused by effects of polymetal industrial dust. – *Acta zoologica bulgarica*, **55**, 2003, 61-71
9. World Health Organization. Cobalt and inorganic cobalt compounds. – In: *Concise International Chemical Assessment Document*, 69, 2006, 13-21.

The Affect of Cobalt Salts on Some Weight Indices in Developing Mice

*Y. Gluhcheva¹, M. Madzharova¹, V. Atanasov²,
R. Zhorova², M. Mitewa², E. Pavlova¹, J. Ivanova³*

¹*Institute of Experimental Morphology, Pathology and Anthropology with Museum – BAS*

²*Faculty of Chemistry, Sofia University “St. Kliment Ohridski”*

³*Faculty of Medicine, Sofia University “St. Kliment Ohridski”*

Although cobalt is an essential trace element long-term exposure and large amounts of its salts can have deleterious effects on humans and animals. Pregnant balb/c mice in late gestation were subjected to cobalt chloride ($\text{CoCl}_2 \cdot 6\text{H}_2\text{O}$) or cobalt EDTA (Co-EDTA) treatment at daily doses of 75 mg/kg or 125 mg/kg. Cobalt compounds were dissolved and obtained from drinking tap water. Sodium EDTA (Na-EDTA) and pure tap water were used as controls. The newborn pups were sacrificed on days 18, 25 and 30 which correspond to different stages of development. Mice were weighed weekly and the experimental cobalt concentration was adjusted accordingly. Preliminary results showed that mice treated with cobalt salts (CoCl_2 and Co-EDTA) have smaller body weight compared to the control group. Liver weight was increased in the Co-EDTA-treated mice for both doses in all experimental groups. Spleen and liver weight was increased in case of high dose CoCl_2 -treated mice. Spleen weight was the largest in high dose CoCl_2 -treated mice compared to all other groups. Liver weight of mice treated with Co-EDTA was the largest in all experimental groups compared to that induced by the other substances and in the control. The experimental results show that organic and inorganic cobalt salts affect body and organ weight.

Key words: mice, cobalt salts, liver, spleen, indices.

Introduction

Heavy metals are widely spread in the environment, food and water and exposure to them is unavoidable. Elevated values of the heavy metals' concentration in various organs of humans, animals and aquatic fish are measured [12].

Although cobalt is an essential trace element long-term exposure and large amounts of its salts can have deleterious effects on humans and animals. Cobalt (II) accumulates in organs such as spleen, kidney, heart and liver [1]. Its salts are shown to affect body weight of patients and experimental animals but the mechanism remains to be elucidated. Data show significant weight loss, as well as decreased food and water consumption in diabetic rats treated with cobalt chloride [10, 11]. No data were found for

the influence of cobalt compounds on animals in different stages of development after long-term treatment.

Ethylenediamine tetraacetic acid (EDTA) is used in medicine, molecular biology and biochemistry; as anticoagulant for blood samples and decalcifying agent in histopathology, in non-alcoholic beverages, etc. Experiments with animals though show that EDTA exhibits cytotoxic and weakly genotoxic effects. Oral exposure causes reproductive and developmental effects as well.

The *aim* of the present study is to investigate the effect of cobalt compounds (CoCl₂ and Co-EDTA) on some somatic indices in developing mice – body weight, liver and spleen weight.

Materials and Methods

Complex synthesis

All chemicals and solvents used were of AR grade. Co-EDTA was synthesized according to modified literature procedures [3, 8], namely adding slowly solution of Co(NO₃)₂·6H₂O (0.291 μg, 1 mmol in 5 ml H₂O) to a mixture containing Na₂EDTA (186 mg, 0.5 mmol in water) and tetraethyl ammonium hydroxide (Et₄NOH) (180 ml, 0.5 mmol, 40% in water) resulting in formation of Co-EDTA. The latter was precipitated as pink suspension with acetone. Then the vessel was covered with parafilm and after approximately a week formation of pink crystals was observed. They were studied using X-ray diffraction method proving a composition of [Co(H₂O)₄(Co-EDTA)]_n with known structure – orthorhombic space group Pna2₁ (CCDC Ref:COEDTA) [8].

The structural data was collected on an Oxford Diffraction Sapphire 2 CCD diffractometer with graphite – monochromated Cu-Kα radiation.

Animal model

Pregnant balb/c mice in late gestation were subjected to cobalt chloride (CoCl₂·6H₂O) or cobalt EDTA (Co-EDTA) treatment at daily doses of 75 mg/kg or 125 mg/kg which continued until day 30 of the newborn mice. Cobalt compounds were dissolved and obtained from drinking tap water. Sodium EDTA (Na₂EDTA) and pure tap water were used as controls. Animals were fed a standard diet and had access to food *ad libitum*. Mice were maintained in the institute's animal house at 23°C ± 2°C and 12:12 h light-dark cycle in individual standard hard bottom polypropylene cages to ensure that all experimental animals obtained the required dose of cobalt compounds.

The newborn pups (5 per group) were sacrificed on days 18, 25 and 30 which correspond to different stages of development. Mice were weighed weekly and the experimental cobalt concentration was adjusted accordingly. After the animals were sacrificed liver and spleen were removed and weighed. Liver and spleen indices – liver/body weight (L/BW) and spleen/body weight (S/BW) were calculated. Significance was determined using Student's *t*-test at *p*<0.05.

The studies were approved by the Ethics Committee of the Institute of Experimental Morphology, Pathology and Anthropology with Museum – Bulgarian Academy of Sciences.

Results and Discussion

The experimental results showed that cobalt salts (Co-EDTA and CoCl_2) affect body and organ weight. Mice treated with CoCl_2 and Co-EDTA have smaller body weight compared to the control group (Fig. 1a, b). Data are in agreement with Garoui et al. [2] showing retarded weight gain in suckling rats. These results suggest that perinatal and postnatal exposure of rats and mice to cobalt, retards the growth of their pups, possibly due to transfer of Co^{2+} through placenta and milk.

Treatment with CoCl_2 and Co-EDTA affects spleen and liver weight as well. The effect depends on the type of compound used, dose and time duration. Results showed that day 18 mice are the most sensitive to cobalt treatment. Our results are not in agreement with those of Mazur [7] who shows that CoCl_2 -treated rats do not have increased spleen weight. In our experimental model, exposure to high dose CoCl_2 (125 mg/kg)

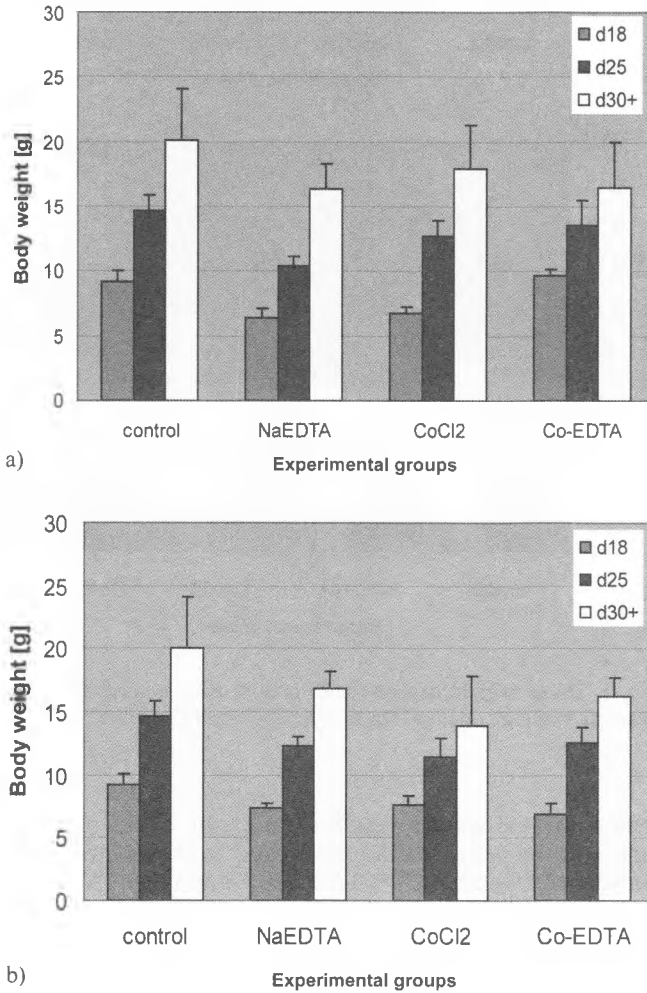


Fig. 1. Body weight of day 18, 25 and 30 mice treated with low dose (a), and high dose (b) Na_2EDTA , CoCl_2 and CoEDTA

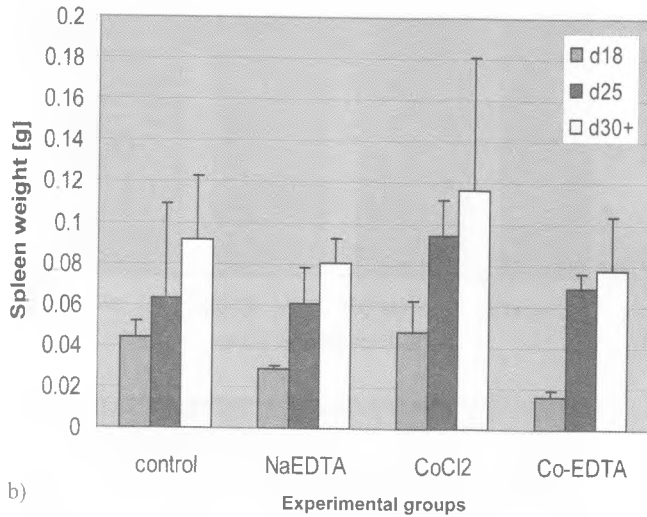
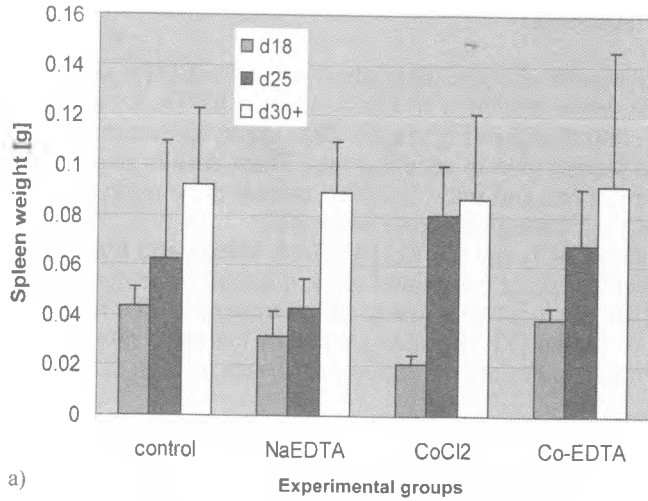
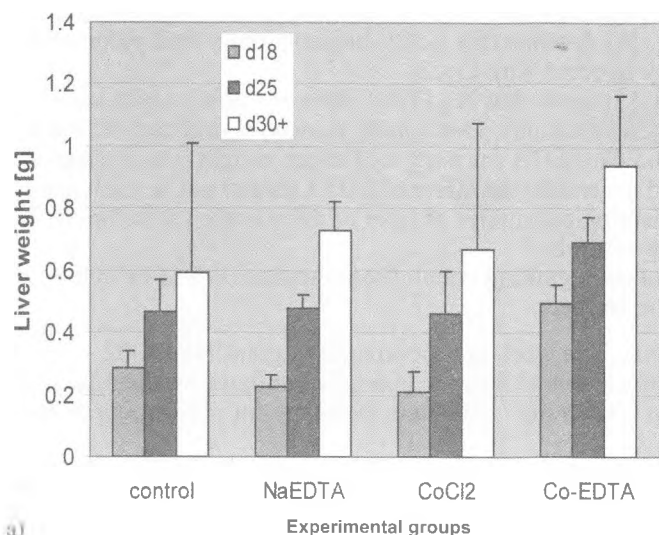


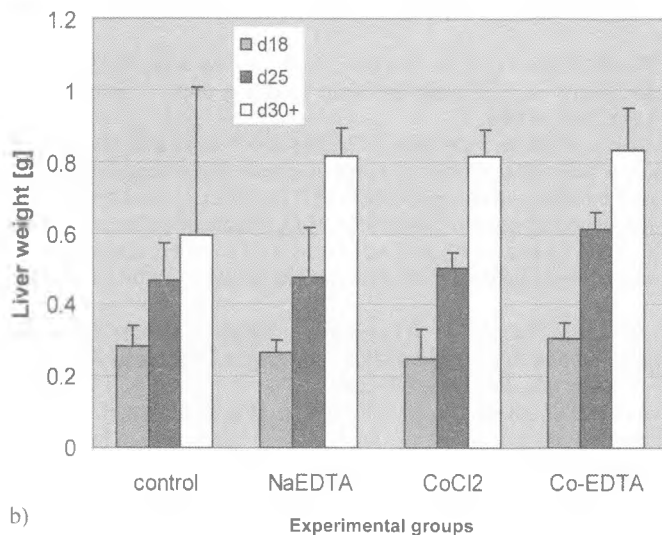
Fig. 2. Spleen weight of day 18, 25 and 30 mice treated with low dose (a), and high dose (b) Na₂EDTA, CoCl₂ and CoEDTA

caused an increase in mouse spleen weight [Fig. 2a, b]. When mice were treated with Co-EDTA though, spleens were smaller compared to the control samples. When the effects of high dose CoCl₂ and Co-EDTA for day 18 and day 25 mice were compared, the differences were significant ($p < 0.004$ and $p < 0.03$, respectively). Spleen index (calculated as a ratio to body weight) was significantly decreased ($p < 0.004$) in low dose CoCl₂-treated day 18 mice and significantly increased ($p < 0.003$) in mice treated with the high dose. High dose Co-EDTA also caused a significant decrease ($p < 0.001$) in spleen index in day 18 mice.

Treatment with high dose CoCl₂ increased liver weight in day 25 and day 30 mice (Fig. 3a, b). Similar results were obtained for mice subjected to both doses (low and



a)



b)

Fig. 3. Liver weight of day 18, 25 and 30 mice treated with low dose (a), and high dose (b) Na₂EDTA, CoCl₂, and CoEDTA

high dose) Co-EDTA for days 18, 25 and 30. Low dose Co-EDTA increased significantly liver weight in day 18 ($p < 0.001$) and day 25 ($p < 0.001$) mice compared to that of CoCl₂-treated mice. For the high dose significance was found only for day 25 mice ($p < 0.01$). Liver index (calculated as a ratio to body weight) was significantly increased in day 18 and day 25 when treated with either low or high dose Co-EDTA. The results suggest stronger effect of Co-EDTA on liver compared to CoCl₂ which is known to induce oxidative stress in rat liver leading to a significant increase in heme oxygenase-1 activity [4]. Garoui et al. [2] show that CoCl₂ treatment leads to infiltration of mononuclear cells, indicating the presence of inflammatory reactions and vascular congestion in livers of rat pups and dams. It also exhibits *in vitro* protective effect on apoptotic

cell death in hepatic cell line HepG2 reducing DNA fragmentation [9]. On the other hand, Liu et al. [6] demonstrate CoCl_2 -hepatotoxicity and pulmonary edema in mice intraperitoneally injected with CoCl_2 .

Hiers et al. [5] show that Na_2EDTA does not affect organ weight as a percentage of body weight in ruminants. Our results showed significant differences in the effects of Na-EDTA and Co-EDTA for body and organ weight which suggests that for proper interpretation of the results the affect of EDTA should not be excluded. Our preliminary results of the histological studies of liver of mice treated with Na_2EDTA show changes compared to the controls.

Further studies regarding cobalt bioaccumulation and its cytotoxicity in liver and spleen will be performed.

Acknowledgments. The work is supported by a grant No DO02 – 351/2008 for Young scientists from the National Science Fund. The authors are thankful to Prof. W. S. Sheldrick from Ruhr University – Bochum, Germany for performing X-ray analysis.

References

1. Ayala-Fierro, F., J. M. Firriolo, D. E. Carter. Disposition, toxicity, and intestinal absorption of cobaltous chloride in male Fischer 344 rats. – *J. Toxicol. Environ. Health A*, **56**, 1999, 571-591.
2. Garoui, E. M., H. Fetoui, F. A. Makni, T. Boudawara, N. Zeghal. Cobalt chloride induces hepatotoxicity in adult rats and their suckling pups. – *Exp. Toxicol. Pathol.*, 2009, doi:10.1016/j.etp.2009.09.003.
3. Gomez-Romero, P., G. B. Jameson, N. Casan-Pastor, E. Coronado, D. Beltran. Low-dimensional bimetallic ordered systems: synthesis and characterization of the isomorphous series of the cobalt nickel complexes $\text{Co}_x\text{Ni}_{2-x}\text{EDTA}\cdot 2\text{H}_2\text{O}$. Crystal structure of $\text{Co}_2\text{EDTA}\cdot 2\text{H}_2\text{O}$ and preferential site occupation in $\text{CoNiEDTA}\cdot \text{H}_2\text{O}$. – *Inorganic Chemistry*, **25**, 1986, 3171-3176.
4. Gonzales, S., A. H. Polizio, M. A. Erario, M. L. Tomaro. Glutamine is highly effective in preventing in vivo cobalt-induced oxidative stress in rat liver. – *World J. Gastroenterol.*, **11**, 2005, 3533-3538.
5. Hiers, J. M., W. J. Miller, D. M. Blackmon. Effect of Dietary Cadmium and Ethylenediaminetetraacetate on Dry Matter Digestibility and Organ Weights in Zinc Deficient and Normal Ruminants. – *J. Dairy Sci.*, **51**, 1968, 205-209.
6. Liu, W., M. Guo, Y. B. Xu, D. Li, Z. N. Zhou, Y. L. Wu, Z. Chen, S. C. Kogan, G. Q. Chen. Induction of tumor arrest and differentiation with prolonged survival by intermittent hypoxia in a mouse model of acute myeloid leukemia. – *Blood*, **107**, 2006, 698-707.
7. Mazur, A. Metabolism of the Stimulated Rat Spleen. I. Ferrochelatase activity as an index of tissue erythropoiesis. – *J. Clin. Invest.*, **47**, 1968, 2230-2238.
8. McCandlish, E. F. K., T. K. Michael, J. A. Neal, E. C. Lingafelter, N. J. Rose. Comparison of the structures and aqueous solutions of [(o-phenylenediaminetetraacetato(4-))cobalt(II)] and [ethylenediaminetetraacetato(4-)]cobalt(II) ions. – *Inorganic Chemistry*, **17**, 1978, 1383-1394.
9. Piret, J. P., C. Lecocq, S. Toffoli, N. Ninane, M. Raes, C. Michiels. Hypoxia and CoCl_2 protect HepG2 cells against serum deprivation- and t-BHP-induced apoptosis: a possible anti-apoptotic role for HIF-1. – *Exp. Cell Res.*, **295**, 2004, 340-349.
10. Vasudevan, H., J. H. McNeill. Chronic cobalt treatment decreases hyperglycemia in streptozotocin-diabetic rats. – *BioMetals*, **20**, 2007, 129-134.
11. Ybarra, J., A. Behrooz, A. Gabriel, M. H. Koseoglu, F. Ismail-Beigi. Glycemia-lowering effect of cobalt chloride in the diabetic rat: increased GLUT1 mRNA expression. – *Mol. Cell Endocrinol.*, **133**, 1997, 151-160.
12. Арнаудова, Д., Е. Томова, И. Велчева, А. Арнаудов. Проучване съдържанието на олово, цинк и кадмий в някои органи на риби от сем. Cyprinidae и сем. Percidae в язовирите „Студен кладенец“ и „Кърджали“. – Юбилейна научна конференция по Екология (Сборник с доклади), Ред. И. Велчева, А. Цеков, Пловдив, 2008, стр. 327–335.

Impact of Cobalt Chloride on Testis and Male Fertility in Adulthood

M. Madzharova, Y. Gluhcheva, E. Pavlova, N. Atanassova

*Institute of Experimental Morphology, Pathology and Anthropology with Museum,
Bulgarian Academy of Sciences, Sofia, Bulgaria*

Our work is focused on the impact of cobalt on male fertility. We used two doses of CoCl_2 (75 and 125 mg/kg/day) that negatively affected body weight (BW), testis weight (TW) and epididymis weight (EW) in early puberty of male mice. In late puberty restoration of BW, TW but not EW was observed at the two doses of CoCl_2 . In adulthood treatment with two doses of CoCl_2 negatively affects BW. At low dose TW as well as testicular/body weight index was elevated on 45 and 60 pnd. At height dose TW was significantly reduced whereas testicular/body weight index remained unchanged. The number of spermatozoa was lower only in mice treated by high dose CoCl_2 .

Key words: cobalt, male fertility, spermatogenesis.

Introduction

Cobalt is a naturally occurring relative rare element of earth crust. It is an essential oligoelement for mammals and it circulates in human body mainly in the form of vitamin B_{12} . Food and beverages are the main source of cobalt for the general population [6]. The adult human body contains approximately 1 mg of cobalt and human dietary intake of cobalt varies between 5 and 50 mg/day [4]. Cobalt is not a cumulative toxin and is excreted rapidly mainly in urine and to a lesser extent via faeces. Cobalt tends to accumulate in different organs and tissues when the threshold of physiological detoxication is reached and this leads to pathological alterations [3]. People exposed to higher doses of cobalt on occupational settings represent the most influenced group of people to the cobalt action. Degenerative changes in adult seminiferous epithelium involving vacuolation of Sertoli cells and germ cell nuclei were reported by Elbetieha et al. [2]. However, the effect of different doses of cobalt is poorly investigated. In this respect the **aim** of our study was to establish the impact of cobalt chloride applied at low and height doses on testis morphology and fertility of adult mice.

Materials and Methods

Female mice in late gestation were divided into two groups and subjected to two different doses of CoCl_2 respectively – low dose (75 mg/kg/day) and high dose (125 mg/kg/day). CoCl_2 were applied via drinking water. Male pups were sacrificed on 45 pnd (early maturity) and 60 pnd (maturity). On 25 pnd male mice were separated in individual cages, the CoCl_2 doses were calculated and actualized weekly on the base of their own weight. The effect of CoCl_2 on testis was evaluated at microscopic level (histological observation) and following quantitative parameters: body weight (BW), testicular weight (TW), epididymal weight (EW), testis/body weight index as well as sperm count. The data obtained were statistically processed using Student's *t*-test.

Results and Discussion

Recently we reported that in early puberty CoCl_2 significantly decreased BW at the two doses applied, whereas in mid puberty no negative influence was observed [5]. Current study in adulthood indicated that CoCl_2 negatively affected BW in dose dependent manner. In our previous study 20% decrease in TW was found at two doses in early but not in mid puberty [5]. In adulthood CoCl_2 negatively and significantly affected TW at high dose only, whereas in low dose CoCl_2 even showed slight stimulatory mode of action (Fig. 1). Testicular/body weight index was not changed in early ages [5] whereas in adulthood this index was significantly increased by low dose of CoCl_2 that reflects its slightly stimulatory effect on TW. The high dose of Co compound did not produced significant effect on this parameter. Interestingly epididymis during puberty was considered as more sensitive organ to cobalt treatment that the testis [5].

The sperm count was not affected by low dose of CoCl_2 on day 45, whereas on day 60 it showed slight stimulatory effect and that correlates with higher TW on this age. The high dose of CoCl_2 induced 70% reduction of spermatozoa number by 45-days old

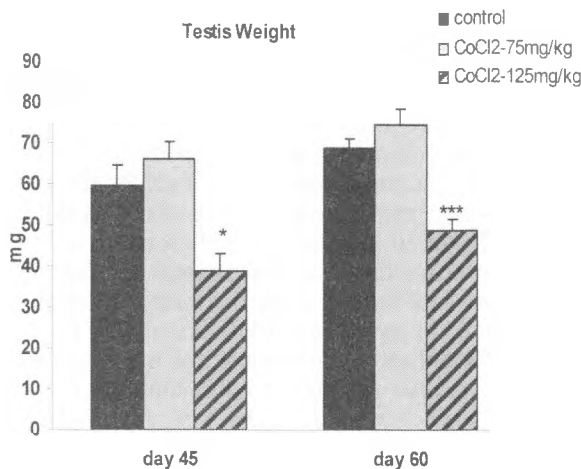


Fig. 1. Testicular weight of control and treated mice with CoCl_2 at low (75 mg/kg/day) and high doses (125 mg/kg/day) on 45th and 60th-day. Data represent mean value \pm SE (* $p < 0.05$; ** $p < 0.01$; *** $p < 0.001$)

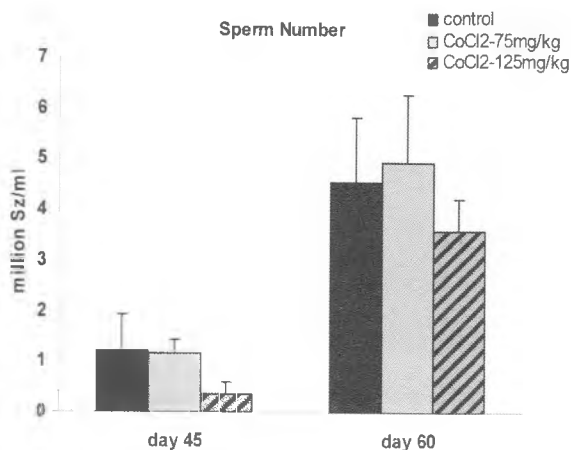


Fig. 2. Sperm number of control and treated mice with CoCl_2 at low (75 mg/kg/day) and high doses (125 mg/kg/day) on 45- and 60-day. Data represent mean value \pm SE (* $p < 0.05$; ** $p < 0.01$; *** $p < 0.001$)

animals whereas on day 60 the same dose caused 30% decrease of this parameter (Fig. 2). Our data did not show statistical significance which is probably due to high heterogeneity within the treated group.

Histological samples taken from animals in early puberty treated with low dose of the compound showed depletion of germ cells in some seminiferous tubules, whereas other tubules demonstrated normal morphology. In the group treated with high dose it was observed the same type of alterations but the frequency of the affected tubules was higher. On mid puberty as well on maturity (day 45 and 60) we found histological changes only in testes treated by high doses of CoCl_2 – germ cell depletion and abnormal formation of tubular lumen (Figs 3, 4). Our findings are in concert with data by Elbeticha et al. [2] about degeneration of seminiferous epithelium.

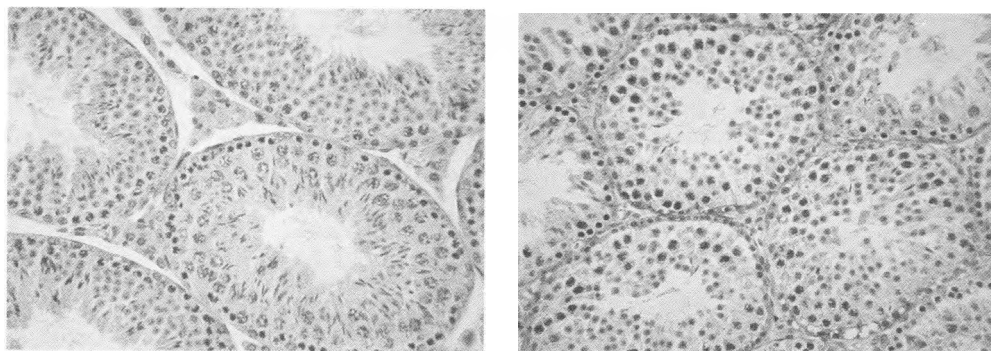


Fig. 3. Testicular cross-sections of control and treated mice with high dose (125 mg/kg/day) on 45 day. $\times 400$

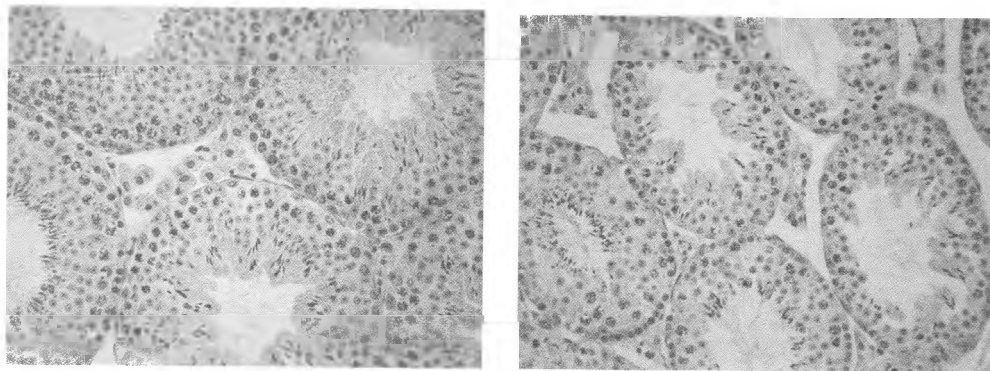


Fig. 4. Testicular cross-sections of control and treated mice with high dose (125 mg/kg/day) on 60 day. $\times 400$

Conclusions

On the basis of our observations as well as data from the literature [1, 2] we could conclude that chronic treatment with cobalt chloride negatively affected male reproductive parameters. Thus its concentrations should be carefully monitored especially on occupational settings with higher quantities in order to protect male reproductive health.

Acknowledgements. This work is supported by grant No DO02 – 351/2008 for Young scientists from the Bulgarian National Science Fund.

References

1. Bitner A. M., N.G. Pedigo, R. P. Katz, W. J. George. Histopathology of testes from mice chronically treated with cobalt. – *Reproductive Toxicology*, **6(1)**, 1992, 41-50.
2. Elbetieha, A., A. S. Al-Thani, R. K. Al-Thani, H. Darmani, W. Owais. Effect of chronic exposure to cobalt chloride on the fertility and testes in mice. – *Journal of Applied Biological Sciences*, **2 (1)**, 2008, 1-6.
3. Kapadia, C. R. Vitamin B₁₂ in health and disease. Part I – Inherited disorders of function, absorption, and transport. – *Gastroenterologist*, **3(4)**, 1995, 329-344.
4. Lison, D. Cobalt. – In: *Handbook on the Toxicology of Metals* (Eds. G. F. Nordberg, B. A. Fowler, M. Nordberg and L. T. Friberg) 3rd Edition, 2007, 511-528.
5. Madzharova, M., Gluhcheva, Y., Pavlova, E., Atanasova, N. Effect of cobalt on male organs during puberty. – *Biotechnol. Biotechnol. Equip.* **24 (2)**, 2010, 321-324.
6. Стоянов, Ст. Тежки метали в околната среда и хранителните продукти. – София, Пенсофт, 1999, с. 288.

Novel Fluorescent Histochemical Technique for γ -Glutamyl Transpeptidase Activity Determination

R. Todorova*, M. Dimitrova*, I. Ivanov**

**Institute of Experimental Morphology, Pathology and Anthropology with Museum,
Bulgarian Academy of Sciences, Sofia*

***University of Sofia "St. Kl. Ohridski", Faculty of Biology, Sofia*

A synthetic fluorescent substrate – γ -L-Glu-N-hexyl-6-hydrazido-1,8-naphthalimide (γ -L-Glu-HHNI) and a novel fluorescent histochemical method based on it for activity determination and localization of γ -glutamyl transpeptidase (GGT) are proposed. Using the new fluorescent technique, GGT activity is visualized in rats and mice organs. Presently, there is a vast interest of GGT because of its aberrant expression during development of diverse malignant diseases and Type 1 and 2 diabetes. Thus, a reliable histochemical method is much needed to elucidate the GGT activity localization and its alterations at normal physiological and different pathological conditions.

Key words: gamma-glutamyl transpeptidase, fluorogenic substrates, fluorescent histochemical methods, enzyme histochemistry.

Introduction

γ -Glutamyl transpeptidase (EC 2.3.2.2, GGT) is a highly glycosylated, membrane associated heterodimeric enzyme [16]. GGT catalyses the cleavage of γ -glutamyl moiety from a donor substrate (mainly glutathione) and transfers it to an acceptor substrate (water, L-amino acids or dipeptides) at pH optimum 8.2 – 9.0 [19]. In mammals, γ -glutamyl transpeptidase shows a high activity in cells with intense secretory or absorptive functions. The physiological function of GGT is to maintain the glutathione cycle and provide the redox regulation of cellular function [3]. Also, enzyme is responsible for cellular detoxification [6], biosynthesis of leukotriene D [14], and amino acid transport in kidneys [8].

Increased activity of GGT is detected in human primary tumors such as ovarian carcinoma [15], colon carcinoma [13], non-small cell lung carcinoma [1], in the metastatic forms of sarcoma [9], melanoma [12] and leukemias [18] as well as in the development of Type 1 and Type 2 diabetes [11]. Besides, GGT is involved in such physiological disorder as Parkinson's disease [17].

The role of GGT for the normal physiology of the mammalian organisms and the significant alterations of the enzyme activity at different pathological conditions make the development of reliable methods for its activity localization in situ very important. The histochemical methods for GGT visualization are based on γ -glutamyl derivatives of 1- or 2- naphthylamine and 4-methoxy-2-naphthylamine [7] as substrates, which are used according to the diazonium salts technique. A more convenient method than the diazo-dye has been suggested by Dikov et al. [2], with the application of tetrazolium salts as better auxiliary reagents. All these histochemical techniques are chromogenic, fluorescent GGT activity determination method is missing hitherto.

In the present paper we propose a novel fluorescent histochemical method for GGT activity localization, based on the fluorescent substrate γ -L-Glu-N-hexyl-6-hydrazido-1,8-naphthalimide, synthesized by us. We provide data about the enzyme localization in rats and mice organs with different GGT activity levels.

Materials and Methods

Synthesis of the fluorochrome 6-hydrazino-1,8-naphthalimide (HHNI). The synthesis was performed according to Gan et al. [4]. First, 6-Cl-1,8-naphthalic anhydride (Fluka) and n-hexylamine (Fluka) were boiled in absolute ethanol for 12 hours to give N-hexyl-6-Cl-1,8-naphthalimide. The last compound was dissolved in dimethylsulfoxide, then hydrazine monohydrate (Fluka) was added and the reaction mixture was heated at 60°C for 3 hours. As a result, HHNI was obtained and immediately recrystallized from 95 % ethanol.

Synthesis of the substrate for γ -glutamyl transpeptidase. The GGT substrate – γ -L-Glu-6-hydrazido-2-hexyl-1,8-naphthalimide (γ -L-Glu-HHNI) was obtained from HHNI and Boc-Glu(OH)-OtBu (Fluka) by TBTU-procedure [10]. The Boc-group was cleaved by stirring the protected substrate in 4N HCl/ dioxane (Fluka) for 6-8 hours at room temperature to give γ -L-Glu-HHNI as hydrogen chloride salt.

Tissue treatment and incubation. Mature Balb/c mice and Wistar rats from both sexes were decapitated under ether anesthesia. Pieces of kidney, pancreas, spleen, epididymis and seminal vesicle were removed and frozen immediately in liquid nitrogen. Ten μ m sections were cut on cryotome Reichert Jung (Nussloch, Germany) at -25°C, mounted on gelatinized glass slides and air dried. Then, they were covered with 0,75 % celloidin for one minute at room temperature and incubated in 0.1 M phosphate buffer, pH 8.2, containing 0,5 mM of the substrate (γ -L-Glu-HHNI), 1 mg/ml aromatic aldehyde (piperonal) and 10mM Glycyl-glycyn (Reanal). The incubation lasted 60-120 min at 37°C. All the samples were post-fixed in 4 % neutral formaldehyde, stained with hematoxyline by the standard histochemical procedure and embedded in glycerol-jelly. Control sections were thermally inactivated (emerged for 10 minutes in hot (80°C) water) and incubated in full substrate media or incubated only in buffered aldehyde (in the absence of the substrate).

The sections were studied under fluorescent microscope OPTON IM 35 with filter combination G 546 FT 580 LP 590. The photos were made on Konica Minolta (Japan) VX 200 colorful films.

Results and Discussion

The principle of the here presented new technique is as follows: GGT catalyzes the hydrolysis of the hydrazide bond in the substrate and HHNI is liberated. The latter com-

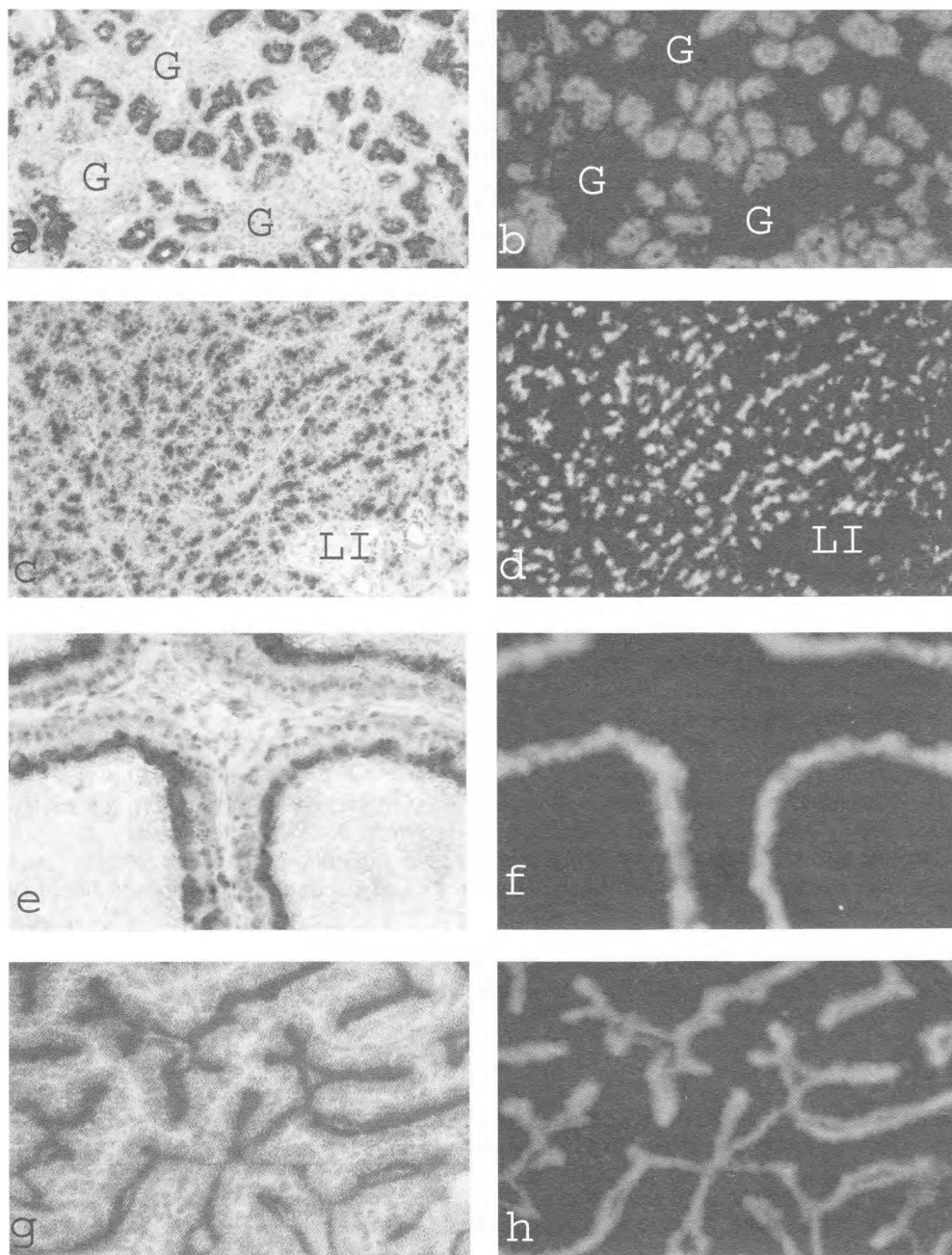


Fig. 1. Localization of GGT activity in Balb/c mice and rats organs.

- a, b – Rat kidney. GGT reaction in the brush border epithelial cells of kidney convoluted tubules. No reaction in the glomeruli. (G-glomeruli)
- c, d – Fluorescent product in the acinar cells of the mouse pancreas. No reaction in the cells of the islet of Langerhans (LI).
- e, f – Final reaction product, restricted to the epithelial cells of the rat epididymis.
- g, h – Amorphous fluorescent product deposits in the epithelial cells of the mouse seminal vesicle. Magn. $\times 200$. Left: light microscopy; Right: fluorescent microscopy

ound reacts simultaneously with the aromatic aldehyde (piperonal), presented in the incubation medium. Thus, a water-insoluble hydrazone is produced, which precipitates on the places with the enzyme activity and visualizes them by intensive red fluorescence. The final reaction product – the hydrazone does not diffuse from the places of its origin which is important for the precise enzyme localization. Another priority of the method is that the hydrazone possesses a fluorescent spectrum different from the tissue autofluorescence, e.g it fluoresces in red upon green light excitation ($\lambda_{\text{excit.}} = 540\text{-}580$ nm, $\lambda_{\text{emiss.}} > 600$ nm), whereas the tissue fluorochromes fluoresce in blue upon violet light excitation ($\lambda_{\text{excit.}} = 290\text{-}400$ nm, $\lambda_{\text{emiss.}} = 400\text{-}470$ nm). This allows enzyme activity to be visualized at the lack of background noise. With the here presented fluorescent histochemical method we managed to determine GGT in several organs, where its activity has been detected biochemically. Both controls did not show any non-specific fluorescent staining. GGT activity was high in kidney and short incubation period was needed (30 minutes). The final reaction product was strictly deposited in the brush border area of the epithelial cells of the convoluted channels. The Glomeruli were entirely negative (Fig.1a,b). In the pancreas the enzyme reaction was seen in acinar cells. The cells in the islet of Langerhans were negative for GGT. (Fig.1c,d). In the epididymis we observed a GGT reaction in the epithelial cells of the channels (Fig.1 e,f). In the seminal vesicle, amorphous final reaction product was observed on the luminal surface of the glandular epithelial cells (Fig.1 g, h). Our investigations confirm that normally GGT has the highest activity in kidney and moderate in pancreas and male reproductive organs, which could be a result of the different glutathione levels in the examined organs. It is known that GGT exists in almost all normal leukocytes [5, 7]. So, we expected to find a GGT activity in spleen, but besides our multiple trials we did not obtain a positive enzyme reaction. Recent studies reported that GGT has different isoforms of tissue-specific expressions [16]. The negative reaction in spleen might indicate that our substrate does not recognize the lymphocytes isoenzyme form of GGT. This has to be tested by further investigations.

The newly proposed fluorescent method for γ -glutamyl transpeptidase can be applied for enzyme activity determination in tissue sections from laboratory animals. Also, we speculate on the possibility that we have obtained a histochemical substrate for GGT isoenzymes presented in the secretory or absorptive cells but not in lymphocytes, however, further studies are needed.

Acknowledgements. This work was supported by the Bulgarian National Science Fund of Ministry of Education and Science. Grant No MUL-1505/05.

References

1. Blair, S. L., P. Heerdt, S. Sachar, A. Abolhoda, S. Hochwald, H. Cheng, M. Burt. Glutathione metabolism in patients with non-small cell lung cancers. – *Cancer Res.*, **57**, 1997, 152-155.
2. Dikov, A., M. Dimitrova, R. Krieg, K.-J. Halbhuber. New tetrazolium method for the histochemical demonstration of gamma-glutamyl transpeptidase. – *Cell. Mol. Biol.*, **45**, 1999, 241-248.
3. Dominici, S., L. Pieri, M. Comporti, A. Pompella. Possible role of membrane gamma-glutamyltransferase activity in the facilitation of transferring-dependent and -independent iron uptake by cancer cells. – *Cancer Cell International*, **3**, 2003, 1-8.
4. Gan, J., H. Tian, Zh. Wang, K. Chen, J. Hill, P. A. Lane, M. D. Rahn, A. M. Fox, D. D. C. Bradley. Synthesis and luminescent properties of novel ferrocene-naphthalimides dyads. – *Organometallic Chem.*, **645**, 2002, 168-175.

5. Girino, M., R. Invernizzi, P. Perseghin, M. Michienzi. Cytochemical study of gamma-glutamyltranspeptidase activity in normal blood cells and in blood malignancies. – *Hematologica*, **70**, 1985, 266-268.
6. Godwin, A. K., A.O. Meister, P. J. Dwyer, C.S. Huang, T.C. Hamilton, M. E. Anderson. High resistance to cisplatin in human ovarian cancer cell lines is associated with marked increase of glutathione synthesis. – *Proc. Natl. Acad. Sci.*, **89**, 1992, 3070–3074.
7. Gossrau, R. Cytochemistry of membrane proteases. – *Histochem. J.*, **17**, 1985, 737-771.
8. Griffith, O. W., R. J. Bridges, A. Meister. Evidence that the γ -glutamyl cycle functions in vivo using intracellular glutathione: Effects of amino acids and selective inhibition of enzymes. – *Proc. Natl. Acad. Sci.*, **75**, 1978, 5405–5408.
9. Hochwald, S. N., L. E. Harrison, D. M. Rose, M. Anderson, M.E. Burt. Elevation of glutathione and related enzyme activities in high-grade and metastatic extremity soft tissue sarcoma. – *Ann. Surg. Oncol.*, **4**, 1997, 303-309.
10. Knorr, R., A. Trzeciak, W. Bannwarth, D. Gillissen. New coupling reagents in peptide chemistry. – *Tetrahedron Lett.*, **30**, 1989, 19-27.
11. Lee, D-H., M-H. Ha, J-H. Kim, D.C. Christiani, M. D. Gross, M. Steffes, R. Blomkoff, D. R. Jacobs. Gamma-glutamyltranspeptidase and diabetes—a 4 year followup study. – *Diabetologia*, **46**, 2003, 359-364.
12. Maellaro, E., S. Dominici, B. Del Bello, M. A. Valentini, L. Pieri, P. Perego, R. Supino, F. Zunino, E. Lorenzini, A. Paolicchi, M. Comporti, A. Pompella. Membrane gamma-glutamyl transpeptidase activity of melanoma cells: effects on cellular H2O2 production, cell surface protein thiol oxidation and NF-kappa B activation status. – *J. Cell Sci.*, **113**, 2000, 2671-2678.
13. Murata, J., P. Ricciardi-Castagnoli, P. Dessous L'Eglise Mange, F. Martin, L. Juillerat-Jeanneret. Microglial cells induce cytotoxic effects toward colon carcinoma cells: measurement of tumor cyto-toxicity with a gamma-glutamyl transpeptidase assay. – *Int. J. Cancer*, **70**, 1997, 169-174.
14. Orning, L., S. Hammarstrom, B. Samuelsson. Leukotriene D: A slow reacting substance from rat basophilic leukemia cells. *Proc. Natl. Acad. Sci.*, **77**, 1980, 2014–2017.
15. Paolicchi, A., A. Pompella, P. Tonarelli, A. Gadducci, A. R. Genazzani, F. Zunito, G. Pratesti, R. Tongiani. Gamma-glutamyl transpeptidase activity in human ovarian carcinoma. – *Anticancer Res.*, **16**, 1996, 3053-3058.
16. Sener, A., T. Yardimci. Activity determination, kinetic analyses and isoenzyme identification of gamma glutamyltransferase in human neutrophils. – *J. Biochem. Mol. Biol.*, **38**, 2005, 343-349.
17. Sian, J., D. T. Dexter, A. J. Lees, S. Daniel, P. Jenner, C. D. Marsden. Glutathione-related enzymes in brain in Parkinson's disease. – *Ann. Neurol.*, **36**, 1994, 356–361.
18. Tager, M., A. Ittension, A. Franke, A. Frey, H. G. Gassen, S. Ansorge. Gamma-Glutamyl transpeptidase – cellular expression in populations of normal human mononuclear cells and patients suffering from leukemias. – *Ann. Hematol.*, **70**, 1995, 237-242.
19. Vesely, J., V. Lisy, M. Cernoch. Partial purification of γ -glutamyl transferase from human brain microvessels. – *Neurochem. Res.*, **10**, 1985, 1325-1334.

TNF- α Augments Enzyme Expression in the Small Intestine of Developing Mice

V. Pavlova, M. Dimitrova, E. Nikolova

*Institute of Experimental Morphology, Pathology and Anthropology with Museum,
Bulgarian Academy of Sciences*

Colostrum and milk are essential for the development and growth of mammals. Among the substances present in colostrum and milk tumor necrosis factor-alpha (TNF- α) has significant role in gut maturation and development. The aim of our study was to determine whether TNF- α has influence on the expression of the enzymes alkaline phosphatase, lactase and dipeptidil peptidase IV (DPP IV). Deposition of reaction products was visualized in thin sections of frozen gut tissue. Our observations showed more vivid results on first day of explants' treatment. Presence of TNF- α didn't show any significant effect on the activity of lactase. However in presence of TNF- α expression of alkaline phosphatase and DPP IV was increased.

Key words: TNF- α , enzyme expression, alkaline phosphatase, lactase, DPP IV.

Introduction

Colostrum and milk are essential for the development and growth of mammals. The composition of human milk provides the infant with all nutritional requirements in its early life [1]. A key cytokine delivered to developing intestine by mammary secretions is tumor necrosis factor alpha (TNF-alpha). Milk TNF- α is secreted by milk macrophages and by mammary epithelium. Levels of the cytokine in colostrum are significantly higher than both transitional and mature milk [8]. Besides participating in humoral and cell immunity, TNF- α also plays an important role in many diseases such as severe hepatitis, septic shock and inflammatory bowel disease [5]. During the first days of lactation TNF- α is physiologically active, enhancing the immune system of the neonate [13]. This includes development of monocytes and IL-1 and IL-10. The effects of milk cytokines and in particular tumor necrosis factor alpha on the maturation and functions of the epithelium, mucosal leukocytes and other specialized cells and structures in the alimentary system is not well documented. For that reason we target our research on TNF- α since it has got protective effect on respiratory system [10], but fewer investigations are held on the alimentary tract. The aim of our study was to trace the enzyme activity of alkaline phosphatase, lactase and DPP IV in the small intestine in organ culture in presence of TNF- α . Quantitative analysis of the number of dividing cells, stimulated or non stimulated with the factor was done.

Material and Methods

Tissue treatment. Balb/c mice 5 days old were used. Segments from duodenum, jejunum and ileum were taken according to the method of Playford et al. [7]. Specimens were incubated in culture medium RPMI 1640 containing 10 % fetal calf serum with 30 pg/ml rm TNF-alpha /Immunotools /Germany/ for 24, 48 and 72 h at 37 °C, 5% CO₂ respectively. All animal procedures were approved by the animal ethics committee at the Institute.

Autoradiography. It was developed by standard procedure and 5 µCi of ³H-Thymidine were added (Amersham, UK) to untreated or TNF-alpha treated cultures 18 h before the end of the culture. Gut explants were put into Tissue Tek embedding medium (Sakura, USA) and frozen at -25 °C. They were cut on cryotom (Reichert Jung, FRG) to 10 µm sections and applied to glass slides. The number of dividing cells was counted using light microscope.

Enzyme localization. For the visualization of alkaline phosphatase activity we followed Burnstone's technique [3]. Sections were incubated in 0.7 mM naphthol-AS-MX-phosphate and 0.8 mg/ml Fast Blue B in 0.1 M TRIS/HCl buffer, pH 9.0 for eight min at 37 °C.

The visualization of lactase activity was performed after Gossrau [4]. We used substrate medium, containing 1 mM 5-Bromo-4-chloro-3-indolyl-beta-D-galactopyranoside and 1.2 mg/ml nitroblue tetrazolium chloride in 0.1 M sodium citrate /citric acid buffer, pH 6.0 for 2 h at 37°C.

For the visualization of DPP IV activity we used a newly developed procedure by Ivanov et al. [6]. The sections were incubated in medium, containing 0.3 mM fluorogenic substrate Gly-Pro-4-hydrazido-N-hexyl-1,8-naphthalimide (Gly-Pro-HHNI) and 0.3 mg/ml piperonal in 0.1 M phosphate buffer, pH 7.7 for two hours at 37°C. Then the sections were post fixed in 4 % neutral formalin for 15 min at room temperature, stained with hematoxylin according to the standard histochemical procedure and embedded in glycerol jelly.

Results and Discussion

The small intestinal mucosa changes rapidly in the first few postnatal weeks. The role of immune system in colostrums and milk is significant in protecting not only the mature, healthy newborn but also premature infant who is more prone to infections and damage caused by inflammatory processes. The human milk-fed preterm infant may experience improved health, such as, lower rate of infection, necrotizing enterocolitis, better gastrointestinal function, and neurodevelopment [14, 9].

TNF- α is synthesized as a 26-kDa transmembrane pro-hormone, which undergoes proteolytic cleavage to yield a 17-kDa soluble TNF- α molecule. Despite the differences in the location, both forms of TNF- α are capable of mediating biological responses [2,18] and together may be responsible for both local and systemic actions of this cytokine [16]. Tumor necrosis factor-alpha that is present in colostrums is a multifunctional cytokine which exerts a myriad of biological actions in different tissues. It has been demonstrated to regulate or interfere with adipocyte metabolism like transcriptional regulation, glucose and fatty acid metabolism and hormone receptor signaling [11]. Other *in vivo* studies demonstrate that elevated levels of serum TNF- α could be an important mediator of bacterial invasion of the intestinal mucosa during acute liver failure [12]. To date most of the cellular actions of TNF- α have been attributed to the activities of two distinct receptors TNFR1 and TNFR2 which are playing primarily a modulatory

role in ligand passing [17]. Both TNF receptors can be released from the cell surface and can exist in soluble form. Elevated levels of soluble TNF receptors are presented in many pathological states like cancers, sepsis, and fever [15].

Murine intestinal mucosa undergoes significant morphological changes like disappearance of large supranuclear vacuoles and decrease in the intestinal permeability towards proteins (gut closure). It has also been observed that activities of some mucosal enzymes are modified during that early postnatal period. For instance lactase which is essential for lactose hydrolysis during the first two postnatal weeks loses part of its activity and concentration [11].

In our previous work we have found positive morphological effect of TNF- α on murine gut development. To complete our study we traced the effect of TNF- α on some small bowel enzymes as described above.

Using autoradiography we counted the number of dividing nuclei. For that purpose we used StatMost for Windows. One-Way ANOVA results were used to prepare graphs. For first day of incubation the number of dividing nuclei was increased for the samples treated with TNF-alpha (Fig.1). On second and third day of incubation we did not see significantly different results for the two groups.

Intestinal alkaline phosphatase (AP) is a brush border protein that hydrolyzes monophosphate esters. It is expressed exclusively in villus enterocytes and is considered as a marker for crypt-villus differentiation. Addition of TNF-alpha to culture medium augmented AP's activity in all parts of the small bowel (Fig. 2a) compared to untreated specimens (Fig. 2b).

Dipeptidyl peptidase (DPP IV) is highly expressed in differentiated enterocytes. It is implicated in the degradation of various peptides and hormones including glucagons, neuropeptides and chemokines. Stimulation of the explants with TNF-alpha resulted in increased activity in all three parts of the small bowel (Fig. 3 a, b – control)

Lactase is essential for lactose hydrolysis during the first postnatal weeks. It also is considered marker of terminal differentiation in enterocytes. In our study addition of TNF-alpha did not affect enzyme's activity (Fig. 4a, b).

The results of our study do raise the possibility that TNF- α can ameliorate the activity of both alkaline phosphatase and dipeptidyl peptidase and has no significant effect on the activity of lactase.

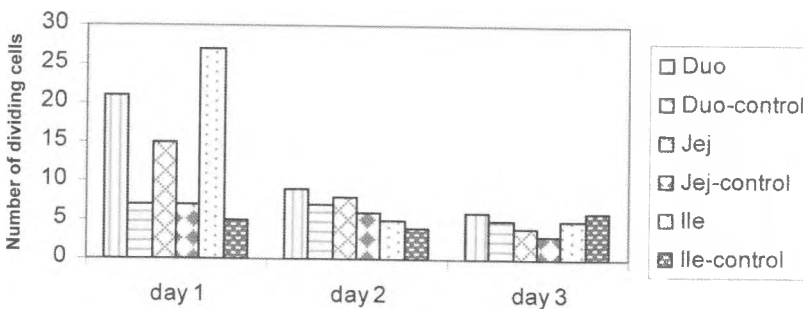
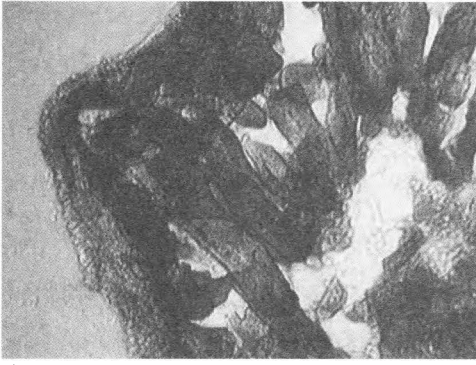


Fig. 1. Incorporation with 3H -Thy in murine enterocytes, treated with TNF- α and controls. Elevated levels of incorporation for the first 24 h after treatment, especially in jejunums

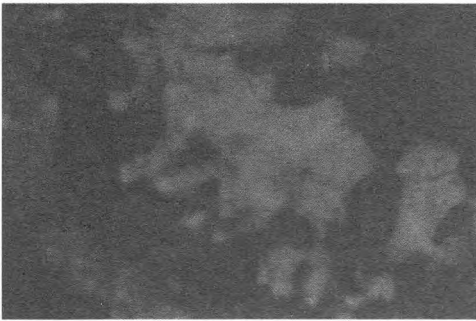


a)

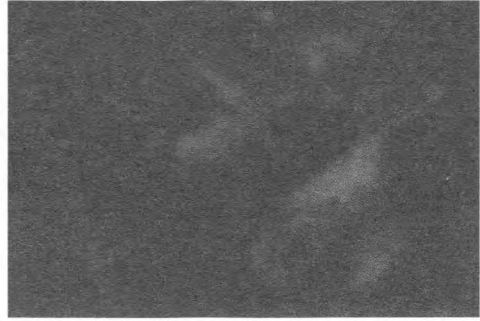


b)

Fig.2. Expression of alkaline phosphatase (AP) in cultured intestinal villi of 5 day old mouse, treated with TNF- α (2a). Lower expression of AP in controls in all parts of the small bowel (2b). Original magnification $\times 40$

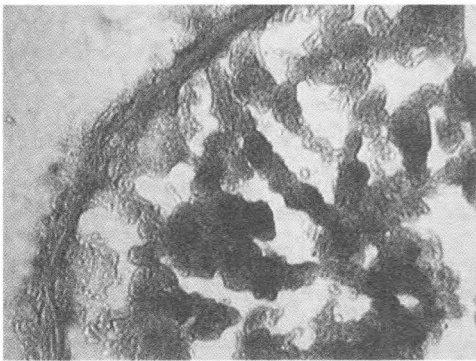


a)



b)

Fig. 3. Expression of dipeptidyl peptidase (DPP IV) in murine intestinal villi. Specimens treated with TNF- α (3a) show more reaction product in comparison to untreated controls (3b). Originally $\times 60$



a)



b)

Fig. 4. Expression of lactase in intestinal microvilli of 5 days old mouse. No significant differences were observed between samples (4a) and controls (4b). Original magnification $\times 40$

Acknowledgements. This study was supported by Grant TKL 1609 from the Ministry of Education, Bulgaria.

References

1. Bernt, K. M., W. A. Walker. Human milk as a carrier of biochemical messages. – *Acta Paediatr Suppl.* 88, 1999; 27-41.
2. Beutler, B. TNF, immunity and inflammatory disease: lessons of the past decade. – *J Invest Med* 43, 1995, 227-235.
3. Burstone, M.S. Enzyme histochemistry and its application in the study of neoplasms. New York-London Academic press, 1962.
4. Gossrau, R., Azoindoxyl methods for the investigation of hydrolases. III. Histochemical studies of beta-D-N-acetylglucosaminidase. – *Histochemistry*, 58, 1978, 203-218.
5. Hong, HL, S. Lu, P. Liu. Tumor necrosis factor-alpha induces apoptosis of enterocytes in mice with fulminant hepatic failure. – *World J Gastroenterol*, 11, 2005, 3701-3709.
6. Ivanov, I., D. Tasheva, R. Todorova, M. Dimitrova. Synthesis and use of 4-dipeptidylhydrazido-N-hexyl-1, 8-naphthalimides as fluorogenic histochemical substrates for dipeptidyl peptidase IV and tripeptidyl peptidase I. – *Eur. J. Med. Chem.*, 44, 2009, 384-392.
7. Krieglner, M., C. Perez, K. DeFay, I. Albert, S. D. Lu. A novel form of TNF/cachectin is a cell surface cytotoxic transmembrane protein: ramifications for the complex physiology of TNF. – *Cell*, 53, 1988, 45-53.
8. Meki, M.A., T. A. Saleem, M.H. Al-Ghazali, A.A. Sayed. Interleukins-6, -8 and -10 and tumor necrosis factor-alpha and its soluble receptor I in human milk at different periods of lactation. – *Nutrition Research*, 23, 2003, 845-855.
9. Montagne, P.M., V.S. Tregoeat, M. L. Cuilliere, M.C. Bene, G.C. Faure. Measurement of nine human milk proteins by nephelometric immunoassays: Application to the determination of mature milk protein profile. – *Clin. Biochem.*, 33, 2000, 181-186.
10. Oddy, W. H., M. Halonen, F.D. Martinez, I.C. Lohman, D.A. Stern, M. Kurzius-Spencer, S. Guerra, A.L. Wright. TGF- β in human milk is associated with wheeze in infancy. – *J Allergy Clin Immunol.*, 112, 2003, 723-728.
11. Peulen, O., Deloyer P., Grandfils, C., Loret, S., Dandrifosse G. Intestinal maturation induced by spermine in young animals. – *Livestock Production Science*, 66, 2000, 109-120.
12. Playford, R. J., T. Marchbank, R. A. Goodlad, R. A. Chinery, R. Poulsom. A. M. Hanby, Transgenic mice that overexpress the human trefoil peptide pS2 have an increased resistance to intestinal damage. – *Proc. Natl. Acad. Sci. U S A*, 93, 1996, 2137-2142.
13. Rudloff, E.T., F.C. Schmalstieg, Jr, A.A. Mushtaha, K.H. Palkowetz, S.K. Liu, A.S. Goldman. Tumor necrosis factor- α in human milk. – *Ped. Research*, 31, 1992, 29 – 33.
14. Schanler, R. J., S. A. Atkinson. Effects of nutrients in human milk on the recipient premature infant. – *J Mammary Gland Biol Neoplasia*, 4, 1999, 297-307.
15. Sethi, J.K., G. S. Hotamisligil. The role of TNF α in adipocyte metabolism. – *Cell & Develop. Biol.*, 10, 1999, 19-29.
16. Song, H. L., S. Lv, P. Liu. The roles of tumor necrosis factor-alpha in colon tight junction protein expression and intestinal mucosa structure in a mouse model of acute liver failure. – *BMC Gastroenterol.*, 9, 2009, 70.
17. Tartaglia, L.A., D. Pennica, D.V. Goeddel. Ligand passing: the 75-kDa tumor necrosis factor (TNF) receptor recruits TNF for signaling by the 55-kDa TNF receptor. – *J. Biol. Chem.*, 268, 1993, 18542-18548.
18. Xu, H., J. K. Sethi, G. S. Hotamisligil. Transmembrane tumor necrosis factor (TNF)-alpha inhibits adipocyte differentiation by selectively activating TNF receptor 1. – *J. Biol. Chem.*, 37, 1999, 26287-95.

Double Staining Technique for Rat Foetus Skeleton in Teratological Studies

M. Georgieva, M. Gabrovska

Medical University of Varna "Prof. Paraskev Stoyanov"

The characteristic staining of the skeleton is an important part of the toxicological studies on the individual development. The precise and full interpretation of the data regarding the skeletal toxicity is possible only if using the "double staining method" with alizarin red and alcian blue. The Wilson section method, which is standard teratological method and still represents the most utilized technique to examine the visceral organs, was used to explore the soft tissues.

The study of teratogenicity required application of the studied substances on pregnant female Wistar rats during the organogenesis. On day 21 after conception were extracted via caesarian section and were explored for skeletal toxicity, using the method of "Double skeleton staining".

The double staining method used in the current study is a fundamental part of the teratological studies for assessment of the toxicity of the xenobiotics and non-chemical factors for the individual development.

Keywords: toxicology, teratogenicity, xenobiotics, Double staining method, Wilson section method.

Introduction

The teratogenic activity of the xenobiotics is studied by means of examination for visceral and skeletal abnormalities of the fetus of laboratory animals (rats).

The characteristic staining of the skeleton is an important part of the toxicological studies on the individual development [6]. The precise and full interpretation of the data regarding the skeletal toxicity is possible only if using the "double staining method" with alizarin red and alcian blue [5, 8]. All cartilages stained in blue, and the ossified bones in red. Thus the cartilaginous and the bone part of the skeleton are examined, and any possible abnormalities could be detected. Despite the latter one requires a lot of labor and time, it is the only one that can be used to study the fetus until the pregnancy is not accomplished (20th day of the pregnancy) [2, 3, 10].

The separate staining with alizarin red for bones is the most commonly used in the routine teratological testing, since it involves a much easier and cheap procedure [1, 5]. However, this turns the staining of the cartilaginous part of the skeleton is impossible

The fetuses were studied microscopically to detect any internal organ (lung, liver, spleen etc.) abnormalities, using 20 body slices with thickness 1 mm. (Wilson Section Method) (Fig. 3).

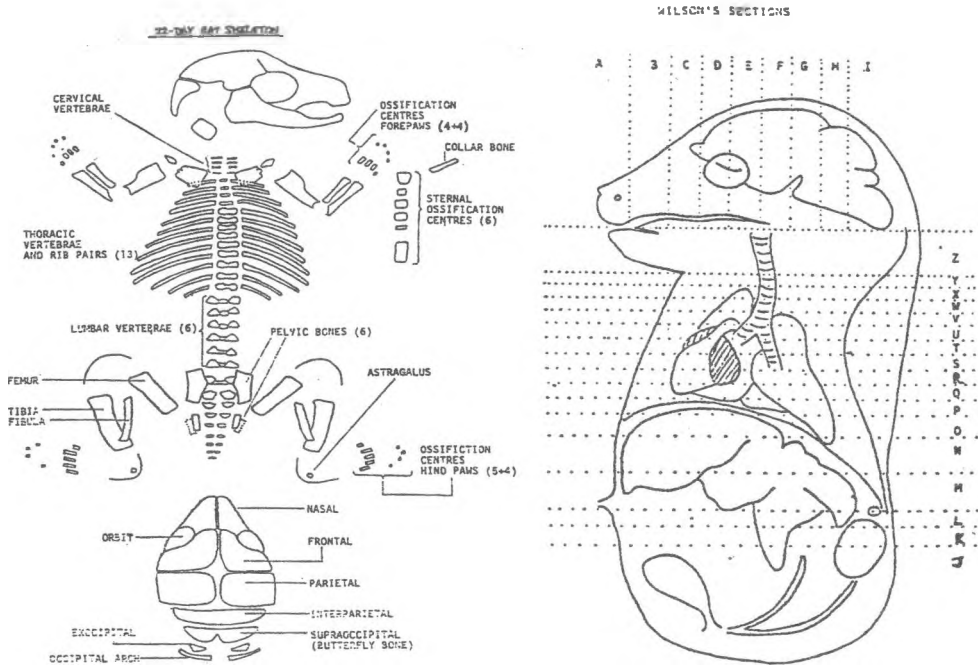


Fig. 3. Wilson Section Method

Results

The body weight and the length of the fetuses, the weight of the placentas and livers of adult rats treated with physiological solution are shown on Table 1.

On inspection of the fetuses from the group with physiological solution no anomalies were seen regarding the skeleton: head, body, extremities. Lack of teratogenic effect was detected, using following indices:

- Gross appearance - external;
- Coloration of the fetus;
- Subcutaneous hemorrhages.

Table 1. Weight and length of fetuses, weight of placentas and livers

	Weight fetuses (g)	Length fetuses (mm)	Weight placentas (g)	Weight livers (g)	n
Controls (phys. sol.)	2.81±0.24	33.48±1.21	0.45±0.007	0.20±0.017	29

Gross abnormalities as: spina bifida, anencephaly, exencephaly, arhinencephaly; cebocephaly;

Head: eyes, ears, nostrils, tongue, palate, mouth.

Extremities: anterior, posterior (number of fingers, syndactyly, micromelia).

Rear part of the body: anus (abnormalities) – atresia ani; tail (deformities, lack of tail; genitals (2 mm for male gender, 1 mm for female gender).

Test for skeletal toxicity

When the physiological solution was tested for skeletal toxicity with the “double staining method” all cartilages stained in blue, and the ossified bones – in red. The examination of the whole skeleton for variations in the level of ossification, lack of cartilages and any possible abnormalities no deviations from the norm were found. For each bone the dimensions, type, relative position, number of bones and ribs were denoted and compared to standarts. The physiological solution that was tested did not induce skeletal toxicity.

Microscopy

On microscopy examination of the fetuses for abnormalities of the internal organs (lung, liver, spleen, kidneys etc.) using the Wilson section method no anomalies were found in any of the explored organs.

Discussion

In the current experiment a test for fetal and maternal toxicity of the physiological solution was done. The body weight, and the length of the fetuses, the weight of the placentas, and livers of rats treated with physiological solution, did not show statistically significant difference compared to normal parameters. The inspection of the fetuses showed no abnormalities.

The physiological solution was tested for skeletal toxicity using double skeleton staining method with alizarin red and alcian blue [8]. All cartilages stained in blue, and the ossified bones in red. Thus the cartilaginous and the bone part of the skeleton were examined, and any possible abnormalities could be detected. The animals treated with physiological solution showed no difference compared to the norm.

The Wilson section method, which is standard teratological method and still represents the most utilized technique to examine the visceral organs, was used to explore the soft tissues [9]. No impairment was found in any of the examined internal organs.

This experiment convincingly demonstrates that physiological solution does not manifest data indicative for teratogenicity.

Conclusion

The double staining method used in the current study is a fundamental part of the teratological studies for assessment of the toxicity of the xenobiotics and non-chemical factors for the individual development. The double staining method described in the study is used by world-wide known toxicological laboratories, by universities and pharmaceutical corporations – Bayer Corporation, Lilly RL, Zeneca, Glaxo, Sanofi, etc. [10, 11, 12].

References

1. Burdan, F. Teratology, 40-years after the thalidomide tragedy. – *Ginekol. Pol.*, 72, 2001, 93-100.
2. Burdan, F, I. Rozylo-Kalinowska, T. K. Rozylo, I. Chahoud, A new, rapid radiological procedure for routine teratological use in bone ossification assessment: a supplement for staining methods. *Teratology*, 66, 2002, 315-325.
3. Christian, M. S Test methods for assessing female reproductive and developmental toxicology. In: Hayes AW (ed.). *Principles and method of toxicology*. 4th Ed. Taylor & Francis, Philadelphia, 2001, 1301-1381.
4. ICH ICH Harmonised tripartite guideline. Maintenance of the ICH guideline on toxicity to male fertility. 2000, An addendum to ICH tripartite guideline on detection.
5. Menegola, E, M. L. Broccia, F. Di Renzo, E. Giavini, Comparative study of sodium valproate-induced skeletal malformations using single or double staining methods. – *Reprod. Toxicol.*, 16(6), 2002:15-23.
6. Miller, D. M, J. Tarpley, An automated double staining procedure for bone and cartilage, *Biotech Histochem.* 71(2), 1996, 79-83.
7. Webb, G. N, R. A. Byrd, Simultaneous differential staining of cartilage and bone in rodent fetuses: an alcian blue and alizarin red S procedure without glacial acetic acid. – *Biotech. Histochem.*, 69(4), 1994, 181-185.
8. Whitaker, J, K. M. Dix. Double staining technique for rat foetus skeletons in teratological studies. *Lab Anim.* 13(4), 1979:9-10.
9. Wilson, J. G, F. C. Fraser, *Handbook of teratology*. Vol. 4. Plenum Publishing Corporation, New York. 1977.
10. Young, A. D, D. E. Phipps, A. B. Astroff, Large-scale double-staining of rat fetal skeletons using Alizarin Red S and alcian blue. – *Teratology*, 61(4), 2000, 273-6.
11. Truman, D, S. W. Jackson, B. Truman. An automated technique for double staining rat and rabbit fetal skeletal specimens to differentiate bone and cartilage. – *Biotech. Histochem.*, 74(2), 1999:98-104.
12. Liberati, T. A, B. J. Roe, M. H. Feuston. An oral (gavage) control embryo-fetal development study in the Wistar Hannover rat. – *Drug Chem Toxicol.* 25(1), 2002, 109-30.

Metabolic Glycogen Activity in Hepatocytes of Fish from a Water Source Containing Heavy Metals

*D. Arnaudova, *At. Arnaudov, **E. Sapundzhiev*

University of Plovdiv "Paisii Hilendarski" – "Lyuben Karavelov" Branch – 6000 Kardzhali

** University of Plovdiv "Paisii Hilendarski", Faculty of Biology – 4000 Plovdiv*

*** University of Forestry, Faculty of Veterinary Medicine – 1756 Sofia*

By a histochemical research it was investigated what the glycogen concentration in the hepatocytes of three species freshwater fish (bleak, perch and rudd) is. By this it is proven that there is bioaccumulation of lead, zinc and cadmium in their livers as a result of the fish's inhabiting water basins containing the same metals.

It was established that heavy metal bioaccumulation in the fish liver causes decrease of glycogen and its uneven distribution in the organ compared to fish in clean water basins. Resulting from the presence of heavy metals, species peculiarities in the disorders of glycogen metabolism were found.

Key words: glycogen, freshwater fish, heavy metals, histochemistry.

Introduction

In the hydrobiomes there is a bioconcentration of persistent pesticides and other xenobiotics including of heavy metals. Metals are not biodegradable and are referred to as mail environment polluters that have a mutagenic and carcinogenic effect on living organisms (More et al., 2003). Dural et al. (2007) and Ploetz et al. (2007) report that the highest levels of cadmium, lead, copper and zinc accumulation can be found in livers and gills of the fish investigated.

Down the Arda river valley there are the reservoirs 'Studen Kladenets' and 'Kardzhali' that are located near sources of strong anthropogenic pollution with heavy metals. Velcheva (1998) indicates morphological changes in liver cells of bleak, carp and perch fish from 'Studen Kladenets' reservoir by increased cadmium, lead, copper and zinc content in this organ. Concerning the physiological role of liver in carbohydrates metabolism, as well as the property of hepatocytes to accumulate polysaccharates in their cytoplasm it is of interest to comparatively study the morphofunctional characteristics of glycogen activity in cells containing accumulated heavy metals.

The aim of the research was to determine the quantitative parameters of the glycogen synthesized in the liver cells of fish inhabiting the basin of 'Studen Kladenets' reservoir down the Arda river containing heavy metals and to compare the results with those of fish of the same species but from unpolluted basins.

Materials and Methods

The study is conducted in the 'Studen Kladenets' reservoir region (Southern Bulgaria). In the investigations are included 30 freshwater fish of each of the 3 species: bleak (*Alburnus alburnus* L., Cyprinidae), rudd (*Scardinius erythrophthalmus* L., Cyprinidae) and perch (*Perca fluviatilis* L., Cyprinidae). As control specimens were used 3 to 5 fish of the same species from the 'Varbitsa' river in a region with no anthropogenic pollution.

The chemical analysis of heavy metals content in the soil and sediment was conducted using the method flame atomic absorbance spectrophotometry air-acetylene (2100-2300°C) with an apparatus "Perkin Elmer 3030 B".

The content of zinc, lead and cadmium in organs samples of the freshwater fish investigated was determined by the atomic absorbance spectrophotometry (AAS „PERKIN-ELMER 3030 B"). The results are calculated in mg.kg^{-1} air-dry sample and are in conformity with the Threshold Limit Value (TLV) regulation for the concentration of toxic stuff in foodstuffs (Regulation No 5 of Health Department 1984).

Treating the histological samples for proving the presence of glycogen in the hepatocytes is conducted using the PAS histochemical method.

Results and Discussion

The permissible lead, zinc and cadmium level in soil depends on the active reaction of soil to water suspension. In the soil around 'Studen Kladenec' reservoir by a $\text{pH}=8.0$ the norm of the concentration Pb is $<80 \text{ mg.kg}^{-1}$, of Zn - $<370 \text{ mg.kg}^{-1}$ and Cd - 3 mg.kg^{-1} . According to our data the quantity of Pb and Cd is more than the norm. The measured Pb concentration is higher than TLV by $60.845 \text{ mg.kg}^{-1}$ and the quantity of Cd is a little more than it by 0.13 mg.kg^{-1} . Unlike these, the content of Zn is under the TLV by $31.189 \text{ mg.kg}^{-1}$.

The data about the heavy metal concentration in the sediment show higher values of those in the soil but our country does not have regulation norms for TLV in it. This is of big methodological importance as water organisms are capable of accumulating heavy metals from different sources including sediment (Labonne et al., 2001).

Researches on heavy metal accumulation in organs of fish from 'Studen Kladenets' reservoir show species peculiarities. The Lead content in the three fish species' organs show that the metal accumulates in the highest concentration in the hepatopancreas of rudd and less in the same organ in the bleak followed by perch but by all three fish the content is above the Threshold Limit Value. Bioaccumulation of zinc is also changed to more than the Threshold Limit Value in all three fish species. Among them, the zinc concentration is highest by perch followed by rudd and bleak. The cadmium content in liver of all three species shows that the metal accumulates in a considerably high level in perch liver. There is an increase over the Threshold Limit Value indicated as well, although in lower grades, in the hepatopancreases of the other two species. The found quantity accumulation and the regularities coincide with some previous researches of ours. Similar results have been reported by other authors when examining heavy metal bioaccumulation in different organs of freshwater fish (Dural et al., 2007; Ploetz et al.,

2007). It is considered that lead and chromium bioaccumulation in liver is due to protein affinity of the protein metallothionein towards these elements (Ikem et al., 2003).

The found accumulation of heavy metals and its species specificity proves right the statements of Tawari-Fufeyin and Ekaye (2007) and Karadede-Akin and Unlu (2007) that fish can serve as a bioindicator for pollution of the water they inhabit.

Normal metabolic activity of liver cells of bleak, rudd and perch

The parenchyma of the hepatopancreas is built by prismatic cells with a light-coloured cytoplasm, distinctive borders between them and centrally located nucleuses. The density of the parenchyma cells cytoplasm is due to the glycogen in them which is the form of granules. By the histochemical investigation on availability of glycogen in the hepatocytes of the control specimens there can be observed that the glycogen granules are present on the whole surface of the histological sections. In the organ are found vacuolised hepatocytes and a great number of lipocytes around them which gives the parenchyma a netlike character (fig. 1a, b).

In the perch liver the hepatocytes are with a more homogeneous cytoplasm and the lipocytes between them are less in quantity which provides the organ with a relative density (fig. 1c).

Metabolic activity of liver cells of bleak, rudd and perch from the 'Studen Kladenets' reservoir

By acquiring the glycogen concentration in the hepatocytes of bleak, rudd and perch from the "Studen Kladenets" reservoir a degranulation in the cell cytoplasm can be observed. (fig. 2). In the bleak samples the positively displayed areas with glycogen are lighter coloured. The vacuolization of hepatocytes is in higher rate while the quantity of lipocytes between them is reduced (fig. 2a).

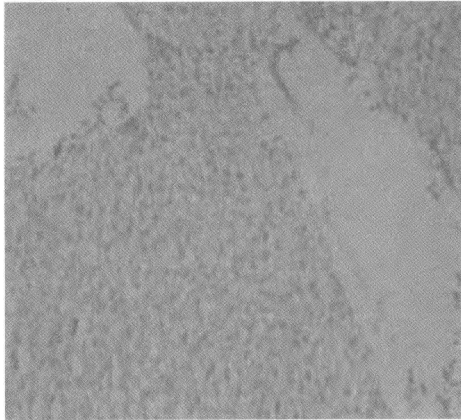
Glycogen by rudd fish is evenly distributed but has a weakened intensity and the parenchyma acquires a looser appearance (fig. 2b). In the perch samples the degranulation of glycogen is increased and the parenchyma density is decreased (fig. 2c).

The lead, cadmium and zinc found in hepatocytes of the fish investigated play a deactivating role on the glycogen synthesized in them. These data are in a correlation with the observed by More et al. (2003) metabolic deficit of DNA and hypofunction of the organism as a result of accumulation of heavy metals in it. Hayat et al. (2007) prove it that these metals have a growth hold-back influence of carp fish. They probably are the cause and consequence of the found morphological changes in fish hepatocytes (Velcheva, 1998). Depending on their aptitude towards bioconcentration, heavy metals take part in the metabolic chains on the highest levels of ecological pyramids where they create critical concentrations. This accumulation can lead to a long-lasting effect and changes in the biological lifecycle of fish.

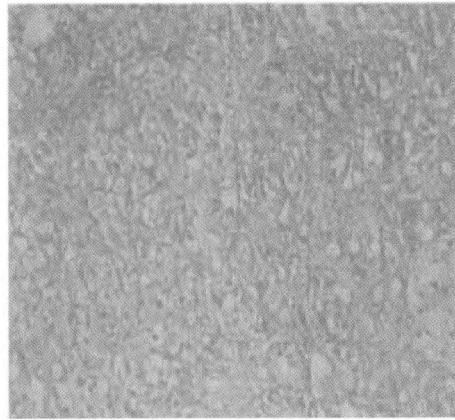
Conclusion

Bioaccumulation of lead, zinc and cadmium in the hepatocytes of bleak, perch and rudd causes the decrease of the glycogen content in them.

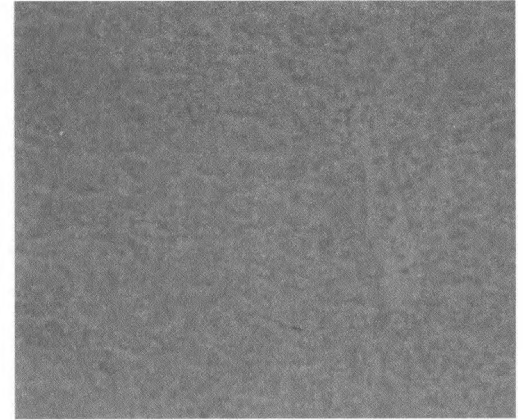
Species peculiarities exist in the glycogen metabolism disorder in the hepatocytes of fresh water fish caused by the presence and action of heavy metals in their organisms.



(a)

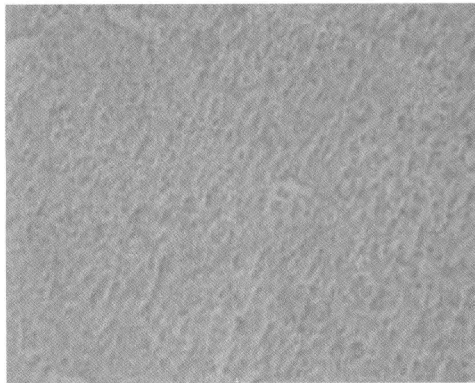


(b)

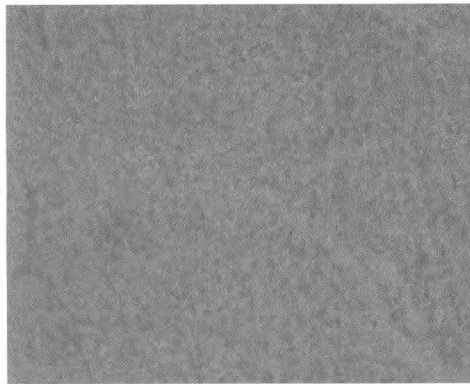


(c)

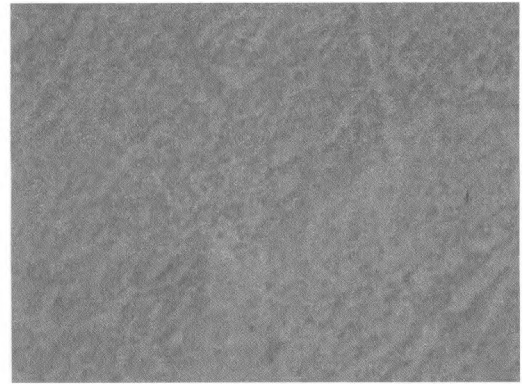
Figure 1. Expression of glycogen by a PAS reaction in a hepatopancreas of bleak (a), rudd (b) and perch (c) from a clean water basin. $\times 40$.



(a)



(b)



(c)

Figure 2. Expression of glycogen by a PAS reaction in a hepatopancreas of bleak (a), rudd (b) and perch (c) from the 'Studen Kladenets' reservoir. $\times 40$.

References

1. Velcheva, I. An ecological research on the cadmium (Cd), lead (Pb) and zinc (Zn) in bleak (*Alburnus alburnus* L.), carp (*Cyprinus carpio* L.) and perch (*Perca fluviatilis* L.) from the reservoirs 'Kardzhali' and 'Studen kladenets'. PhD thesis. University of Plovdiv. 1998. 135 p.
2. Durali, M., M. Z. L. Goksu, A. A. Ozak. Investigation of heavy metal levels in economically important fish species captured from the Tuzla Lagoon. – *Food Chem.*, 102, 2007, 415-421.
3. Hayat, S., M. Javed, S. Razzaq. Growth performance of metal stressed major carps viz. Catla catla, *Labeo rohita* and *Cirrhina mrigala* reared under semi-intensive culture system. – *Pakistan Vet. J.*, 27, 1, 2007, 8-12.
4. Ikem, A., N. O. Egiebor, K. Nyavor. Trace elements in water, fish and sediments from Tuskegee lake, Southeastern USA. – *Water Air Soil. Pollut.*, 149, 2003, 51-75.
5. Karadede-Akin, H, E. Unlu. Heavy metal concentrations in water, sediments, fish and some benthic organisms from Tigris river, Turkey. – *Environ. Monit. Assess.*, 131, 2007, 323-337.
6. Labonne, M., D. B. Othman, J. M. Lucc. Lead isotopes in muscles as tracers of metal sources and water movements in a Lagoon (Thau Basin, S. France). – *Chem. Geology*, 181, 2001, 181-191.
7. More, T. G., R. A. Rajput, N. N. Bandel. Impact of heavy metals on DNA content in the whole body of freshwater bivalve, *Lamelleiden marginalis*. – *Environ. Sci. Pollut. Res.*, 22, 2003, 605-616.
8. Ploetz, D. M., B. E. Fitts, T. M. Rice. Differential accumulation of heavy metals in muscles and liver of a marine fish (King Mackerel, *Scomberomorus cavalla*, Cuvier) from the Northern Gulf of Mexico, USA. – *Bull. Environ. Contam. Toxicol.*, 78, 2007, 134-137.
9. Tari-Fufeyin, P., S. A. Ekeye. Fish species diversity as indicator of pollution in Ikpoba river, Benin City, Nigeria. – *Rev. Fish Biol. Fisheries*, 17, 2007, 21-30.
10. Regulation No 5 for hygiene norms of Threshold Limit Value of chemical and biological pollutants in food products. Health Department of Republic of Bulgaria, State Gazette, 39, 18.05.1984.

Comparative Analysis of Two Embryo Freezing Methods

E. Sapundzhiev

*Faculty of Veterinary Medicine University of Forestry
1756 Sofia, 10, Kl. Ohridski, Bulgaria*

Two rates of methods are mainly conducted to establish the influence of the deep embryo freezing protocol on the post-thawing viability during the embryobiotechnology procedure.

The aim of the present study is to compare reliability of both so call conventional slow-rate freezing and vitrification high-speed method, respectively for preservation the viability of animal preimplanted embryos.

Using slow-rate freezing live offspring were produced from Romanovska sheep frozen-thawed embryos subsequently transferred to synchronized different breed recipients. The viability rate ranged between 40% and 57% when 1.37 M glycerol was used in two experiments. The beef cattle embryos were treated just the same speed protocol and their viability was 40% and 25% when 1.37 M glycerol and 1.5 M ethyleneglycol were used respectively, when new-born calves were obtained. In comparison vitrified mouse embryos survive the freezing with 6.85 M glycerol cryoprotectant and viability was saved up to 44% after in vitro culture.

Key words: freezing, embryo, embryobiotechnology.

Introduction

Embryo freezing is a cryobiology method achieving arrest of the biological processes in their blastomeres. Following manipulations of thawing and dilution of the cryoprotectant restore the embryo viability and give as an attractive tool of controlling animal reproduction. After the first successful approach of freezing-thawing mouse embryos [12], various mammalian embryo cryopreservation procedures have been developed and gave acceptable in vitro or in vivo results abroad and also in our country [9]. These procedures can be divided into two main types – conventional slow-rate freezing and vitrification. Various cryoprotectants were used for freezing of animal embryos and their influence on viability rate was examined after thawing in proper conditions – in vitro culture or embryo transfer.

Conventional freezing is the method in which the cryoprotectant concentration reaches to 10% and good post-thawing viability rate has been achieved. Many kinds of cryoprotectants such glycerol, DMSO, ethyleneglycol and propyleneglycol were used. The disadvantage of this method is the necessity of special costly equipment which real-

ized the computerized program for a long time period (2-3 h) of freezing. The method was elaborated earlier and has wider application in practice.

Vitrification method has the advantages of being much quicker (a couple of min) and cheaper. Otherwise, this method is still experimental and higher up to 50% concentration a mixture of various cryoprotectants has expressive toxicity.

The aim of the present investigation was to compare viability rate of animal pre-implanted embryos after freezing, thawing and subsequent embryobiotechnology of so called slow-rate procedure and vitrification method respectively.

Materials and Methods

Animal donors and embryo recovery

Sheep. Two subsequent experiments A and B were provided with 8 Romanoska sheep respectively 5 and 3. Superovulation of the donors was induced by intramuscular injection of 1000 IU PMSG (Pregmagon, Germed, Germany) on day 10 of the sexual cycle (estrus = day 0). The donors were treated 48 h later with analogue of PGF2 α – 125 μ g Cloprostenol (Oestrophan, Spofa, Czech Republic). The sheep were artificially inseminated twice in 12-hour interval with fresh semen when clinical signs of estrus were observed. A total of 28 embryos respectively 19 in trial A and 9 in trial B were recovered on day 6 of gestation by midventral laparotomy and flushing uterine horns. The obtained embryos were in blastocyst stage in experiment A and morula and early blastocyst in experiment B. Manipulating medium (MM) was phosphate buffered saline (PBS) solution – Dulbecco's medium supplemented with 20% de complemented fetal calf serum. The freezing medium (FM) was prepared by addition of 1.4 M glycerol to MM on three steps for 30 min. The embryos individually were placed in 0.5 ml straws (IMV, Cassue, France) containing FM. The experiment A with frozen-thawed sheep embryos was done in Bulgaria. The experiment B was international and embryos in frozen condition were ship to Poland.

Cattle. A total of 17 beef cattle (breed Hereford – n=12, Salers – n=3, and Aberdeen-Angus – n=2) were hormonally stimulated with 3500 IU Pregmagon (Dessau, Germany) intramuscular injection on the day 10 or 11 of the estrus cycle. The cows exhibited heat after 2 days were inseminated twice with frozen-thawed sperm of a relevant breed bull at a 12-hours interval. The embryos at morula and blastocyst stage were recovered on the day 7 after insemination by a transcervical flushing of the uterine horns using catheters type Foley (Willy Rush, Germany) and solution MM. Altogether 81 embryos only intact morulae and blastocysts were included in the freezing programme. The FM was two modifications. The first one was compounded of cryoprotectant 1.4 M glycerol for 50 embryos. The second was consisted of 1.5 M ethyleneglycol for 31 embryos. The final concentration was obtained by addition on three increasing steps for 30 min. The embryos were separately placed in 0.5 ml straws (IMV, Cassue, France) previously filled with corresponding FM. All the embryos were ship to the Russia in frozen condition and embryo transfers to 27 Holstein-Friesian recipients altogether were accomplished.

Mice. Hormonal stimulation was induced to 7 female BALBc fertile mice by intraperitoneal injections of 5 IU PMSG (Gestyl, Organon, Holand) and 5 IU hCG (Pregnyl, Organon, Holand) given 48 h apart and couple was made. The presence of the vaginal plug on the next day was evidence for mating. The embryos were collected 72 h after that by forceps of the oviduct at 8-16 blastomeres stage. The mice were in general narcosis and the ethical principles and legal requirements for the welfare with the animals

were kept during the embryo recovering using MM. The freezing medium (FM) was prepared by addition of 6.85 M glycerol to MM. The embryos in a group were placed in 0.5 ml straws (IMV, Cassue, France) with content of FM.

Freezing and thawing procedure

The sheep and cattle embryos were frozen by conventional slow-rate method in program biofreezer Minicool AS 25 (L'Air Liquide, France) according to the so called "two-step method":

1. Cooling of the straws from temperature 20°C to -7°C with rate 1°C/min.
2. Equilibration for 5 min, seeding of the crystals and subsequent 5 min equilibration.
3. Freezing to temperature -30°C with a rate 0.3°C/min.
4. Transfer of the straws directly to container with liquid nitrogen to temperature -196°C.

Thawing was accomplished by immersion of the straws in water bath at temperature 37°C. Cryoprotectant dilution was done in accordance of the cryoprotectant. Glycerol was diluted in four steps by transfer the embryos in equilibrated at room temperature solution with decreasing concentration 1 M, 0.7 M, 0.3 M for 5 min each step and finally in culture medium. Ethyleneglycol was diluted by placing the embryos in fresh freezing medium containing 0.25 M sucrose for 10 min at room temperature and than placed in manipulating medium.

The mouse embryos were frozen by direct transfer of the straws in liquid nitrogen at -196°C. They were thawed by immersing of the straws in water bath at 38°C for 1 min. For cryoprotectant diluted medium (DM) 0.35 M sucrose was added to FM and the embryos remained for 10 min.

Biotechnological assessment of the viability.

Sheep embryos were surgically transferred to 17 recipients from the breeds Bulgarian Cigai in experiment A and Polish plane crossbreed in experiment B respectively 10 and 7 in number.

Cattle embryos were nonsurgically transferred to synchronized 27 Holstein-Friesian breed recipients in Russia.

Pregnancy and parturition in all trials were registered in comprehensive protocol.

Mouse embryos were in vitro cultured in 5% CO₂ incubator at 38°C in tissue culture medium. Development to the stage expanded or hatched blastocyst was sign for embryo viability.

Results and Discussion

The viability of sheep embryos at morula and blastocyst stage frozen conventionally with 1.4 M glycerol was evaluated in two experiments summarized in Table 1. In experiment A from 19 frozen embryos 10 were chosen for transfer. A total of 9 frozen embryos were excluded of the experiment after thawing and dilution of the cryoprotectant for presence of morphologic discrepancy. The viability of frozen embryos was evaluated up to 40% and 4 offspring were obtained from 10 recipients. In experiment B viability of 9 frozen embryos reached to 57% and 4 newborn lambs were registered from 7 transferred embryos after thawing and dilution of the cryoprotectant to 7 recipients. Only 2 embryos were evaluated as unsuitable for embryo transfer because of degeneration and lysis after dilution of the cryoprotectant.

Our results with sheep embryos demonstrated that conventional slow-rate freezing method using 1.4 M glycerol is proper for preimplanted stage of development. Our originally experience has shown that embryo viability depended upon the stage of embryo development, rates of cooling and thawing or choice of cryoprotectant. Some authors were used DMSO or ethyleneglycol for freezing sheep embryos but the success is variable [1, 2].

The viability of cattle embryos was estimated after slow-rate freezing method comparing two kinds of cryoprotectants – glycerol and ethyleneglycol and the result is shown in Table 2. From 50 frozen with 1.4 M glycerol embryos belonged to Hereford breed cattle after thawing and stepwise dilution of the cryoprotectant 24 (48%) were evaluated as proper for embryo transfer to 15 recipients. As a result 7 pregnant cows were registered by rectal palpation on the third month of gestation. The viability achieved for this group was 6 (40%) newborn calves, respectively male and female equally. The cow suffer abortion was pregnant with twins. In the group of 31 cattle embryos frozen with 1.5 M ethyleneglycol 5 were Hereford 17 – Salers and 9 – Aberdeen-Angus. After thawing-dilution procedure 12 (39%) embryos were eliminated of the trials as unsuitable for embryo transfer. A total of 19 (61%) embryos were transferred to 12 recipients. The viability rate was registered as 3 (25%) offspring female calves 1 of them Hereford and 2 Salers. As a final result 9 newborn calves were registered. Out of them 7 calves were Hereford breed and 2 – Salers breed. No Aberdeen-Angus breed was delivered of transferred embryos.

The presence of a cryoprotectant is required to avoid damage to embryos during freezing and thawing. Since the presence of a cryoprotectant significantly increases the medium's osmolality which could damage the embryos, these substances have been mostly added in a step-wise manner [4, 7]. Our results show that different cryoprotectants preserved embryo survival in accordance of their permeability, respectively 1.4 M glycerol up to 48% and 1.5 M ethyleneglycol up to 61%. They are comparable to the obtained pregnancy rate following the transfer of frozen-thawed embryos of the other authors using similar approach [5, 6]. On the other hand the subsequent effectiveness is discussible because the viability was saved up to 40% when glycerol was used. Contrary to expectation the viability was decreased up to 25% for embryos frozen with ethyleneglycol. The distinctions may probably due to different approach of cryoprotectant dilution and expressed toxicity.

The results of vitrified than thawed and in vitro cultured mouse embryos are summarized on Table 3. The experimental group of 152 embryos in early morula stage of development with expanded blastomeres and intact zona pellucida were assessed morphology normal and divided in 2 groups. After vitrification and following thawing procedure of 138 embryos the blastomeres were contractive and zona pellucida was intact at 113 (82%) embryos and they were morphologically evaluated as survived. Dilution of the cryoprotectant indicates initial shrinkage and subsequent swelling to the normal isotonic volume. A signs of zona pellucida hardening was also observed which reduced permeability of the cryoprotectant. Nevertheless the procedure decreased the survival rate and 96 (70%) embryos showed rehydration of the blastomeres. The results of in vitro embryo culture on 24 h demonstrated viability rate reached to blastocyst stage for 78 (56%) embryos and comparable saved viability on 48 h of cultivation up to stage hatched blastocyst of about 61 (44%) embryos respectively. A control group of 14 embryos were only cultured without applying on the freezing program. Their viability was 86% on 24 h of cultivation at blastocyst stage and 71% on 48 h at expanded or hatched blastocyst respectively.

During the vitrification of mouse embryos the movement of the cell volume and decreasing of the space between blastomeres and zona pellucida were additional indica-

Table 1. Survival and in vivo viability of conventionally frozen sheep embryos using different recipients

Trial	Donors (n)	Frozen embryos	Transferred embryos	Recipients (n)	Newborn lambs (%)
A	Romanovska (5)	19	10	Cigai (10)	4 (40)
B	Romanovska (3)	9	7	Polish plane (7)	4 (57)

Table 2. Survival and in vivo viability of conventionally frozen beef cattle embryos using different cryoprotectants

Cryoprotectant	Donors (n)	Frozen embryos	Transferred embryos	Recipients	Pregnant on 3rd month	Newborn calves (%)
Glycerol	Hereford 10	50	24	15	7	6 (40)
Ethyleneglycol	Hereford 2	5	5	5	2	2
	Salers 3	17	10	5	1	1
	Aberdeen-Angus 2	9	4	2	-	-

Table 3. Survival and in vitro viability of vitrified preimplanted mouse embryos

Methods	Treated embryos	Embryo survival rate		Embryo viability rate	
		normal embryos after thawing (%)	normal embryos after dilution (%)	after 24 h culture <i>in vitro</i> (%)	after 48 h culture <i>in vitro</i> (%)
Vitrification	138	113 (82)	96 (70)	78 (56)	61 (44)
Nonvitrified	14	-	-	12 (86)	10 (71)

tions for embryo survival. Symptoms of lysis and hypertension were signs for embryo morphology destroy. The dilution of the cryoprotectant by one-step procedure using 0.35 M sucrose is commonly used in other vitrification protocols [8, 10]. Our results also demonstrated that achievement of high viability rate dependent on every method's step. It is also showed that development of mouse embryos were preserved after vitrification procedure like gene expression in mouse pronuclear zygotes [3]. In comparison similar results have been reported when the same protocol was applied to mouse and bovine early preimplanted embryos or using mixture of ethyleneglycol and propanediol vitrification solution [7, 11].

Conclusion

The present study demonstrated that slow-rate freezing and high-speed vitrification methods can be routinely used for animal embryos cryopreservation and their viability is saved ranged between 25-57 % *in vivo* and 44-56 % *in vitro*, respectively.

References

1. Cocero, M. J., R. Procureur, J. DeLa Fuente, D. Chupin. Glycerol or ethylenglycol for cryoprotection of deep-frozen ewe embryos. – *Theriogenology*, **29**,1, 1998, 238.
2. Cognie, Y., G. Baril, N. Poulin. Current status of embryo technologies in sheep and goat. – *Theriogenology*, **59**, 2003, 171-188.
3. Dhali, A., V. M. Anchamparathy, S. P. Butler, R. E. Pearson, I. K. Mullarky, F. C. Gwazdauskas. Gene expression and development of mouse zygotes following droplet vitrification. – *Theriogenology*, **68**, 2007, 1292-1298.
4. Galli, C., R. Duchi, G. Crotti, P. Turini, N. Ponderato, S. Colleoni, I. Lagutina, G. Lazzari. Bovine embryo technologies. – *Theriogenology*, **59**, 2003, 599-616.
5. Jousan, F. D., M. D. Utt, S. S. Whitman, R. H. Hinshaw, W. E. Beal. Effects of varying the holding temperature and interval from collection to freezing on post-thaw development of bovine embryos in vitro. – *Theriogenology*, **61**, 2004, 1193-1201.
6. Martinez, A. G., G. M. Brogliatti, A. Valcarcel, M. A. de las Heras. Pregnancy rates after transfer of frozen bovine embryos: a field trial. – *Theriogenology*, **58**, 2003, 963-972.
7. Massip, A. Cryopreservation of embryos of farm animals. – *Reprod. Domest. Anim.*, **36**, 2001, 49-55.
8. Rall, W. F. Cryopreservation of oocytes and embryos methods and applications. – *Anim. Reprod. Sci.*, **28**, 1992, 237-245.
9. Sapundzhiev, E. Freezing of preimplanted mouse embryos by vitrification. – *Acta Morphologica et Antropologica*, **13**, 2008, 116-120.
10. Scheffen, B., P. Van Der Swalmen, A. Massip. A simple and efficient procedure for preservation of mouse embryos by vitrification. – *Cryo-Letters*, **7**, 1986, 260-269.
11. Vajta, G. Vitrification of the oocytes and embryos of domestic animals. – *Animal. Reprod. Sci.*, **60-61**, 2000, 357-364.
12. Whittingham, D. G. Survival of mouse embryos after freezing and thawing. – *Nature*, **233**, 1971, 125-126.

Eyeball Plastination with Polyester Co-Polymers

D. Sivrev¹, Zl. Trifonov²

¹*Department of Anatomy*

²*Department of Ophthalmology*

Faculty of Medicine, Thracian University, Stara Zagora, Bulgaria

Polyester co-polymers are contemporary plastination materials, used for brain preserving. The aim of the experiment is to investigate the possibility of preparing exact anatomic models of whole eyeballs, which are safe for the health of the trainees and durable and resistant to mechanical trauma. We used 2 pig and 2 calf eyes of animal corpses and some chemical and physical agents: Fixators – 5% water solution of formaldehyde (methanol by IUPAC – HCHO); Dehydrant – acetone 98-100%; Impregnator – polyester co-polymer Hardener – UV.

Plastinated with co-polymers eye preparations have a good quality and mechanical resistance. The preparations are safe for the human health and are practically everlasting, that is why they can be used for teaching students of medicine and ophthalmology residents.

Key words: Plastination, Polyester co-polymers, eyeball, anatomy.

Introduction

Polyester co-polymers colored or not colored [1, 2] are contemporary plastination materials, used for brain preserving [8, 9, 13] or preservation of other body partes [3, 4, 6, 12]. The parts of the brain treated with it are practically everlasting and safe for human health.

A combined method is used to plastinate a whole eyeball, offered by the same authors (1997), using two plastination materials- polyethylene glycol and Biodur S10 [5]. The preparation made by using this method is soft and elastic as well as harmless to human health but it is not resistant to mechanical trauma [5]. That is why we assume that polyester co-polymers are more suitable for plastinating eyeball in order to make a preparation with greater resistance [10, 11].

Plastination of eyeball with polyester co-polymers has not been performed worldwide so far.

Aims and tasks

The aim of the experiment is to investigate the possibility of preparing exact anatomic models of whole eyeballs, which are safe for the health of the trainees and durable and resistant to mechanical trauma.

In order to realize the described aim we had the following specific tasks:

1. To choose an appropriate biological material
2. To choose the optimal duration of the stages of plastination of the eyeball.

Materials and Methods

We used 2 pig and 2 calf eyes of animal corpses because their size, structure and availability are most suitable for the purpose.

The chemical and physical agents needed for treating the biological material are:

Fixators – 5% water solution of formaldehyde (methanol by IUPAC – HCHO);

Dehydrant – acetone 98-100%;

Impregnator – polyester co-polymer

Hardener – UV

The plastination material was treated by using a standard technology with polyester co-polymers, offered by Gunther von Hagens(1994) for brain plastination, modified according to the eyeball specificity. We used “hylase” for the liquification of the vitreous body as in the combined method for plastinating the eyeball (1997).

Results and Discussion

The preparations we made have better quality and mechanical resistance compared to the ones prepared using the combined method (fig.1 and fig.2) and can be used for teaching eye anatomy. This result is according to other authors [10, 11].



Fig. 1 Eye, treated using the combined method with Biodur S10 and polyethylene glycol

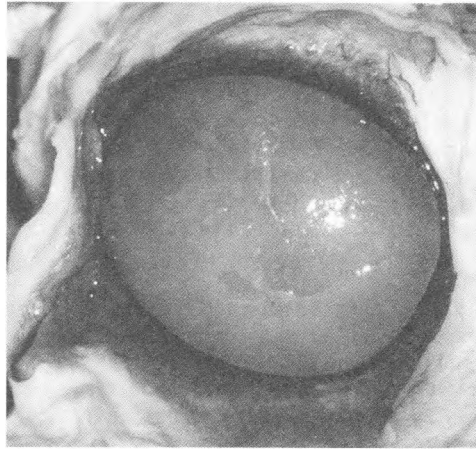


Fig.2 Eye, prepared with polyester co-polymer

It is not well defined in this case when to fixate and dehydrate as with eye slices, because the eventual damage of the retina does not matter for the final preparation.

In both methods – combined and plastination with co-polymers, the danger of shriveling of the cornea exists in the stage of dehydration. We compensate the shriveling by injecting plastination material in the anterior eye chamber, polyethylene glycol in the first method and polyester co-polymer in the second one.

We manage the shrinking of the eyeball after the liquification of the vitreous body with “hylase” in the same way but here comes the difficulty with hardening the polyester co-polymer because of the incapability of UV light to penetrate inside the sclera.

Before the impregnation we do not use the stage “immersion” which is analogical to the preparation of eye slices, but the impregnation itself we perform at room temperature, not at -25°C . This is synchronized with the investigation of Sora et al (1999) [6].

We harden the material using UV light (200W/180 min), as we constantly control the quality of the preparation. Unlike the hardening when preparing eye slices, we do not observe cracking of the material, because the proportion between the polyester co-polymer and the biological material is in favor of the biological material.

After the stage of drying the preparation we have to put it in an open container under the sunlight for several weeks because the impregnation material is not dry yet in the end of the procedure as the UV light does not penetrate through the wall of the sclera. To harden the material in this case we rely on the fact that heat also initiates reaction in the polyester co-polymers and they harden for a few weeks even though more slowly.

The preparation that we make is hard and non-elastic but more resistant to mechanical trauma. It is safe for human health.

Conclusions

1. Plastinated with co-polymers eye preparations have better quality and mechanical resistance compared to the combined method.

2. The preparations are safe for the human health and are practically everlasting, that is why they can be used for teaching students of medicine and ophthalmology residents.

References

1. Baeres, F. M. Muller. Plastination of dissected brain specimens and Mulligan stained sections of human brain. – *Eur. J. Morphology*, **39**(5), 2001, 307-311.
2. Barnett, R., G. Lyons, J. Driscoll. Improved staining and Berlin blue staining of whole human brain. – *Stain technology*, 1980, 235-239.
3. Genster-Strobl, B., M. Sora. Potential of P40 plastination for morphometric hip measurements. – *Surg. Radiol. Anat.*, **27**(2), 2010, 147-151.
4. Latorre, R., A. Arencibia, F. Gil, M. Rivero, G. Ramirez, J. Vaquez-Autin, R. Henry. Sheet Plastination with Polyester: An Alternative for all Tissues. – *J Int. Soc. Plast.*, **19**, 2004, 33-39.
5. Sivrev, D., J. Kayriakov, Zl. Trifonov, D. Djelebov, M. Atanasov. Combined Plastination Method for Preparation of Improved Ophthalmologic Teaching Models. – *The Journal of International Society on Plastination*. **12**(2), 1997, 12-14.
6. Sora, M., P. Brugger, H. Traxler. P40 Plastination of Human Brain Slices: Comparison between different immersion and Impregnation conditions. – *J Int. Soc. Plast.*, **14**(1), 1999, 22-24.
7. Steinke, H., S. Pfeiffer, K. Spanel-Borovski. A new plastination technique for head slices containing brain. – *Annals of Anatomy*, **184**(4), 2002, 353-358.
8. Von Hagens, G. Heidelberg Plastination Folder. – University of Heidelberg, Heidelberg, 1986.
9. Von Hagens, G., K. Tiedmann, W. Kriz. The current potential of Plastination. – *Anatomy and Embryology*, **175**(4). 1987, 411-421.
10. Von Hagens, G. Personal contacts, 1996.
11. Weiglein, A. Plastinated brain specimens in the Anatomical curriculum at Graz University. – *J Int. Soc. Plast.*, **7**(3), 1993, 3-7.
12. Sheet Plastination. – Universidad de Murcia. <http://www.um.es/anatvet/Documentos/P40-PROTOCOL-web.pdf>
13. Plastination preserves in traumatic brains for medico-legal evidence. – Mahidol University, 2004. <http://mulinet10.li.mahidol.ac.th/e-thesis/4236021.pdf>

Preparing Eye Slices with Biodur P40

D. Sivrev¹, Z. Trifonov², A. Georgieva¹

¹*Department of Anatomy*

²*Department of Ophthalmology*

Faculty of Medicine, Thracian University, Stara Zagora, Bulgaria

The aim of the experiment is to prepare slices of the eyeball, that are safe for the health of the trainees, that are durable and give an exact idea of the macrostructure of the eye. We used 14 pig and 4 calf eyeballs of animal corpses and prepared them with Biodur P40 polymer. We get the best slices by freezing (-25°C) before fixation of the biological material. Plastinated eye slices are difficult to prepare, but they are practically everlasting.

Eye plates are safe for human health and can be used for educating eye anatomy of the students and residents. Treating of eye plates can be done using the classic technology of the author of the plastination method but modified according to the particularities of the specific anatomic preparation.

Key words: Plastination, Biodur P40, eyeball, anatomy, eyeslices.

Introduction

Biodur P40 and old Biodur P35 are contemporary plastination materials used for preserving brain slices [5, 10, 13]. Treated with them parts of brain are practically everlasting and safe for the human health [3, 6]. The obtained plates demonstrate the macrostructure of the white and grey matter and their proportion [1, 8] and they are suitable for medical student and post-graduate students [4, 7, 12]. We experimented to plastinate the eyeball using Biodur P40. Plastination of eye slices has not been performed worldwide so far.

Aims and tasks

The aim of the experiment is to prepare slices of the eyeball, that are safe for the health of the trainees, that are durable and give an exact idea of the macrostructure of the eye.

In order to realize the described aim we had the following main tasks:

1. To choose a suitable biological material;
 2. To define the method of preparing the slices of the used biological material;
 3. To fix the stage of the plastination procedure most suitable for performing the cuts.
- To define the optimal duration of the stages for plastinating the slices.

Material and Methods

We used 14 pig and 4 calf eyeballs of animal corpses that are most suitable for the purpose according to the size, structure and availability.

The chemical and physical agents needed for treating the biological material are:

Fixators – 5% water solution of formaldehyde (methanol by IUPAC – HCHO);

Dehydrant – acetone 98-100%;

Impregnator – Biodur P40;

Hardener – UV.

The slices were prepared in different stages of the plastination process – before fixation (10 cases), after fixation (2 cases), after dehydration (1 case), after impregnation (1 case). After the fixation we froze the eyeball (25°C) and using eye scalpel (9 cases) or a special cutting tissue machine (1 case) we cut it into plates 3-4 mm wide.

We fixed the eye plates with 5% water solution of formaldehyde (-25°C) for 72 hours and after that we put them into cold acetone (-25°C) for 12 h. The technique used after the fixation of the biological material is analogical but we put the eye slices directly into cold acetone (-25°C).

The prepared slices were impregnated using a standard plastination technology with Biodur P40, submitted by Gunther von Hagens(1986) [9] for plastinating brain slices, modified according to the specificity of the eyeball(fig. 1). We put the eye plates in a container with cold Biodur P40 (-25°C) and under constant observation we slowly increased the vacuum until the signal bubbles disappeared. Because of the small capacity of the wall of the eyeball the stage of impregnation continued (including the pauses) for about 2 h (10mmHg=13 mbar)

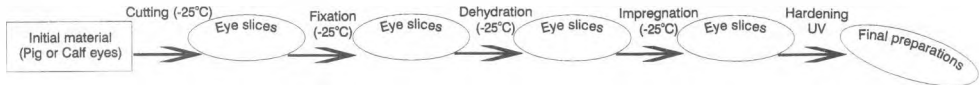


Fig. 1. Scheme of preparing the eye plates with Biodur P40

In the phase of “hardening” we first put into the matrix a thin (1-2 mm) layer of Biodur P40 and we put it under the influence of UV radiation (200W/30 min). Over the semi-hardened layer of the polymer we put a dehydrated slice of the eyeball and using an anatomic pincet we shaped it so that more details could be observed. Carefully and slowly we filled the matrix with new Biodur in order to cover the eye slice 1-2 mm. We irradiated the ready matrix with UV light (200W/30 min) constantly controlling the quality of the hardening.

Results and Discussion

We performed a subjective visual assessment of the anatomic preparations of the eyeball.

The preparations had a satisfactory quality and could be used for educating anatomy of the eye.

The best eye slices were the ones made before the fixation using scalpel despite the technical difficulties in cutting the eyeball.

The plates prepared after the fixation with 5% water solution of formaldehyde had worse quality due to the lower level of hardening of the biological material. This is according to investigations of other authors [2, 9].

The dehydrated eyeball was tearable despite the low temperature (-25°C), that is the reason why we didn't get equal cuts. The same result but in bigger size we got when we impregnated with Biodur P40 biological material.

The periods of step by step treating of the eye slices were significantly shorter compared to the analogical procedure in preparing brain plates [9, 13], which can be explained with the smaller size of the material. The other difference is that when plastinating the eyeball we avoided the stage of "immersion" [5], and after the dehydration we directly impregnated.

The phase of "hardening" is particularly difficult and important because the Biodur P40 is more sensitive to any change in the condition in this stage. To make a valuable preparation we stuck to the guidelines received in a personal conversation with Gunther von Hagens (1996) – the author of the plastination method. The appearance of cracks or darkening of the plate is a sign of quick polymerization and implies short interruption of the radiation, followed by lowering the power of UV radiation [11], and when the hardening is insufficient we need extension of the stage. The power increasing is not desirable because better results are received when using lower radiation.

Conclusions

1. Plastinated eye slices are difficult to prepare, but they are practically everlasting.
2. Eye plates are safe for human health and can be used for educating eye anatomy of the students and residents.
3. We get the best slices by freezing (-25°C) before fixation of the biological material
4. Treating of eye plates can be done using the classic technology of the author of the plastination method but modified according to the particularities of the specific anatomic preparation.

References

1. Bickley, H. The staining of Brain slices by impregnation. – *J. Int. Soc. Plast.*, **10**(1), 1996, 8-15.
2. Brown, M., R. Reed, R. Henry. Effects of Dehydration Mediums and Temperature on Total Dehydration Time and Tissue Shrinkage. – *J. Int. Soc. Plast.*, **17**, 2002, 28-33.
3. Latorre, R., A. Arencibia, F. Gil, M. Rivero, G. Ramirez, J. Vaquez-Autin, R. Henry. Sheet Plastination with Polyester: An Alternative for all Tissues. – *J. Int. Soc. Plast.*, **19**, 2004, 33-39.
4. Lozanoff, S., B. Lozanoff, M. Sora, J. Rosenheimer, M. Keep, J. Tregear, L. Salland, J. Jakobs, S. Saiki, D. Alverson. Anatomy and the Access Grid: Explored Plastinated brain sections for use in distributed medical education. – *Anat. Records* **270**(1), 2003, 30-37.
5. Sora, M., P. Brugger, H. Traxler. P40 Plastination of Human Brain Slices: Comparison between different immersion and Impregnation conditions. – *J. Int. Soc. Plast.*, **14**(1), 1999, 22-24.
6. Steinke, H., S. Pfeiffer, K. Spänel-Borovski. A new plastination technique for head slices containing brain. – *Annals of Anatomy*, **184**(4), 2002, 353-358.
7. Szarvas, B., L. Szarvas, P. Groscurth. Use of plastination brain sections for medical education. – *J. Int. Soc. Plast.*, **9**(1), 1990, 23-24.
8. Ulfig, Staining of human fetal and adult brain slices combined with subsequent plastination. – *J. Int. Soc. Plast.*, **4**(1), 1990, 33-38.

9. Von Hagens, G. Heidelberg Plastination Folder. – University of Heidelberg, Heidelberg, 1986.
10. Von Hagens, G., K. Tiedmann, W. Kriz. The current potential of Plastination. – *Anatomy and Embryology*, **175**(4). 1987, 411-421.
11. Von Hagens, G. Personal contacts, 1996.
12. Weiglein, A. Plastinated brain specimens in the Anatomical curriculum at Graz University. – *J. Int. Soc. Plast.*, **7**(3), 1993, 3-7.
13. Weiglein, A. Preparing and using S10 and P35 brain slices. – *J. Int. Soc. Plast.*, **10**(10), 1996, 22-25.

Dynamics of Changes in Central and Peripheral Lymphoid Organs in Rats Treated Intraperitoneally with Lipopolysaccharide of *E. Coli*

N. Dimitrov¹, D. Sivrev¹, M. Andonova², I. Borissov³

¹*Department of Anatomy, Faculty of Medicine*

²*Department of Pathophysiology, Faculty of Veterinary Medicine*

³*Department of Surgery, Faculty of Veterinary Medicine*

^{1,2,3}*University of Thrace, St. Zagora, Bulgaria*

The arising question is what morphological changes occur in various organs and systems of the human body under the effect of LPDs. The purpose of this study is to identify and record the dynamics of changes in central and peripheral lymphoid organs in rats treated intraperitoneally with lipopolysaccharide of *E. Coli*. 30 rats were injected intraperitoneally with lipopolysaccharide of *E. Coli*. The typical changes in the spleen occurred through apoptosis: cytoplasmic eosinophilia, nuclear pyknosis and fragmentation. In the spleen and lymph nodes alike, together with the continued action of LPDs, there is an increased number of lymphocytes.

During the action of LPDs, there is an increase of lymphoid organs -splenomegaly, lymphonodomegaly. LPDs induces apoptosis with the occurrence of apoptosis cells and increase the number of lymphocytes in lymphoid organs.

Key words: Bacterial endotoxin, lipopolysaccharide, apoptosis, *E. Coli*, lymphoid organs.

Introduction

Bacterial endotoxin lipopolysaccharide (LPS) is a component of the outer surface of the cell membrane in the Gram-negative bacteria. It consists of three elements: O antigen (O polysaccharide), central oligosaccharide and lipid A. LPDs causes changes in metabolism of the cell, its immune status and acid-base balance [1].

Over the past 20 years, some authors describe substances that add to the pathogenic effects of LPDs in the cell – Interleukin 1 (IL-1) [3], Interleukin 6 [6], Prostaglandin E [8].

There are many changes in the normal physiology of the whole organism under the effect of LPDs: erythropenia and leucopenia in the blood [9], subjective complaints – gastrointestinal disorders [2], reduced physical activity [5].

The arising question is what morphological changes occur in various organs and systems of the human body. Since LPDs, which is a bacterial lipopolysaccharide, is perceived by the animal and human organism as a signal for microbial invasion, invasion is first to be expected in systems that are related to the protection of the organism.

Purpose and objectives

The purpose of this study is to identify and record the dynamics of changes in central and peripheral lymphoid organs in rats treated intraperitoneally with lipopolysaccharide or *E. Coli*.

To fulfill the objective we set ourselves the following tasks:

1. To determine what gross changes occurring in lymphoid organs under the influence of bacterial LPDs.
2. To register tissue changes in the central and peripheral lymphoid organs.

Materials and Methods

Experiments were conducted on 36 male Wistar rats with an average weight of about 190.00 g. Six of them are left as a monitoring group and the remaining 30 were injected intraperitoneally with lipopolysaccharide of *E. Coli* 0111B4 (Sigma Aldrich Chemie GmbH). LPDs is injected at a dose of 1.0 mg per kg body weight dissolved in sterile solution of 0.9% NaCl.

Samples for light microscope were obtained at each experimental period: second, fourth, sixth hour and the first, third, sixth, 10th and 15th day, until the sixth day – from 6 rats per day, while on the 10th and 15th day – from 3 rats. Material from half of the rats were fixed with 10% aqueous solution of formaldehyde and the other – with a solution of Carnoustie.

Results and Discussion

Macroscopic changes. There is hepatosplenomegaly in experimental animals, but these changes are absent in the monitoring group. There is an increase in close lymph nodes, and after the tenth day there is an increase in distant lymph nodes along the path of the ductus thoracicus. These results coincide with those published by Shao et al [7], but they concentrate on the changes in the liver.

Microscopic changes. The typical changes in the spleen occurred through apoptosis. Such changes detected Zhou et al. [11], but in thymus and Peyer's patches. They apply smaller dose of LPDs (0.5 mg / kg body weight) because deoxinivalenol was injected simultaneously with LPS (25.00 mg/kg T.M.). Deoxynivalenol is a synergist of LPS [12]. According to these authors, the characteristics of lymphocyte apoptosis are: condensation of nuclear chromatin, fragmentation of the nucleus and the appearance of apoptotic bodies in the tissues of experimental animal. Zhou et al [11] decide that the immune system is the first target of the interactive effects of bacterial toxins, and the first signs of programmed cell death seen in germ centers of the spleen. Since we do not have Cell Death Detection Kit, we identify as apoptotic the cells that are collapsed, with Cytoplasmic eosinophilia, nuclear pyknosis and fragmentation.

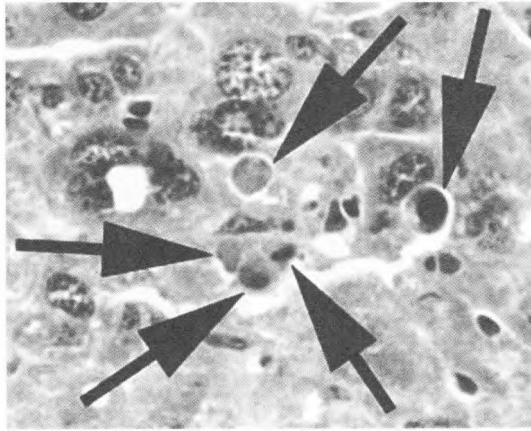


Fig. 1. Apoptosis

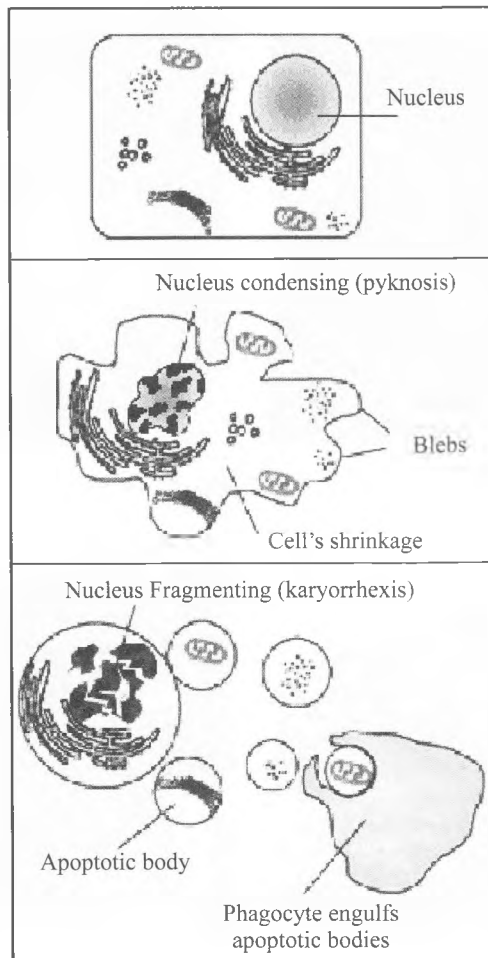


Fig. 2. Scheme of apoptosis

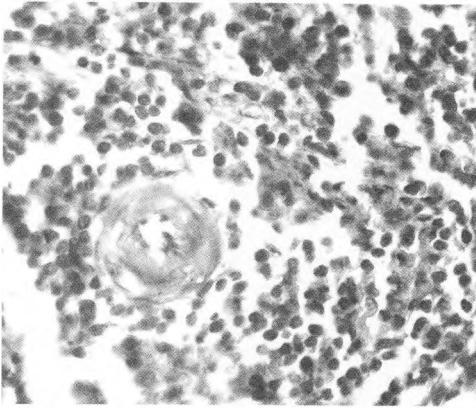


Fig. 3. Spleen – white pulp, the sixth hour, increase 100×0.25

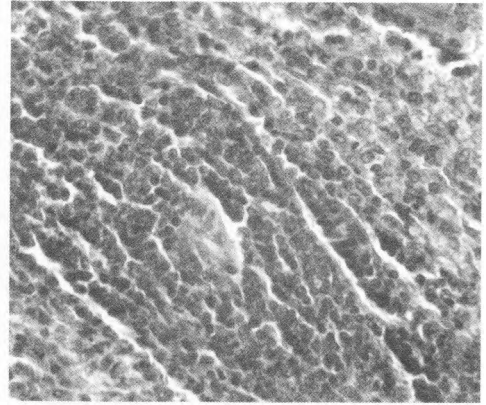


Fig. 4. Spleen – white pulp, the first day, increase 40×0.65

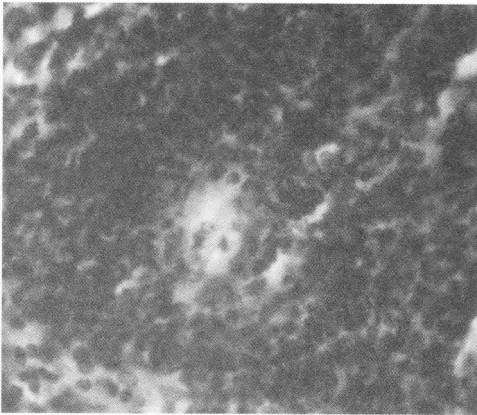


Fig. 5. Spleen – white pulp, the sixth day, increase 40×0.65

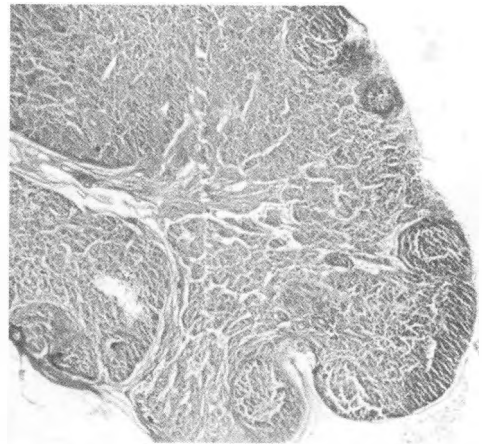


Fig. 6. Lymph node – the controls, increase 32×0.10

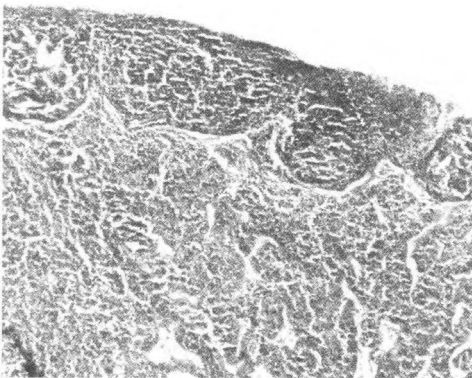


Fig. 7. Lymph node – the second hour, increase 32×0.10

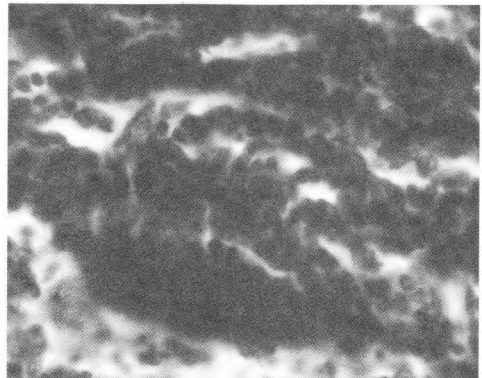


Fig. 8. Lymph node – the third day, increase 32×0.10

In the spleen and lymph nodes alike, together with the continued action of LPDs, there is an increased number of lymphocytes.

This is contrary to the assertions of some authors [4, 10], whereby the difference between the number of lymphocytes in control and treatment groups is small.

Conclusions

1. During the action of LPDs, there is an increase of lymphoid organs – splenomegaly, lymphonodomegaly.
2. LPDs induces apoptosis with the occurrence of apoptosis cells and increase the number of lymphocytes in lymphoid organs.

References

1. Andonova, M., D. Goundasheva, V. Ivanov. – Lipopolysaccharide-induced changes in interleukin β , some biochemical and hematological parameters in rats after an intraperitoneal administration. – *Veterinary Medicine*, **4**(1), 1998, 45-47.
2. Bluthe, R. M., R. Dantzer, K. W. Kelley. Interleukin 1 mediates behavioural but not metabolic effects of tumor necrosis factor in mice. *Eur J Pharmacology*, **209**, 1991, 281-283.
3. Dinarello, C. A. Role of interleukin 1 and tumor necrosis factor in systemic response to infection and inflammation. – In: *Inflammation Basic Principles and Clinical Correlates* (Gallin JI, Goldstein IM, Synderman R eds). 2nd Ed Raven Press Ltd New York, 1992, 211-232.
4. Liu, Y, J. Lu, J. Shi, Y. Hou, H. Zhu, S. Zhao, H. Liu, B. Ding, Y. Yin, G. Yi. Increased expression of the peroxisome proliferator-activated receptor gamma in the immune system of weaned pigs after Escherichia coli lipopolysaccharide injection. – *Vet Immunol Immunopathol.* **124**(1-2), 2008, 82-92.
5. Saperas, E. S, H. Yang, C. Rivier. Central action of recombinant interleukin 1 to inhibit acid secretion in rats. *Gastroenterology*, **99**, 1990, 1599-1606.
6. Schindler, R, J. Mancilla, S. Endres, R. Ghorbani, S. C Clark, C.A. Dinarello. A Correlations and interactions in the production of interleukin 6 (IL-6), IL-1 and tumor necrosis factor (TNF) in human blood mononuclear cells: IL-6 suppressed IL-1 and TNF. – *Blood* **75**,1, 40-47.
7. Shao, B., M. Lu, S. Katz, A. Varley, J. Hardwick, T. Rogers, N. Ojogun, D. Rockett, R. DeMatteo, R. Munford. A Host Lipase Detoxifies Bacterial Lipopolysaccharides in the Liver and Spleen. – *J. Biol. Chem.*, **282**, 2007, (18).
8. Templeton CB, GD Bottoms, JF Fessler, JJ Turek. Hemodynamics, plasma eicosanoid concentrations and plasma biochemical changes in calves given multiple injections of Escherichia coli endotoxin. – *Am J Vet Res*, **49**, 1, 1988, 90-95.
9. Ulich T. R., J. Castillo, Ni. R. X., N. Bikhazi, L. Calvin. Mechanisms of tumor necrosis factor alpha induced lymphopenia, neutropenia and biphasic neutrophilia: a study of lymphocyte recirculation and hematologic interactions of TNF α with endogenous mediators of leukocyte trafficking. *J Leukocyte Biol*, **45**, 1989, 155-167.
10. Zhang, X. M., Morikawa, A., Takahashi, K., Jiang, G. Z., Kato, Y., Sugiyama, T., Kawai, M., Fukada, M., and Yokochi, T. Localization of apoptosis (programmed cell death) in mice by administration of lipopolysaccharide. *Microbiol. Immunol.* **38**, 1994, 669-671
11. Zhou, H., J. R Harkema, D. Yan, J. Pestka. Amplified proinflammatory cytokine expression and toxicity in mice coexposed to lipopolysaccharide and the trichothecene vomitoxin. *J. Toxicol. Environ. Health*, **56**, 1999, 115–136.
12. Zhou, H., J. Harkema, J. Hotchkiss, D. Yan, R. Roth, J. Pestka. Lipopolysaccharide and the Trichothecene Vomitoxin (Deoxynivalenol) Synergistically Induce Apoptosis in Murine Lymphoid Organs. – *Toxicological Sciences*, **53**, 2000, 253-263.

A Modern View on the Bulgarian Anatomical Terminology

P. Kancheva

Medical University – Sofia, Department of Language Training and Students' Sport

The modern Bulgarian anatomical terms are formed in conformity with the basic term formation methods in Bulgarian literary language: lexico-morphological, lexico-syntactical and lexico-semantic. Alongside them, word-borrowing in its two varieties – borrowing through translation (literal and free) and borrowing existing foreign terminological items – has had an impact on the terminological norm and is currently an active modern process lending itself to control.

Key words: Bulgarian anatomical terminology, Term formation methods, Linguistic borrowing.

Introduction

The modern Bulgarian anatomical terminology has been established and developed in strict conformity with the Latin anatomical nomenclature.

The Latin anatomical nomenclature is an orderly, standardized, internationally unified system of names of anatomical entities presented as a list, reflecting the inherent consistency of anatomical terminology. An expression of that consistency is the generic relationships and those of the part-whole, which are the foundation of the nomenclature structuring and classification in anatomy.

By Bulgarian anatomical terms we mean the names established by scientific tradition, duplicating the Latin anatomical terms and coined with the means of the Bulgarian language or loan-words which are grammatically integrated (assimilated) into the Bulgarian anatomical text and are written in the Cyrillic alphabet. In their integrity and systemic relationships, the Bulgarian anatomical terms make up the Bulgarian anatomical terminology (3).

The modern Bulgarian anatomical terms are formed in conformity with the basic term formation methods in Bulgarian literary language: lexico-morphological, lexico-syntactical and lexico-semantic (5: p.6). Alongside them, word-borrowing in its two varieties – borrowing through translation (literal and free) and borrowing existing foreign terminological items – has had an impact on the terminological norm and is currently an active modern process lending itself to control.

1. Lexico-Semantic Term Formation Method

The lexico-semantic term formation is the creation of terms by changing the meaning of words from the general language (4: p.220). In anatomical terminology, two lexico-semantic term formation processes can be distinguished: specialization of commonly used vocabulary and transfer of meaning (metaphorisation) of commonly used vocabulary. These include commonly used nouns of Bulgarian origin.

1.1. Specialization

Commonly used words start being used in a special context, the relationship with their denotations preserved. Complete or partial coincidence of the general and the terminological denominations is achieved and this phenomenon can be defined as weak terminologisation of the commonly used vocabulary (2: p.280). Although the commonly used word and the term both preserve identical denotative reference, it is possible for changes in the meaning of the newly coined term to take place in a functional aspect – it can be narrowed, extended or differentiated (specified).

Most numerous are the cases of specialization of the nouns from the ‘Parts of the body’ class. Examples: *зъби* ‘teeth’, *език* ‘tongue’, *бузи* ‘chicks’, *нос* ‘nose’ etc.

1.2. Metaphorisation

Of the various divisions of the metaphor, of importance to the anatomical terminology is the one into identifying (objective, substantive) and attributive (predicative) metaphor (1: p.159-169).

The identifying metaphor serves as a means for autonomous (indirect) secondary nomination, i.e. for independent denotation (8: p.19). This phenomenon can be defined as strong terminologisation of the commonly used vocabulary (2: p.286). Using it, metaphorical terms are coined in anatomy, for instance the names of the hearing ossicles – *чукче* ‘hammer’(malleus.), *наковалня* ‘anvil’ (incus) and *стреме* ‘stirrup’(stapes).

Quite common are the cases when, in addition to the identifying metaphor, also another term is incorporated which becomes a microcontext for the metaphor, i.e. into the content of the term both the name-metaphor and the smallest nominative context explaining the reference of the metaphorical name are included (7: p.29). Example: *покрив на тъпанчевата кухина* ‘roof of the tympanic cavity’ (tegmen tympany) etc.

The attributive metaphor is a means of a non-autonomous (indirect) secondary nomination (8: p. 19), i.e. not of independent naming but rather together with another name to which it plays a characterizing role. The name created through an attributive metaphor is a term-element of a term combination. The examples for metaphorical adjectives representing term-elements are numerous: *охлювно каналче* ‘snail shell’ (cochlea), *скалиста част* ‘rock-like part’ (pars petrosa), *люспеста част* ‘scale-like part’ (pars squamosa) etc. In contrast to them, the ones for metaphorical participles representing term-element are few in number: *блуждаещ нерв* ‘vagus nerve’ (nervus vagus), *пробиващи артерии* ‘perforant arteries’(arteriae perforantes), *катерещи се влакна* ‘climbing fibers’(neurofibra ascendens) etc.

2. Lexico-Morphological Term Formation Method

The lexico-morphological term formation is based on affixation and composition. In the anatomical terminology these processes are directly linked to the strong trend of loan translation.

2.1. Affixation is the addition of word-building formants to the root forms of various parts of speech with the aim of forming new term words.

2.1.1. By adding prefixes a number of Bulgarian anatomical terms and term elements, pertaining to nouns and adjectives are formed. The use of the following Bulgarian prefixes is rather common: *зад-* 'behind', *над-* 'above', *под-* 'below', *пред-* 'in front of', *между-* 'between', *около* 'around' etc. They are connected to the bases of nouns, e.g. *задстомашен* (pancreatic), *надкостница* (periosteum), *подлигавица* (submucosa), *предмишница* (forearm), etc. Together with the borrowed anatomical terms, a number of foreign language affixes were introduced, such as: *епис-* (epi-), *мета-* (meta-), *диа-* (dia-), *пери-* (peri-) etc., e.g. *епифиза* (epiphysis), *метафиза* (metaphysis), *диафиза* (diaphysis), *перикраний* (pericranium) etc.

2.1.2. Sufficsation is used to form: a) Noun terms through the following suffixes: *-еи*, *-ник*, *-ица*, *-ач*, *-тел*, *-ък*, *-ак*, *-ка*, *-ло*, *-ост*, *-не*, *-ние*, *-ие*, *-ице*, *-че*, *-ица²*, *-ка²*, *-ичка*, *-ен*, *-це*, e.g. *кръстец* (os sacrum), *гръдник* (sternum), *коремница* (peritoneum), *междинница* (perineum) etc.; b) Adjective terms through the following suffixes: *-ест*, *-ист*, *-ен*, *-ов* (*-ев*), *-ен²*, *-ов²*, *-ен³*, *-ов³*, *-телен* (*-ителен*, *-ателен*), e.g. *гъбест* 'spongy' – *гъбесто вещество* (substantia spongiosa), *скалист* 'rocky' – *горен скалист синус* (sinus petrosus superior), *долен скалист синус* (sinus petrosus inferior) etc.

2.1.3. By confixation (prefix-suffix word formation method) a number of terms are created. Examples: *надгръклянник* (epiglottis), *надкостница* (periosteum), *надсеменник* (epididymis).

2.1.4. Term formation without suffixes (zero suffixation). Only one example was found – *просвет* (lumen).

2.2. By composition a great number of noun and adjective terms are formed.

2.2.1. Formation of compound noun terms. Depending on the relationship between the initial root bases two groups exist: a) Terms with syntactically equal bases, e.g. *назофаринкс* (nasopharynx); b) Terms with syntactically unequal root bases, e.g. *хранопровод* (esophagus).

2.2.2. Formation of compound adjective terms: a) Compound adjectives with a conjunctive link between the two bases. Example: *стомашно-чревен* (gastro-intestinal); b) Compound adjectives, formed by binominal word combinations with a subordinating link between the two bases. Example: *горночелюстен* 'of the upper jaw' (maxillaries); c) Compound adjectives formed by using Bulgarian word bases: *-виден*, *-образен* 'shaped'.

3. Lexico-Syntactic Term Formation Method

The word combination terms in anatomical terminology have been analyzed on the basis of syntactic models representing the syntactic relationship between the word combination components – attributive, objective, adverbial – and on structure-positional models which represent a) the structural elements (term elements) of the word combination as parts of speech; b) the linear position (word order) of the structural elements and c) the presence or absence of grammatical words (6: p.107-108).

3.1. Non-prepositional word combination terms. These are of two types.

3.1.1. Principal part – a noun and a subordinate part – one or more (2, 3) adjectives or an ordinal number (+/- adjective-s), or a participle (+/- adjective-s) with a syntactic relationship between the term elements of attribute coordinated type. Examples: *бедрена кост* (os femoris), *голям объл мускул* (m. teres major), *четвърто мозъчно стомахче*

(ventriculus quartus), *блуждаещ нерв* (n. vagus). The word combination terms of this kind are characterized according to the basic lexico-grammatical and semantic features of the subordinate element. The cases studied are: of a subordinate element being an adjective with a general meaning of: 'relation to an object' (relation to size, place and location, shape, surface), 'characteristic' (structure, colour), 'relation to sequencing and quantity', or 'relation to action'.

3.1.2. Two-element word combination terms with the formal structure of noun + noun (S+S) with an attributive syntactic correlation between the term elements of the application type. Examples: *мускул дъвкач* (m. masseter), *мускул квадратен пронатор* (m. pronator quadratus).

3.2. Prepositional word group terms. With regard to the syntactic relation between the term elements these are: 1) attributive or 2) objective.

3.2.1. Attributive word group terms are a type of non-concord attributes with the preposition *на* (of). The formal structure is S+of+S with possible extensions by concordant adjectives. Example: *ос на таза* (axis pelvis). The general semantics is one of 'possession and belonging' and is related to the intra-systematic partonomic relations in anatomy. The preposition *на* 'of' can be used once, twice or three times in the word group, corresponding to a one degree, two degree or three degree attribute.

3.2.2. Object word group terms with the preposition *на* 'of'. Formal structure S+S+of+S with a possible extension S+A+S+of+A+S. This structure is used in the cases when the motivating feature for the terminological nomination is the function of the anatomical structure – the work done by them, together with the objects of that work. Example: *мускул отвеждач на палеца* (m. abductor hallucis).

4. Linguistic Borrowing as a Term Formation Method

In Bulgarian anatomical terminology the sources of borrowing are the Greco-Latin nomenclature terms.

4.1. Borrowing through translation. Translation is a lasting trend in modern Bulgarian anatomical term formation, supported by the necessity to strictly comply with the Nomina Anatomica standards. As a term formation method it has two varieties – literal translation, realized by word formation and phraseological loan translation and free translation.

4.2. Borrowing of existing terms. Related to word loan implementation mechanisms in the Bulgarian anatomical text, two cases emerge:

4.2.1. Unchanged borrowed terms. Examples: *брегма* (bregma), *вертекс* (vertex), *оципунт* (occiput) etc.;

4.2.2. Assimilated (Bulgarianized) terms: Examples: *енифиза* (epiphysis), *диафиза* (diaphysis), *метафиза* (metaphysis), etc. The terminological borrowings become a basis for a further morphological and syntactical term formation.

Conclusion

At present, the Bulgarian anatomical terminology is a subsystem of the Bulgarian literary language having an orderly internal structure. It has its own well-defined terminological norm.

The Bulgarian anatomical terminology is open system to the relationships with the generally used vocabulary and the Latin anatomical terminology. With regard to the language structure and the origin several groups of anatomical terms are outlined:

■ – Word-terms, created by changing the meaning of commonly used nouns of Bulgarian origin. Examples: *китка* (carpus), *чукче* (malleus), *наковалня* (incus), *стреме* (stapes).

■ – Artificial world-terms. Their creation is directly linked to the strong trend of loan translation. Example: *предмишница* (antebrachium).

■ – Borrowing of existing nomenclature world-terms. Examples: *мускул* (musculus), *нерв* (nervus), *стернум* (sternum), *дуоденум* (duodenum), *колон* (colon).

■ – Word group terms, created from Bulgarian term elements. Example: *петна върга* (tuber calcanei).

■ – Word group terms, created from Bulgarian term elements and assimilated (Bulgarianized) Latin term elements. Example: *хипофизна яма* (fossa hypophysialis).

■ – Word group terms, created from assimilated (Bulgarianized) Latin term elements. Example: *висцеларна плевра* (pleura visceralis).

■ – Eponyms. Examples: *поленце на Брока* (area subcallosa), *Лангерхансови острови* (insulae pancreaticae).

References

1. А р у т ю н о в а, Н. Д. Языковая метафора (синтаксис и лексика). – В: Лингвистика и поэтика, М. 1979, 159-169.
2. К ъ н ч е в а, П. Лексикално-семантични взаимоотношения между българската анатомична терминология и общоупотребимите съществителни имена за части на тялото. – Език и литература, 2008, кн. 1-2, 278-289.
3. К ъ н ч е в а, П. Българската анатомична терминология *днес*. София, Медицинско издателство „АРСО“, 2009.
4. М а н о л о в а, Л. Образуване на научно-техническа терминология (с оглед на силикатната терминология). – Известия на Института за български език, 1980, кн. 24, с. 203-233.
5. М а н о л о в а, Л. Българска терминология. София, Държавно издателство „Народна просвета“, 1984.
6. П о п о в а, М. Термини-словосъчетания. София, Издателство на БАН, 1985.
7. П о п о в а, М. Метафората като средство за номинация (с оглед на терминологичната номинация). Български език, 1986, кн. 1, 22-31.
8. П о п о в а, М. Метафоричният пренос при назоваване на свойството в българската терминология. Български език, 1997–1998, кн. 4, 17-29.

Dr. Zaharina Dimitrova (1873-1940): A Pioneer in Research of the Pineal Gland's (Corpus Pineale) Microstructure

D. Paskalev¹, D. Radoinova², B. Galunska³

¹*Clinic of Nephrology and Dialysis,*

²*Department of Forensic Medicine,*

³*Department of Biochemistry*

Medical University "Prof. Dr. Paraskev Stoyanov" – Varna, Bulgaria

Dr. Zaharina Dimitrova is a still forgotten Bulgarian scientist who did ground breaking research in the field of histology of the pineal gland. Born in Ressen, Macedonia on 26th November 1873, Dimitrova left to study Medicine in France. Under the supervision of Prof. M. Nicolas, she researched the fine structure of epiphysis cerebri and for the first time made an accurate description of the pinealocytes. Dr. Zaharina Dimitrova pointed out the characteristic vacuoles in the nuclei of the cells and related the finding with a possible endocrine function. At present, it is known that the pinealocytes produce the hormone melatonin. She graduated with honors from the Medical School in Nancy, France, and published her PhD thesis "*Recherches sur la structure de la glande pineale chez quelques mammiferes*". Her highly acclaimed work was awarded the Gold Medal from the Medical School and published in *La Nevraxe Journal* (vol. 2, 1901, 257-361). Dr. Zaharina Dimitrova died on April 14, 1940.

Key words: Dr. Zaharina Dimitrova, pineal gland, morphology, history of medicine.

The name of Dr. Zaharina Dimitrova cannot be found in *Encyclopaedia Bulgaria*, *Concise Bulgarian Encyclopaedia* or any of the specialized biographical reference books for famous and not so famous Bulgarian physicians. A little over a century ago, she completed a fundamental research on the pineal gland producing the hormone melatonin. Today modern science uses melatonin to fight aging, insomnia, some hormonal dysfunctions, oxidative stress, etc. [2, 9]. Famous scientists have cited Dimitrova's dissertation. She was also awarded a gold medal for her accomplishments [6, 7].

Short History of the Pineal Gland and its Function

It is accepted that the first more accurate description of the pineal gland was made by the famous Roman physician Claudius (Clarissimus) Galenus of Pergamon (129-200 A.D.). He stated that the anatomists from the renowned Alexandrian School were also familiar with the organ. Galenus named the gland "conarium" because of its resemblance to a

pine or the cone-like tip of the pine twig. The organ's Latin name, Corpus Pineale (from the Latin word for pine – pinus) derived from this resemblance as well. Galenus was one of the first to notice and document the accumulation of small increments in the pineal gland known as acervuli (from Latin acervus – accumulation) or sabula (from Latin sabulum – one-grain sand). For a long time scientists have believed the brain sand to be closely linked to some mental diseases. This belief spread even wider after the famous French philosopher Rene Descartes (1596-1650) declared that corpus pineale was the throne of the soul in the human body [3, 5].

Today it is accepted that the pineal gland develops as a pine-like caudal excrescence of the epithalamus. The phylogenetic predecessor of this small organ is the parietal eye found in some reptiles (Reptilia), which is partly responsible for the pigmentation [10]. In 1958 A. Lerner confirmed that an extract from bull's pineal gland caused paling of a frog's skin due to the melatonin [4, 5]. The melatonin was officially recognized as a hormone in 1963 [5, 10]. Pinealocytes, the main cells of the pineal gland [3, 5] produce melatonin. In 1901 Z. Dimitrova was the first to describe these cells in detail [1].

Dr. Zaharina Dimitrova: Life and Work

Dr. Z. Dimitrova was born on the 26th of November 1873 in Ressen, Macedonia, which at that time was under Turkish rule. As a result of the decisions made at the Berlin congress in 1878 the region remained under Turkish governance even after the neighboring regions gained their independence. This fact would have a serious impact on the life of the talented Bulgarian woman. Simeon Radev (1879-1967), a famous Bulgarian historian and diplomat, was also born in Ressen. He was Bulgarian ambassador extraordinary and envoy plenipotentiary in many countries such as Romania (Bucharest, 1913-1916), Switzerland (Bern, 1916-1917), Netherlands (Hague, 1920-1921), USA (Washington, 1925-1933), UK (London, 1935-1938), and Belgium (Brussels, 1938-1940). S. Radev, remotely related to Dr. Z. Dimitrova, described their birthplace Ressen as a beautiful valley “960 meters above the sea level – surrounded from all three sides by tall mountains and expanded southward by the Lake of Prespa... It is (Ressen) particularly beautiful in the spring when the numerous gardens and cherry trees blossom and give the lawns multiple colors above which rise the narcissi spraying their hypnotic scent. Here the land is fruitful...” [8].

Dr. Z. Dimitrova comes from an old ancestry with deeply rooted Bulgarian traditions. Her grandfather on her father's side, Velyo, fought against the Ottoman Empire for religious and national freedom. In 1848 he became a member of the first Bulgarian province in Istanbul. Later, in 1871, he was elected representative of the Ohrid-Prespan eparchy in order to participate in the National Convocation [8]. Simeon Radev elaborated further on Dr. Z. Dimitrova's ancestry in his book *Early Memories*:

“I have to mention some other leaders whose patriotism was on par with everyone's but who also avoided being constantly present in the public eye. One of them was Mitse Velyov, the son of Z. Dimitrova's grandfather Velyo, whose role in the Istanbul's church matters I already discussed. Tall and a little hunched over, dry and with a fairly dismal character, he kept to himself. Everyone who knew him praised his wisdom... One of Mitse's daughters, Zaharia (Zaharina), graduated with Medicine in Nancy and for her excellent results received a gold medal. Ressen can be proud that it gave the Bulgarian nation one of the first female physicians.” [8].

Dr. Z. Dimitrova (Fig.1) graduated from the Bulgarian Ladies' High School in Thessaloniki, Greece and left for Russia to study Obstetrics. Her thirst for knowledge brought her in 1895 to Nancy, France, where she enrolled in medical school. One of her mentors was Prof. M. Nicolas. He was internationally renowned for his research work on the histology and embryology of the intestinal epithelium and absorption mechanisms



Fig.1. Dr. Z. Dimitrova's photo at the time of her graduation

[7]. On February 27, 1901 Dr. Z. Dimitrova graduated with honors. Her dissertation "Recherches sur la structure de la glande pineale chez quelques mammiferez" was distinguished and received the honorary award of the Faculty of Medicine along with a gold medal bearing her name. Later, her interest-stirring work was published in the popular Belgian Journal – *La Nevraxe*, 1901, 2, 257-361. With her impressive research work started during her years at the medical school in Nancy, Dr. Z. Dimitrova could be recognized as the first Bulgarian histology scientist [7].

Dr. Z. Dimitrova's scientific work was partly studied during one of the congresses of the French Anatomical Association by both Prof. P. Petkov and Prof. E. Leger – General Secretary of the Association and Director of the Faculty of Anatomy in the University in Nancy [7]. Later, the work of Dr. Z. Dimitrova found a place in the already classic textbooks of the famous Bulgarian Professor Assen I. Hadjiyolov (1903-1998) – Head of the Department of Histology and Embryology at the Medical faculty in Sofia (1930 – 1968) [3].

During her study in Nancy, Prof. M. Nicolas drew Dr. Z. Dimitrova in his research team. He provided her with a rich collection of pineal glands of mammals, including human, and opportunities for all kinds research work in his lab. She used the modern for the time impregnation methods for cell staining in the nerve tissue, originally developed by the Nobel Prize winners Camillo Golgi (1843-1926) and Santiago Ramón y Cajal (1852-1934) [7]. For the first time in her dissertation Dr. Z. Dimitrova described accurately the main cells in the pineal gland – pinealocytes. She depicted them as extended or cone-like cells with heavily granulated cytoplasm and large bright eccentrically located nucleus. In addition, the young researcher documented for the first time the typical for the pinealocytes nuclear vacuoles [1]. Later, Prof. A. Hadjiyolov called them the "Dimitrova's Nuclear Spheres" [3]. They most commonly appear during puberty and their size reaches 4-5 μm and stain in blue by the method of Mann (eosine – methylene

blue) [3]. Today it is known that these spheres or vacuoles are cytoplasmic intrusions in the nucleus that encompass membranes of the granular endoplasmic reticulum. They are also characteristic of other cells with internal secretion when activated. Dr. Z. Dimitrova considered them quite interesting: "If the presence of granules is enough to classify a certain cell as glandular, then the pineal cells are at least glandular if nothing else." [1]

Dr. Z. Dimitrova's dissertation was cited more than 30 times in the publication of Dr. Bargmann, one of the founding fathers of the research of neurosecretion [7].

Unfortunately, after her return to Macedonia, Dr. Z. Dimitrova could neither continue her promising research nor practice medicine (Fig. 2). At that time Macedonia was still under Turkish rule and women were not allowed to work as physicians. Therefore Dr. Z. Dimitrova left for Sofia. After passing a rigorous state exam she received the right to practice medicine in Bulgaria [7].



Fig. 2. Dr. Z. Dimitrova's photo as a medical doctor in Bulgaria

From 1901 to 1910 Dr. Z. Dimitrova worked in the town of Sliven where she started a family with the military pharmacologist Major Panaiot Dimitrov. Her family moved to the South-Bulgarian town of Tatar-Pazardjik where she became a school and regional physician and later a freelance doctor. In 1930 she discontinued her practice due to illness. Dr. Z. Dimitrova died on April 14, 1940 [6]. During the last ten years of her life she was engaged in a lot of charity work serving as head of the charity organization "Budna Makedonka" and the ladies' organization "Prosveta". Through her charity activities Dr. Z. Dimitrova and her family provided support to many homes

for old people and birth centers. They also assisted refugees and their children in need of financial support for their education. One of the most beautiful public fountains in Pazardjik is “Gergana”, built with the financial support of Dr. Z. Dimitrova and her husband.

References

1. Dimitrova, Z. Recherches sur la structure de la glande pineale chez quelques mammiferes. *La Nevraxe*, **2**, 1901, 257-361.
2. Galunska, B., T. Tchervenkov, D. Paskalev et al. Melatonin and oxidative stress: some effects in patients on hem dialysis. *Nephrology Forum of Varna*, **I**, 2009, 38-43.
3. Hadjiyolov, A. I. Histology and Embryology. “Medicina i Fizkultura Edition”, Sofia, 1973, 444-448.
4. Lerner, A. B., Case, J. D., Takahashi, Y., Lee, T. H., Mori, N. Isolation of melatonin, pineal factor that lightens melanocytes. *J. Am. Chem. Soc.* 1958; **80**:2587.
5. Nordio, M. Melatonin – myth and reality. “Bolid Edition”, Sofia, 2005, 127.
6. Obituary. Dr. Zaharina P. Dimitrova died. In newspaper “Podem” (Pazardjik), No 541, 20. April 1940.
7. Petkov, P., A. Kanev. World-wide famous, little known in Bulgaria. *Asklepios*, **XVII**, 2004, 184-186.
8. Radev, S. In: Early memories. “Streletc Edition”, Sofia, 1994, 18-79.
9. Velkov, Z.A., Velkov, Y.Zh., Galunska, B.T. et al. Melatonin: Quantum-chemical and biochemical investigation of antioxidant activity. *European journal of medicinal chemistry* 2009; **44**:2834-9.
10. Voss, H. Grundriss der normalen Histologie und mikroskopischen Anatomie (Neu bearbeitet von G. Geyer), VEB Georg Thieme, Leipzig, 1977, 267.

Cases of Bodily Injuries During Arrest and in Custody

D. Radoinova¹, Y. Kolev²

Department of Forensic Medicine, Medical University of Varna¹

Department of Forensic Medicine, District Hospital MBAL, Gabrovo²

Cases of bodily injuries to two groups of victims are presented: 1) police officers during their professional duties by persons subject to detention or detained; 2) detainees (citizens) – during arrest, in pre-trial detention or in custody (cells or prison). A retrospective study was performed for all cases of examination of living persons for a 5-year period (2005-2009). The number of cases of police violence slightly prevail over the number of police officers who were victims of detainees' violence. In all of the cases examined there was a minor injury (low battery) ruled, with the exception of one case of the detainee – victim to another inmate, ruled as a medium grade of battery. The violence in the studied two groups is relatively rare and there are no serious cases of physical violence or death from the described period.

Key words: police violence, violence against police officers, medico-legal investigation.

Introduction

The incidence rate of injured law enforcement officers – police officers, judicial security and prison officers is not high, but have a social importance as accidents while performing their professional duties. On the other hand, during the arrest of citizens by police and at the places of detention (pre-trial detention or in custody), detainees complain from physical violence exerted on them.

The aim of this work is the parallel study of these two groups to compare the incidence of violence based on the collected data from forensic medicine units.

A cases of physical violence and a grade of bodily injuries to two groups of victims are studied: 1) police and judicial security officers during their professional duties by persons subject to detention or detained; 2) Physical abuse of detainees (citizens) – during arrest, in pre-trial detention or in custody (cells or prison).

Material and Methods

A retrospective study was performed and all cases of examination of living persons in the Department of Forensic Medicine in Medical University of Varna were analyzed, for a 5-year period (2005-2009), total number of 854.

Results

Of these 854 examinations of living persons, 11 relate to the subject, which are 1,29% of all examinations. From the first group there were 4 cases of police officers at work (0,47% of all the examined persons). There were 3 cases of violence during arrest of suspected persons, and the 4th case is during the attempted escape from the district police office. The police officers were struck, tossed, pressed or bitten by the detainees. The average age of police detainees was $42,3 \pm 3$ years. The examination revealed a number of abrasions, bruises and wounds, which differ by localization and grade, and one case of 5th finger of the left hand sprained (by bending and twisting). Objects by which were inflicted the injuries were basic blunt objects – hands, feet, teeth (bites), etc. Injuries were interpreted as minor injuries (lowest level of battery). From the second group (trauma during arrest or in custody) there were 7 citizens (0,82% of total reviewed). Six of them were injured by police in various incidents in detention or prison, and one was injured by another prisoner. The average age of the group was $34,6 \pm 5$ years. In all the 6 cases there were external mechanical injuries – abrasions, bruises and superficial lacerated wounds, which also were justified as minor battery.



Fig. 1, 2. A strangulation mark on the neck of a living person

The injuries were inflicted by hands, kicks, handcuffs, sticks (batons). The seventh case was a prisoner injured by another prisoner who has tried to strangle him by thin rope from behind. The examination took place on the third day after the incident and found a double groove strangulation on the anterior surface of the neck. Since the patient had severe pain on swallowing and a fully hoarse voice, an oedema of plica vocalis (consulted and established by ENT specialist), the injury was qualified as a medium grade of battery (temporarily life-threatening disorder). There were no recorded cases of severe injury or death occurred for the processed period.

Discussion

Our country lacks a system for investigation and registration of physical and mental violence, both for the police and prison officers and for citizens detained or in custody.

Kruse M et al. [2] presented data from three sources in Denmark — from a national register of the patients, statistics of victims and death register. Over 70% of the victims were men. Data for most of the victims can be found in emergency units or from the police reports, and some from the death register. Sometimes there was an overlap of data, so the authors concluded that there is a potential disadvantage in the use of different sources for the accuracy of incurred epidemiological, health, social and other analysis and conclusions.

Chaudhry M. A. et al. [1] studied police violence in Pakistan on forensic documents and court files. They found that most frequent was a blunt trauma. At the time of the survey most of the victims had visible evidence of psychotrauma and the distribution of the data by sex was markedly in favor of men.

Lorin de la Grandmaison G. et al. [3] investigated the police violence in the suburbs of Paris in 2004. In over 60% of the examined the authors established superficial injuries, localized mainly in the head and neck. All the recorded injuries were verified by police reports. In less than 2% of the victims there were secondary neurological complications from being handcuffed. There was no death case observed during the survey period, and in approximately 5% of the cases needed an emergency hospitalization.

We did not find out any published data on the subject in Bulgaria.

Conclusion

The violence in the studied groups is relatively rare – 1,29% of all the examined living persons for the period of 2005-2009 and there were no serious cases of physical violence nor a cases of death. The number of cases of police violence (0,82% of all the examined living persons) slightly prevail over the number of police officers who were victims of detainees' violence (0,47%). In all of the cases examined there was a minor injury (low battery) ruled, with the exception of one case of the detainee – victim to another inmate, ruled as a medium grade of battery – an attempted strangulation.

The problem discussed did not attract researchers' interest in Bulgaria so there is no data for other regions, and therefore more global conclusions can not be made.

It would be a good idea to consider creating a national register in forensic medicine units, for registration and in-depth study of this kind of violence.

References

1. Chaudhry, M. A., W. Haider, A.H. Nagi, Z. Ud-Din, Z. Parveen. Pattern of police torture in Punjab, Pakistan. – *Am. J. Forensic Med. Pathol.* **29**, 2008, (4):309-11.
2. Kruse, M, J. Sørensen, H. Brønnum-Hansen, K. Helweg-Larsen. Identifying victims of violence using register-based data. – *Scand. J. Public Health.* **38**, 2010, (6):611-7.
3. Lorin de la Grandmaison, G., C. Houssaye, N. Bourokba, M. Durigon. Frequency of traumatic lesions alleged by victims of assault during police custody. – *J. Forensic Leg. Med.* **14**, 2007, (6):364-7.

Anthropology

Psychometric Characteristics of Adolescents from Plovdiv, Aged 19-20

E. Andreenko

*University of Plovdiv "P. Hilendarski" – Faculty of Biology,
Department of Human Anatomy and Physiology*

Introduction

The problems of developing the motional habits and skills of humans have drawn various experts' attention for a long time, such as sports anthropologists, psychologists, teachers, etc.; because these problems are closely related to the functional condition and the level of working capacity of individuals during different age periods in their lives. In connection with studying the human psychomotor status, it is often applied an assortment of psycho-diagnostic approaches – attention analyses, speed of visual-motor reactions, emotional stability, mobility of the higher nervous activity, etc. Psychological research, done in this direction, show that personal characteristics, psychology and human consciousness are important factors that affect biological functions, somatic condition, health and development of individuals (1, 2, 3, 4, 5, 6).

The purpose of the present study is to research the inter-sexual differences in the psychometric characteristics of adolescents from Plovdiv, at the age of 19-20.

Key words: tremor measurement, tapping-test, speed, dexterity, attention.

Material and Methods

192 people were tested – 80 boys and 112 girls, aged 19-20, university students in their first year, from different specialities of the University of Plovdiv. The research was conducted in the period of years 2009-2010. In the present work we used a part of transversely measured data, in connection with the realization of the scientific project БФ-031 "Physical development, functional activity and psychological status of students".

We included a total of 9 directly measured psychometric indications. The common psychomotor profile of the students we surveyed represents a collective portrait of the

psychomotor, emotional and nervous-dynamic characteristics of the nervous system. Table 1 shows the main nervous characteristics of the students and the psycho-diagnostic tests used.

Table 1. Psychometric profile and tests used for psycho-diagnosis

Psycho-metric profile of the students	Tests applied
Psycho-emotional characteristics	Tremor measurement (static)
Coordination characteristics	Finger dexterity
Nervous-dynamic characteristics	Tapping-test Speed of the sensorimotor reaction
Characteristics of attention	Correction test with geometric shapes

➤ **Static tremor measurement (number of touches)** – the Polish electro-mechanical testing apparatus for psycho-physiological and technical research “Tremor-meter” was used. The person tested holds in hand, with their arm stretched, a metallic pencil in a circular aperture (d=5mm) in 10 seconds, without touching the walls of the aperture. *The number of touches (errors) was read.*

➤ **Finger dexterity (in seconds)** – a special block-board, with sockets for insertion of pins of three different sizes, was used. *We read the time that it takes to arrange all the removed pins in their places.*

➤ **Tapping-test (number of knockings)** – the apparatus “Tremor-meter” was used; you strike with a metallic pencil the top plate as quick as possible in 10 seconds. *The number of knockings on the plate of the apparatus was read.*

➤ **Speed of the sensorimotor reaction (number of correct hits)** – we used the reflex-meter “Piorkowski – I.C. – 6”. When submitting a series of simple light signals in a random order, the test subject responds as quickly as possible by pressing the appropriate button. The survey was conducted in two consecutive programmed pace of work – 75 pulses/min and 105 pulses/min. *The number of correct hits in the apparatus was read.*

➤ **Correction test with geometric symbols (for the intensity of attention)** – we used a blank-test with evenly spaced different geometric shapes (circle, square, rhombus, etc). The test subject strikes out with a vertical line only a single shape (a small circle) in 1 minute. *We read the number of correctly struck figures, the number of mistaken ones and the number of omissions.*

All data were processed using SPSS statistical package. The reliability of intersexual differences was checked through the t-criterion of Student at the level of significance $P < 0.05$.

Results and Discussion

The average values of the psychometric features in the surveyed students of both sexes are presented on Table 2 and illustrated in Figure 1 and Figure 2.

One of the important qualities of human emotions is their balance or stability. The lowered processes of active internal retention are the basis of a lesser degree of stability in the emotional sphere.

Table 2. Average values of the psychometric features of 19-20-year-old students

Tests		Boys N = 80		Girls N = 112		T ♂/♀
		X	SD	X	SD	
Static tremor measurement (number of touches)		5,18	6,76	5,33	6,61	
Finger dexterity (in seconds)		43,81	8,31	41,21	7,52	*
Tapping-test (number of knockings)		77,34	13,71	64,17	12,60	****
Speed of the sensor motor reaction (number of correct hits)	75 pulses/min	41,50	9,02	36,34	11,87	**
	105 pulses/min	35,40	4,33	35,61	4,30	
Correction test with geometric symbols (for the intensity of attention)	Number of correctly	67,30	14,13	67,58	12,49	
	Number of mistaken	0,039	0,19	0,050	0,26	
	Number of omissions	22,69	14,13	22,28	12,34	

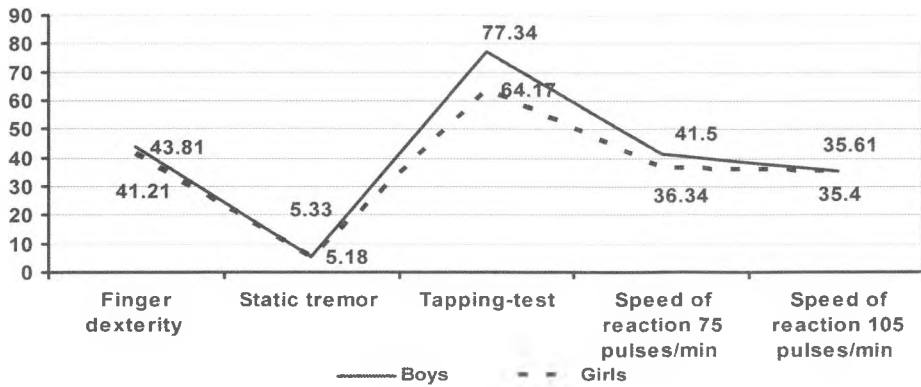


Fig. 1. Average values of the psychometric features of 19-20-year-old students

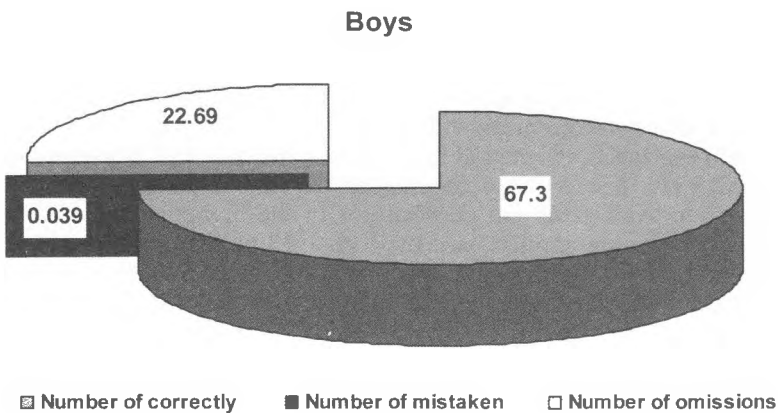


Fig. 2. Intensity of attention – Correction test with geometric symbols (Boys)

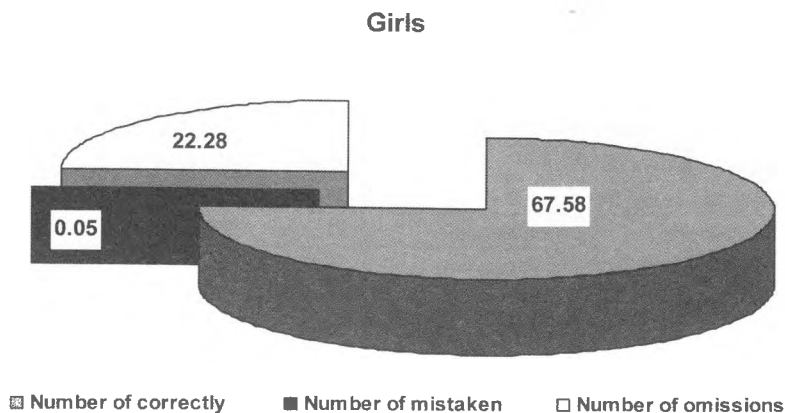


Fig. 3. Intensity of attention – Correction test with geometric symbols (Girls)

The tremor measurement makes possible to assess the functional status and emotional instability of the nervous system; it has a clearly-expressed individual nature. The results of this study show similar physiological type of tremor in both sexes. The average value of this feature for boys was 5.33 touches, while for girls they are 5.18. The recorded fluctuations in the psycho-emotional stability between the sexes do not reach statistical value ($p > 0.05$). The boys and girls tested have similar processes of controlled micro-movements in carrying out the task.

Finger dexterity is a psychometric feature that refers to the speed parameters of the nervous activity. Besides speed, the major components of this test are also the coordinated movements of the fingers and the quickness of mind. The average time to arrange the pins for boys was 43.81 sec, and for girls – 41.21 sec. The difference in averages between the sexes was significant ($p < 0.05$) and it showed that the girls solved the task 2.6 sec faster than boys.

Tapping-test appears to be a simple and effective practice for individual or group diagnostics of the functional status and the degree of activation of the nervous system. It aims to determine the power of neural processes and it is based on the changes in the time of the maximum rate of wrist movement. The results show that the number of movements with a maximum frequency is higher in boys (77.34 taps) than in girls (64.17 taps). In 10 seconds the boys made an average of 14 taps more than girls. The gender differences were statistically significant ($p < 0.05$). Therefore, in boys, it is recorded a higher functional mobility and speed of the neural processes.

Speed of reaction is an integral indication of the speed of implementation of excitation in reflex arc. It very much depends on the functional condition of the central nervous system as well as on the peculiarities of the higher nervous activity. In the survey we used two programmed pace of work – 75 pulses/min and 105 pulses/min. When comparing the data for speed of reaction at the lower frequency (75 pulses/min), we had better results for boys. For them there is a statistically significant greater amount of correct responses (correct hits 41.50) than girls (36.34 correct hits) – ($p < 0.05$). This shows a better level of functional status of CNS in boys.

With regard to the higher pulse frequency (105 pulses/min), significant differences between the sexes were not observed ($p > 0.05$). The girls equaled their speed of response (correct hits 35.61) to that of boys (35.40 correct hits).

Intensity of attention represents a focused or intent consciousness, suggesting an increased level of the sensory, intellectual or physical activity of individuals. The most common group of research methods of attention is the blank methods grouped under the general title "Correction tests". In the present study we used the widely popular "Correction test with geometric symbols". The amount of the basic mark (a small circle), which must be struck out according to the instructions, is 90. The test gives the opportunity to assess the speed of information processing in the central nervous system. The results show the same averages with regard to the quantity of properly struck geometric shapes in both sexes. Boys struck out properly 67.30 symbols, and girls – 67.58 symbols ($p < 0.05$). In terms of numbers of the wrong strikes and omitted geometric symbols, gender differences also were statistically insignificant ($p < 0.05$). The boys gave average 0.039 wrong answers and 22.69 omissions, while the girls respectively – 0.05 errors and 22.28 omissions. The resulting data show a similarity in the quality of attention. Obviously, solving the mental task of the correction test runs in both sexes at an equal degree of attention expression.

Summarizing the data from this study, we can conclude that students' nervous-dynamic and coordination characteristics play a better demarcating role in their psychometric profile in comparison with their psycho-emotional characteristics and features of attention. Some results from the psycho-diagnostic tests allow us to get to the following

Conclusions

- For students of both sexes there is a similar physiological tremor, and therefore similar levels of emotional stability.
 - Boys show a higher speed of response and they make more movements in a short time, while girls are more skillful and quick-witted.
 - Both sexes maintain a high level of concentration and have a similar level of attention expression.

References

1. Балтаджиева, Й. 1990. Факторен анализ на характеристиките на вниманието. – Сп. Психология, 2, 42-46.
2. Банковска, Р., Минкова, Н. 1985 Психофизиологични изследвания при някои професии в тютюневата промишленост в зависимост от трудовия стаж. – Сп. Психология, 2, 33-38.
3. Мартиросов, Э. Г. 1998. Соматический статус и спортивная специализация. Автореф. дис., М., с. 87.
4. Клаучек, С. В., Г. А. Севрюкова, Т. Н. Кочегура, М. О. Красильникова, 2004. Оценка адаптивных реакций студентов на воздействие моделируемых эмоциогенных нагрузок. Вестн. Волгогр. гос. мед. ун-та, № 11, 18-20.
5. Шмидт, С. А., Т. Н. Кочегура, Т. А. Аристова, Е. Л. Шатова, 2006. Метод диагностики параметров психомоторного статуса человека–оператора. – Современные наукоемкие технологии, № 1, 59-60.
6. Robertson, I., A., Kinder. The validity of the occupational stress indicator. – Work and Stress, 4, 1990, 1, 29-39.

Relation Between Body Composition and Some Social Factors and Habits in Children and Adolescents

*M. Nikolova**, *D. Boyadjiev***

**Department Human Anatomy and Physiology, University of Plovdiv*

***Department Applied Mathematics and Modelling, University of Plovdiv*

The purpose of this study is to assess how essential the individual factors and social habits and their combination are for body composition of a body. It was made a transversal analysis of 1155 girls and 1114 boys aged 7 to 17 years in 2008/2009 by the anthropometric and bioimpedance-metric methods. The estimation of body type nutritional status was made by the discriminatory values of BMI for underweight and normal status, overweight and obesity. The survey showed that the complex issue of socio-economic factors have a determinative role regarding the main body components. The socio-economic status can be used as a starting point for predicting the body nutritional status of adolescents.

Key words: Body composition, anthropometry, bioelectrical impedance analysis, socioeconomic factors, children and adolescents.

Introduction

Studying the influence of the socioeconomic factors on growth and development of children and adolescents has a long history. In recent years, attention is drawn to body composition of growing organisms and the assessment of body components that make up the weight. Experts' attention is focused on the information which BMI gives to assess the type of body nutritional status [1, 4]. To some extent, the individual differences during the intense growth and development also depend on the socio-economic living conditions [2, 5, 8]. The socioeconomic factors traditionally are related to parents' education and occupational status, residential living conditions, income, living standards, etc.

The purpose of this study is to assess how essential the individual factors and social habits and their combination are for body composition of a body. If it is possible to predict the level of body nutritional status on the basis of socio-economic factors and habits.

Materials and Methods

We tested anthropometrically and by the method of bio-impedance analysis 2269 children and adolescents from Plovdiv /1114 boys and 1155 girls/, aged 7 to 17 years, in 2008/2009. The anthropometric program includes 31 indicators, directly measured, – height weight, 5 body diameters, 11 circumferential features of the torso and limbs, 9 skin folds and 4 bone diameters. Through the means of Matiegka's method [6] we estimated the fat, muscle and bone components of body composition, and through Skerlj's method – the subcutaneous fat mass [7, 8]. We estimated the absolute and relative values of fat and fat-free masses and active cell mass with a bioelectrical impedance analyst ABC – 01 “Medas”, equipped with special software [3]. On the basis of anthropometric features we estimated BMI and its two components – index of active body mass /IABM/ and index fat mass /IFM/. The estimation of body type nutritional status was made by the discriminatory values of BMI for underweight and normal status, overweight and obesity. Through inquiry method we collected information on the following determinative socio-economic factors and habits: father's and mother's educational and professional qualifications, both parents' job, number of family members and household standard of living, floorage and average income per family member; sports, alcohol drinking and smoking.

The data on body components are standardized according to the age and gender. The significance of the relation between body components and social factors was assessed using factor analysis with Student's criterion /in 2 levels of the factor/ and Fisher's /in more than 2 levels of the factor/. We applied linear discriminatory analysis for modelling and predicting the levels of body nutritional status by the social factors and habits.

Results and Discussion

Table 1 presents the results of the analysis of the influence of socio-economic stratification and habits on components of body composition in the tested children and adolescents. In both sexes, the dependencies of most body components on father's educational level and number of family members are significant. There were also gender differences. Girls' body composition depends on the family living standard as well, and in boys – on the type of family. For both sexes, sports activity is in a significant dependence on muscle tissue, while alcohol drinking on fat mass. Only in girls, fat mass and subcutaneous fat mass showed a significant relation to smoking. Differences can also be seen in the different levels of a factor. Sons and daughters of fathers with secondary school education have values of fat component and BMI above average. Father's educational levels are also a differentiating factor regarding muscle and bone tissue, but only in girls, while the type of family is a differentiating factor for BMI and subcutaneous fat in boys.

The next task was to examine the possibility of predicting the level of body nutritional status /according to the discriminatory levels of BMI/, basing on socioeconomic factors and habits. For this purpose linear discriminatory analysis was applied. In the model which we used there were four groups of the classification variable: underweight, normal status, overweight and obesity. Using the version of behavioural discriminatory analysis of all 11 socio-economic factors, we identified 8 predictors in girls and 7 in boys, which can be seen on Table 2. With their help we predicted to which of the groups of body nutritional status each child belongs. Results for girls are given in Fig.1. They show that the model works best for obese girls /50% correctly predicted by the model/,

Table 1

Body composition components with statistically significant differences in the different levels of social factors and habits											
Body components	Social factors and habits (where $p \leq 0.1$ according to T/F criterion)										
	Father's education	Mother's education	Father's profession	Mother's employment status	Type of family	Number of family members	Average income	Lifestyle	Sports activity	Alcohol	Smoking
Fat mass	0.066 0.014				- 0.007	0.016 0.004				0.023 0.025	0.006 -
Fat-free mass								0.096 -	0.006 -	- 0.072	
% Fat mass	0.041 0.015				- 0.001	0.029 0.010					
Active cell mass								0.009 -	0.000 -		
Subcutaneous fat mass					- 0.078	0.045 0.024				0.000 -	0.000 -
Muscle tissue	0.036 -			- 0.089		0.022 -			0.007 0.072		
Bone tissue	0.092 -		- 0.098		0.065 -	0.081 -				0.002 -	
Body Mass Index	0.059 0.016				- 0.068	0.007 0.025		0.073 -		0.017 0.032	
Fat-free mass index	0.002 0.019	0.003 -	- 0.083		0.065 0.095	0.017 -	0.015 -			0.000 0.000	0.003 0.023
Fat Mass Index	0.024 0.005	0.060 -			- 0.002	0.015 0.007	0.067 -	0.058 -		0.000 -	

Table 2

Discriminative socio-economical predictors in girls and boys	
girls	boys
Factors included in the model	
Mother's profession	Father's education
Father's profession	Floorage
Average income	Average income
Mother's education	Family members number
Lifestyle	Mother's education
Father's employment status	Family type
Floorage	Mother's profession
Family members number	
Factors outside the model	
Father's education	Father's profession
Mother's employment status	Father's employment status
Family type	Mother's employment status
	Lifestyle

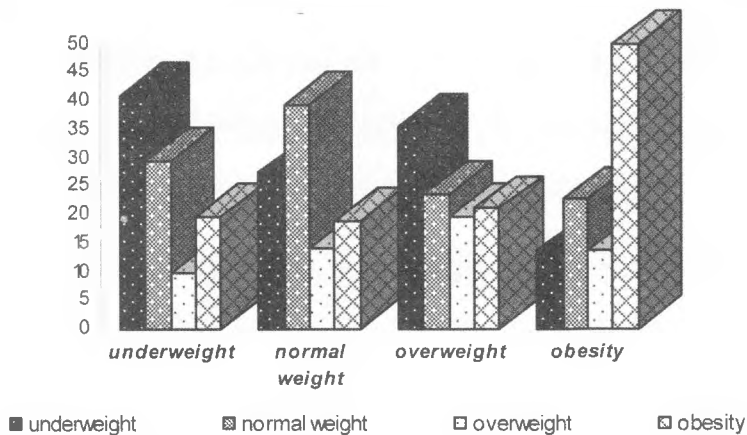


Fig. 1. Percentage of posteriori classification by social factors – girls

followed by those of underweight /41%/ and the lowest is the prediction for girls with overweight – probably because they are an intermediate group. The total percentage of correctly classified by the model girls is 36.8%.

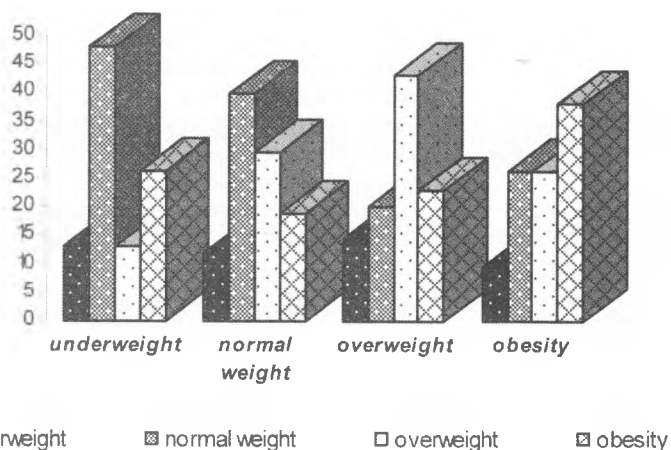


Fig. 2. Percentage of posteriori classification by social factors – boys

Table 3

Discriminative socio-economical and behavioral predictors in girls and boys	
girls	boys
Factors included in the model	
Alcohol	Sports activity
Lifestyle	Father's employment status
Father's profession	Mother's education
Floorage	Father's education
Mother's employment status	Family members number
Average income	Alcohol
Family members number	Mother's employment status
	Lifestyle
	Smoking
	Family type
Factors outside the model	
Sports activity	Father's profession
Smoking	Mother's profession
Father's education	Floorage
Mother's education	Average income
Mother's profession	
Father's employment status	
Family type	

For boys (Fig.2) the model gives the best prediction for those who are overweight (42.9%) and the lowest – the boys with underweight (13%). The total percentage correctly classified by the model for boys was 38.4%.

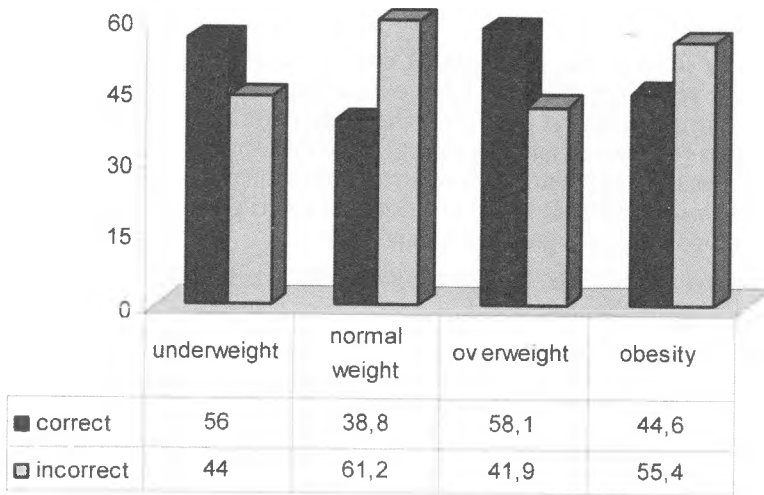


Fig. 3. Percentage of posteriori classification by social factors and habits – girls

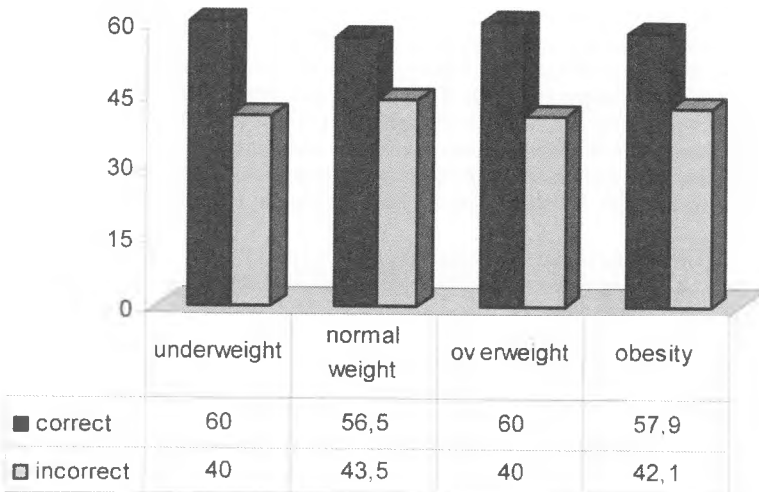


Fig. 4. Percentage of posteriori classification by social factors and habits – boys

The next step was the habits of children to be added to the model. In this case, adolescents over 11 years were included and the last two groups of the classification variable were united. The discriminatory variables in the new models are shown on Table. 3. The predicted body nutritional status in girls, as shown in fig. 3, is best for overweight (58.1%) and underweight (56%). In boys (fig. 4), the model gives 50% correct classification for all three levels of body nutritional status. The total correct classification rate after including the habits increases in both sexes – girls from 36.8% to 44.6%, and for boys from 38.4% to 57.9%.

Conclusion

The survey showed that the complex issue of socio-economic factors have a determinative role regarding the main body components. The socio-economic status can be used as a starting point for predicting the body nutritional status of adolescents. It appeared to be a good predictor for predicting the occurrence of certain bad habits and upcoming changes in body status. It is a matter of big interest to what extent the statistical approach is also applicable to the creation of a priori prognoses for the age changes in the body components of a growing organism.

Acknowledgements. This work is supported by grant No ВУ-Л – 313/2007 from the Bulgarian National Science Fund.

References

1. Година, Е. З., Задорожная, Л. В., Пурунджан, А. Л., Третьяк, А. В., Хомякова, И. А. Некоторые особенности состава тела у детей и методические проблемы его изучения. «Вопросы антропологии», 2007, 93: 18-39
2. Година, Е. З., Задорожная, Л. В. Влияние некоторых факторов окружающей среды на формирование особенностей соматического развития детей и подростков. – *Вопр. Антропол.*, 1990, вып. 84, с.18-30
3. Николаев, Д. В. Биоимпедансный анализатор АВС-01 „Медас“. Руководство пользователя, Москва, 2001. 24 с.
4. Пурунджан А. Л., Година, Е. З., Хомякова, И. А., Задорожная, Л. В., Савостьянова Е. Б., Бердникова М.С., Третьяк, А. В. Возрастные изменения состава тела у московских детей и подростков. – В: Сборник трудов ученых РГУФК, М., 2006, 8-15.
5. Godina, E., Khomyakova, I., Purundzhan, A., Zadorozhnaya, L. Some differences in body composition in Moscow adolescent children according to the level of their physical activity: comparison of anthropometric and bioelectrical impedance methods of assessment. // *Human Body Composition*. Eds. S.P.Singh, Rajan Gaur. Kamla-Raj Enterprises, Delhi: India, 2007, 63-74.
6. Matiegka, J. The testing of physical efficiency. – *Am. J. Phys. Anthropol.*, 1921, 223-30.
7. Smirnova, N. S., Shagurina, T. P. Methods of Anthropometric Investigations, pp.16-22. In: *Methods of Morphophysiological Investigations in Anthropology*. Moscow State Univ. Publishers. 1981.
8. Parizkova, J. *Body Fat and Physical Fitness*, 1977, Nijhoff: The Hague.

Morpho-Functional Characteristics of Students from Plovdiv

Sl. Tineshev

*Faculty of Biology, Paisii Hilendarski University of Plovdiv
Department of Human Anatomy and Physiology*

The purpose of this study is to characterize the morphological status and functional abilities of students, aged 19-21 years, from the University of Plovdiv. The morphologic characteristic showed that: in the boys are taller and heavier than girls; the transverse and sagittal diameters of the chest have higher values in boys, as in both genders, functionally well-fitted conic shapes are more common; limbs circumferences are bigger in boys, as the intersexual differences are more expressed for the circumference of the forearm in comparison with the circumference of the shank. This presents the bigger plasticity of muscles and subcutaneous fat tissue in the distal segment of the upper limb in comparison with that of the lower limb. Physiometric characteristic showed that hypertension occurs more often in boys, and hypotension – in girls. In both genders, the percentage of individuals with quickened pulse rate is the highest.

Key words : morphological status, functional abilities, students.

Introduction

Human ontogenesis is a long and multifarious process, whose stages are characterized by processes different in power and nature. The correct assessment of health status of the body is impossible without the systematic monitoring of physical development [3]. Modern concepts of physical development are best matched in its definition as a process of formation of the structures and functions of the body, in accordance with the genetic potentialities and environmental conditions [4, 5]. To clarify the common tendencies in body changes during ontogenesis, functional studies are of great importance [1, 2]. Their results have essential importance in medico-biological practice and give interesting information of a higher hierarchical level about humans. Such complex anthropological studies that are related to a big number of morpho-functional indicators aim to characterize more fully and completely the somatic development and functional reactivity of the organism.

The great originality in form and structure of a body through the stage of maturity, and the overlap of the opinion for the integrity and indivisibility of the body, for the unity of its morphology and function, determine the interest toward the present research.

Material and Methods

To solve this purpose, we used transversally collected data of students, in their first year at university, at the Faculty of Biology of the University of Plovdiv. 192 students – 80 boys and 112 girls, aged 19 to 21 years, were measured. The anthropological features were measured by the conventional method of Martin-Saller (1957), using the original anthropometric equipment. The study included height, weight, and chest diameters and limbs circumferences. The recording of the systolic pressure, diastolic pressure and pulse rate was made with OMRON MX3 Plus. The measurement was performed in a seated position of the body, on the left hand.

Results

The height (Table 1) is a basic anthropometric feature of leading significance also for the interpretation of the metric data for a big part of the other anthropometric characteristics. This feature is characterized with great changeability and it shows distinct sexual, age and territorial differences.

Analyzing our results, we found that the tested boys in the age interval of 19-20 years are taller than girls with 14.04cm. The intersexual differences are statistically reliable at the level of significance $p \leq 0.001$. In our excerpt, boys' height varied from 163.40 to 191.20 cm, and in girls – respectively from 142.00 to 181.10 cm. The most common frequency of occurrence are the boys between 171.99cm and 182.83cm ($X \pm 1SD$), while girls – in the interval between 157.17cm and 169.57cm.

In contrast to the height, which is genetically determined, the body weight (Table.1), except its coded hereditary potential, it is also influenced by a lot of exogenous factors, social-economical status of the family, and last but not least by the food quality and type. These peculiarities make it exclusively important in determining the health status of a body throughout the postnatal ontogenesis.

The average value of body weight in boys was 76.19, and in girls – 57.39 kg. Intersexual differences of the order of 18.8 kg and they are characterized with a high level of reliability $p \leq 0.0001$. The big variation range was also proved with the big variability of weight of the students we surveyed.

The transverse and sagittal diameters (Table 1) of the chest are the features whose values determine the form and size of the chest. The sagittal diameter presents the depth of the chest, and the transverse diameter characterizes its width. The chest shape depends on the inclination and curves of ribs, on the position of the chest bone, collar-bones, blades and the spinal column.

Analysis of the results fully substantiates the well-known facts from the scientific literature that boys have bigger values of chest diameters. In both genders, the functionally well adjusted conic shapes are more (thoracic index 70.0-73.0). In our excerpt, we found that 19% of the boys and 17% of the girls have cylindrical chest shape, which is typical for sports individuals. As a whole, in both genders, the chest is well-developed and it has typical shape and size intrinsic to grown individuals

Limbs circumferences (Table 1) are morphologic characteristics that present the physical abilities of the skeletal muscles. Together with their measuring the amount of subcutaneous fat tissue was also recorded. The average values of these two features were higher in boys – respectively the circumference of the forearm – boys – 26.83 cm, girls – 22.39 cm; the circumference of the shank – boys – 37.45 cm, girls – 34.16 cm. The intersexual differences are higher for the circumferences of the forearm, where boys have 16.55% bigger size in comparison with girls, while for the shank the dif-

Table 1. Biostatistics data on morphological characteristics

No	boys							girls							T♂/♀
	n	χ	SD	SEM	V	min	max	n	χ	SD	SEM	V	min	max	
Height	80	177,41	5,42	0,62	29,39	163,4	191,20	112	163,37	6,20	0,58	38,49	142	181,10	**
Weight	80	76,19	12,59	1,44	158,65	51,20	121,40	112	57,39	10,48	0,99	110,01	41,40	112	***
Transverse diameter	80	29,19	2,34	0,26	5,48	22,10	35,20	112	24,38	1,57	0,14	2,50	21,20	28,50	**
Sagittal diameter	80	21,27	2,87	0,31	8,27	14	28,80	112	17,56	1,86	0,17	3,48	14,20	25,20	***
Circumference of the forearm	80	26,83	2,24	0,25	5,03	22,40	32,90	112	22,39	2,14	0,20	4,59	17,90	29,80	****
Circumference of the shank	80	37,45	3,16	0,36	10,02	31,20	44,70	112	34,16	3,74	0,35	14,04	20,50	52,50	***

Table 2. Biostatistics data on physiological characteristics

No	boys							girls							T♂/♀
	n	χ	SD	SEM	V	min	max	n	χ	SD	SEM	V	min	max	
Systolic blood pressure	80	133,26	13,94	1,59	194,51	100	170	112	116,67	11,97	1,13	143,28	90	152	****
Diastolic blood pressure	80	76,02	11,62	1,33	135,03	53	110	112	76,00	9,42	0,79	88,88	60	103	
Pulse rate	89	86,75	16,47	1,89	271,48	54	135	112	86,25	13,53	1,27	183,16	60	122	

ferences between sexes are almost twice smaller – 8.79%. These kind of intersexual differences represent the bigger plasticity of muscles and the subcutaneous fat tissue in the distal segment of the upper limb compared to the distal segment of the lower limb.

Pulse rate (Table 2). The average values of pulse rate, in both genders, were relatively similar – 86 beats per minute. The lowest pulse rate measured in young men was 54 beats per minute, but in girls – 60 beats per minute. The highest pulse rate measured in boys was 135 beats per minute, and in girls – 122 beats per minute. The average pulse rate does not give a clear picture of the characteristics of heart activity, because that we would characterize the data on the frequency of individuals with slow pulse rate (to 59 beats per minute), quick (80 beats per minute) and normal pulse rate (between 60 and 80 beats per minute). In our sample, we found that slow pulse rate occurred only in boys, with very low frequency – 2.5%. The percentage of boys with normal pulse rate is relatively equal to that of girls (boys – 36.71%, girls – 35.71%). It is worrying that in both sexes individuals with quickened pulse rate dominate, which in future may possibly be a prerequisite for the occurrence of arterial hypertension – 60.79% in boys and 64.29 in girls.

Systolic blood pressure (Table 2). The average values of the systolic blood pressure in the boys surveyed were 133.26mmHg, and 116.67mmHg in girls. The comparison between genders showed that in girls it is 12.45% (16.59mmHg) lower than that of boys. Since the average values of systolic blood pressure do not give information about any abnormal aberrations, we analyzed data of individuals according to the categories hypotension (up to 109mmHg of mercury) norm tension (from 110 to 140mmHg of mercury) and hypertension (over 140mmHg of mercury). Result analysis showed that individuals with normal systolic blood pressure are more (boys – 62.5%, girls – 69.46%). It is interesting to note that hypotonic systolic blood pressure has higher frequency of occurrence in girls (26.78%) (7.5% boys), but hypertension in boys (30%), (3.86% in girls); which shows that boys are in higher risk of occurrence of risk situations.

Diastolic blood pressure (Table.2). Our records, according to the average values of the diastolic blood pressure, do not present any intersexual differences – 76mmHg. We calculated the frequency of occurrence in individuals in the three categories of the diastolic blood pressure with the following limiting values – up to 69 mmHg, from 70 to 90 mmHg and over 90 mmHg. In both genders, most individuals had diastolic blood pressure between 70 mmHg and 90 mmHg (boys – 66.25%, girls – 68.75%). The percentage of boys with diastolic blood pressure bellow 69 mmHg is 25%, and girls – 23.21%. The least frequency of occurrence was in students with diastolic blood pressure over 90 mm Hg (boys – 8.75%, girls – 8.03%).

Conclusion

The summary results from the analysis of the data of the arterial blood pressure in students, aged 19-21 years, showed that in both genders these with normal values are more. For our students the hypertension is more common in boys, and hypotension – in girls, i.e. students tested at this age have physical status typical for the grown-up men and women.

1. The morphologic characteristic showed that:

- * boys are taller and heavier than girls;
- * the transverse and sagittal diameters of the chest have higher values in boys, as in both genders, functionally well-fitted conic shapes are more common;
- * limbs circumferences are bigger in boys, as the intersexual differences are more expressed for the circumference of the forearm in comparison with the circumference of

the shank. This presents the bigger plasticity of muscles and subcutaneous fat tissue in the distal segment of the upper limb in comparison with that of the lower limb.

2. Physiometric characteristic showed that:

* hypertension occurs more often in boys, and hypotension – in girls. In both genders, the percentage of individuals with quickened pulse rate is the highest.

References

1. Андреевко, Е. Особенности в психометричната характеристика на Пловдивски студенти. Юбилейна национална научна конференция с международно участие, СУБ, клон Смолян, 947–955.
2. Andreenko, E., 2007. Factors, defining psychomotor reactivity and personal profile of men with different physical activity. Номо, Научни трудове, Биология, ПУ „П. Хилендарски“, том 40, кн.6, 13–24.
3. Година, Е. Динамика процессов роста и развития у человека: пространственно-временные аспекты. Автореф. докт. биол. наук. Москва, 2001.
4. Година, Е. З., Задорожная, Л. В. Влияние некоторых факторов окружающей среды на формирование особенностей соматического развития детей и подростков. – *Вопр. антропол.* 84, 1990, 18–30.
5. Николова, М. Генетични и средови основи на морфологичната изменчивост. Научни трудове ПУ „П. Хилендарски“, 4, 2000, 267–284.

Dependence Between Maternal Weight Gain During Pregnancy and Some Newborns Anthropometrical Sizes

I. Yankova, Y. Zhecheva

*Institute of Experimental Morphology, Pathology and Anthropology with Museum,
Bulgarian Academy of Sciences*

The aim of our study is to determine the relationship between the maternal weight gain during pregnancy and some anthropometric parameters of newborns.

During 2001 a total of 219 (110 boys and 109 girls) clinically healthy, fullterm neonates born in Sofia (38 to 42 weeks of gestation, with body weight of more than 2500 g) were examined.

The maternal prepregnancy body weight and weight gain during pregnancy exert a significant influence of the newborns body dimensions. Mothers with higher body weight before pregnancy gain less. Women who gain weight during pregnancy more than 20.0 kg give birth to heavy babies. Newborns whose mothers gain during pregnancy more than 20.0 kg have values of the anthropometrical features above the means. Infants born by mothers who gain less than 20.0 kg have values of the anthropometrical features around and below the means.

Key words: newborn infants, maternal weight gain, pregnancy, anthropometrical sizes.

Introduction

The physical development of newborn infants is influenced by a complex of exogenous and endogenous factors. The impact of environment on foetal growth is mediated by the mother through her womb (i.e. the function of the placenta, uterine blood flow and central uterine circulation, placental and umbilical circulation). Some authors consider that the maternal factor, characterized meanly by age, weight and stature of mother, birth order and etc. is most important for the foetus [5]. (Kaliszewska-Drozdowska, 1996).

During pregnancy and in postnatal period, nutrition, socioeconomic status, diseases and other factors significantly influenced growth [1, 2]. Nutritional status of the mother before and at the time of pregnancy, as well as pregnancy weight gain are important for foetal growth [3] and also affect perinatal mortality, postnatal morbidity and postnatal growth of children [4]. It is considered that poor nutritional status and low weight gain of mother during pregnancy are associated with low body weight at birth [6]. According to some authors, the women who gain more than 18 kg during pregnancy

give birth to heavy babies two times more frequently than these who gain weight within the recommended levels (11.5-16.0 kg).

The study of inheritable and environmental factors on the physical development of newborns, as well as on the growth and development during early childhood could help to detect some genetic abnormalities.

The aim of the study is to determine the relationship between the maternal weight gain during pregnancy and some anthropometric parameters of newborns.

Material and Methods

During 2001 a total of 219 (110 boys and 109 girls) clinically healthy, fullterm neonates born in Sofia (38 to 42 weeks of gestation, with body weight of more than 2500 g) were examined. The babies were studied within 24 hours after birth in the Department of Neonatology at II Hospital of Obstetrics and Gynaecology "Sheynovo". The gestational age was determined according to the date of mother's last regular menstruation. The anthropometrical measurements were realized by Martin – Saller's classical methods [7], in lying position of the child, from the right side of the body.

From a total of 38 directly measured anthropometrical features in the analysis 19 of them are included and grouped according to their morphofunctional identity and biological information, which they provide.

Mathematical and statistical data processing was realized using statistical software for Windows – SPSS 13.0, using the following analysis:

– Z – score transformation – to standardize the values of the compared features, regardless of their measure units. Using was the formulae:

$$Z \text{ score} = (X_i - \bar{X}) / SD$$

where X_i – is the individual value of an anthropometrical feature, \bar{X} – is the mean values of this features in the sample and SD – standard deviation of the trait in the sample. After standardizing $\bar{X} = 0$, $SD = 1$ for the given feature.

– One-way ANOVA analyses – to establish the relation between mean anthropometrical characteristics of neonates and maternal weight gain during pregnancy.

According to the factor pregnancy weight gain were formed 5 groups: Group I – mothers who gained 5 to 10 kg; II gr. – mothers who gained 11 to 15 kg.; III gr – mothers who gained 16 to 20 kg.; IV gr. – mothers who gained 21 to 25 kg and V gr. – mothers who gained more than 25 kg.

– Post hoc Tukey Honestly Significant Difference Test (HSD-test for unequal N) – to establish the inter-group differences.

– T – test of Student – for assessment of the statistically significant gender differences ($P \leq 0.05$).

Results

The maternal body weight varied from 40.0 kg to 100.0 kg and the mothers were divided into three groups: weighing less than 60.0 kg; from 61.0 to 70.0 kg and weighing over 70.0 kg.

The mothers with body weight between 61.0 and 70.0 kg gain most during pregnancy – an average of 18.0 kg. Mothers with body weight less than 60.0 kg gain weight an average of 17.0 kg and those weighing over 70.0 kg gain least of all – between 10.0 and 15.0 kg (Fig. 1).

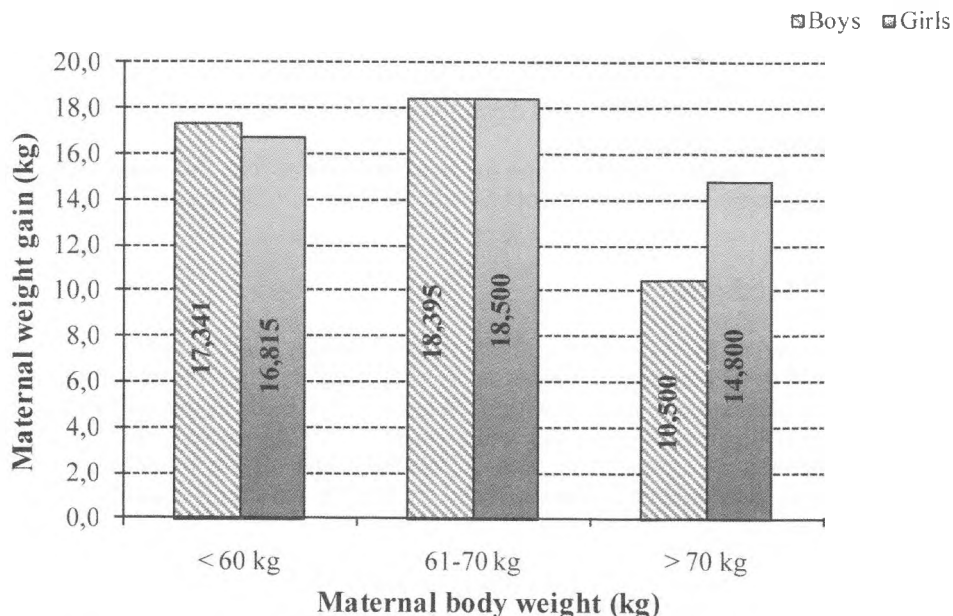


Fig. 1. Pregnancy weight gain, according to the maternal body weight

Figure 2 shows the distribution of pregnancy weight gain (5-kg groups) in the three maternal body weight groups. The highest percentage of mothers (28.0%) of newborn boys, weighing less than 60.0 kg gain weight during pregnancy from 10.0 to 15.0 kg, and only 8.0% of women gained more than 25.0 kg. Most of the mothers (27.0%) in the second group, with body weight between 61.0 and 70.0 kg, gain weight from 15.0 to 25.0 kg. Twenty five percents of the mothers with body weight over 70.0 kg before pregnancy gain weight from 5.0 to 10.0 kg.

In the group of mothers of newborn girls weighing less than 60.0 kg the tendency of pregnancy weight gain are similar to this in the group of the boys' mothers. The highest is the frequency of the women who gain weight during pregnancy from 10.0 to 15.0 kg (36.0%) and the mothers gained over 25.0 kg are only 9.3%. Forty three percents of women weighing between 61.0 and 70.0 kg gain from 10.0 to 15.0 kg. Only 9.5% of women gain between 15.0 kg and 20.0 kg and also 9.5% – over 25.0 kg. Most of the mothers (33.3%) weighing over 70.0 kg gain between 15.0 and 20.0 kg, and only 8.3% of women in the same group gain between 20.0 -25.0 kg.

The maternal weight gain during pregnancy strongly affects the infants birth weight (Fig. 3).

The mean birth weight of boys is 3.390 kg, as the newborns of mothers who gain weight during pregnancy above 25.0 kg are heaviest (3.661 kg) and those whose mothers gain from 5 to 10 kg are lighter (3.169 kg).

The newborn girls have mean birth weight of 3.290 kg, as those whose mothers gain weight from 21.0 to 25.0 kg are heaviest (3.625 kg). The newborn girls of mothers increasing their weight during pregnancy with 11.0 to 15.0 kg are lightest.

Figure 4 illustrates a marked positive dependence between pregnancy weight gain and body sizes of newborn infants.

The specificity of anthropometrical status of newborn boys and girls depending on the pregnancy weight gain of their mothers is similar. With pregnancy weight gain over

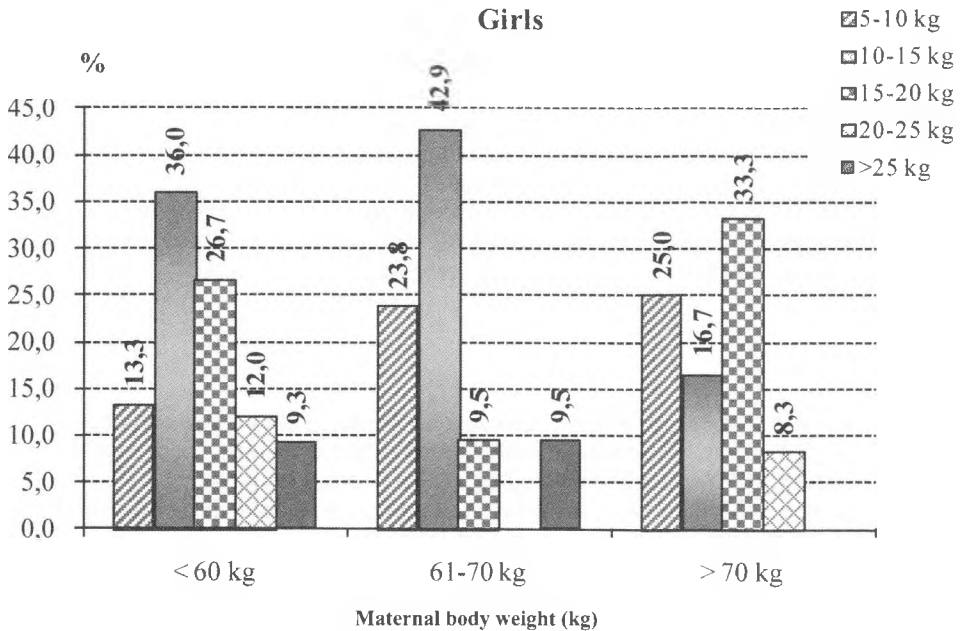
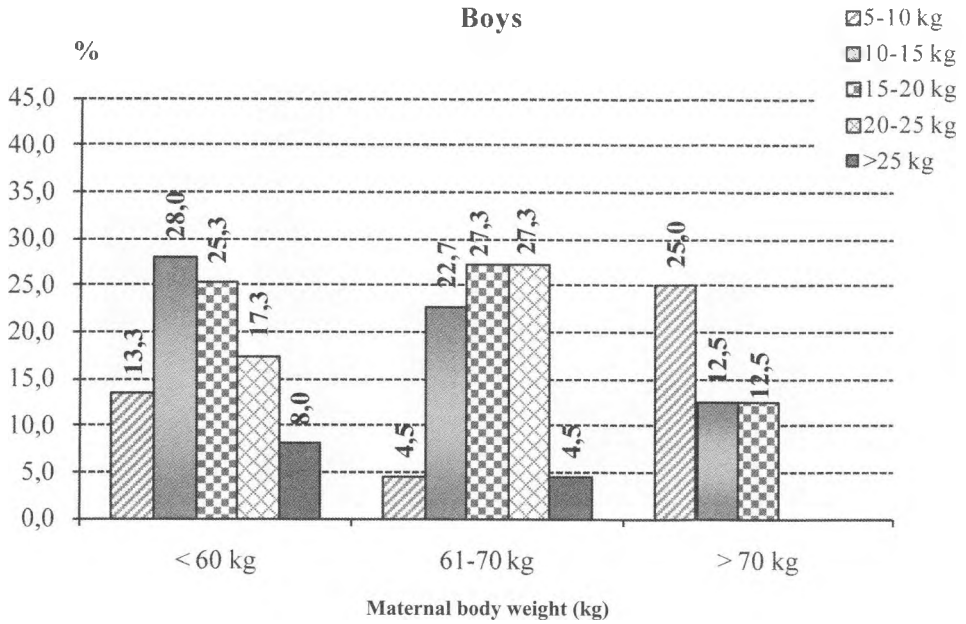


Fig. 2. The distribution of pregnancy weight gain, in three groups, according to the maternal body weight

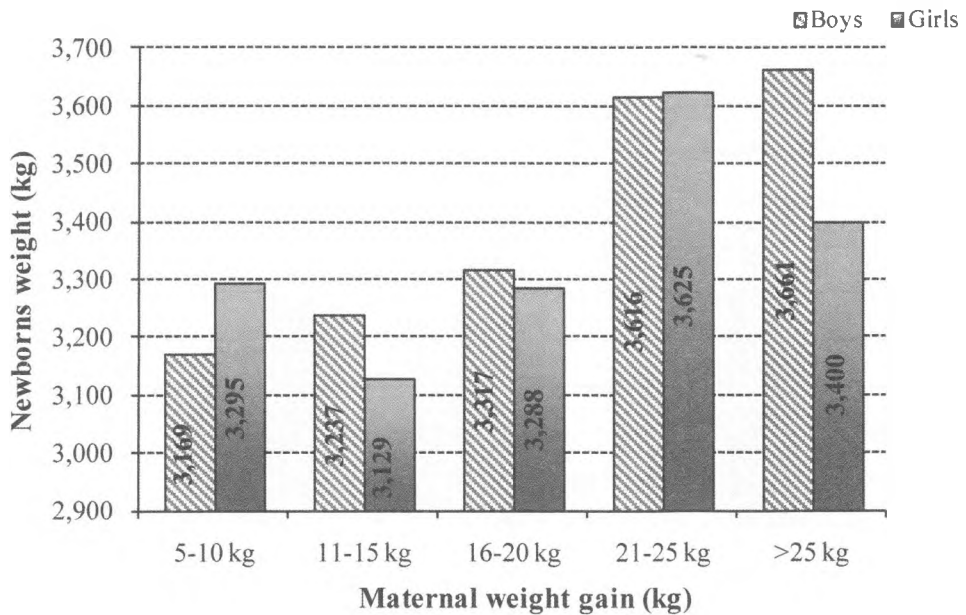


Fig. 3. The newborns birth weight, according to the maternal weight gain during pregnancy

20.0 kg a manifest increase of body sizes is observed in both genders. In girls the three features make exception: stature, upper extremities length and lower extremities length. Its values are around and below the means for the group.

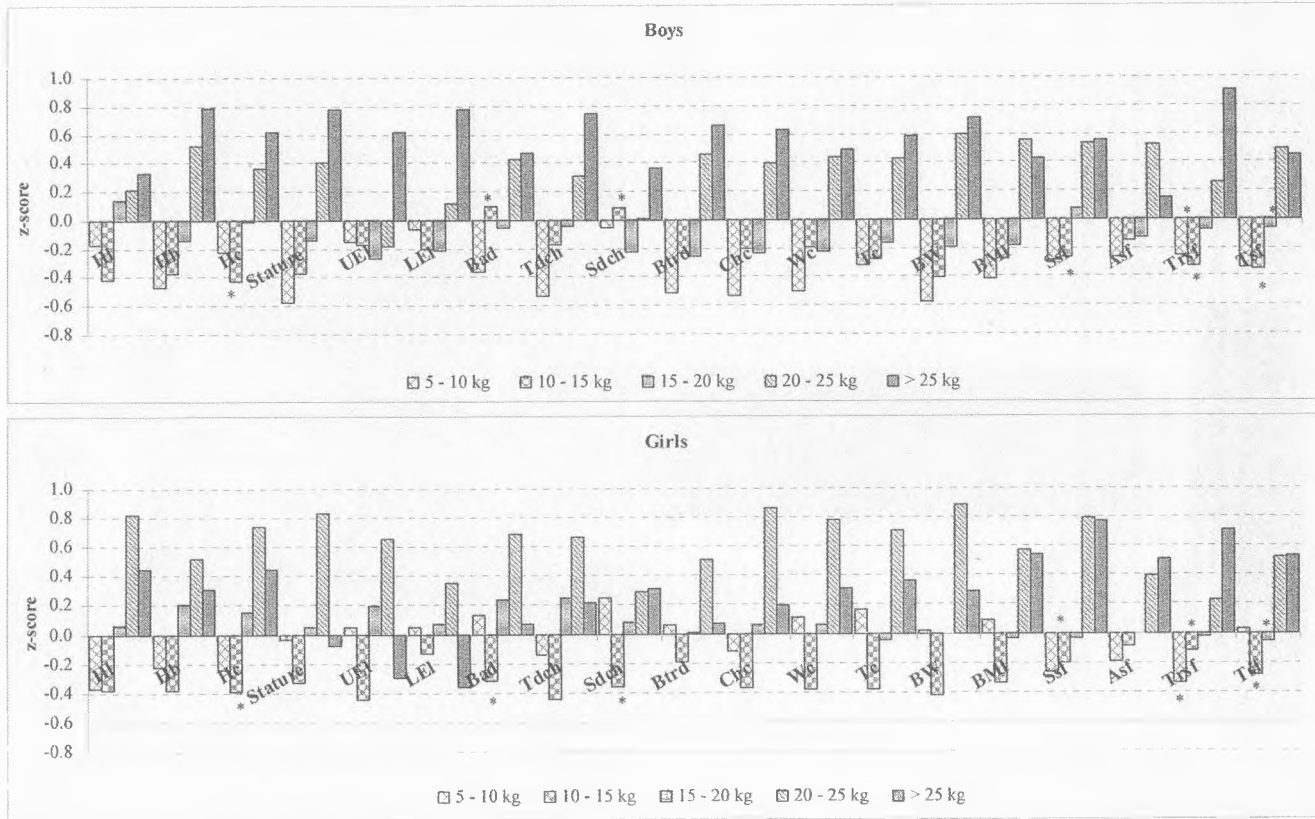
Boys born by mothers who gain weight during pregnancy from 5.0 to 20.0 kg have values for most anthropometrical features below or close to means.

Girls born by mothers increasing their weight up to 15.0 kg during pregnancy have the smallest body dimensions and those whose mothers gain weight from 16.0 to 20.0 kg have values of studied anthropometrical features close to means.

Conclusions

We can conclude that the maternal prepregnancy body weight and weight gain during pregnancy significantly influence the anthropometrical characteristics of newborns.

- Mothers with higher body weight gain less during pregnancy.
- Mothers who gain weight during pregnancy more than 20.0 kg give birth to heavy babies.
 - There exists a positive dependence between the weight gain of the mothers and the body sizes of their babies:
 - Infants born by mothers who gain during pregnancy more than 20.0 kg have values of the anthropometrical features above the means.
 - Infants born by mothers who gain less than 20.0 kg have values of the anthropometrical features around and below the means.



Hl-head length, Hb-head breadth, Hc-head circumference, UEl-upper extr. length, LEl-lower extr. length, Bad-biacromial diameter, Tdch-transversal diameter of chest, Sdch-sagital diameter of chest, Btrd-bitrohanterial diameter, Cxc-chest circumference, We-waist circumference, Tc-high circumference, BW-body weight, BMI-body mass index, Ssf-subscapular skinfold, Asf-abdominal skinfold, Trsf-triceps skinfold, Tsf-thigh skinfold

Fig. 4. Anthropometrical characterization of the newborn infants, according to the maternal weight gain during pregnancy

References

1. A b r a m s, B. Weight gain and energy intake during pregnancy. – *Clinical Obstetrics and Gynecology*, **37**, 1994, 515-527.
2. A b r a m s, B., L a r o s, R. Pregnancy weight, weight gain, and birth weight. – *American Journal of Obstetrics and Gynecology*, **154** (3), 1986, 503-509.
3. A b r a m s, B., A l t m a n, S., P i c k e t, K. Pregnancy weight gain: still controversial. – *American Journal of Clinical Nutrition*, **71** (suppl), 2000, 1233-1241.
4. A n d e r s o n, G., B l i n d e r, I., M c C l e m o n t, S., S i n c l a i r, J. Determinants of size at birth in Canadian population. – *American Journal of Obstetrics and Gynecology*, **150**, 1984, 236-244.
5. K a l i s z e w s k a - D r o z d o w s k a, M. Influence of mother's age and child's birth order on birth body mass. – *Variability and Evolution*, **5**, 1996, 43-48.
6. K i r c h e n g a s t, S., B. H a r t m a n n. Maternal prepregnancy weight status and pregnancy weight gain as major determinants for newborn weight and size. – *Annals of Human Biology*, Vol. **25**, No 1, 1998, 17-28.
7. M a r t i n, R., K. S a l l e r. *Lehrbuch der Anthropologie in systematischer Darstellung*. – Bd. I. Stuttgart, Gustav Fischer Verlag, 1957, 322-324.

Body Fat Distribution in Bulgarian Children and Adolescents Estimated by the Conicity Index

Y. Zhecheva, I. Yankova

*Institute of Experimental Morphology, Pathology and Anthropology with Museum,
Bulgarian Academy of Sciences*

The aim of our study is to present data for Conicity Index (CI) in newborns, children and adolescents aged 3 to 17 years, and to assess its relation with other anthropometric indexes of body fatness and body fat distribution.

For newborns the values of CI are higher in girls but sexual differences are not statistically significant. However in all investigated age groups from 3 to 17 years boys have higher values of CI, which is indicative of a more central distribution of body fat. Sexual differences in all age groups are well defined and statistically significant ($P < 0.05$), marking the sex specificity of the feature. The correlation between CI and both body weight and BMI is slightly expressed. The positive correlation with the indicators of body fat distribution – waist circumference and trunk-to-extremities skinfold ratio shows that CI is a good measure of central fat distribution during the growth period.

Key words: body fat distribution, conicity index, children.

Introduction

Over the last few years, many epidemiological studies show that the risk of developing various metabolic complications (hypertension, hyperlipidemia, coronary heart disease, type 2 diabetes) depends not so much on the amount of body fat, but being mostly associated with the distribution of fats in the body. Individuals with high central fatness – i.e. these in which the accumulation of excess adipose tissue is concentrated in the abdominal area are at an increased health risk [1, 5, 6].

There are many anthropological approaches for determining body fat distribution and one of them determines it through the Conicity Index (CI). CI evaluates waist circumference in relation to body height and weight, quantifying the deviation from the circumference of an imaginary cylindrical shape modelled from the height and weight of the individual [2, 7]. Theoretically its values vary between 1.0 (perfect cylinder) and 1.73 (perfect double cone) and the higher index values are associated with more central fat distribution [8].

It is well established that most disturbances related with high central fatness have their onset during early childhood [3, 4] and in this sense the results of such studies in children and adolescents are extremely important for pediatric practice. Data of body distribution for Bulgarian children are less available in the literature, which led us to the choice of paper's topic.

The aim of our study is to present data for CI in children and adolescents and to assess its relation with other anthropometric indexes of body fatness and body fat distribution.

Material and Methods

Object of the study are 219 newborns (investigated through 2001), 640 preschool children – 3-6 years of age (investigated through 2004-2005) and 2291 children and adolescents between 7 and 17 years of age (investigated through 1993-2002), or totally of 3150 boys and girls relatively evenly distributed into 16 age groups for both sexes separately. The actual number of the groups is shown on Table 1.

Table 1. Investigated contingent

Age	n ♂	n ♀	Total ♂ and ♀
0	110	109	219
3	80	80	160
4	80	80	160
5	80	80	160
6	80	80	160
7	110	110	220
8	100	101	201
9	100	101	201
10	100	98	198
11	99	100	199
12	97	100	197
13	101	99	200
14	99	101	200
15	100	100	200
16	119	120	239
17	118	118	236
Total	1573	1577	3150

Anthropometry

Height is measured to the nearest millimeter with anthropometer and weight is measured with scales to the nearest 0.1 kg. Body mass index (BMI; in kg/m²) is calculated.

The thickness of 8 skinfolds – 4 on the trunk (subscapular, X-th rib, suprailiac, abdominal skinfolds) and 4 on the extremities (triceps, biceps, thigh and calf skinfolds)

are measured triplicate on the right side of the body with Holtain skinfold caliper to the nearest 0.2 mm. The trunk-to-extremity skinfold ratio is calculated.

Waist circumference is measured in duplicate with an anthropometric tape at the minimum circumference between the iliac crest and the rib cage.

The conicity index is calculated as follows:

Conicity index = waist circumference / (0.109 × square root of weight/height) where waist circumference and height are measured in meters and weight is measured in kg.

Statistical analyses

Mathematical and statistical data processing are performed with Statistical Package for Social Science – SPSS 13.0, using the following analyses:

Descriptive statistics – mean (\bar{x}), standard deviation (SD) and the minimum (min) and maximum (max) values are calculated.

One-way ANOVA – to establish statistically significant age differences. The analysis is applied separately for both sexes.

Student's *t*-test – to establish statistically significant sexual differences ($P < 0.05$).

Correlation analysis – to determine the linear relationship between the CI and other anthropometric indexes using the Pearson's correlation coefficient ($P < 0.05$ and $P < 0.01$).

Results

Mean values about CI by sex and age in newborns and in children and adolescents aged 3 to 17 years are presented in Fig. 1.

For newborns the values of CI are higher in girls but the sexual differences are not statistically significant. However in all investigated age groups from 3 to 17 years, the boys have significantly higher values of CI than girls, which is indicative of a more central distribution of adiposity. Other words boys establish a preferential accumulation of body fat in and around the abdominal area (Table 2).

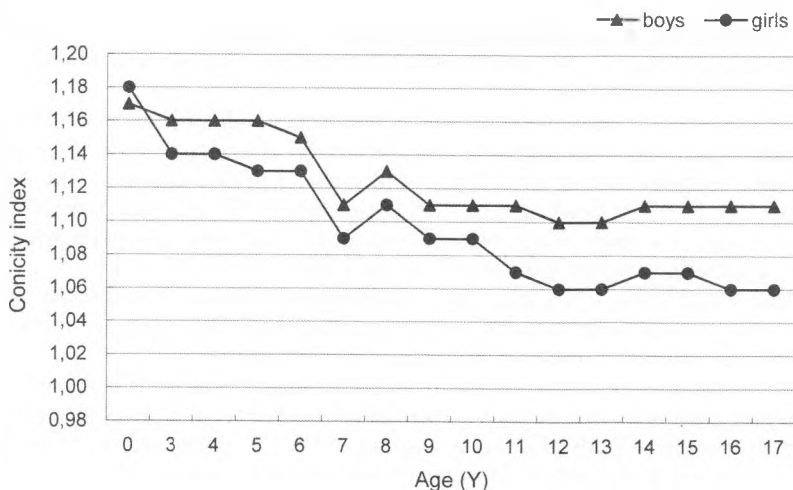


Fig. 1. Mean values of CI in boys and girls

Table 2. Biostatistical data about CI by age and sex

Age (Y)	Boys					Girls				
	n	mean	SD	min	max	n	mean	SD	min	max
0	110	1.17	0.03	1.10	1.25	109	1.18	0.04	1.10	1.29
3	80	1.16	0.03	1.11	1.28	80	1.14	0.04	1.07	1.26
4	80	1.16	0.03	1.07	1.27	80	1.14	0.03	1.07	1.23
5	80	1.16	0.05	1.07	1.39	80	1.13	0.03	1.06	1.28
6	80	1.15	0.04	1.09	1.32	80	1.13	0.04	1.05	1.30
7	110	1.11	0.04	1.03	1.24	110	1.09	0.05	0.96	1.25
8	100	1.13	0.05	0.99	1.28	101	1.11	0.05	1.00	1.25
9	100	1.11	0.05	0.99	1.22	101	1.09	0.05	0.98	1.22
10	100	1.11	0.05	1.02	1.27	98	1.09	0.05	0.94	1.22
11	99	1.11	0.05	0.94	1.24	100	1.07	0.05	0.97	1.22
12	97	1.10	0.04	1.00	1.22	100	1.06	0.04	0.95	1.15
13	101	1.10	0.05	0.92	1.30	99	1.06	0.05	0.96	1.18
14	99	1.11	0.04	0.99	1.22	101	1.07	0.04	0.98	1.20
15	100	1.11	0.05	1.01	1.30	100	1.07	0.04	0.97	1.20
16	119	1.11	0.05	1.00	1.26	120	1.06	0.04	0.96	1.18
17	118	1.11	0.04	1.02	1.21	118	1.06	0.04	0.96	1.18

The differences between boys and girls in the separate age groups are very well defined and statistically significant ($P < 0.05$), marking the sex specificity of the feature. (Fig. 1) Our results illustrate also the dependence of sexual differences on age. They are considerably more pronounced after 10 years of age, an expected result being due to the transformation of childish body type into those of a grown up individual with characteristic differences in male (*android*, or apple-shaped) and female (*gynoid*, or pear-shaped) body type (Fig. 2).

The values of CI decrease with age in both sexes, which is associated with a reduction in trunk fats and waist shaping. The reduction is greater in girls – CI value is 1.18 at birth and reaches 1.06 in the 17 year old girls (0.12 decrement). The index in boys decreases from 1.17 in newborns to 1.10 at the age of 17 (0.07 decrement). This reduction continues till 9 years of age in boys and till 11 years for girls, after which the index remains relatively constant till the end of the studied period (Fig. 1).

Table 3 and Table 4 illustrate the relationship between CI and some generally accepted indicators of body fatness and body fat distribution: body weight, BMI, waist circumference and the trunk-to-extremities skinfold ratio.

The correlation between CI and both body weight and BMI is slightly expressed, in some age groups even a negative correlation is observed. This is probably related to the normal growth of body and waist shaping. Positive significant correlation, higher in boys, is observed at the end of the investigated period – between 15 and 17 years when the body and its parts increase in smaller rate and weight gain is already associated with the massiveness of the body. However, our results show very well expressed relation-

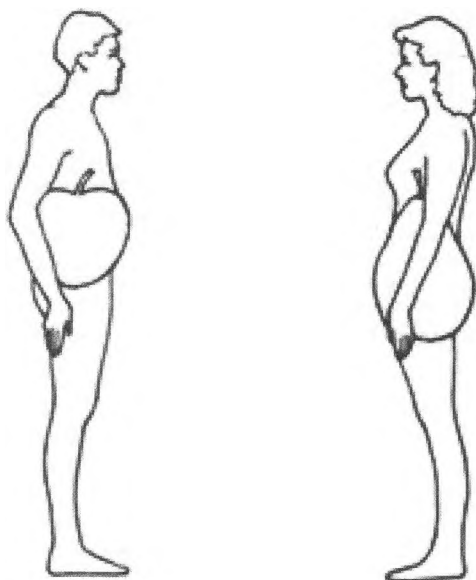


Fig. 2. Android (apple) and gynoid (pear) fat deposition patterns in men and women

Table 3. Correlation between CI and body weight, BMI, waist circumference and trunk-to-extremities skinfold ratio by age groups in boys

Age (Y)	Body weight	BMI	Trunk-to-extremities skinfold ratio	Waist circumference
0	-0.17	-0.23*	-	0.41**
3	-0.11	0.03	0.11	0.42**
4	0.22	0.16	0.18	0.54**
5	0.48**	0.47**	0.54**	0.77**
6	0.28*	0.37**	0.29**	0.62**
7	0.13	0.05	0.26**	0.54**
8	-0.06	-0.03	0.14	0.49**
9	0.00	-0.01	0.39**	0.45**
10	0.20*	0.24*	0.42**	0.55**
11	0.31**	0.42**	0.53**	0.70**
12	0.17	0.21*	0.35**	0.57**
13	0.09	0.21*	0.34**	0.56**
14	0.18	0.28*	0.42**	0.55**
15	0.38**	0.36**	0.22*	0.68**
16	0.35**	0.32**	0.28**	0.66**
17	0.33**	0.39**	0.21*	0.63**

* $P < 0.05$

** $P < 0.01$

Table 4. Correlation between CI and body weight, BMI, waist circumference and trunk-to-extremities skinfold ratio by age groups in girls

Age (Y)	Body weight	BMI	Trunk-to-extremities skinfold ratio	Waist circumference
0	-0.22*	-0.32**	-	0.38**
3	0.15	0.24*	0.47**	0.69**
4	-0.23*	-0.19	0.38**	0.27*
5	0.02	0.17	0.15	0.53**
6	0.34	0.49**	0.56**	0.71**
7	0.21	0.09	0.24*	0.62**
8	-0.04*	-0.02	0.36**	0.52**
9	0.03	0.03	0.27**	0.43**
10	0.21*	0.23*	0.50**	0.59**
11	0.25*	0.29**	0.47**	0.59**
12	0.12	0.19	0.59**	0.50**
13	0.08	0.13	0.32**	0.43**
14	0.03	0.07	0.42**	0.50**
15	0.24*	0.27**	0.38**	0.63**
16	0.27**	0.24**	0.45**	0.61**
17	0.21*	0.21*	0.42**	0.60**

* $P < 0.05$

** $P < 0.01$

ship between CI and the indicators of body fat distribution (waist circumference and trunk-to-extremities skinfold ratio) indicating that CI is a good measure of the central fat distribution in children and adolescents.

Conclusions

1. Our results confirmed the dependence of body fat distribution on sex and age.
2. The preferential accumulation of body fat on the trunk, typical for adult men, begins early in life (established even in 3-year-old boys).
3. The CI adequately reflects the changes in body shape during childhood and adolescence. Its positive correlation with other indicators of body fat distribution, especially with waist circumference shows the ability of this index to assess the central fatness during growth period.

References

1. American College of Sports Medicine. ACSM's guidelines for exercise testing and prescription. 7th ed. Philadelphia, Lippincott Williams and Wilkins, 2006.
2. Bose, K., C. G. N. Mascie-Taylor. Conicity index and waist-hip ratio and their relationship with total cholesterol and blood pressure in middle-aged European and migrant Pakistani men. – Annals of human biology, **25**, 1998, 11-16.

3. Daniels, S. R., J. A. Morrison, D. L. Sprecher, P. Khoury, T. R. Kimball. Association of body fat distribution and cardiovascular risk factors in children and adolescents. – *Circulation*, **99**, 1999, 541–545.
4. Gillum, R. F., Distribution of waist-to-hip ratio, other indices of body fat distribution and obesity and associations with HDL cholesterol in children and young adults ages 4-19 years: The Third National and Nutrition Examination Survey. – *Int J Obes Relat Metab Disord*, **23**, 1999, 556-563.
5. Pinto-Sietsma, S. J., G. Navis, W. M. Janssen, D. de Zeeuw, R. O. Gans, P. E. de Jong. A central body fat distribution is related to renal function impairment, even in lean subjects. – *Am J Kidney Dis*, **41**, 2003, 733-741.
6. Sönnichsen, A. C., W. O. Richter, P. Schwandt. Body fat distribution and serum lipoproteins in relation to age and body weight. – *Clinica Chimica Acta*, **202**, 1991, 133-140.
7. Taylor, R., I. Jones, Sh. Williams, A. Goulding. Evaluation of waist circumference, waist-to-hip ratio, and the conicity index as screening tool for high trunk fat mass, as measured by dual-energy X-ray absorptiometry, in children aged 3-19 y. – *Am J Clin Nutr*, **72**, 2000, 490-495.
8. Valdez, R. A simple model-based index of abdominal adiposity. – *J Clin Epidemiol*, **44**, 1991, 955-956.

Discrimination Effect of the Biomarkers Minor Physical Anomalies Between Schizophrenic Patients and Mentally Healthy Subjects

F. Ahmed-Popova¹, M. Mantarkov², S. Sivkov¹, V. Akabaliev²

¹ Department of Anatomy, Histology and Embryology, Medical University – Plovdiv

² Department of Psychiatry and Medical Psychology, Medical University – Plovdiv

The aim of the study is to analyze the predictive value of minor physical anomalies in the binominal model schizophrenic patients-mentally healthy subjects as an index of neurodevelopmental etiology of schizophrenia.

128 schizophrenic patients (66 men, 62 women) and 103 normal controls (49 men, 54 women) are examined with modified Waldrop Physical Anomaly Scale. Predictive value of minor physical anomalies is analyzed with discriminant analysis.

The two-group discriminant analysis distinguishes well between schizophrenic patients and control subjects with 8 independent predictor variables. The variables that contribute to prediction of schizophrenic patient-control subject include high/steepled palate, fine electric hair, third toe³ second, big gap between I and II toes, epicanthus, abnormal head circumference, hypertelorism, abnormal hair whorls, malformed ears have significant independent contribution to prediction of patient-control status. The model classifies correctly the two groups in 79.57% of the cases and slightly better the controls than the schizophrenics (85.4% vs. 74.8%).

The data of the study show discernible prevalence of morphological anomalies in large cohort of schizophrenic patients in comparison with control subjects. The studies of minor physical anomalies in schizophrenic patients allude to a disturbed neurodevelopment and increased predisposition to development of schizophrenia that could be used for stratification of the risk in future prevention attempts.

Key words: schizophrenia, neurodevelopmental hypothesis, minor physical anomalies, Waldrop scale.

Introduction

Validity of psychiatric disorders as a whole and schizophrenia in particular is determined to some extent by detection of discernible biomarkers. Biomarkers are measurable indicators of underlying disease process (Buchsbaum, M.S., R.J. Haier, 1983), which appear predominantly in psychotic individuals, show greater incidence in their family members and predict development of psychotic disorders in children with high

genetic risk. Biomarkers should be irreversible and allow non-invasive and reliable measurement (Garver, D.L., 1987). Plausible biomarkers at advanced stage of validation in schizophrenia include neurocognitive deficits, characteristic alterations in some evoked potentials, disorders in the smooth eye tracking, increased frequency in smooth (non-localizing) neurological signs and neuroimaging findings of brain structural abnormalities (Szymanski S, J.M. Kane, J.A. Lieberman, 1991; Ivleva, E.I. et al., 2009).

The presence of the biomarkers mentioned at the disease onset or even earlier appears a major argument in favour of the neurodevelopmental hypothesis put forward in the schizophrenia etiology (Weinberger, D.R., 1987; Murray, R., 1994). In its contemporary formulation the neurodevelopmental hypothesis share three assumptions: 1) the primary pathogenetic defect is an early derangement of the central nervous system development that occurs in the early prenatal period; 2) the period of action is relatively short, i.e., it is essentially static; and 3) the consequences of this static process remain relatively latent until long after the primary effect (Woods, B., 1998). Symptoms, typical of the disease, might occur some decades later, perhaps after functional maturation of the nervous system, i.e., in the process of neuronal pruning in adolescence that might occur excessively or improperly (Feinberg, I., 1982/1983; McGlashan, T.H., R.E. Hoffman, 2000).

The concept that early brain disruptions predispose to schizophrenia development is supported by the findings that some schizophrenic patients present morphological evidence of slight developmental abnormalities with probably prenatal origins (Petronius, A., 2004). Minor physical anomalies (MPAs) are slight dysmorphic features mainly in the craniofacial region and limbs that normally have no functional or cosmetic significance (Buckley, P.F., 1998; Weinberg, S.M., E.A. Jenkins, M.L. Marazita, B.S. Maher, 2007), but deserve interest as markers of prenatal maldevelopment. The anomalies appear of particular importance when they are found in ectodermal derivatives or in structures on which aberrant brain morphology can be projected. Regarding the ectodermal origin of the brain, presence of excess of such anomalies may be related to CNS maldevelopment (Waldrop, M.F., F.A. Pedersen, R.Q. Bell, 1968; Steg, J.P., J.L. Papoport, 1975). As the anomalies indicate adverse events during critical periods of the prenatal development, usually the first or early second trimester, MPAs may contribute to understanding the nature and time of occurrence of certain disruptions (Persaud, T., 1979).

The aim of the present study is to analyze the predictive value of MPAs in the binominal model schizophrenic patients-mentally healthy subjects as an index of neurodevelopmental etiology of schizophrenia.

Material and Methods

Subjects

The subjects for this study were 128 schizophrenic inpatients (66 men, 62 women) consecutively admitted in the Clinic of psychiatry in Plovdiv. Their mean age was 32.09 (SD=9.73) years, mean duration of illness 8.02 (SD =7.33), mean number of hospitalizations 4.98 (SD= 5.36). The patients satisfied DSM-IV criteria for a diagnosis of schizophrenia (American Psychiatric Association, 1994) on the basis of case records review, semistructured interview (by V.A. the study psychiatrist) based on a checklist of items from DSM-IV and information obtained from relatives in order to enhance the validity of the diagnosis. Potential subjects were excluded if they had a history of drug or alcohol abuse, identifiable neurological disorder (seizure disorder, head injury, multiple sclerosis etc.), any signs of mental retardation or somatic disorder with neurological components.

The normal comparison group comprised 103 mentally healthy subjects (49 men, 54 women) with a mean age 39.65 (SD=10.68) years and socio-economic background comparable to that of the patients. Normality was defined as the absence of a major axis I or axis II disorder according to DSM-IV (American Psychiatric Association, 1994). They satisfied exclusion criteria similar to those applied to the patients. In addition, to better separate the control from the schizophrenic group, potential normal controls were excluded if they had a first-degree relative with a history of a psychotic disorder, major affective disorder or suicide.

To avoid eventual confound due to the lack of ethnic and racial references of MPA both the patients and normal controls were of Bulgarian origin; individuals with parental or grandparental ethnicity other than Bulgarian were also excluded.

The study was approved by the local Ethics Committee and all subjects gave written informed consent to participate.

Assessment of Minor Physical Anomalies

The subjects were examined with a slightly modified Waldrop Physical Anomaly Scale (Waldrop et al., 1968). It includes 19 morphological abnormalities (Table 2) from six body regions: head, eyes, ears, mouth, hands, and feet. Most of the abnormalities are scored qualitatively as present (1) or absent (0). The variables fine electric hair, head circumference, epicanthus, intercanthal distance, low seated ears, high/steepled palate and third toe ³ second are scored in a graded manner – 1 or 2, according to severity.

All examinations were performed by the same examiner (S.S., the study anatomist). Reliability studies were conducted using a second assessor (Z.L.), who was not otherwise involved in the study. Cohen's *k* for concordance between categorical/ordinal scores were all >0.75 and intra-class correlation coefficients for continuous measures – > 0.78. Acceptable level of reliability was not reached for curved 5th finger (*k* < 0.60).

Statistical Analysis

To assess the predictive value of MPA in schizophrenia a two-group discriminant analysis was performed. The analysis allows discrimination between groups on the base of several predictor variables. The correlations between the variables are controlled and the variables analyzed in group. In our model the predictor variables are the 19 MPAs from the Waldrop Scale.

The data were analyzed with SPSS 14.0. Statistical significance was defined as $p < .05$, two-tailed.

Results

The two-group discriminant analysis distinguishes well between schizophrenic patients and control subjects with 8 independent (predictor) biomarkers, classifying correctly 79.57% of the cases (Fig. 1).

Among the biomarkers entered into the equation (Fig. 1), high/steepled palate, fine electric hair, third toe ³ second, big gap between I and II toes, epicanthus, abnormal head circumference, hypertelorism, abnormal hair whorls, malformed ears have significant independent contribution to prediction of patient-control status.

The model classifies correctly the two groups and slightly better the controls than the schizophrenics (85.4% vs. 74.8 (Fig. 2).

Predictor biomarkers	Wilks' lambda		% Correctly classified by step
	F	p	
Entering the model			
1. High/steepled palate	56.1515	.000	68.40%
2. Fine hair	38.0653	.000	72.73%
3. Gap between I and II toe	30.0457	.000	76.62%
4. Epicanthus	25.4624	.000	78.35%
5. Head circumference	22.1005	.000	76.96%
6. Hyper(hypo)telorism	20.2454	.000	77.39%
7. Hair whorls ≥ 2	18.8440	.000	76.52%
8. Malformed ears	17.6057	.000	79.57%

Fig. 1. Two-group discriminant analysis between schizophrenic patients and control subjects with independent variables – biomarkers MPAs

Actual group	Cases	Predicted group affiliation	
		Controls	Schizophrenia
Controls	103	88 85.4%	15 14.6%
Schizophrenia	127	32 25.2%	95 74.8%
Totally		79.57%	

Fig. 2. Classification results

Discussion

The data of the study show discernible prevalence of morphological anomalies in large cohort of schizophrenic patients in comparison with control subjects. The results comply with the data published in a number of other publications (Petronis, A., 2004; Buckley, P.F., 1998; Weinberg, S.M., E.A. Jenkins, M.L. Marazita, B.S. Maher, 2007). In the present study an attempt to deal with the methodological shortcomings of previous studies is made. Main advantages appear the precise clinical evaluation using clear morphological characteristics, reliable statistical methods and adequate power compared with previous studies.

Despite the general tendency to craniofacial localization of MPA, the analysis does not support the hypothesis of craniofacial model of MPA regional distribution. Discriminant analysis determines a set of biomarkers that distinguish sufficiently enough the schizophrenic patients from the control subjects. The independent variables with significant contribution to prediction of the status schizophrenic patient-control subject are high/steepled palate, fine electric hair, third toe – second, big gap between I and II toes, epicanthus, abnormal head circumference, hypertelorism, abnormal hair whorls,

malformed ears. As the discriminant analysis creates one possible biomarker profile, it could be accepted that as a whole the results of the study suggest more frequent but not unique localization of the biomarkers MPAs in the head and face region.

The pattern of changes in the morphological characteristics in our study is not unidirectional. So, the changes in the intercanthal distance can present with both increased and decreased values. That suggests that the changes can be a casual outcome of general neurodevelopmental defect or define different neurodevelopmental defects, which in turn allow better characterisation of the subgroups of schizophrenic patients.

The studies of MPA biomarkers in schizophrenic patients allude to a disturbed neurodevelopment and increased predisposition to development of schizophrenia. They offer a suitable way to throw a bridge across the time (to the pre- and perinatal period), in search of the effect of presumptive disontogenic events. The potential diagnostic value of each of these biomarkers for evaluation of diathesis-stress conditions is limited in terms of time and character of the neurodevelopmental processes as well as degree of disease susceptibility when applied alone. These should be used in combination to create a diagnostic profile, which defines specific psychiatric syndromes with greater accuracy on the diagnosis than just the clinical standards.

Although MPAs are not specific for schizophrenia, they suggest a risk of development of that disease in presence of neurodevelopmental abnormalities. Some anomalies, nasal volumes, palate anomalies or craniofacial dysmorphology in particular, could be informative in further evaluation of the specific pathogenesis of schizophrenia. Depending on the possibilities of high-tech microarray technologies and recent data of investigations on spontaneous mutations, MPAs could prove to be useful in identification of etiological subtypes or loci of genetic anomalies in schizophrenia. It has to be elucidated whether MPAs, being fixed markers throughout childhood and adolescence, far preceding the prodromes and psychosis onset, could be used for stratification of risk in future prevention attempts.

References

1. Buchsbaum, M. S., R. J. Haier, 1983. Psychopathology: Biological approaches. – Annual Review of Physiology, **34**,401-430.
2. Buckley, P. F., 1998. The clinical stigmata of aberrant neurodevelopment in schizophrenia. – J. NervMentDis., **186**, 79-86.
3. Feinberg, I., 1982/1983. Schizophrenia: caused by a fault in programmed synaptic elimination during adolescence? – J. Psychiatr. Res., **17**, 319-334.
4. Garver, D. L., 1987. Methodological issues facing the interpretation of high-risk studies: Biological heterogeneity. – Schizophrenia Bulletin, **13**, 525-529.
5. Ivleva, E. I. et al., 2009. Genetics and intermediate phenotypes on the schizophrenia-bipolar disorder boundary. – Neurosci. Biobehav. Rev. (2009), doi 10.1016/j.neubiorev., **11**.022.
6. McGlashan, T. H., R. E. Hoffman, 2000. Schizophrenia as a disorder of developmentally reduced synaptic connectivity. – Arch. Gen. Psychiatry, **57**, 637-48.
7. Murray, R., 1994. Neurodevelopmental schizophrenia: The rediscovery of dementia praecox. – British Journal of Psychiatry, (165Suppl. 25) 6-12.
8. Persaud, T., 1979. Teratogenesis: Experimental Aspects and Clinical Implications. VEB Gustav Verlag; Jena, Germany.
9. Petronis, A., 2004. Schizophrenia, neurodevelopment, and epigenetics. – In: M.S. Keshavan, J.L. Kennedy, R.M. Murray (Eds.) Neurodevelopment and Schizophrenia. Cambridge University Press, Cambridge, 174-190.
10. Steg, J. P., J. L. Papoport, 1975. Minor physical anomalies in normal, neurotic, learning disabled, and severely disturbed children. – J. Autism Childhood Schizophr., **5**, 299-307.
11. Szymanski, S, J. M. Kane, J. A. Lieberman. A Selective review of biological markers in schizophrenia. – Schizophrenia Bull. **17**(1), 1991, p. 99.

12. Waldrop, M.F., F.A. Pedersen, R.Q. Bell, 1968. Minor physical anomalies and behavior in pre-school children. – *Child Dev.*, **39**, 391-400.
13. Weinberg, S. M., E. A. Jenkins, M.L. Marazita, B. S. Maher, 2007. Minor physical anomalies in schizophrenia: a meta-analysis. – *Schizophr. Res.*, **89**, 72-85.
14. Weinberger, D.R., 1987. Implications of normal brain development for pathogenesis of schizophrenia. – *Arch. Gen. Psychiatry*, **44**, 660-669.
15. Woods, B., 1998. Is schizophrenia a progressive neurodevelopmental disorder? Toward a unitary pathogenetic mechanism. – *American Journal of Psychiatry*, **155**, 1661-1670.

Anthropological Characterization and Correlations of Mandibular Branch

N. Atanassova-Timeva, A. Katsarov

*Institute of Experimental Morphology, Pathology and Anthropology with Museum,
Bulgarian Academy of Sciences, Sofia*

The issue of symmetry in the development of the facial skeleton and particularly of mandibular bone and its branch is extremely important. The aim of the present work is to make a detailed anthropological characteristics of the mandibular branch, to trace the manifestations of asymmetry and to establish correlations between features of the branch, as well as, between the main profile angles of the facial skull region and the main measurements of the mandible and its branch. In this investigation are used 120 dry mandibles of Bulgarian adult men who were participants in the wars at the beginning of the 20th century. The bilateral differences are greatest in width measurements of the branch. Correlations are positive between angular facial dimensions on the one hand and between linear features of the mandibular bone on the other hand, and the relationships are negative between facial angles and length dimensions of the mandible.

Key words: mandible bone, mandibular branch, anthropological characterization, correlations.

Globally, the study of human population history often focuses on the anatomy of the mandibular bone, because it is influenced by many external factors (geographical, adaptation, etc.) [3, 5, 6, 8, 9]. Therefore, in anthropology the mandibular features are used for comparison and differentiation between bone remains belonging to individuals of both sexes and different population groups [1, 2, 7, 11].

The lower jaw is the only mobile-joined bone in the skull. For that reason the morphological features of the mandibular branch (where masticatory muscles are attached), and articular processes (involved in the formation of temporomandibular joint) are very important for the development of a number of secondary changes. The issue of symmetry in the development of the facial skeleton and particularly of mandibular bone and its branch is extremely important [14].

For these reasons, we set about to make a detailed anthropological characteristics of the mandibular branch, to trace the manifestations of asymmetry and to establish correlations between features of the branch, as well as between the main profile angles of the facial skull region and the main measurements of the mandible and its branch.

Material and Methods

The presented data are result from metrical investigation of 120 dry mandibular bones (from the Ossuary at the National Museum of Military History, Sofia). The investigated material belongs to Bulgarian adult men, participants in the Wars at the beginning of the 20th Century. Measurements were conducted using the methods of Martin-Saller [4], Madzarov [16] and Polichronov [17]. In the present work are interpreted the data for 19 linear signs (7 unilateral and 12 bilateral), 5 angular and 2 scopical features.

The data are statistically processed by variation and correlation analysis. Correlations are calculated by the coefficient of Pearson. The strength of correlation was assessed by empirical rules of Kalinov [15]:

Table 1. Correlation degrees (by Kalinov, 2001)

Calculated value of r	Interpretation of correlation
0.00 to 0.30 (-0.30 to 0.00)	Very low positive (negative)
0.31 to 0.50 (-0.50 to -0.31)	Low positive (negative)
0.51 to 0.70 (-0.70 to -0.51)	Moderate positive (negative)
0.71 to 0.90 (-0.90 to -0.71)	High positive (negative)
0.91 to 1.00 (-1.00 to -0.91)	Very high positive (negative)

The valuation of bilateral asymmetry is made by the absolute metrical differences and their relative share, as well as by their standardization according to the Index of Relative Group Differences (IRGD) of Wolański [12], in this case to determine the bilateral differences and called index of bilateral differences (IBD). Its values represent differences in Relative Index Units (IU).

$$IBD = 2 \times [(\bar{x}_{right} - \bar{x}_{left}) \times 100] / (\bar{x}_{right} + \bar{x}_{left}).$$

Values of IBD, which are equal to zero, show absence of asymmetry; the positive values display relative priority for right side of the bone, and the negative ones – for the left side.

The t-criterion of Student at $P \leq 0.050$ is used to determine the authenticity of the established differences.

Results and Discussion

Estimation of the values of IBD shows that differences are greatest in width measurements of the branch. These signs show the largest differences (according to literature review and data from our other studies) between individuals of both sexes, as well as, between individuals from different historical periods and from different populations [2, 7, 8, 9, 11, 13]. Bilateral differences are large for the sizes of *lingula mandibulae*, where *ligamentum sphenomandibulare* has caught, limiting the movements of the mandibular bone in a downward direction, i.e. the tension in this area of *ramus mandibulae* is very high and most likely this is the reason for high degree of bilateral asymmetry. With the lowest values of IBD is the lowest height of the branch – only 0.22 IE.

Descendant formula for the degree of bilateral differences:

Width of the branch (2,63 EI) > Distance between lingula mandibulae and the lowest point of the incisura mandibulae (2,39 IE) > Branch thickness at the level of lingula

mandibulae (2,01 IE)> *Smallest width of the branch* (1,88 EI)> Distance between *lingula mandibulae* and *angulus mandibulae* (1,64 IE)> Retromolar distance (1,50 IE)> Thickness of the condyle (0,88 IE)> Length of the *canalis mandibulae* (0,67 IE) > Width of *incisura mandibulae* (-0,54 IE)> Depth of *incisura mandibulae* (-0,47 IE)> *Width of condyle* (-0,38 IE)> *Smallest height of the branch* (0,22 IE)

It should be noted that the manifestations of asymmetry (for the majority of measurements) are in favor of the right side. This fact can be regarded as a special case of the manifestation of the overall body asymmetry. Exceptions are only three indicators: the *breadth and depth of incisura mandibulae*, and the *condyle width*, which are larger in the left branch.

Anthroposcopy characterization showed that the majority of investigated mandibles have moderate width for both branches. Very low percentages of bones have a narrow branch. Both metrical and scopical analysis found that the cases with a large width of the right branch prevail.

For the second investigated scopical feature (height of *processus coronoideus* and *processus condylaris*) there is observed similar percentage distribution for the right and left branch – most are the cases (50%) with equal height of *processus coronoideus* and *processus condylaris*, on the second place are the bones with higher *processus condylaris* (which involved in *articulatio temporomandibularis*) and the lowest is the percentage of mandibles with higher *processus coronoideus* (affords insertion to the temporal and masseter muscles).

The question of harmony and balance between the individual components of the face attracts and retains the attention of many scientists, orthodontists, plastic and maxillofacial surgeons for many years [6, 9, 10]. In this connection, we set the goal to calculate correlations between signs of *ramus mandibulae*, as well as, between the main profile angles of the facial skull region and the main dimensions of the mandible and its branch (Table 1).

The highest positive correlations are found between the *height of the branch* and *projection length from condyle*, as well as, between *facial and nasal profile angle*, and negative – between the *mandibular angle* and *projection length from condyle*.

Overall correlations are positive between angular facial dimensions on the one hand and between linear features of the mandibular bone on the other hand, and the relationships are negative between facial angles and length dimensions of the mandible. There is a negative correlation between the *height of ramus mandibulae* and the values of the *profile angle* and *mandibular angle*. Namely, when the mandibular length and height of the branch are lower, values of facial angles are higher and the front part of the skull has a flat shape. On the other hand, at lower values of the profile angles and higher length of the mandible, the degree of protrusion of the facial skull region is greater.

Detailed anthropological study of mandible allows for the assessment of development and relationships between knots, branches, body and teeth, and to assess the impact and effects of articulation and occlusion on the shape and size of the mandibular bone.

References

1. Ari, I., I. M. Kafa, Z. Basar, M. A. Kurt. The Localization and Anthropometry of Mental Foramen on Late Byzantine Mandibles. – Coll. Antropol., **29(1)**, 2005, 233-236.
2. Gungor, K., M. Sagir, I. Ozer. Evaluation of the Gonial Angle in the Anatolian Populations: From Past to Present. – Coll. Antropol., **31(2)**, 2007, 375-378.
3. Lavelle, C. L. B. A comparison between the mandibles of Romano-British and nineteenth century periods. – Am. J. Phys. Anthropol., **36**, 1972, 213-219.

4. Martin R, K. Saller. Systematische Anthropologie. In: Lehrbuch der Anthropologie in systematischer Darstellung. Stuttgart, Bd. I. Gustav Fischer Verlag, 1957, 429-500.
5. Moore W. J., C. L. B. Lavelle, T. F. Spence. Changes in the size and shape of the human mandible in Britain. – Br. Dent. J., **125**, 1968, 163-169.
6. Nicholson, E., K. Harvati. Quantitative Analysis of Human Mandibular Shape Using Three-Dimensional Geometric Morphometrics. – Am. J. Phys. Anthropol., **131**, 2006, 368-383.
7. Rai, B., S. C. Anand, R. K. Jain. Effect of Age and Sex: Antegonial and Gonial Notch of Mandible. – Int. J. Biol. Anthropol., **1(1)**, 2007, online available on: <http://www.ispub.com/ostia/index.php?xmlFilePath=journals/ijba/>.
8. Rai, R., V. A. Ranade, V. L. Prabhhu, M. M. Pai, S. Madhyastha, M. Kumaran. A pilot study of the mandibular angle and ramus in Indian populations. – Int. J. Morphol., **25(2)**, 2007, 353-356.
9. Spoor, F., M. G. Leakey, L. N. Leakey, Kaifu, Y. Changes in mandibular morphology from the Jomon to modern periods in Eastern Japan. – Am. J. Phys. Anthropol., **104**, 1997, 227-243.
10. Strajnić, L., D. Stanišić-Sinobad, D. Marković, L. Stojanović. Cephalometric indicators of the vertical dimensions of occlusion. – Coll. Antropol., **32(2)**, 2008, 535-541.
11. Vodanović, M., J. Dumančić, Ž. Demo, D. Mihelić. Determination of Sex by Discriminant Function Analysis of Mandibles From two Croatian Archeological Sites. – Acta Stomatol. Croat., **40(3)**, 2006, 263-277.
12. Wolanski, N. A symmetria ciała człowieka i jej zmienność w świetle funkcji kończyn. – Przegl. Anthropol., **23**, 1957, 461-464.
13. Yordanov, Y., M. Botschev. Zusammenhang zwischen dem retromolaren Raum und den Massen des Unterkieferknochens beim Bulgaren. – Stomatol., **28**, 1978, 263-8.
14. Зия, Д. Рентгенологично проучване върху особеностите в развитието на долночелюстните израстъци. Дис., С., МА, 1987.
15. Калинин, Кр. Статистически методи в поведенческите и социалните науки. С., НБУ, 2001, 79.
16. Маджаров, Д. Рентгенова анатомия на лицево-челюстната област. Дис., С., МА, 1981.
17. Полехронов, Н. Реконструктивни операции на челюстните кости при деформации. Дис., С., ВМИ, 1992.

Bioelectrical Impedance Analysis (BIA) of Body Composition in Children with Diabetes Mellitus Type 1

A. Baltadjiev, G. Baltadjiev

Medical University Plovdiv, Department of Anatomy, Histology and Embryology

The purpose of this study is to determine the components of active body mass, skeletal muscle mass, body water and skeletal (bone) mass of the body composition of children suffering from type 1 diabetes by the means of bioelectrical impedance analysis. 150 children with Diabetes mellitus 1 were tested, grouped by gender and in two age groups – 7-12 and 12-17 years of age. We defined the following components of body composition: active body mass /ATM/, skeletal muscle mass /SMM/, skeletal (bone) mass /SM/and body water /BW/, which were measured by Tanita apparatus. The results show that the relative (percentage) values of the main features of body composition in age comparison are higher in 12-17-year-old diabetic boys and the statistical reliability varies from the absence of such to a high level. The exception is %SM, since the values are higher in 7-12-year-olds and the statistical significance is of a high level. In diabetic girls, the percentage values are higher in the age group 7-12, with a statistical significance from absent to a high level. Intersexual comparisons of the relative values of the components show that they generally are higher in diabetic boys compared to girls in both age groups.

Key words: BIA, diabetes mellitus type 1, body composition, children.

Introduction

Diabetes mellitus is a socially significant disease with a progressively increasing number of patients [6, 9]. Diabetes mellitus type 1 is a nosology that appears in childhood and it is 1.5-2% of the total number of patients with diabetes. Its effect on body composition is in a correlation with the changes occurring with the upcoming puberty [6]. The most sensitive to changes they are in fat-free mass, also called active body mass [3, 7, 8]. Attention is drawn as well to the change in total body water [9] and changes in bone mass [4, 7, 8].

Bioelectrical impedance method is fast, mobile, noninvasive; it provides accurate data on body composition which are comparable to those obtained by other research [7].

The purpose of this study is to determine the components of active body mass, skeletal muscle mass, body water and skeletal (bone) mass of the body composition of children suffering from type 1 diabetes by bioelectrical impedance analysis.

Material and Methods

150 patients with Diabetes mellitus were tested; they are children from South Bulgaria (Central Southern region). The children were grouped into two gender groups: 75 girls and 75 boys, as well as into two age groups: 7-12- and 12-17-year-olds. The following components of body composition were examined: active body mass (ATM), skeletal muscle mass (SMM), skeletal (bone) mass (SM) and body water (BW) measured with the apparatus TANITA. For data processing we used the statistical programs SPSS and INSTAT. Comparing the average values, we calculated the coefficient t , and the statistical significance was set at four levels: high – $P \leq 0.001$, average – $P \leq 0.01$, low – $P \leq 0.05$, no significance $P > 0.05$.

Results and Discussion

The quantitative data of body composition components in children with diabetes are presented on Table 1.

1. Active body mass (ABM)

This component shows the value of lean mass (fat-free mass) in diabetic children's bodies.

The interage comparison within gender groups showed that boys with diabetes tend to have a higher percentage of that feature in the age group 12-17 years in comparison with that of the group 7-12 years, but there is lack of statistical reliability. In girls with diabetes, the relative value of the feature is much higher in the age group 7-12 years compared with that in 12-17 years, as the statistical reliability is high.

Intersexual comparison of ABM shows that the relative value of the feature for 7-12-year-olds is higher in boys compared to girls with diabetes, but the statistical significance is at the limit of standard ($P=0.05$). Comparing the age group 12-17 years shows that there is a clear predominance of the relative values of ABM in boys compared to girls and the statistical reliability is high.

2. Skeletal muscle mass (SMM)

This component of body composition shows the proportion of skeletal muscle, which is a major component of the indicator ABM.

The interage comparing of the relative values of this feature in boys with diabetes shows that the value in the age group 12-17 years is higher than that of 7-12 years, as the statistical reliability is of a high level. In diabetic girls, the relative values of SMM in both age groups are very close and there is a trend for higher value in 7-12-year-olds but without any statistical reliability.

The intersexual comparisons show that in both age groups SMM has higher relative values in diabetic boys than these of girls and the statistical reliability is of average to high level.

3. Skeletal (bone) mass (SM)

This feature defines the proportion of bones of the skeleton in body composition and it is a part of fat-free body mass.

The interage comparing of the relative values of this component in boys and girls with diabetes shows that they are higher in the 7-12-year-olds compared to those of 12-17 years and the statistical reliability is high.

Table 1. Relative values of the body composition indices of children with type 1 diabetes mellitus

Girls						Boys					
Age groups	Count	Mean	SD	SE	♂/♂	Count	Mean	SD	SE	♀/♀	♀/♂
Fat-free mass											
<12	75	79.48	6.53	1.69	-	75	81.50	5.99	2.44	-	p=0.05
>12	75	73.33	5.20	1.30	p<0.0001	75	82.49	5.05	1.46	p>0.05	p<0.0001
Skeletal muscles											
<12	75	38.04	5.20	1.34	-	75	45.23	6.91	2.82	-	p<0.0001
>12	75	36.87	3.94	0.99	p>0.05	75	49.01	4.38	1.27	p<0.0001	p<0.0001
Bone mass											
<12	75	37.17	4.34	1.12	-	75	41.20	4.20	1.72	-	p<0.0001
>12	75	34.95	5.48	1.37	P=0.0067	75	34.08	4.88	1.41	p<0.0001	p>0.05
Body water											
<12	75	58.68	5.05	1.30	-	75	59.97	4.62	1.89	-	p>0.05
>12	75	53.66	3.81	0.95	p<0.0001	75	60.39	3.69	1.06	p>0.05	p<0.0001

The intersexual comparison of the relative values of SM shows that in the age group 7-12 years they are higher in boys compared to girls and the statistical reliability is high. In the age group 12-17 years, the values are very close and there is no statistical reliability.

4. Body water (BW)

This component of body composition indicates the percentage of water in the body of diabetic patients. It is part of the lean mass of body composition. The interage comparison of water values in boys with diabetes shows that the proportion is likely to be higher in the age group 12-17 years, but there is no statistical reliability. The comparison in diabetic girls shows a higher % share of water in the age group 12-17, compared to 7-12, and the statistical reliability is high.

Intersexual comparison of the relative values of water in the age group 7-12 tends to have greater value in boys, compared to girls with diabetes, but there is no statistical reliability. The age group 12-17 years has a significantly higher value in boys than in girls and the statistical reliability is high.

Conclusion

Bioelectrical impedance analysis provides an accurate picture of the effect of type 1 diabetes on body composition in children with diabetes in the age and gender aspects.

The relative (percentage) values of the main features of body composition, in the age comparison in diabetic boys, are higher in 12-17-year-olds and the statistical reliability ranges from the absence of such to a high level. The exception is %SM, since the values are higher in 7-12-year-olds and the statistical significance is high. In diabetic girls, the percentage values are higher in the age group 7-12, where the statistical significance varies from absent to a high level.

Intersexual comparisons of the relative values of the components show that they generally are higher in boys, compared to girls with diabetes, in both age groups.

References

1. Eisenmann, J. C., K. A. Heelan, G. J. Welk. Assessing body composition among 3- to 8- year-old children: anthropometry, BIA and DXA. – *Obes. Res.*, 12, 2004, 1633-1640.
2. Gomez, J. M., F. J. Maravall, J. Soler, M. Fernandez-Castaner. Body composition assessment in type 1 diabetes mellitus patients over 15 years old. – *Horm. Metab. Res.*, 33, 2001, 670-673.
3. Hui, S. L., S. Epstein, C. C. Jr. Johnston. A prospective study of bone mass in patients with type 1 diabetes. – *J. Clin. Endocrinol. Metab.*, 60, 1985, 74-80.
4. Ingberg, C.M., S. Sarnblad, M. Palmer, E. Schvarcz, C. Berne, J. Aman. Body composition in adolescent girls with type 1 diabetes. – *Diabet. Med.*, 20, 2003, 1005-1011.
5. Ingberg, C. M., M. Palmer, J. Aman, B. Arvidsson, E. Schvarcz, C. Berne. Body composition and bone mineral density in long-standing type 1 diabetes. – *J. Intern. Med.*, 255, 2004, 392-398.
6. Lamendola, C. J. *Cardiovasc. Nurs.*, 18, 2003, 103-107.
7. Phillips, S. M., L. G. Bandini, D. V. Compton, E. N. Naumova, A. Must. A longitudinal comparison of body composition by total body water and bioelectrical impedance in adolescent girls. – *Nutritional Methodology*, 2003, 1419-1425.
8. Weber, G., L. Beccaria, M. de' Angelis, S. Mora, L. Galli, M. A. Cazzuffi, F. Turba, F. Frisone, M. P. Guarneri, G. Chiumello. Bone mass in young patients with type 1 diabetes. – *Bone Miner.*, 8, 1990, 23-30.
9. Карамфилова, В. Съвременно лечение на захарен диабет тип 2. – *MedInfo*, VIII, 2008, 26-30.

Epiphyseal Complex and Growth Arrest

*A. Katsarov, N. Atanassova-Timeva, E. Ivanova**

*Institute of Experimental Morphology, Pathology and Anthropology with Museum,
Bulgarian Academy of Sciences, Sofia*

**Emergency Care Institute "N. I. Pirogov" – Sofia*

Bone tissue in human is connective tissue with mineralized extracellular matrix. It originates from mesoderm layer. There are specific zones in every bone known as epiphyses. These are the parts of the bone where the growth is accomplished. Different kind of injuries at these zones could lead to growth disturbances.

Key words: epiphysis, bone, bone growth, growth disturbance, growth arrest, epiphyseal injury.

Introduction

During the third week of the fetal period shaping of limbs begins. The three parts of lower and upper limb are distinguished during the sixth week [1]. At that time also appears primary ossification center. At the sixth lunar month begins forming of the medullary canal.

There are two kinds of bone formation – endochondral ossification and membranous ossification.

Long bones in human are formed by endochondral osteogenesis. Mature bone is formed over cartilage mould built of fibroblasts. Length of the new formed bone grows by the division of these fibroblasts. Long bones with unfinished growth are built of diaphysis (primary ossification nucleus or center), metaphysis and epiphyseal complex. Primary ossification center takes 70-80% of bone length.

Metaphysis is zone of big metabolic activity. Here the cartilage of the physis ossifies.

Epiphyseal complex is more clinical conception than anatomical, which includes the epiphysis, physis (growth plate) and that part of the metaphysis which lies immediate to the physis, perichondral sheath of Ranvier and bone ring of LaCroix. Epiphysis grows of the secondary ossification center. It has its own blood supply for the physis and articular cartilage.

Material and Methods

The physis is a cartilaginous formation between the metaphysis and epiphysis. Its main function is the longitudinal bone growth. It is a complex of cell groups situated in three zones:

1. Zone of growth - the most important, situated immediately to the epiphysis. It holds all the genetic growth potential. The layer main characteristic is cell proliferation and matrix synthesis.

- Layer of resting cells or “reserve” layer – it serves as a depot for nutritive substances. Cells are well differentiated, spherical, with robust endoplasmic reticulum – a sign for active protein synthesis. Collagen fibers of the matrix are irregularly situated.
- Layer of active cells or “proliferative” layer – These are the only dividing cells in the whole epiphysis. Their division is strong in longitudinal and transversal direction. It borders on with reserve layer to which is situated one basic cell which divides and gives birth to the cellular line.

The growth is calculated by formula at which the number of new cells multiplies to the size of the chondrocytes. Terminal number of cell division is 50.

Layer of the columnar cells – in this layer the final outlook and number of cell columns and extracellular matrix forms. It is built of II type of collagen.

2. Maturation zone – characterizes with stop of cell division and calcium depot. It divides into three layers: layer of hypertrophy, layer of calcification, layer of degeneration.

A. Layer of hypertrophy is built of big cells with a spherical shape and a lot of vacuoles.

B. Calcification layer – the number of vacuoles increase, degeneration and loss of cellular organelles is seen. Cells are with anaerobic metabolism. There is a lack of blood vessels. A process of calcium deposition in mitochondria and extracellular matrix is accomplished.

C. Degeneration layer – cells here are in terminal phase of destruction with lysis of the nucleus.

Maturation zone seems to be the most fragile point of the epiphyseal complex.

This is the point where the epiphyseal fracture happens.

3. Zone of transformation – here the cartilage of the physis gradually turns into the bone of metaphysis. There are two layers in that zone:

A. Layer of blood vessels penetration – capillaries along the cell columns.

There is a chondrolysis of the cartilage of the blood cells, which is the end part of the physal growth.

B. Layer of ossification – free of cartilage spaces are full of growing bone synthesized by osteoblasts.

4. Remodelling zone – actually belongs to metaphysis than to physis. There are two layers. Layer of primary spongiosis and layer of secondary spongiosis.

The perichondrial groove of Ranvier and the perichondrial ring of LaCroix surround each physis circumferentially at the periphery [2].

Perichondrial groove of Ranvier is described in 1873 and named after its author. This is a fibrous-cartilage sheath which covers the physis by its circumference and deepens to the periosteum of the metaphysis and joint cartilage of the epiphysis. Part of the perichondrial sheath, is the described of Lacroix, bone ring. It looks like a protrusion around the physis as a continuation of the metaphyseal cortex.

We classify actually types of epiphyses:

1. Spherical or radial – consists of primary ossification nucleus. Little bones and carpal bones have epiphyses of that kind.

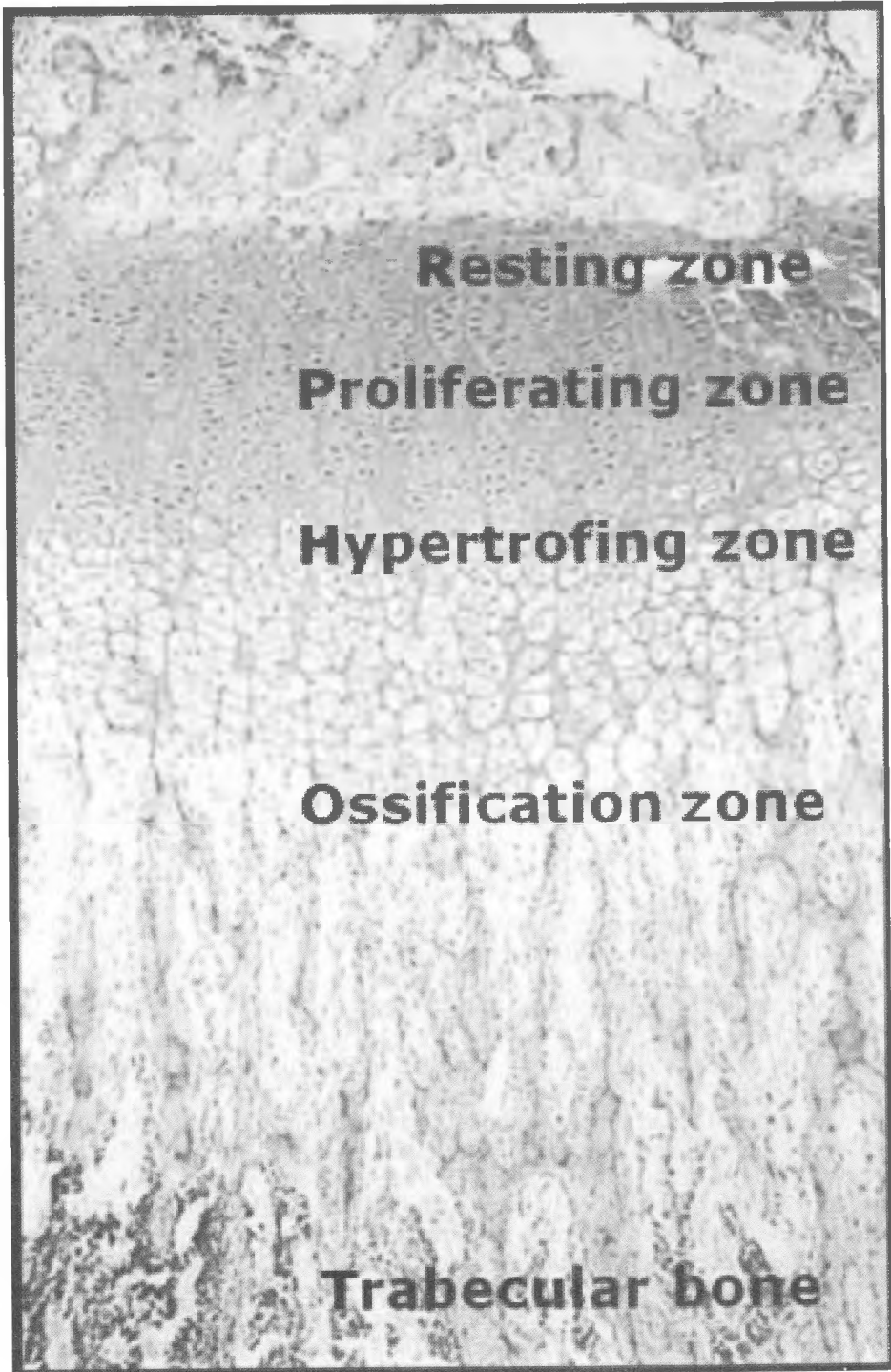


Fig. 1. Epiphyseal plate – zones

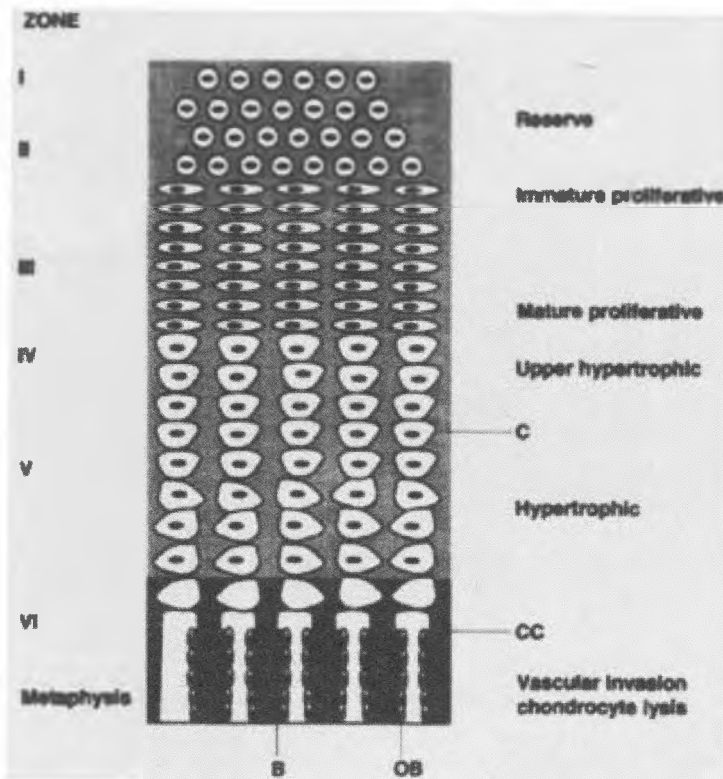


Fig. 2. Epiphyseal cell columns

2. Discoidal – consists of primary and secondary ossification centre – they divide in three subtypes:

- A. Pressure epiphyses
- B. Traction epiphyses or apophyses
- C. Mixed epiphyses

Blood supply of the epiphyseal complex is complicated and could be divided in three types.

1. Metaphyseal blood supply – its disturbance do not tend to significant growth problems.

2. Epiphyseal blood supply – normally there is a single central artery which gives branches to the joint cartilage and the physis. Blood vessels divide at the boundary of the physis and penetrate it through cartilage channels, forming a net which sends capillaries to the layer of resting chondrocytes. Single arteriole supplies 4 to 10 columns. Blood vessels cross the growth plate very rarely (only till 6 years of age) and anastomose with the blood vessels from metaphyseal circulation. The epiphyseal blood supply is formed of central arteriole and venules around it. These channels are not anastomosing and probably are the source of chondroblasts which provide the interstitial growth of the epiphysis, and after ossification create the secondary ossification nucleus.

3. Perichondrial blood supply – this is the blood vessels net of the perichondrial artery and its variables with different anastomoses with epiphyseal and metaphyseal circulation. Injuries of the peichondrial circulation are followed by angular deformation because of the disturbance of the appositional growth.

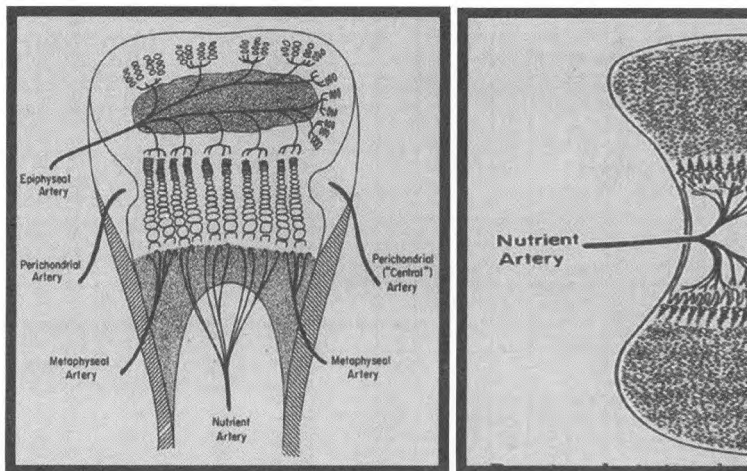


Fig. 3. Epiphyseal blood supply

Results

The above described circulation system of the epiphyseal complex is valid for the most of discoidal (pressure) epiphyses. According to Dale and Harris there are two epiphyses in human bones, which are totally covered by cartilage and its nutrient blood vessels [3]. They enter from the periphery of the metaphysis and after that unite with blood vessels of the growth plate outside. These are the proximal femoral epiphysis and proximal radial epiphysis. Haraldson adds also the epiphysis of the radial humeral condyle [4]. The situation of these epiphyseal arteries is so, that they are injured after every epiphyseal injury. Connecting these anatomical preconditions for the prognosis, Dale and Harris classified the blood supply of the physis in 2 types:

Type A – like femoral head and radial head blood supply – with poor prognosis after injury.

Type B – for the rest of the epiphyses – good prognosis after injury.

Epiphyses in different parts of the bones have different participation in the bone growth. As it is seen on table 1, the proximal epiphysis of the radius gives 25 % of the bone growth and only 10% of the limb length. It is seen also that for the upper extremity most active epiphyseal complexes are in its ends and for the lower extremity are around the knee.

The appearance of the secondary ossification centre in bone depends on bone age. Around the birth secondary ossification centres of proximal tibia, distal femur and navicular bone appear. After the first year secondary centre in most of the bones appear. At the 4th year of age secondary ossification center in bigger trochanter and proximal fibula appears. Lately, at 11 years of age secondary centre of humeral radial condyle and tibial tuberosity appears.

Table 1. Participation of different epiphyseal complexes in bone growth

Bone	Proximal epiphysis		Distal epiphysis	
	Bone	Total limb	Bone	Total limb
Humerus	80%	40%	20%	10%
Radius	25%	10%	75%	40%
Ulna	80%	–	20%	–
Femur	30%	15%	70%	40%
Tibia	55%	27%	45%	18%
Fibula	60%	–	40%	–

Injury in the zone of epiphysis is known as epiphysiolysis or fracture of the physis. Mechanism of injury is indirect in common. The answer of the epiphyseal complex to the trauma could be:

1. Overgrowth – symmetrical or asymmetrical;
2. Growth arrest;
3. Asymmetrical growth – with or without shortening;
4. Delayed growth – especially in disturbance of the metaphyseal circulation;
5. Normal growth – only in pure tears.

After series of investigations, Schenk generalizes that there are several factors having influence on bone growth [5]. Growth hormone stimulates the cell proliferation directly and thyroxine – indirectly. Cell proliferation is inhibited by adrenocorticotrophic

hormone and corticosteroids. They also inhibit the matrix synthesis. Matrix synthesis is also inhibited by vit. C and vit. D deficiency. Vit. D and its metabolites stimulate the mineralization of bone and cartilage.

When there is a disturbance in the diaphyseal circulation, overgrowth at length is seen. This leads to collateral hyperemia in metaphysis and stimulation of the epiphyseal complex. It answers with growth acceleration.

When the disturbance is at metaphyseal circulation some effects are available:

1. Pure tear of the epiphysis and moderate trauma tends to temporary growth acceleration but not to overgrowth.

2. When the injury is heavier, with tear of larger metaphyseal blood vessels, total growth delay is seen but it is temporary.

3. When disturbance in epiphyseal circulation occurs growth arrest is seen after epiphyseal artery tear.

4. Isolated injuries of the perichondrial artery with preserved germinative layer do not influence over the nutrition and growth of the epiphyseal complex.

Disturbances in epiphyseal growth could appear not only after blood supply injuries but in other conditions as [6, 7]:

1. Disturbances after not functioning – prolonged plaster immobilization, crutches walking, direct traction healing, DDH, rheumatoid arthritis, polyomyelitis, tuberculosis, Perthes disease, etc.

2. Radiation injuries – X-ray radiation inhibits the growth and leads to destructive effect over the growth cartilage.

3. Disturbances after infection – septic arthritis, osteomyelitis with metaphyseal localization, when premature stop of growth occurs fast.

4. Reason for epiphyseal disturbances could be tumors, blood vessels trauma or disease, metabolic disturbances, frostbites, burn trauma, iatrogenic reasons.

Discussion

Epiphyseal complex is growth zone of the long bones. Trauma in that zone leads to different growth disturbances. Knowing the function and structure of the epiphyseal complex is a precondition for the right treatment and prognosis of the injuries in that zone.

References

1. Bardeen, C. R., W. H. Lewis. Development of the limbs, body wall and back in man. – *Am. J. Anat.*, 1, 1960, 47-49.
2. Wood, W. L., R. B. Winter, T. Raymond. *Morrissy in Lovell and Winter's pediatric orthopaedics*, Vol.2, 6th ed., September 2000, 1433.
3. Dale, G. G., W. R. Harris. Prognosis of epiphyseal separations. An experimental study. – *J. Bone Joint Surg.*, **40B**, 1958, 116-122.
4. Haraldson, S. Osteochondrosis deformans juvenilis capituli humeri including investigation of the intra-osseous vasculature in the distal humerus. – *Acta Orthop. Scand.*, **38**, 1959, 93-97.
5. Schenk, R. K., W. Hofstetter. Connective tissue and its heritable disorders. – In: *Molecular, genetic and medical aspects* (Ed. P. Royce and B. Steinmann), Chapter 1, Part Morphology and Chemical Composition of Connective Tissue: Bone, Wiley-Liss, 2002, 67.
6. Simpson, Jr, W. C., D. F. Fardon. Obscure distal femoral epiphyseal injury. – *South Med. J.*, **69**, 1976, 1338-1340.
7. Clarke, T. A., D. K. Edwards, A. Merritt. Neonatal fracture of the femur: Iatrogenic?. – *Am. J. Dis. Child.*, **136**, 1982, 69-70.

Cephaloscopic Characterization of Acromegalic Patients

Preliminary announcement

S. Todorov

*Institute of Experimental Morphology, Pathology and Anthropology with Museum
Bulgarian Academy of Sciences –Sofia, Bulgaria*

Acromegaly is a hormonal disorder that results from too much growth hormone (GH) in the body. The excess of GH comes from noncancerous tumors on the pituitary. The most common symptoms are abnormal growth of the hands and feet, brow and lower jaw protrude, the nasal bone enlarges, and the teeth space out.

This announcement concerns cephaloscopic characterization of investigated group till this moment, composed of 57 acromegalic patients, aged 26-77 years, 16 men and 41 women and distribution of cephaloscopic signs within.

The present results are only preliminary at early stage of the research. To terminate this study is necessary to examine more patients, anthropometric and anthroposcopic characteristics to be compared with in healthy persons. The data has to be statistically analyzed and the obtained result has to be discussed.

Key words: acromegaly, cephaloscopy.

Introduction

Acromegaly (from Greek – ‘acros’-end, and ‘megalos’-big) is a hormonal disorder that results from too much growth hormone (GH) in the body. Due to its low frequency and “hidden” onset it is hard to diagnose. In Bulgaria there are 400 registered cases of acromegaly and no full anthropological characterization of specific anomalies (enlargement) that occur the hands and feet as a consequence of the disease.

History

Ancients manuscripts describe legendary giants, as king Og from Basan ,who was so tall, that he was able to bake a fish in his hand only by stretching it to the sun. And the murder of Goliath by David, which are maybe the first balance-sheets of a physical disorders caused by a pituitary adenomas [7].

In 1886 Pierre Marie (1853 Paris (France) – 1940 Paris (France) used the term “acromegaly” for the first time and gave a full description of the characteristic clinical picture [3].

At this time he did not realize the role of pituitary, because the knowledge of endocrine system marked a remarkable progress not until Renaissance. Endocrinology is formed as a discipline after the appearance of experimental medicine whose “father” is Claude Bernard who proposed the theory of “internal secretion” after he had investigated cells with glandular structure [6].

Marie, however, was not the first physician to give a clear description of the clinical picture of acromegaly. Others had done this years before him, like (possibly) the Dutch surgeon and active opponent of superstition and witch-burning, Johannes Wier (1515–1588) already in 1567, or Saucerotte in 1772. Other physicians had also given the disease different names including Alibert in 1822 calling it “Ge’ant scrofuleux”, Verga in 1864 calling it “Prosopoectasia” and Lombroso in 1869 calling it “Macrosomia”. A total of more than 20 physicians had already published on disorders, which later could be reclassified as cases of acromegaly [3].

Symptoms

The name acromegaly comes from the Greek words for “extremities” and “enlargement”, reflecting one of its most common symptoms – the abnormal growth of the hands and feet. Swelling of the hands and feet is often an early feature, with patients noticing a change in ring or shoe size, particularly shoe width. Gradually, bone changes alter the patient’s facial features: The brow and lower jaw protrude, the nasal bone enlarges, and the teeth space out. Overgrowth of bone and cartilage often leads to arthritis. When tissue thickens, it may trap nerves, causing carpal tunnel syndrome, which results in numbness and weakness of the hands. Body organs, including the heart, may enlarge [1, 2].

Morbidity

Used data for 700 patients between 1970-2009 show the following distribution by sex and age:

- Middle age 42,3y.*
- Top age of morbidity-40-50y.*
- 63% women и 47% men (for Bulgaria)*.

In medical literature the separation by sex is 50/50 %, no data for sexual dimorphism.

In Bulgaria the different separation is assigned by endocrinologists to more rarely visit at the doctor from men’s side [9].

Medico-anthropological aspects

Since acromegaly is often difficult to diagnose until later in life, recent studies are focusing on the best and most efficient way to determine a problem before major irreversible damage occurs. Unfortunately, since the disease is so rare, major symptoms generally have to occur before the afflicted is even tested for the disease. The problem is until recently, scientists have based their diagnoses almost entirely upon phenotypic characteristics and what is known about pituitary adenomata; So further medico-anthropological studies on metric and scopic characteristics of patients with acromegaly and comparison with control groups are needed to determine the level of abnormal changes occurring orofacial and somatic structures, and some anthropological signs evoking eventual onset of the disease may be discovered [5, 6].

*According to unpublished data from national clinics of endocrinology.

Anthropological research

This announcement concerns cephaloscopic characterization of investigated group till this moment, composed of 57 acromegalic patients, aged 26-77 years, 16 men and 41 women.

Investigated cephaloscopic symptoms :

Macroglosia , exophtalmus, prognatism, tufts of distal phalanx and level of expression of sulcus mentolabialis.

For anthropological investigation are used anthropological methods proposed by R. Martin–K. Saller, 1957 y., defining bite type by R. Martin–K. Saller, 1957 y. [4], and defining level of expression of sulcus mentolabialis by E. Eickstedt, 1943 y. [8].

Intermediate results

Distribution of cephaloscopic signs shows high percent of patients with Exophtalmus and macroglosia (Fig. 1).

Separation by sex does not show a sexual dimorphism (Fig. 2).

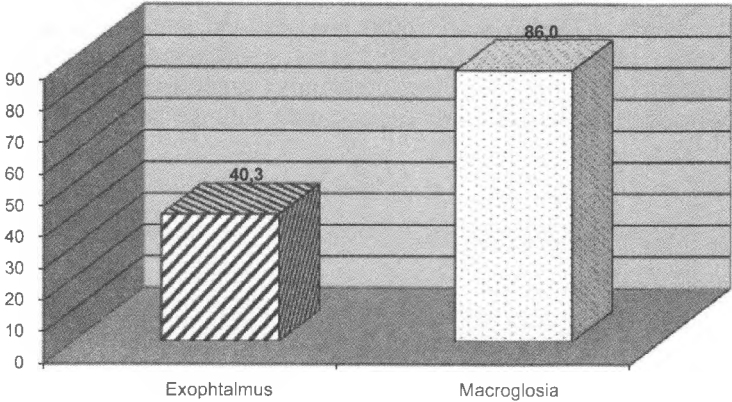


Fig. 1. Exophtalmus, macroglosia distribution

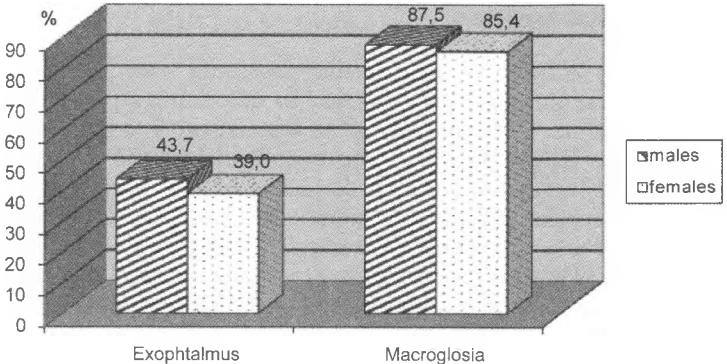


Fig. 2. Exophtalmus, macroglosia separation by sex

The research shows most recently level of expression 2 (well developed) Sulcus mentolabialis in both sexes (fig. 3).

The investigation of bite shows high percent of progenia in patients of both sexes but mostly in men (fig. 4).

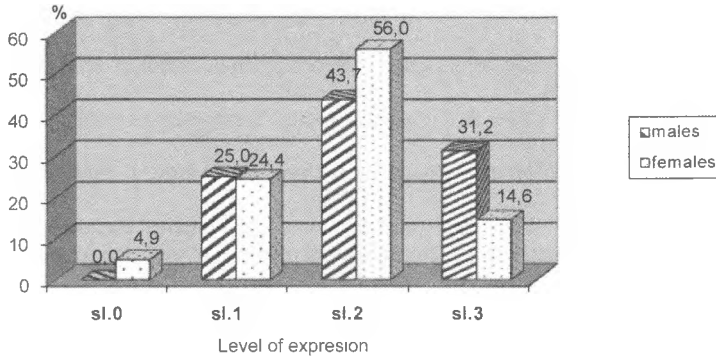


Fig. 3. Distribution of Sulcus mentolabialis by sex

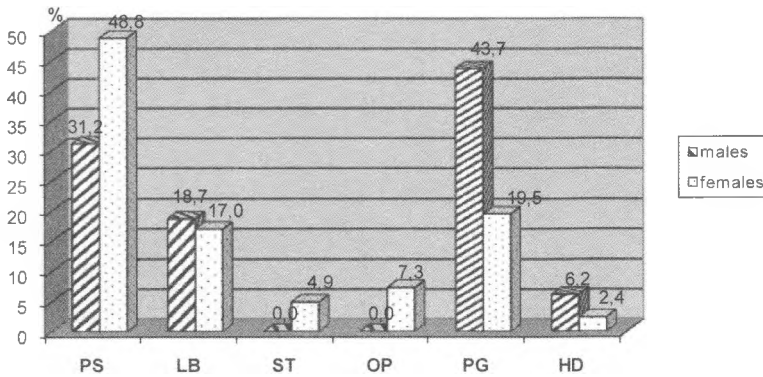


Fig. 4. Separation of bite type by sex

The present results are only preliminary at early stage of the research. To terminate this study is necessary to examine more patients, anthropometric and anthroposcopic characteristics to be compared with those ones in healthy persons. The data has to be statistically analyzed and the obtained result has to be discussed.

This study aims to present detailed anthropological characterization of acromegalic patients, which presents an interest for theoretical physical (medical) anthropology and medical practice as well.

The discovery of a metric or scopic symptoms presented in statistically significant values would give assistance to diagnose acromegaly.

References

1. Hurley, D. M., Ho KKY. Pituitary disease in adults. – *The Medical Journal of Australia*. April 19, 2004, **180**:419-425.
2. Levy, A. Pituitary disease: presentation, diagnosis, and management. – *Journal of Neurology, Neurosurgery, and Psychiatry*. 2004; **75**:47–52.
3. Marie, P. Sur deux cas d'acromégalie; hypertrophie singulière non congénitale des extrémités supérieures, inférieures et céphalique. *Rev. Med. Liege*, **6** 1886:297-333.
4. Martin, R., Kessler. *Lehrbuch der Anthropologie*, Stuttgart, Gustav Fischer Verlag, 1961, No 11, 1810-1926.
5. Melmed, S. Medical progress: acromegaly. – *New England Journal of Medicine*. December 14, 355(24) 2006: 2558–2573.
6. Muller, A. F., van der Lely, A. J. Pharmacological therapy for acromegaly: a clinical review. – *Drugs*. **64**(16): 2004, 1817–1838.
7. Pearce, J. M. Nicolas Saucerotte: acromegaly before Pierre Marie. *J. Hist. Neuroscience*, **15**(3) (2006): 269-275.
8. Wouter, W. de Herder. Acromegaly and gigantism in the medical literature. Case descriptions in the era before and the early years after the initial publication of Pierre Marie (1886) Published online: 6 August 2008 at Springer.
9. Начев, Е., Лозанов Л. Акромегалия. Изд. „СЕМАРШ“, 2002 ред. проф. С. Захариева, 2002: 2–8.
10. Йорданов, Й. Наръчник по антропология за медици и стоматолози. УИ „Св. Климент Охридски“, 1997, 41–42.

INSTRUCTION TO AUTHORS

SUBMISSION: Original papers and review articles written in English are considered and should be sent to the Editor-in-Chief.

Address: Bulgarian Academy of Sciences

Institute of Experimental Morphology and Anthropology with Museum

Acad. G. Bonchev Str., Bl. 25,

1113 Sofia

Bulgaria

Our e-mail address is: <iemabas@bas.bg>

Manuscripts should not exceed 4 standard pages including abstract, captions, references and figures (3 copies — two copies in English and one copy in Bulgarian, and a disc using WINWORD 7.0, Times New Roman 12 pt).

CONDITIONS: In submitting a paper, the author should state in the covering letter that the article has not been published elsewhere and has not been submitted for publication elsewhere.

All manuscripts are subject to editorial review.

ARRANGEMENT:

Title page. The first page of each paper should indicate the title, the authors' names and institute where the work was conducted, followed by abstract and key words.

Abstract. It should contain no more than 150 words.

Key words. For indexing purposes, a list of up to 5 key words in English is essential.

Tables and illustrations. Tables and captions to the illustrations should be submitted on separate sheets. The proper place of each figure in the text should be indicated in the left margin of the corresponding page. All illustrations (photos, graphs and diagrams) should be referred to as "figures" and given in abbreviation "Fig.". The author's name, the number of the figure with indication of its proper orientation (top, bottom) should be slightly marked on the back of each figure. All illustrations should be submitted in duplicate too.

References. They should be indicated in the text by giving the corresponding numbers in parentheses. The "References" should be typed on a separate sheet. The names of authors should be arranged alphabetically according to family names, first the articles in Roman alphabet, followed by the articles in Cyrillic alphabet. Articles should include the name(s) of author(s), followed by the full title of the article or book cited, the standard abbreviation of the journal (according to British Union Catalogue), the volume number, the year of publication and the pages cited. For books - the city of publication and publisher. In case of more than one author, the initials for the second, third, etc. authors precede their family names. Example:

Tuohy, V. K., Z. Lu, R. A. Sobel, R. A. Laursen, M. B. Lees. A synthetic peptide from myelin proteolipid protein induces experimental allergic encephalomyelitis. — *J. Immunol.*, 141, 1988, 1126-1130.

Norton, W. T., W. Cammer. Isolation and characterization of myelin. — In: *Myelin* (Ed. P. Morell), New York, Plenum Press, 1984, 147-180.

Further details. Use only standard symbols and abbreviations in the text and illustrations. Manuscripts, figures and diagrams should not be folded.

Full address. The exact postal address completed with postal code of the senior author must be given. If correspondence is handled by someone else, indicate this accordingly.

ISSN 0861-0509

AIMS AND SCOPE

Acta morphologica et anthropologica publishes original and review articles in the following sections:

Section A – Morphology:

1. Neurobiology;
2. Structure and Metabolism of the Cells;
3. Cell Differentiation and Kinetics;
4. Cellular Immunology;
5. Experimental Cytology;
6. New Methods;
7. Anatomy.

Section B – Anthropology:

1. Physical Development;
2. Somatotype and Body Composition;
3. Population Genetics and Medical Anthropology;
4. Paleoanthropology and Paleopathology.